Universitat Autònoma de Barcelona

The role of mesenchymal stem cell products in experimental asthma

Rubén Osuna Gómez

TESIS DOCTORAL

The role of mesenchymal stem cell products in experimental asthma

presentada por

Rubén Osuna Gómez

DIRECTOR

David Ramos Barbón

TUTOR

Silvia Vidal Alcorisa

Programa de Doctorado en Inmunología Departamento de Biología Celular, Fisiología e Inmunología IIB Institut de Recerca Hospital de la Santa Creu I Sant Pau Universitat Autònoma de Barcelona, 2020

DEPARTAMENTO DE BIOLOGÍA CELULAR,
FISIOLOGIA E INMUNOLOGÍA

FACULTAD DE BIOCIENCIAS
UNIVERSIDAD AUTÓNOMA DE BARCELONA

Memoria presentada por

Rubén Osuna Gómez

Para optar al grado de

DOCTOR EN INMUNOLOGÍA

Tesis realizada en el laboratorio de Neumología del *Institut del Hospital de la Santa Creu i Sant Pau* de Barcelona bajo la dirección del Dr. David Ramos y el Dr. Eder Mateus.

El doctorando	El director	El codirector
	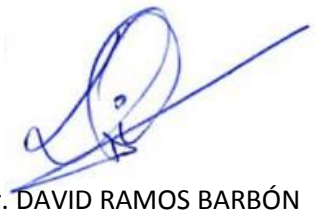	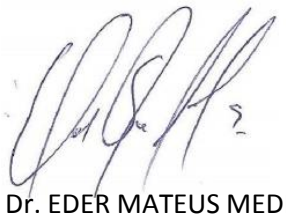
RUBÉN OSUNA GÓMEZ	Dr. DAVID RAMOS BARBÓN	Dr. EDER MATEUS MEDINA

Barcelona, Enero del 2020

Thesis committee members

President

Dra. Victoria del Pozo Abejón, PhD

Secretary

Dr. Carlos Zamora Atenza, PhD

Commite member

Dra. María Jesús Cruz Carmona, PhD

Este trabajo ha sido financiado con subvenciones concedidas por el Instituto de Salud Carlos III del Ministerio de Ciencia en Innovación (becas operativas FIS PI14/00257 y PI18/01102).

This work has been supported with grants from *Instituto de Salud Carlos II,I Ministerio de Ciencia en Innovación,* (*becas operativas* FIS PI14/00257 and PI18/01102).

A mi familia

“Learn from yesterday, live for today, hope for tomorrow. The important thing is not to stop questioning'”

Albert Einstein

INDEX

INDEX

Index of figures

Index of tables

SUMMARY

Traditional models of experimental asthma have been developed by followed intraperitoneal sensitization and airway challenge, but do not have the ability to reproduce how humans get sensitized to airborne allergens. This is an important point due to the crucial interaction between allergens and airway mucosa that promotes a specific immune response. In the present work, we developed a rat model of allergic asthma based on local airway exposure to a natural allergen. Following sensitization and after fifteen intranasal challenges, the model developed airway hyperresponsiveness to MCh, mucus overproduction, subepithelial collagen deposition, an increased airway contractile mass and developed a Th2 response with eosinophilic recruitment in the upper and lower airways.

An infiltration of T cells into the airways is a major feature of asthma, where these cells contribute to the ongoing inflammation through the release of cytokines and chemokines. Airway smooth muscle (ASM) cell proliferation is a major feature of airway remodeling, in which many mediators are implicated. The increase in ASM mass may be the main contributing factor to airway hyperresponsiveness and asthma severity. Therefore, it is crucial to find an effective treatment to suppress the development of airway remodeling in asthma. Mesenchymal stem cells (MSC) may offer a therapeutic potential for asthma due to their immunomodulatory and anti-inflammatory properties, as well as their allogeneic tolerance. However, MSC administered for therapeutic purposes in asthma may have a dual therapeutic and pathogenic potential of reducing inflammation while serving as a precursor to originating new airway structural cells. For this reason, it is necessary to understand their immunomodulatory mechanisms and mediators.

In the second part of this work, we showed that adipose-MSC had a suppressive effect on $CD4^+$ T cell-induced ASM proliferation only when separated by Transwell upper chamber. Further, this suppressive effect was generated by soluble factors that were secreted into the medium and not carried by exosomes. This conditioned media was separated into different molecular weight ranges and it was observed that the suppressive effect was only in a fractionated group of proteins. Following a proteomic analysis, we obtained different candidates to suppress the development of airway remodeling in asthma.

To demonstrate that conditioned media may drive immune regulation and has suppressive effect on airway remodeling, we tested the effect of conditioned media in the previously developed rat model of allergic asthma *in vivo*. We showed that only primary exposure to repeated low doses of conditioned media decreases airway remodeling with subsequent deviation of profile to Th1 and Th17 responses, whereas high or single repeated doses

may be non-effective. These findings suggest a role of conditioned media in the attenuation of the asthma features. Further work is warranted to better define the suppressive effect of conditioned media and the proteins that may be implicated.

ABBREVIATIONS

ADAM: A disintegrin and metalloproteinase domain
AERD: aspirin-exacerbated respiratory disease
AHR: airway hyperresponsiveness
ALOH3: aluminium hydroxide
ANOVA: analysis of variance
APC: allophycocyanin
ASM: airway smooth muscle
AD: adipose derived
ATP: adenosine triphosphate
AwCT: airway contractile mass
BAL: bronchoalveolar lavage
bFGF: basic fibroblast growth factor
BM: bone marrow
BN: Brown Norway
BSA: bovine serum albumin
CCL: C-C chemokine ligand
CCR: C-C chemokine receptor
cDC: conventional dendritic cell
CFU: colony-forming unit
CM: conditioned media
COX1: cytochrome c oxidase subunit 1
COX2: cytochrome c oxidase subunit 2
CRSwNP: Chronic rhinosinusitis with nasal polyps
CTLA-4: cytotoxic T-lymphocyte antigen
CY: cyanine dye
DFSC: dental follicular stem cell
DERP 1: Dermatophagoides pteronyssinus 1
DMEM: Dulbecco's Modified Eagle Medium
DN: double negative
DNA: deoxyribonucleic acid
DP: double positive
EAR: early asthmatic responses
ECM: extracellular matrix
EdU: 5-ethynyl-2’-deoxyuridine
EGFR: epidermal growth factor receptor
EMTU: epithelial-mesenchymal thropic unit
ESC: embryonic stem cell
EV: extracellular vesicle
FBS: foetal bovine serum
FCERB: Fc Epsilon Receptor Beta-Chain
FEV1: forced expiratory volume in the first second of forced expiration
FITC: fluorescein isothiocyanate
FOT: forced oscillation technique
G-CSF: granulocyte-colony stimulating factor
GM-CSF: granulocyte-macrophage colony-stimulating factor
HB-EGF: heparin-binding epidermal growth factor
HBSS: Hank's Balanced Salt Solution
H-E: haematoxylin eosin
HDM: house dust mite
HGF: hepatocyte growth factor
HLA: human leukocyte antigen
HRP: horseradish peroxidase
IFN-y: interferon gamma
ICAM-1: inter-cellular adhesion molecule-1

IDO: indoleamine-pyrrole 2,3-dioxygenase
i.e.: id est
Ig: immunoglobulin
IL: interleukin
IL4RA: interleukin 4 receptor alpha chain
IL1R1: interleukin 1 receptor type 1
IL2R: interleukin 2 receptor
IL7R: interleukin 7 receptor
ILC2/3: type 2/3 innate lymphoid cell
i.n.: intranasal
i.p.: intraperitoneal/intraperitoneally
IPF: idiopathic pulmonary fibrosis
IRF4: interferon Regulatory Factor 4
i.v.: intravenous/intravenously
kDa: kilodalton
LAR: late asthmatic responses
LFA-1: lymphocyte function-associated antigen 1
LW: Lewis
MAPK: mitogen-activated protein kinase
MBP: major basic protein
MCh: acetyl-β-methylcholine chloride
MHC: major hystocompatibility complex
MMP: matrix metalloproteinases
mOD: mean optical density
mRNA: messenger ribonucleic acid
MSC: mesenchymal stem cells
NFKB: nuclear factor kappa-light-chain-enhancer of activated B cells
NK: natural killer
NO: nitric oxide
NOD: nucleotide-binding oligomerization domain
nTreg: natural regulatory T cell
OVA: ovalbumin
PAMP: pathogen-associated molecular patterns
PAR: protease-activated receptor
PAS: periodic acid Schiff
PBM: perimeter of the basal membrane
PBS: phosphate buffer saline
PD-1: programmed death 1
PDGF: platelet-derived endothelial cell growth factor
PDL-1: programmed death-ligand 1
PE: phycoerythrin
PEEP: positive end expiratory pressure
PGE2: prostaglandin 2
PI3K: phosphoinositide 3-kinase
PMA: phorbol 12-myristate 13-acetate
PRR: pattern recognition receptors
PSG: penicillin-Streptomycin-Glutamine
RANTES: regulated on activation, normal T cell expressed and secreted
RNA: ribonucleic acid
RL: lung resistance
ROD: range of detection
RT: room temperature
SA: Staphylococcus aureus
SAE: Staphylococcal enterotoxins

s.c.: subcutaneous
SCF: epithelial cells release stem-cell factor
SD: Sprague Dawley
SE A/B: Staphylococcus enterotoxins A/B
SEM: standard error of the mean
SMA: smooth muscle actin
STAT: signal transducer and activator of transcription
TCR: T cell receptor
TGFB: transforming growth factor beta
Th1/2/3: type 1/2/3 helper T lymphocyte
TIM: transmembrane immunoglobulin and mucin domain
TMB: 3,3′,5,5′-Tetramethylbenzidine
TIMPS: tissue inhibitors of metalloproteinases
TLC: total lung capacity
TLR: Toll-like receptor
TNFA: tumor necrosis factor alpha
Tr1: inducible type 1 regulatory T cells
Treg: regulatory T cell
TSLP: thymic stromal lymphopoietin
TSST-1: toxic shock syndrome toxin-1
VCAM-1: vascular cell adhesion molecule-1
VEGF: vascular endothelial growth factor
VLA-4: very late antigen-4

INTRODUCTION

1. ASTHMA

1.1. General aspects

Asthma is generally described as a chronic inflammatory alteration of the airways, which is represented by heterogeneous clinical phenotypes and is characterized by airway hyperresponsiveness (AHR) and inflammation [1], [2]. The term “asthma” originates from the Greek verb “aazein”, which means “to pant or exhale with the open mouth” [3]. Since the 1960s, substantial research efforts have been put into understanding the pathobiology of asthma [4].

The lack of understanding of the immunologic mechanisms leading to this disease has made it difficult to give a clear and concise definition [5]. In addition to the cardinal features of asthma (AHR, airflow obstruction and inflammation), another hallmark termed “airway remodeling” has been recently described in the pathogenesis of asthma and has become a significant area of research. Airway remodeling is defined by the structural changes of the airways that occur over time in response to certain stimuli. These changes correlate with the severity of the disease. The most common features of airway remodeling are subepithelial fibrosis, epithelial damage, collagen deposition; goblet cell hyperplasia, angiogenesis, and increased airway smooth muscle (ASM) mass [6], [7]. These features are described in further detail in a subsequent section. Moreover, respiratory virus infections are strongly associated with asthma and, in combination with allergen sensitization, increase the risk of exacerbation [8], [9]. Commonly involved viruses include the respiratory syncytial virus in children and rhinoviruses in adults [10].

This disease affects approximately 300 million people worldwide and its impact accounts for 1 in every 250 deaths [1]. Most of these deaths are due to the lack of medical treatments and are a common phenomenon in countries with poor economic resources [11].

In the industrialized world, the prevalence of asthma has increased dramatically during the last decades [11] and has brought the research of this disease into an important point in the health systems of the European Union and North America. Curiously enough, such prevalence of asthma in these areas remains understudied. However, the prevalence of this disease is associated with industrialization and the occidental lifestyle, and this trend is correlated with the increase of autoimmune diseases and allergies [10].

In Spain, the general population has a prevalence of asthma that ranges from 5.1 to 7.5%, and in from 9 to 13% in children aged 13-14 [12]. Moreover, approximately 20% of asthmatics are hospitalized following acute asthma attacks, which are very common in children [13]. Therefore, acute asthma attacks amount to high costs for public health systems and are responsible for a loss of productivity of approximately €9.8 billion per year in European countries with poor asthma control [10].

Classically, there are two forms of asthma defined according the clinical features [6]. Most children and approximately 50% of adults have allergic asthma, in which the disease is associated with allergic sensitization. Conversely, non-allergic asthma often develops later in life in the absence of allergic sensitization [6].

1.2. Etiology of asthma

Asthma has become a downright endemic in the industrialized parts of the world, and its incidence is still increasing in developing countries [14]. The rise in the prevalence of diseases of the allergy spectrum (allergic rhinitis, asthma, food allergies, urticaria, atopic eczema, and anaphylaxis) has been attributed to a westernized lifestyle [14]. This trend has generated the so-called “hygiene hypothesis” and the concept of allergies as not only genetic but also environmental diseases [14].

1.2.1. Genetic factors

It has long been known that the predisposition to developing an allergic disease is, to some extent, an inheritable trait [14]. Previous studies have shown that there is a 60% risk of atopy when both parents are atopic, and maternal asthma seems to be more influential than paternal asthma [15]. Early linkage analyses have identified loci on chromosomes 5 and 11 containing the *IL9* and *FCERB* genes and the *IL4* gene cluster, relevant to both atopy and asthma [14]. Nevertheless, meta-analyses have identified several genes that have been reproduced in several independent cohorts as being associated with atopy, sensitization and allergy spectrum diseases. Among the top hits are genes for type 2 helper T (Th2)-associated and proinflammatory cytokines and chemokines (*IL4*, *IL4RA*, *IL13*, *IL6*, *IL10*, *TNFA*, *IL33*, *TSLP* and *RANTES*) and their receptors (IL4RA, IL1R1), transcription factors (STAT6), subunits of the high-affinity immunoglobulin E (IgE) receptor (*FCER1A*, *FCER1B*), genes of the MHC-II gene cluster (*HLADRB1*, *HLADQB1*) and innate pattern recognition receptor genes (*CD14*, *TLR7*, *TLR9* and *S100A7*) [15].

Moreover, the genes associated with different T cell domains and *ADAM33,* which are localized in chromosome 20p13 and have recently been correlated with this disease [16].

1.2.2. Environmental factors

There are epidemiological studies that have demonstrated a strong correlation between environmental factors and the development and progression of asthma [17]. However, the prevalence and incidence of this disease are represented by an extensive geographical variation and increase in parallel with “western development” [14]. It has progressively become apparent that the “westernized lifestyle” may impact on the predisposition to developing allergic diseases [14]. Epidemiological studies have suggested the existence of both harmful and protective environmental and lifestyle factors that may play an important role during early childhood and adolescence, and possibly in utero as well [14]. Growing up in a rural environment in contact with farm animals, nutrition rich in dietary fibers, ample food diversity and early contact with siblings or peers have been identified as protective factors [14]. A feature common to all such environmental factors is that they favor the establishment of a highly diverse microbiome on the body’s barrier tissues such as the skin and the mucosa of the respiratory, urogenital, and gastrointestinal tracts [14]. The early interaction of environmental and commensal microbes with the host′s developing immune system, including epithelial pattern recognition receptors, seems instrumental for the adjustment of the innate immune system [14]. Such interactions likely set activation thresholds for the pattern recognition receptors and their downstream signaling pathways, which in turn influence the immune homeostasis and reaction capacity later in life [14]. Harmful environmental factors, in contrast, include obesity, lack of exercise, industrially manufactured foods and life in an urban context, which reduce microbial diversity and increase the the probability of employing antibiotic treatment [14]. Significant research have focused has focused on understanding to allergic diseases [16]. Moreover, the genetic and environmental factors that interact and regulate allergic diseases remain understood [16]. Therefore, further advances in the genetics of atopic asthma and the understanding of the way asthma genes possibly interact with environmental factors may enhance the development of new treatments [16].

1.3. Asthma Phenotypes

There are multiple phenotypes and endotypes of asthma [18], and in the last decades, it has been postulated that asthma was is an allergic disease caused by allergen exposure

[5]. Traditionally, asthma phenotypes have been classified into extrinsic (allergic) and intrinsic (non-allergic) asthma [19].

Asthma triggered by the presence of allergens has been more extensively researched. Individuals with an early sensitization to an allergen such as house dust mite (HDM) have a higher risk of persistent asthma [20]. This leads to the distinction between allergic (atopic) and non-allergic (non-atopic) asthma. Atopy is the term used to indicate the predisposition to sensitization that results in the Th2 response pattern of the immune response defined by the presence of specific IgE serum and cytokines such as interleukin (IL)-4, IL-5 and IL-13 that gives rise to allergic conditions. To qualify as allergic, individuals must demonstrate a positive skin prick test or specific IgE antibodies against allergens [21]. Although asthma is usually divided into allergic and non-allergic asthma, there can be the presence of atopy in non-asthmatics. In fact, less than half of asthma cases in the developed world are due to atopy and even less in the developing world [22].

Non-allergic asthma appears later in life (at approximately 40 years of age), and is strongly correlated with aspirin-exacerbated respiratory disease (AERD). Further, this form of asthma is not associated with allergic sensitization, whereas inflammatory markers related to Th2 response and IgE have not been identified (i.e. by skin prick test) on a panel of different allergens. Further, pathobiological studies in humans have reported that no differences can be observed in Th2 cytokine levels between allergic and non-allergic asthma subjects when compared. Moreover, they have shown that inhaled corticosteroid is a good treatment in mild to moderate asthma patients, whereas the classification between allergic and non-allergic asthma is complicated to define [19]. Moreover, some reviews have contrasted clinical and immunopathological features of allergic and non-allergic asthma [19].

However, this classification does not explain the global asthma patterns [5]. These questions have led to the need to evaluate and improve the atopic/non-atopic classification of asthma phenotypes [21].

This purpose to classify asthma phenotypes by pathological features [23] beyond to clinical pattern has the result to enhancing the medical treatment and understanding why asthmatic patients respond to conventional treatment while others do not [5]. However, most reported studies do not use methods for obtaining samples from the target organ (sputum induction and nasal lavage) or new technologies based on biomarker detection (microbiome and epigenetics analysis). Therefore, several works have classifed asthma phenotypes based on airway inflammation biomarkers. Moreover, Simpson *et al.* showed

that there are four inflammatory subtypes of asthma: eosinophilic, neutrophilic, mixed granulocytic and paucigranulocytic asthma [24]. Later, Haldar *et al.* reported a characterization of these subtypes, but some comparable clinical and biological features were identified [25].

The concept of asthma phenotypes is rapidly developing with the objective to correlate clinical characteristics and phenotype biology patterns [19]. Perhaps a breakthrough analysis reports a strong correlation between a Th2-high phenotype in up to 50% of people and asthma of any severity [19]. However, the percentage of early allergic asthma that has this same phenotype remains understood. An increase of complexity and severity in the disease is probably associated with an increase in the complexity of immune response with adaptive immune elements and structural changes in the airways. Further, Th2 immunity is a hallmark in asthma of any severity and evidence of this disease with other types of immune response remains understood [19]. Recently, other studies have reported the role of Th17 response in neutrophilic asthma [19].

Therefore, our understanding of asthma phenotypes remains incomplete [19]. The need to obtain data from genomic and proteomic profiling studies of well-characterized phenotypes could improve the development of animal models to study the immunological response and the environment obtained from human reports [19].

1.4. Pathophysiology of asthma

Asthma is a chronic inflammatory disorder of the respiratory tract where many cells implicated in innate and adaptive immune responses interact with epithelial cells to develop airway narrowing, mucus overproduction, airway wall remodeling and AHR, in which smooth muscle cells react to nonspecific stimulus as well as cold air or exercise [6]. In asthmatic patients, this leads to repeated periods of shortness of breath, wheezing and chest tightness [6]. Airway narrowing during acute episodic deterioration (exacerbations) results in persistent chronic inflammation and structural alterations that may be associated with the appearance of persistent symptoms and reduced lung function [8].

The pattern of features can vary between patients, as does their severity, ranging from mild asthma with occasional symptoms to severe forms where the symptoms are persistent and have an impact on daily life [18]. Over the long term, airway remodeling with thickening of the epithelium and underlying smooth muscle can also lead to a fixed, non-reversible airflow obstruction [18]. As has been explained before, various factors that

are responsible for the rise in asthma prevalence include aeroallergens, environmental factors and genetic factors [18].

Moreover, there is an infiltration of T cells that secrete a panoply of cytokines which contribute to the pathophysiology and, ultimately, the appearance of the symptoms [26]. These cytokines are believed to be predominantly Th2 cytokines such as interleukin IL-13, IL-4 and IL-5 [26]. Recent data suggests that other Th cells may contribute to the initiation and perpetuation of the disease. Th2 cytokines stimulate mast cells, cause eosinophilia and may participate in the development of airway remodeling [26]. This will be discussed in further detail.

1.5. Airway hyperresponsiveness

First described in 1946, airway hyperresponsiveness is the airway response to an inhaled bronchoconstrictor such as methacholine (MCh) or histamine [27]. It is used to diagnose and follow asthmatic patients [27]. MCh works as an acetylcholine analog that induces direct constriction on the airway smooth muscle cells [28]. Typically, patients are asked to inhale increasing doses of the bronchoconstrictor and the test is continued until there is a 20% fall in the forced expiratory volume in 1 second (FEV_1) or the highest concentration of methacholine or histamine (16mg/ml) has been aerosolized. The test is aimed at mirroring the airway responsiveness to non-specific bronchoconstrictive stimuli such as cold air. The MCh test is very sensitive and has a high negative predictive value [28]. AHR is present in almost all asthmatic patients and is more present during exacerbations, such as allergen exposure [28], [29]. Moreover, it correlates with the severity of the disease and non-asthmatic subjects do not exhibit any AHR [28], [29].

Many mediators have been suggested to play an essential role in the appearance of AHR in asthmatic patients. The underlying AHR may be due to airway wall thickening, which may be due to subepithelial or bronchial smooth muscle thickening and edema [30]. However, to date, it is unknown which of these mediators is directly involved in AHR. Another critical factor that is involved in AHR is epithelial cell damage, which is evidenced by an excess of bronchial epithelial cells found in bronchoalveolar lavage (BAL) and sputum of asthmatic patients [31]. This may be explained by loss of the epithelial cell layer, while bronchoconstrictors may reach the smooth muscle layer and amplify the response [31].

Changes in AHR in asthmatic patients over time have been observed. This may be due to chronic eosinophilic inflammation [32]. However, inhaled glucocorticoid administration does not eliminate AHR but significantly reduces it, suggesting that eosinophilic inflammation is not the main reason for changes in AHR [32].

1.6. Airway remodeling

The term “airway remodeling” in asthma can be defined as an alteration due to a response to chronic airway inflammation that induced structural changes in the airway respiratory tract [33]. This chronic airway inflammation may develop airway remodeling, and the reversible changes of airflow obstruction may develop the chronic obstruction and an irreversible deterioration of airway wall [33].

It was first described by Huber and Koessler in the early 1920s in studies of fatal asthma. They observed a thickening of the airway wall, subepithelial fibrosis, mucus metaplasia, epithelial hyperplasia and increased ASM in asthmatic subjects compared to control subjects. These structural changes lead to airway wall thickening in small and large airways [30], airway narrowing and airflow obstruction [33]. It has been reported that airway remodeling could improve a pathophysiological environment for AHR development, which start in an early phase of the disease whereas clinical symptoms not have been appeared [28]. In the following sections, features of airway remodeling will be discussed in further detail.

1.6.1. Epithelial damage

The respiratory epithelium is specially thickened in asthmatic subjects. Epithelium deterioration and desquamation has also been described in asthma [34], and the most important changes noted are epithelial shedding and loss of ciliated cells in asthmatic subjects [35]. A crucial role of the airway epithelium in the pathogenesis and immunological mechanisms of asthma has been reported by studies that have shown the presence of epithelial dysfunction and deterioration in their tight junction integrity [36]. The increase in epithelial injury is correlated to AHR and disease severity [37]. Moreover, the loss of epithelium may result in a loss of protection and an increase of allergen entry and damage [37].

Airway epithelium alterations in this disease may be developed by a dysregulation in the interaction between the epithelium and subjacent mesenchymal elements, which include fibroblasts. This effect modifies the airway's microenvironmet and alters lung development, repair, and regulation of the inflammatory process [38]. Further, fibroblasts have the ability to differentiate into myofibroblasts, which secrete proinflammatory factors and cellular matrix components [38]. Moreover, chronic inflammation induces an increase in epithelium damage and fragility, which in turn activates epithelial cells and the secretion of of proinflammatory factors, such as cytokines, growth factors and metalloproteases). These factors improve the chronic inflammation development and the airway remodeling progression that results in airway thickening [39]. Further, globet cell hypertrophy and mucus hypersecretion contribute to thickening of the respiratory epithelium in the airways [39].

1.6.2. Goblet cell hyperplasia and increased number of mucous glands

Another contributing to the narrowing of the airways of asthmatic subjects is the increase in the number of goblet cells and an increase in the size of submucosal glands [40]. Mucous glands appear in bronchioles of asthmatic subjects in comparison to healthy subjects in which these are absent [30]. Moreover, mucous glands have been observed in high proportion when fatal asthma patients have been evaluated [30]. Further, there is a reduction in mucociliary clearance induced by an increase in mucous viscosity [41], which promotes an incomplete response to inhaled bronchodilators [40]. As a result of these features reported that over 50% of the peripheral bronchioles can be obstructed by mucous accumulation during a fatal asthma exacerbation [42].

The increase in goblet cell number is associated with mucus overproduction. Among mediators that contribute to goblet cell hyperplasia and mucus hypersecretion are related are Th2 cytokines, such as IL-9 and IL-13, or other cytokines IL-1β or COX2 [43]–[45]. Further, mucus hypersecretion and the hyperplasia of mucus glands induce excess of mucus accumulation in the airways [40].

1.6.3. Subepithelial fibrosis

Subepithelial fibrosis is the consequence of induced by airway epithelium dysfunction and deterioration, which may promote an impaired response to repair injured tissues [36].

The basement membrane in the airway epithelium is composed by the basal lamina and the lamina reticularis, which are developed by conjunctive tissue cells [46]. The accumulated deposition of extracellular matrix in asthmatic patients causes thickening of the lamina reticularis and induces subepithelial fibrosis [46]. The fibrotic response, present in all stages of asthma and in allergic rhinitis, is due to an increased deposition of fibronectin, collagens I, III and V [46]. Physiologically, subepithelial fibrosis has been associated with disease severity, where there seems to be more airway wall thickening in asthmatic subjects [47].

Subepithelial fibrosis is also caused by an imbalance of matrix metalloproteinases (MMPs) and tissue inhibitors of metalloproteinases (TIMPs) that regulate the synthesis/degradation of the extracellular matrix [48], [49]. MMPs such as MMP-2,-3, -8 and -9 are responsible for the degradation of the ECM. For example, MMP-9 is implicated in the migration of airway smooth muscle cells and MMP-2 is also implicated in airway smooth muscle hyperplasia [48]. Elevated sputum levels of MMP-8 and -9 are associated with a decrease in FEV_1 following allergen challenge and disease severity [49].

1.6.4. Angiogenesis

Lamina propria is composed of a network of capillaries by the systemic circulation and promotes immunological and inflammatory responses [42]. Further, there is a neovascularization that promotes alterations in the membrane permeability and improves airway narrowing and AHR [42]. The increase in airway vasculature is associated with higher levels of vascular endothelial growth factor (VEGF), basic fibroblast growth factor (bFGF), platelet-derived endothelial cell growth factor (PDGF) and hepatocyte growth factor (HGF) [50]. This increase also leads to an increase in the delivery of mediators through higher permeability that may contribute to airway inflammation and remodeling [50].

1.6.5. Increased airway smooth muscle mass

The importance of airway smooth muscle in asthma was established over 150 years ago [51]. An increase in ASM mass has been reported in all stages of asthma and all age groups. In fact, ASM mass may triple in thickness compared to control subjects [51]. Airway smooth muscle mass is defined as the accumulation of airway smooth muscle cells in the peripheral bronchioles. Airway smooth muscle mass accumulation is an important feature in asthma, and is induced by hyperplasia and hypertrophy mechanisms [52]. This feature was observed in small and large airways and may thus be associated to the clinical severity and progression of asthma [53]. In fact, airway smooth muscle cells promote myofibroblast recruitment in the lamina propria [54]. Recently, it has recently been reported that fatal asthma patients show an increase in bronchial smooth muscle mass [55]. These observations demonstrate that increased smooth muscle mass is an important feature and is strongly associated with AHR and thus with asthma severity [55].

1.6.5.1. Hyperplasia

Hyperplasia is defined as the increase in the number of ASM cells within the airways [51]. The increase in the number of cells can be due to the increase in cell divisions or a decrease in rates of apoptotic cells [51]. Hyperplasia has been reported both *in vitro* and *in vivo* [51]. Further, previous studies have reported hyperplasia of smooth muscle cells in patients with mild-to-moderate asthma. However, this biopsy study demonstrated that this smooth muscle cells not increase in size [51]. Many mediators have been shown to have the potential to be implicated in ASM cell hyperplasia [51]. Moreover, other studies have shown that hyperplasia and hypertrophy appear in children with mild to severe asthma, although hyperplasia has been reported to better supply an increase in smooth muscle than does the hypertrophy mechanism [56]. BAL fluid from atopic subjects collected 48 hours following an allergen challenge induces cell proliferation of ASM cells from normal subjects compared to BAL from healthy subjects or from BAL pre-challenge [57]. This study suggests that BAL fluid contains specific mediators favoring ASM cell proliferation [57]. Some of these mediators include growth factors such as PDGF, tryptase, sphingosine-1-phosphate and leukotriene D4 [57]. Also, a co-culture model of damaged and healthy primary bronchial epithelial cellsand human ASM cells demonstrated an increase in ASM cell proliferation in conjunction with an increase in IL-6, IL-8, monocyte chemotactic protein-1 and MMP-9 concentrations [57]. These findings support the notion that ASM cell proliferation may be present in allergic asthma [58].

1.6.5.2 Hypertrophy

Hypertrophy is defined as an increase in cell size. To date, little is known about the hypertrophy of ASM cells [59]. It is still debatable if this phenomenon occurs *in vivo*. It has been argued that hypertrophy must be present in mild-to-moderate asthmatics while it must be strongly marked in severe subjects [60]. However, there is no evidence of ASM cell hyperplasia as shown by the lack of Ki67 expression, a marker of cell division [60]. Further, it has been shown that IL-1β and transforming growth factor beta (TGF-β) act as hypertrophic mediators in rabbit ASM cultures. In addition, it has been shown that ASM cell hypertrophy is associated with phosphorylation and inactivation of glycogen synthase kinase, which enhances translation of muscle-specific genes [61]. Moreover, other studies have demonstrated that mechanical stretch induces smooth muscle hypertrophy and it has been suggested that micro-RNA-126a is involved [62].

2. Immunology of allergic asthma

2.1. General aspects

Allergic asthma is characterized by an abnormal response to common aeroallergens such as HDM, pollens and animal dander [6]. However, most inhaled allergens induce tolerance and do not trigger an inflammatory response [6]. The epithelial cell layer has a crucial role due to its molecular network function, as it excludes inhaled molecules and pathogens according the molecular weight range [63], [64]. The epithelial barrier recognizes inhaled pathogens by pattern recognition receptors (PRRs) such as the toll-like receptor (TLR) and protease-activated receptors (PARs), which recognize microbial motifs and allergens, respectively [63]. Moreover, epithelial cells secrete stem-cell factor (SCF), which recruits eosinophils via CCR3 by the CCL11 secretion and contribute to mast cell recruitment in the airways [65]. However, it has been reported that allergens have the ability to stimulate mast cells that previously sensitized by surface-bound IgE to secrete to many mediators, such as bronchoconstrictor and prostaglandin D2 [65], [66].

Moreover, it has been reported that epithelial cells and lung conventional dendritic cells (cDCs) express pattern-recognition receptors that promote direct interaction with allergens. On the one hand, when such interaction occurs lung epithelial cells activate and

secrete many chemokines that promote immature pre-cDCs recruitment. On the other hand, these activated epithelial cells secrete other cytokines, such as GM-CSF, IL-25, IL-33 and TSLP, which induce cDCs maturation. This cascade attracts neutrophils, basophils, type 2 innate lymphoid cells (ILC2), mast cells, eosinophils and induces an antigen-specific response [63], [64]. IL-33 activates ILC2, which mainly produces IL-5 and IL-13 and may thus contribute to eosinophil recruitment and mucus overproduction [6], [64]. Basophils and ILC2 may secrete IL-4 and IL-13 to favor the Th2 response and avoid a tolerance response to allergens [6], [67]–[69]. Further, TGF-β increases the production of collagen and extracellular matrix components [64]. Moreover, activated lung cDCs are recruited and promote Th2 and Th17 responses in mediastinal lymph nodes [6].

2.2. T lymphocyte development

Initial studies have shown that T lymphocytes are of great importance in the development and progression of the disease [70]. These cells originate in the thymus, where Pro-T cells and early T cell populations, express the specific T-cell receptor (TCR) but not specific correceptors (CD4 or CD8) [71]. These double negative (DN) thymocytes have the ability to proliferate and develop in the T cell lineage due to their interaction with thymic stromal cells [71]. An important immunological checkpoint in this process is the pre-TCR formation, which keeps the rearrangements on the β-chain locus and permits the maturation process [71]. Besides, there is a pre-TCR:CD3 complex formation that induces both CD4 and CD8 expressions in the cell surface, defined as double-positive (DP) thymocytes [72]. When these cells stop their proliferation phase, the α-light chain rearranges and promotes the TCR formation [72].

This process allows DP thymocytes to survive due to the recognition and engagement with self-peptide when interacting with the self-major histocompatibility complex (MHC) expressed by thymus stromal cells. This interaction is defined as “positive selection”. Afterwards, thymocytes increase their viability and exude the IL-7 receptor (IL7R), a characteristic biomarker in this process [73]. The next step is the CD4/CD8 lineage selection, which is explained by the kinetic signaling model [74]. When thymocytes differentiate into $CD4^+$ T cells, TCR regulated positive selection signaling is maintained with the progressive loss of surface CD8. Conversely, when thymocytes differentiate into $CD8^+$T cells, TCR regulated positive selection signal is blocked when the CD8 transcription is absent, which promotes the loss of CD4 expression and the re-

expression of CD8 [75]. In summary, $CD4^+$T cell formation is a TCR signal-dependent mechanism, while $CD8^+$T cell differentiation is promoted if TCR signaling is blocked and CD8 transcription is upregulated by IL7R signals [74]

While positive selection is occurrs in the thymus, there is a lymphocyte maturation process. This step promotes the apoptosis of thymocytes that strongly recognize self-peptide:self-MHC, while a weak interaction induces survival and maturation of lymphocytes [76]. The next important process is negative selection. When this mechanism occurs in the thymus or BM it is defined as central self-tolerance, whereas if it takes place in secondary lymphoid organs it is defined as secondary self-tolerance [77].

Therefore, the T lymphocyte bears a single TCR with unique antigen specificity [70]. The adaptive response is initiated by T lymphocytes bearing α/β TCRs. Among this family, we count the $CD4^+$ and $CD8^+$ T lymphocytes which differ in their cell surface co-receptors, their interactions with different MHC molecules and their responses to different antigens [70].

2.1.1. $CD4^+$ T lymphocytes

When T cell maturation develops in the thymus, naïve T cells are transferred to the blood [78], [79]. These cells are qualified “naïve” because their specific antigen has never been encountered [80]. These cells enter the peripheral lymphoid tissues, which include mucosal-associated lymphoid tissue, spleen and lymph nodes. This process is induced by specific adhesion receptors, such as selectins and integrins [78], [79]. Afterwards, the antigen:MHC complex expressed by antigen-presenting cells may interact with specific TCR of T cells in the secondary lymphoid organs. When the specific TCR does not interact with the antigen:MHC complex, T cells enter to the blood and go to the next organ. When a recognition between naïve T cell and antigen-presenting cell (DCs, macrophages or B cells) occurs, the T cell activation mechanism initiates [81].

2.2. Antigen presentation

Allergic asthma is characterized by an abnormal response to common aeroallergens such as house dust mite, pollens and animal dander as described above [6]. Most inhaled allergens induce tolerance and do not trigger inflammatory responses [6]. However, DCs

may recognize an array of antigens via the TLRs, cytokine receptors, protease-activated receptors and NOD-like receptors allowing a cascade of signaling [82], [83].

The ovalbumin (OVA) model of allergic asthma shows that administration of OVA by the nose or the lung in the presence of an adjuvant such as aluminum hydroxide induces an immune response with significant tissue eosinophilia and accumulation of inflammatory cells around the bronchi [84]. In the absence of the adjuvant, OVA alone fails to induce this response, thus inducing immunological tolerance [84]. Some allergens exert this adjuvant signal through the expression of proteolytic enzymes that can activate the DCs and induce a Th2 response [85].

Following the capture of the antigen, DCs migrate to the draining lymph nodes in the T cell area [86]. On their way, DCs process these antigens through proteolytic degradation and present them on the cell surface in association with the MHC-II complex [86]. This allows the DCs to acquire a mature phenotype and upregulate the co-stimulatory molecules [86].

When recognition between T cell and antigen-presenting cell takes place thought a specific antigen, T cells are activated and induce proliferation in a clone effector cells with an identical specificity to the antigen [87]. This process is defined as “clonal expansion”, and specific TCR:peptide:MHC formations with co-stimulatory signals are needed to get through this process [87].

One of these co-stimulatory proteins includes B7 molecule, a dimeric and trans-membrane protein that pertains to the immunoglobulin superfamily [87]. This molecule is expressed when antigen-presenting cells are activated in the lymph nodes, and interact with CD28 (B7 target receptor) expressed by naïve T cells [87]. When a CD28:B7 complex is formed, T cell activate survival signaling pathways, which are a crucial point in the clonal expansion development [87]. Moreover, this complex formation induces IL-2 secretion and IL2R expression, which in combination with other cytokines promote the differentiation of T cells into different types of effector T cells [88].

The lymph node is composed by B cells, which are localized into follicles, and T lymphocytes, which are included in pericortical areas [83]. When B cells interact with their specific antigen and T cells there is a proliferation of B cells which promotes formation of germinal centers in the follicles [83]. When effector T cells activate, they enter the efferent lymph circulation system as well as the blood and arrive at sites of inflammation [83].

2.3. T helper 1 cells (Th1)

The Th1 subset of $CD4^+$ T lymphocytes is involved in the response to chronic infections and has an important role in elimination of pathogens which survive inside the phagocytic cells [89]. The Th1 cells secrete interferon-y (IFN-y) and IL-12 and promote macrophage and cytotoxic T cell activation and stimulate B cells to secrete IgG, which opsonizes pathogens [90]. This process has a crucial role in the response to viruses and other intracellular pathogens [89]. Their differentiation is induced by the same cytokines they secrete, IL-12, directly, and IFN-y indirectly [90]. As they develop, they acquire the expression of IL-12 beta-2-chain receptor. Thus they become more responsive to IL-12 produced by antigen-presenting cells [90]. IFN-y inhibits the differentiation of Th2 cells and is decreases in mild allergic asthmatic patients [91].

2.4. T helper 2 cells (Th2 cells)

The Th2 immune response has the ability to eliminate extracellular pathogens and parasitic worms, which are implicated in allergic diseases [92]. This second subtype secretes IL-4, IL-5 and IL-13 cytokines and is involved in humoral response, which promotes the production of B cell antibodies by IL-4 and IL-13 [90]. Moreover, IL-5 is an important cytokine and has a crucial role in the maturation and recruitment of eosinophils [93]. It has been reported that Notch signaling is involved in the induction of the Th2 response, but the mechanism responsible for this process remains unclear [94].

Moreover, a higher affinity of the antigenic peptide-MHC-II complex for TCR, as well as a high dose of antigen favors the Th1 response. Instead, with lower antigen doses the Th2 response is favored. Concerning asthma, it is believed that, although an individual is exposed to many allergens, their dose is minimal, thus inducing a strong Th2 response [95].

It has long been believed that Th2 lymphocytes are the predominant subset in asthmatic airways [90]. Although they represent a small percentage of leukocytes in the airways, Th2 lymphocytes play a significant role in the inflammatory response through the secretion of their cytokines. Asthma has been described as an imbalance between Th1 and Th2 cells with an overproduction of Th2 cells [96].

2.5. T helper 17 cells (Th17 cells)

The Th1/Th2 paradigm has been strongly challenged in the last 10 years with the introduction of a new subset of T lymphocytes, Th17 cells [97]. When dendritic cells interact with a pathogen, they induce the secretion of IL-6 and TGF-β, which in turn induce Th17 differentiation of naïve $CD4^+$ T cells and inhibit Th1 and Th2 deviation [97], [98]. These cells were described and characterized in the 1990s, demonstrating that IL-17 cytokine produced by T cells is secreted when in interaction with specific pathogens [99]. Moreover, these cells have the ability to produce IL-17 in the airways, which promotes the secretion of the granulocyte colony-stimulating factor (G-CSF) and induce granulocyte infiltration in the airways [100]. Further, IL-17 secretion stimulates the production of IL-6 and IL-8 by stromal cells *in vitro*, demonstrating a crucial role in the monocyte differentiation and neutrophil recruitment in the airways [101]. It is now believed that the immune mechanisms involved in allergy are more complex and cannot be explained by the imbalance between Th1 and Th2 cells [102] *In vivo* models of asthma have shown that Th17 lymphocytes recruit neutrophils into the lungs [102]. In addition to Th2 lymphocytes, these cells are involved in the increase of AHR [102].

2.6. Regulatory T cells (Treg)

In addition to the aforementioned Th cells mentioned, a further subset of T cells with immunosuppressive functions is termed regulatory T (Treg) cells [103]. Moreover, Treg cells can be further divided into two subsets: naturally occurring $CD4^+CD25^+FoxP3^+$ Treg cells (nTreg) and inducible type 1 Treg cells (Tr1) [103]. Healthy individuals exhibit all T cells subsets in different proportions where Tr1 cells are the dominant subset against environmental allergens. The immunosuppressive function of Tr1 cells is achieved through the release of IL-10 and TGF-β [104].

2.7. Eosinophilic asthma as a Th2 disorder

In the last decades, asthma has been described as a Th2 immune response disorder of the airways due to eosinophilia infiltration observed in induced sputum and lung biopsies, regardless of allergic or non-allergic features [6]. However, increased levels of IL-4 and IL-5-producing $CD4^+$ T cells have been observed in mild to moderate asthma biopsies and have been associated with eosinophil infiltration in the lungs [6].

It has been reported that an important role of IL-5 in this process, which include the maturation and differentiation of eosinophils in BM and their recruitment in the airways through the secretion of different chemokines, such as CCL24, CCL11 and CCL26 [6]. These cells produce different granules, such as eosinophil peroxidase that promote AHR and stimulate DCs to promopt an adaptive Th2 immune response [6]. However, these granules induce the formation of DNA traps that concentrate eosinophilic granules, which inlcude cationic proteins (eosinophil peroxidase) and the major basic protein (MBP), thus deteriorating airway structural cells [6]. Curiously, recent studies have suggested a possible role in antigen presentiaton on effector T cells by eosinophils [6].

Moreover, in germinal centers of the lymph nodes, helper T cells differentiate towards follicular helper T cells (TFH), which are mediated by IL-21 production [6]. These cells have an important role in the IgE class switching by B cells, which is mediated by IL-4 production of the Th2 cells [6]. As described before, Th2 cells have a crucial role in the development of allergic diseases. Moreover, during allergen challenges, antigen-presenting cells are responsible for recruiting Th2 cells and stimulating lung-resident cells through the secretion of different cytokines, such as CCL17 or CCL22 [6]. These cells secrete IL-4 and IL-13 to activate the production of IgE by B lymphocytes, and synthesize IL-5 and IL-9 to recruit and stimulate eosinophils and mast cells, respectively [6]. Moreover, it has been reported that asthmatic patients present an alteration of the Treg cell levels that favors the Th2 immune response [6].

2.8. Neutrophilic asthma as a Th17 disorder

During the last years, there have been described cases of asthmatic patients that show strong neutrophil infiltration without a Th2 immune response [6]. This is in contrast with the classically defined phenotype of asthma, which is characterized by eosinophil recruitment and the Th2 hallmark pattern [6]. These neutrophilic patients have severe forms (of asthma) and a late-onset profile, for which a combined Th1 and Th17 immune response deviation has been observed [6]. Moreover, these subjects have a less reversible airflow obstruction and are associated with exposure to diesel exhaust particles, which increase the levels of IL-17A in serum [6]. All of this exacerbates asthma symptoms and airway remodeling has been observed in these more severe forms [6]. In rodents and humans, HDM exposure increases IL-17A levels, which induces fibroblast hyperplasia and contributes to airway remodeling development [6]. Curiously, it has been reported that IL-17 promotes AHR and smooth muscle cell hyperplasia without neutrophil recruitment [6].

Other sources of IL-17 production have been described, which include TCRγδ^{+} T cells, invariant natural killer T (NKT) cells and innate lymphoid type 3 (ILC3) cells [6].

Classical observations that define eosinophilic asthma as a Th2 immune response and neutrophilic asthma as a Th17 disorder are general views that describe the extremes of a continuous spectrum [6]. Some cases have shown an overlay of Th1 and Th17 cytokines in different asthma phenotypes [6]. However, Th1 produces cytokines such as IFN-y, observed in eosinophilic and neutrophilic asthma phenotypes [6]. In mice, it has been reported that OVA-specific Th2 and Th1 cells are associated with AHR and the levels of IFN-y and IL-13, which are involved in smooth muscle thickening and Th2 recruitment and homing in the airways [6]. This corresponds to other studies in humans that have observed increased levels of IFN-y in patients with severe asthma forms [105]. In contrast, other reports have suggested that antigen-specific Th1 cells fail to compensate the AHR induced by Th2 cells and may promote the disease [91].

2.9. T lymphocytes and airway remodeling

Although much is known about the role of epithelial cell-derived mediators in the increase in ASM cell proliferation, little is known about the role of T lymphocytes in this process. Lazaar *et al.* were the first to introduce the notion that T lymphocytes adhere through CD44 and intercellular adhesion molecule-1 (ICAM-1) to ASM cells and induce ASM cell proliferation and DNA synthesis [106]. Subsequently, Ramos-Barbon *et al.* have shown that the CD4^{+} T cell subset is responsible for this process [107]. In their study, specific-CD4^{+} T cells were administered *i.p.* in a rat asthma model and a direct interaction between these cells and ASM cells was shown. Further *in vitro* studies have demonstrated direct cell to cell contact [107]. Moreover, there is a strong association between T cell infiltration and smooth muscle hyperplasia, which are correlated with asthma severity [108]. However, cytokines produced by Th1 and Th2 cells do not have the ability to induce ASM proliferation. In fact, it has been shown that IL-4 and IL-13 have anti-proliferative effects and it has been demonstrated that Th2 cytokines are not implicated in ASM hyperplasia [109], [110].

2.9.1 CD4$^+$ T lymphocytes and airway remodeling

Recent studies have reported a crucial role of CD4$^+$ T cells in the development of airway remodeling. Previous studies have shown via mouse asthma models that monoclonal antibody depletion of CD4+ T cells inhibits AHR and avoids eosinophilic infiltration in the lungs [111]. Further, other reports have suggested a notable decrease of AHR and specific features of airway remodeling epithelial thickening, mucus cell hyperplasia and subepithelial fibrosis, when induced asthma in mice resulted in a depletion of CD4+ T cells [112]. Moreover, human *in vitro* studies have indicated that activated T cells may adhere to human ASM cells via integrins such as VCAM-1, ICAM-1 or CD44 and induce ASM cell proliferation [106]. Observations consistent with this mechanism of ASM growth have been reported in Brown Norway (BN) rats, where activated CD4$^+$ T cells interact directly with ASM cells *in vivo* and induce ASM cell proliferation *in vitro* [107]. To date, the nature of the T cells responsible for proliferation has not been determined. However, recent findings have shown that the novel Th17 cell subset may be involved in airway remodeling [113]. Wang *et al.* have shown an increase of Th17 cells in the lung and their presence has been associated with the degree of airway remodeling using a C57BL/6 mouse asthma model [113]. In fact, a decrease in ASM mass, mucus production, peribronchial collagen deposition and expression of heparin-binding epidermal growth factor (HB-EGF) has been observed in mice when treated with an anti-IL-17 monoclonal antibody [113].

Curiously, these features, except for peribronchial collagen deposition, also decreased when mice had a specific inhibitor of the epidermal growth factor receptor (EGFR) and a HB-EGF monoclonal antibody, which suggests a relationship between the Th17 response and these proliferative pathways [113]. On the contrary, Doherty *et al.* have shown in a murine model that CD4$^+$ T cells are not necessary for the development of airway remodeling during allergen challenges after the development of acute eosinophilic lung infiltration [114]. This study suggests that once the sensitization process is fully developed the CD4$^+$ T cell may not be essential for remodeling [114]. These conflicting data may highlight the importance of timing in the context of interventions [115]. However, although CD4$^+$ T cells may be implicated in airway remodeling, the role of CD8$^+$ T cells remains understood [114]. It has been described that depletion of CD8$^+$ T cells during repeated antigen challenges in Brown Norway rats enhances ASM mass and number of epithelial cells suggesting a protective role for these cells in the development of airway remodeling [115].

2.10. Therapeutic targets for airway remodeling

There are two main therapies for the treatment of asthma. Firstly, there are anti-inflammatory treatments used regularly to prevent asthma attacks, which include inhaled corticosteroids, leukotriene inhibitors and therapies based on anti-IgE administration. Secondly, there are therapies based on long-acting bronchodilators to help open airways and bronchodilators with short action, which are defined as rescue treatments [116]. Aerosolized corticosteroids are the main anti-inflammatory treatment for asthmatic patients and are generally effective. However, there is a substantial number of asthmatics who remain symptomatic after these therapies [116]. In addition, variability in immune challenge and response to therapy makes asthma a disease difficult to monitor and manage [116]. These treatments focus on minimizing asthmatic exacerbations and concurrent inflammation [116]. Current therapies can reduce the inflammation process in responsive asthmatic subjects, but in contrast, cannot minimize or reverse the airway remodeling process [116].

Asthma treatments targeted towards airway remodeling reduction have not been widely developed due to the difficulty in obtaining sample collections in clinical studies. To date, no asthma drug treatment has been developed to act directly on airway remodeling [117], [118]. Traditionally, corticosteroids have been the primary treatment for asthma, which has prompted investigators to determine their effect on airway remodeling [118]. Currently, bronchial thermoplasty is the only treatment for reducing airway remodeling features, but the results and effects obtained are unclear [118], [119]. It has been reported that clinical trials have focused on personalized medicine based on specific antibodies that target a characterized cytokine associated with a Th profile (i.e. anti-IL-13 in patients with Th2 eosinophilic disorder) [118], [119]. Moreover, there is a need to understand implicated airway remodeling mechanisms and the prevention of this feature during childhood [118]. Therefore, airway remodeling is an essential target because it may often be present even at the time of the asthma diagnosis [120].

3. Animal models

It is now widely accepted that asthma is a complex multifactorial disorder with different phenotypes underlined by different pathological mechanisms [18]. In order to fully understand the pathophysiology and immunologic mechanisms of asthma, there is a need for a detailed characterization of the different subtypes of asthma in addition to making good experimental models that reflect such different phenotypes [18]. As a result, animal

models have been extensively developed to study the pathophysiology of a variety of diseases [121]. However, there are concrete explanations as to why researchers have used a specific animal model [121]. The first reason is that studies cannot be developed in human clinical trials due to ethical considerations [121]. Secondly, results obtained for *in vitro* models are reductionistic considerations when compared to *in vivo* models [121]. Finally, *in vivo* studies in certain animal species do not reflect and mimic the conditions seen in humans, and the results must be considered with caution [121].

Animal models have an important role in understanding the pathogenic and immunological mechanisms of asthma and continue to evolve to improve knowledge of airway remodeling [122].

3.1. Animal models of experimental asthma

Asthma models have been used for more than 100 years [121]. A great variety of species have been used to study airway allergic diseases [121]. These include guinea pigs, cats, mice, horses, sheep, dogs and rats [121]. The guinea pig model was the first model of asthma described and has had an important role in the development of corticosteroid and β2-adrenergic agonist therapies [121]. Moreover, murine models of experimental asthma have been the most used model to understand this disease [123]. Further, many outbred animal strains naturally develop allergic airway diseases with similar human features, but no laboratory animal is known to generate asthma spontaneously [121]. Dogs and sheep are used to study allergic diseases due to their ability to develop natural sensitization similar to humans', which is accompanied by elevated IgE levels and AHR [124]–[126]. Further, cats can develop airway inflammation and AHR similar to human asthma [127], [128]. Moreover, it has been reported that horses can naturally develop sensitization and "heaves" disease, which generates airflow obstruction, airway remodeling and neutrophilic infiltration [129].

Extrapolation of results from animal models to human asthmatics is critically dependent on the animal species selected [121]. Species and strain differences are restricted by the lack of genetic modifications, specific reagents, costs and biological differences from humans [121]. Moreover, variations in sensitization and airway challenge protocols, and the method by which drugs are delivered to the lungs (*i.e.*, intranasal [*i.n.*] or intratracheal instillation of solutions) are parameters that can influence the outcome of a study [121].

3.2. Murine models of experimental asthma

Rodents have been the most used animals to develop experimental asthma models and study pathobiological and immunological mechanisms that are implicated in this disease [130].

Mouse models of allergic asthma offer numerous advantages [130]. Mice are the most used specie to develop models for a wide variety of diseases due to their genetic knowledge, which improves transgenic manipulation, and the extensively commercially available products to develop the experiments [131]. Further, this specie has a humoral response characterized by the presence of IgE, similar to humans [130]. Therefore, murine models have an important role in the study of the molecular and immunological mechanisms that are implicated in asthma, and thus, currently developing treatments are studied in mice [130].

However, there are important physiological differences between human and mice, which show that extrapolation of results to human therapy must be evaluated with care [130]. Therefore, the problems with translating results found in mice into human clinical practice could be explained by these physiological differences, which include tracheobronchial tree changes [130]. In mice, the primary distal airway is the non-alveolarized bronchiole, whereas in humans and primates it is the respiratory bronchiole [18]. Moreover, the type and location of cells can vary. Basal cells are found throughout the tracheobronchial airways of humans, but only in the trachea of mice, which have a larger Clara cell population in the small airways [18].

Moreover, mouse airways have fewer tree formations than does the human respiratory tract, and do not show lung bronchioles [132]. Among such differences, remarkable ones affect the anatomy and differentiation of the airway and the bronchial circulatory system [132]. Mice only have pulmonary circulation in the respiratory system, lacking bronchial circulation, which could affect mechanisms of leukocyte recruitment, while mouse airways have substantially less smooth muscle, and do not respond readily to pharmacologic agents affecting bronchial tone [18]. Mouse models of experimental asthma have an immunological profile similar to human asthmatic subjects, which include eosinophil infiltration and a Th2 immune response profile [133]. However, an important limiting factor in all asthma animal models is the difficulty in developing a chronic model similar to human asthma [130].

Recently, rats have been used by numerous investigators over other animals to demonstrate many features of airway allergic responses that are similar to human asthma [134]. The rat, compared to other laboratory animal species, shows a respiratory system anatomy and a bronchial circulation closer to those exhibited in humans [121]. Moreover, the rat exhibits immediate and late airway asthmatic responses, airway hyperresponsiveness, airway inflammation, and obstruction after an allergen challenge [121]. These features provide rat models with significant advantages over mouse models [121]. Furthermore, there has recently been an increase in the variety of reagents available and transgenic technology applications for rat studies [121]. Also, rats can easily develop allergic diseases using OVA, house dust mite extracts or *Ascaris* antigens [121]. Conversely, a disadvantage of the rat models of asthma is the difficulty in performing protocols, which result in the chronic changes in the airways associated with asthma. However, they have been useful in understanding the mechanisms of asthma and modulation of tolerance in allergy [135].

Therefore, it is possible to reproduce human allergic asthma features in the rat, which include their ability to develop a Th2 immune response against allergens with an eosinophil infiltration, airway remodeling and AHR [130]. There are, however, relevant differences among different rat strains [121]. The first studies of airway remodeling in an animal were performed on the sensitized and repeatedly challenged Brown Norway rat, a strain with an allergic disposition that has many features in common with human allergic asthma. These studies were focused on the induced increase in airway smooth muscle [136]. The Brown Norway strain is naturally atopic and presents features similar to human asthma which include high IgE levels, early and late airway allergic responses, eosinophilia and Th2 cytokine production [121]. This strain is genetically Th2-predisposed and has been the most widely used strain for studying allergic inflammation [137]. However, Wistar rats can also be asthmatic with OVA sensitization, but less asthmatic features were observed when compared with BN rats [121] In Fisher and Lewis rats, there is an absence in IgE levels and airway inflammation after allergen sensitization [121]. In contrast with the Brown Norway rat, Sprague Dawley rats are not so genetically Th2-predisposed and do not develop allergic reactions or increased IgE production under the same conditions and have been used as a control group for Brown Norway rats [121], [137].

Recently, some new strategies for asthma therapies tested in mouse models have not been effective in human clinical trials [18]. As a result, numerous investigators in asthma

are currently using rats [138]. The improved ability to extrapolate data from rat studies to humans is one of the paramount advantages of rat models [18].

3.3. Sensitization and allergen nature

Given the complexities of the asthmatic condition, it is challenging to create animal models that can capture the full range of components and mimic the human disease [18].

There are many different sensitization and challenge protocols to develop asthma animal models and the species or strain differences are essential parameters that can influence the outcome of the study [138]. Acute sensitization protocols usually require multiple systemic administrations of the allergen (such as intranasal, intratracheal or intraperitoneal) in the presence of an adjuvant [138]. The route for allergen administration is important for developing asthma models without inducing tolerance [138].

Classically, the innocuous antigen OVA has been used to induce an allergic reaction in animals as it allows to reproduce many of the features of the asthmatic lung [139]. This model generates specific IgE levels, Th2-associated eosinophilic inflammation, early and late asthmatic responses (EAR and LAR), airway hyperresponsiveness and associated tissue remodeling [139]. However, it has been noted that the use of OVA with an artificial adjuvant such as aluminum hydroxide does not correctly mimic how asthmatic patients become sensitized to aeroallergens [139]. While the ovalbumin model has primarily provided an extensive understanding of asthma pathophysiology, criticism has been raised that questions its physiological relevance to human asthma [20]. Firstly, extended provocation with OVA leads to tolerance in at least some mouse strains, thus reducing its applicability to modeling chronic asthma [20]. Secondly, the route for OVA sensitization is usually via intraperitoneal injection, whereas asthmatic subjects are sensitized through primary exposure in the airways [20]. Last, ovalbumin is not an actual aeroallergen triggering asthma in humans. All such limitations have motivated researchers to develop more appropriate methods to induce allergic airway disease [20].

For this reason, alternative allergens with more significant clinical relevance for human asthma have been introduced into the models, such as HDM, cockroach, ragweed and *Aspergillus* [138]. The most commonly employed allergen is HDM, a multifaceted allergen to which 50-85% of asthmatics are allergic [20]. HDM extract contains a complex array of allergens, including chitin, fungal spores, fecal spores and immunogenic epitopes [140]. Their major mite component is *Dermatophagoides pteronyssinus 1* (*Der p* 1), which

exhibits serine and cysteine protease activities that produce paracellular access to intraepithelial DCs, and increase the permeability of epithelial cells allowing the passage of immune cells and other allergens across the epithelium [20]. Therefore, HDM seems to be more successful in developing allergy models because of the intrinsic enzymatic activity of this allergen [138]. Moreover, antigenic sensitization occurs depending on immunological factors that affect innate and adaptive immune responses [20].

During the last years, HDM extracts have been studied due to their role in the development of allergic diseases, and a broad range of allergens with similar characteristics have been reported [141]. This detailed knowledge of HDM promotes an interest in inducing allergic asthma in animal models and mimicking human asthma features [142]. However, the complex range of antigens and enterotoxins composed by HDM hinder experimental standardization [142]. In fact, the allergens used will have advantages and limitations and their selection will depend on the aims of each study [142].

Moreover, adjuvants are used to improve the immune response to antigen in asthma models, which include aluminum hydroxide or heat-killed *Bordetella pertussis* [121]. Aluminum hydroxide, administered in combination with antigen, induces a Th2 response [121]. In addition, lipooligosaccharide from *Bordetella pertussis*, often used as well as an adjuvant as well, contributes to driving a Th2 response [121]. The disadvantage of the use of adjuvants is their effects on the immune system, limiting a parallel comparison between humans and animals after the interaction with a specific allergen [121]. However, a strain specific effect has been reported when mice were *i.n.* sensitized in the absence of adjuvants, through which method a closer asthmatic immune response is obtained [121]. Therefore, these limitations on simulating an available comparison with humans have promoted the investigation and enhancement of more appropriate methods [121].

Staphylococcus aureus (SA) is one of the most common bacteria to appear in the human airways and it has the ability to produce toxins and superantigens, which include Staphylococcus enterotoxin A (SEA), B (SEB), C, D, E (up to U), and toxic shock syndrome toxin-1 (TSST-1) [143].

It has been reported that SA and their secreted factors are associated with the development of allergic diseases, including asthma, since it is found in about 67% of patients [144]. Atopic individuals are susceptible to allergic sensitization as well as microbial colonization [18]. Recent microbiome analyses support the notion that microbes,

in particular *Staphylococcus aureus*, play a role in the initiation and chronification of allergic rhinitis and allergic asthma [145]. However, no direct studies in asthma models have been developed. The SAE acts as superantigens and they potentially activate T cells via the linkage of the β chain of the TCR to MHC-II expressed by antigen-presenting cells outside the peptide-binding complex [145].

Staphylococcal enterotoxin B is a superantigen which has been attributed a fundamental role in the induction of human sensitization to aeroallergens. Patients with asthma generate a specific IgE response to staphylococcal superantigens and, in mice, SEB breaks tolerance to both inhaled and contact allergens and aggravates local inflammatory responses in the airways [144].

In addition, it has been demonstrated that SEB, but not other superantigens such as SEA and TSST-1, aggravates allergic airway inflammation, bronchial hyperresponsiveness and increased IgE levels in mouse serum [144]. All these data strongly suggest that SEB plays a role in the modulation of severe airway inflammation [144]. So far, it remains unknown how airway exposure to bacterial enterotoxins may condition the development of asthma [144]. Concerns for the use of artificial adjuvants, which influence the development of Th2 responses in a complex understood mechanism, as well as questions on the representativeness of OVA as an allergen, have promoted the use of alternative allergens and sensitization methods considered more appropriate to represent the pathophysiology of human asthma [18].

4. Mesenchymal stem cells

4.1. General aspects

Currently, mesenchymal stem cells (MSC) are a good possible candidate for cell-based therapies for a wide range of diseases due to their regenerative and differentiation capacity [146]. During the last years, two main groups have been used to classify stem cells, which are those composed by embryonic and non-embryonic stem cells [146]. On the one hand, embryonic stem cells (ESC) have the ability to differentiate into cells coming from all germ layers and developed from blastocysts in the inner cell layer [146]. However, these cells will promote development of teratoma and there are controversies

over the ethical use of these cells, which prompt investigators to use of non-ESC [146]. These cells, mainly adult stem cells, have a restricted differentiation capacity and can be obtained from many tissues [146]. In fact, MSC are adult stem cells with specific biological features that are of high interest for investigators [147]. MSC are a heterogeneous cell population and may differentiate into a variety of specific cell phenotypes, having great potential for regenerative medicine applications [148]–[150].

It has been reported that these cells can be identified by surface molecular markers in combination with their ability to differentiate into other cells [151]. Moreover, the Mesenchymal and Tissue Stem Cell Committee of the International Society for Cellular Therapy has proposed minimal criteria by which we can define human multipotent mesenchymal stem cells. These cells should be multipotent and form colony forming units (CFU) when cultured in plastic-adherent culture conditions. Further, these cells can express antigen surface molecules, such as CD73, CD90 and CD105 and lack expression of CD14, CD11b, CD19, CD34, CD45 or CD79a. In addition, lack of expression of CD34 remains unclear [152]. Further, these cells have the ability to differentiate into chondroblasts, osteoblasts and adipocytes when cultured *in vitro* under specific conditions [151]. These cells are obtained from different tissues and have biomarkers specific to tissue origin, which include CD29, CD44, CD140b, and CD146 [152]. Moreover, it has been reported that stem cell marker Stro-1 is expressed in dental and BM MSC, whereas it is absent in human adipose-derived (AD)-MSC [152]. These cells can be isolated from a wide variety of tissues, which include BM, adipose tissue, skeletal muscle, dental pulp, umbilical cord, synovial membranes, periodontal ligaments, saphenous veins, amniotic fluid, placentae, Wharton's jelly, dermal, lung, cervical and liver tissues [147]. Therefore, these cells are good candidates for treating a wide variety of diseases due to their capacity to proliferate *in vitro* under specific conditions and their ability to differentiate in multiple cell lineages, which allow the secretion of trophic soluble factors that are implicated in immunomodulation and tissue remodeling [147].

4.2. Immunomodulatory features

Several studies have shown that MSC escape recognition by the immune system and inhibit immune responses. Modulation of the immune system has been observed in both BM-MSC and AD-MSC. This property of MSC facilitates the clinical use of MSC in an allogeneic manner in both immune diseases and regenerative medicine approaches [151].

There are wide reports in humans and animal models that demonstrate the immunomodulation function of MSC in various immune disorders [146]. However, the mechanisms that promote this immunomodulatory effects remain unclear [146]. Further, it has been demonstrated that MSC regulate immune response due to their ability to interact with other cells by cell-to-cell contact or the secretion of soluble factors [146]. This regulation of adaptive and innate immune responses through these mechanisms includes the suppressive effects on T and B cells, inhibits the maturation of DCs, modulates the cytotoxicity capacity on NK cells and induces the proliferation of regulatory T cells, which are reported *in vitro* and *in vivo* [153].

4.2.1. Immunomodulation by soluble factors

During the last years, some studies have reported soluble factors secreted by MSC that have a suppressive effect on the immune response, such as indoleamine-pyrrole 2,3-dioxygenase (IDO), HGF, prostaglandin E2 (PGE2), TGF-β, IL-10 and nitric oxide (NO) [153]. Further, some factors secreted by MSC do not release spontaneously and require previous stimulation with proinflammatory cytokine. Moreover, it has been reported that IFN-y, alone or in combination with other cytokines, such as TNF-α or IL-1β, stimulates MSC to release immunosuppressive soluble factors, which include PGE2 and IDO [154]–[156]. Further, co-culture studies have shown that PGE2 is secreted by MSC and has anti-proliferative effects on T-cells from peripheral blood [157]. On the other hand, IDO-expressing DCs, which catalyze the transformation of tryptophan to kynurenine, have the ability to regulate the immune system and induce kidney allograft tolerance by inhibition of allogeneic-T cell proliferation [157], [158]. In addition, NO molecules can also suppress T-cell proliferation [159]. Further, there are other soluble factors, which include galectins and IL-6 that have regulatory effects on the immune system [160]–[162]. Therefore, there are soluble factors that have the ability to modulate the immune response, but the implicated mechanisms implicated remain unclear [153].

It has been shown that microenvironment is implicated in the function of MSC by soluble factors [153]. Therefore, released soluble factors and detailed biological mechanisms that regulate the immune response are important points for understanding the strongly suppressive effects of MSC [153].

4.2.2. Immunomodulation by cell-to-cell contact

There are crucial factors implicated in the suppressive effect of MSC through a direct cell-to-cell contact mechanism. Several reports have shown a reduction in the proliferation of T cells when BM-MSC directly interact with these cells in a co-culture model, which increases the induction of Tregs [163]. These data are consistent with other studies that have shown a dependent cell-to-cell contact mechanism by MSC to promote their suppressive effect on T-cell [164].

The ligands implicated in the direct contact mechanism include ICAM-1/LFA-1, VCAM-1/VLA-4, and programmed cell death complex (PDL-1/PD-1), which are induced when MSC interact with T cells [165], [166]. Moreover, it has been reported in mice that ICAM-1 is an important surface molecule for MSC:lymphocyte interaction, whereas ICAM-1 blockade increases T-cell proliferation and accumulation around the MSC [166]. These molecules are also implicated in the suppressive effect of BM-MSC and the interaction between T cells and antigen-presenting cells in mice [166]. Further, other important molecules are PD-1 and PDL-1, negative costimulatory molecules that have the ability to suppress a wide variety of cells through direct interaction with human MSC [165].

It has been reported that previously stimulated MSC with IFN-y promote the secretion of CD274, vascular cell adhesion molecule-1 and galectin-1, which enhance the cell interaction and the suppressive effect of these cells [153]. There is a complex system that involves the role of soluble factors and the interaction with other cells that are implicated in the immunomodulation by MSC [153]. This network is necessary to regulate a wide variety of immune cells in response to different stimulus and make MSC a possible candidate for asthma therapy [153].

4.3. Mesenchymal stem cells in asthma

During the last years, preclinical studies in models of asthma have demonstrated good safety and efficacy of MSC due to their paracrine effects [167]. Recently, it has been shown that MSC have a possible role in the treatment of airway inflammation due to their immunomodulatory ability and their regenerative effect in the injured airways [168].

Previous studies in our laboratory have shown that the administration of MSC on an experimental murine model of asthma rapidly decreases airway inflammation and mucus production and is correlated with an increase in Th1 cytokines in the lungs. Still, such

effects decline under sustained allergen challenge despite a persistent presence of the MSC [169]. The data suggests that a fading immune deviation mechanism may be, at least in part, responsible for the loss of the anti-inflammatory effect [169]. Conversely, airway contractile mass undergoes a late reduction, associated with a tendency to attenuate airway hyperresponsiveness, in spite of the continued pathogenic stimuli and inflammatory rebound [169].

A growing number of studies have reported that MSC have the ability to reduce pathological changes and AHR in the airways with a Th2 deviation that has been associated with a reduction in IgE levels [170]. Previous studies have shown a significant decrease in asthma features, such as airway inflammation and remodeling, after administration of MSC in OVA murine models [171]. Moreover, MSC have the ability to modulate hyaluronic levels and decrease excess matrix deposition in lamina propria in OVA asthma models [172]. It has been reported that airway inflammation is suppressed in experimental rat asthma models when human placenta mesenchymal stem cells are administered [173]. Furthermore, another study has shown that pathological changes and allergic inflammation are reverted after administration of BM-MSC in OVA murine models [170]. This local administration induces a decrease in AHR, eosinophil infiltration in the airways, reduces mucus overproduction in the lungs and decreases OVA-specific IgE serum levels, which are associated with an increase in immunosuppressive cytokines [170]. It has been reported that MSC have the ability to recruit and activate IL-10-producing monocytes that decrease airway inflammation and AHR [174].

It has been reported that neutrophilic infiltration and Th17 cells are regulated after MSC administration in a murine neutrophilic model, which suggests that these cells might have an important role in steroid-resistant asthmatic patients [175], [176]. These results are consistent with other studies that have shown an immunomodulatory role of MSC due to the deviation of Th2 to Th1 responses [167]. It has been reported that MSC derived from adipose tissue or bone marrow have the ability to migrate and recruit into the airways, where they reduce pathological asthmatic changes by a Th2 deviation [170]. In addition, dental follicular stem cells (DFSC) reportedly inhibit $CD4^+$ T cell proliferation in asthmatic patients [12]. DFSC co-cultured with PBMC from asthmatic patients exhibit increased IFN-y and IL-10 levels but decreased IL-4 and GATA3 expression [167]. DFSC also inhibit the production of costimulatory molecules in PBMC. These results suggest that DFSC inhibit the function of Th2 cells, transform T lymphocytes into Th1 cells, and regulate Th2-mediated allergic asthma [167]. In addition, other studies have suggested that

immunosuppressive effects on MSC are modulated by Treg dependent and independent mechanisms [177].

4.3.1. Immunomodulatory properties of MSC-derived secretome

Due to their specific anatomical and histological characteristics, the lungs are suitable typified organs in which BM-MSC and their conditioned media (MSC-CM) can be delivered by local or systemic administration [178]. During the last decades, there has been controversy regarding to the role of MSC in airway inflammation [179]. Studies in chronic mouse models of asthma have reported that administered MSC reduce collagen matrix deposition and eosinophil recruitment due to an immune response deviation [180]. Cell administration immediately after allergen sensitization results in appropriate immune response deviations in Th2 to Th1 phenotypes [179]. Conversely, other reports have shown that AD-MSC fails to reduce asthmatic features in feline asthma models [181]. Moreover, previous studies have shown that systemic administration of BM-MSC, but not MSC-CM, reduces airway inflammation and pathological changes in OVA-challenged asthmatic changes in a rat model [182].

Since the survival and differentiation rate of stem cells in the inflammatory niche is significantly low, possibly due to its ischemic microenvironment, it has been proposed that the paracrine fashion is the principal mechanism for the therapeutic effects of MSC under pathological conditions [183]. Two main contributory effects of MSC, including paracrine activity and capacity for transdifferentiation, have been previously documented in target tissues[184]. Subcutaneous (*s.c.*) administration results in limited factors, which include immunologic reactions, waiting time for cellular migration and the tumorigenicity risk. This result promotes the use of soluble paracrine factors due to their ability to regenerate target tissues [182]. Stem cell-secreted growth factors are responsible for some of the therapeutic effects of stem cells inside the body, and it seems logical that the paracrine functions of MSC driven by secretome could be monitored in the supernatant MSC-CM [182]. Therefore, the paracrine interaction hypothesis has inspired a novel alternative therapeutic modality that might warrant more efficient consequences than current stem cell-based therapies [183]. The administration of MSC-CM alone could alone attenuate some of the disadvantages associated with direct transplantation of MSC such as immune responses, tumorigenic risk, infectious agents, total costs, and long-term stem cell expansion [179].

Increasing evidence in animal models of lung injury reveals that systemic transplantation of MSC or MSC-CM could significantly shift $CD4^+$ T lymphocyte population from Th2 cells toward a Th1 phenotype, alleviating airway inflammation during lung injury [185]. Moreover, a reduction in T cell activation has been reported, alongside a phenotype switch to Tregs and an induction of apoptosis to suppress T lymphocyte activation by MSC [186]. This suppressive effect on T cells is induced by MSC' secreted soluble factors, which have been demonstrated when MSC have been co-cultured with T cells separated by the Transwell membrane and a reduction of T cell proliferation has been observed [187]. In contrast, direct cell-to-cell contact mechanisms are involved in T cell regulation when human or cat MSC are used [187]. It has been reported that previous stimulation with IFN-y or other cytokines were required to induce immunomodulatory functions on MSC [188]. Other studies have shown a suppressive effect of feline AD-MSC, which secrete PGE2, IDO, IL-8 and TGF-β and are similar to human MSC. Conversely, unlike human MSC, studies have reported a reduction in the production of IDO and PGE2 when AD-MSC were not in direct cell contact [187]. Several reports have demonstrated that AD-MSC from a wide variety of species, such as dogs, horses, cats and humans, have the ability to inhibit T cell proliferation by increasing the levels of IFN-y [187]. Several soluble factors secreted by MSC have been identified and reported to have suppressive functions, which include HGF, NO, IL-6, and IL-10 [170]. These soluble factors can decrease DCs activation and recruitment in the airways, thus lowering Th2 cytokines and allergic airway inflammation [170]. These effects on the immune regulation response could be controlled by paracrine effect monitoring [170]. These observations show that there are differences between the immunomodulatory effects of MSC derived from different tissues and species, and that it is important to explain the preclinical results reported [170].

However, underlying mechanisms commanded by MSC during asthma remain understudied. On the contrary, studies have reported that systemic administration of MSC-CM in single doses has inert effects on the levels of Th1/Th2 cytokines in lung tissues of sensitized rats [185]. Later, these same authors revealed that systemic administration of MSC-CM in repeated dosages, but not in a single dose, could have a therapeutic effect on asthmatic changes, presumably by regulating the differentiation of naïve T cells [185]. It has been shown that in OVA-sensitized male rats, $CD4^+$ T cells deviate into Th1/Th2 effector cells via regulation of T-bet and GATA-3, respectively [185]. On the contrary, some experiments have shown that systemic injection of rat BM-MSC, but not MSC-CM, significantly diminishes the inflammation rate by the modulation of

interleukins and CAMs to normal levels in sensitized rats [189]. On the contrary, MSC-CM do not yield any effects in asthmatic lung tissues [189]. Unlike our results, some experiments have shown that the systemic injection of MSC-CM could positively modulate the inflammatory responses in experimental lung injury [189]. The authors have declared that therapeutic outcome solely depends on the MSC-CM volume and the secretome profile [179], [185]. Although the costs and benefits of a continuous and repeated dose of MSC-CM injection should be described, many reports have unveiled the lack of rejection of MSC-CM in various experiments [190], [191]. To our knowledge, there is little data related to the administration of the repeated doses of MSC-CM in asthmatic models [189].

During the last years, studies have reported suppressive effects of extracellular vesicle (EV) fractions in conditioned media, which include exosomes, microvesicles and microparticles [192].

There are several reports that have demonstrated the protective effect of MSC-CM and MSC-exosomes in animal asthma models, due to their ability to reduce inflammation, matrix collagen depositionand repair injured epithelium in the airways, similar than human MSC [192], [193]. Moreover, other reports have demonstrated a reduction in airway inflammation and remodeling in asthmatic animals after MSC-CM and MSC-exosomes therapies [193]–[195]. Studies have also reported a reduction of eosinophil infiltration and matrix collagen deposition in the airways in OVA murine asthma models when administered with MSC-exosomes [194]. Other studies have shown a decrease in neutrophil and eosinophil infiltration with a reduction in macrophages and lymphocytes in the airways after systemic administration of BM-MSC-CM or BM-MSC-exosomes in mouse asthma models [192]. Moreover, reduced airway inflammation by antigen-specific $CD4^+$T cells has been observed due to their phenotype switching and altered secretome after BM-MSC administration [192]. This secretome has the ability to modulate Th2 and Th17 response by a reduction in the production of IL-5, IL-4 and IL-17 in asthmatic airways, whereas IL-10 producing $CD4^+$ T cells increase and promote an immunosuppressive microenvironment [192].

4.3.2. Clinical studies

During the last years, MSC therapy has been evaluated to determinate the safety and reliability in patients with idiopathic pulmonary fibrosis and acute respiratory distress disease [146]. However, the results obtained in clinical trials have not been correlated with

the immunomodulatory effect observed in preclinical asthma models, which does not warrant finances for the development of this cell-based therapy [167]. There are several problems to solve before a realistic use of MSC in clinical trials is feasible, which explains why its use for the amelioration of inflammatory diseases remains avoided. Moreover, it has been reported that MSC-EVs could alleviate asthma features and lung mechanics [177], [196]. However, more knowledge of MSC secretome is needed, which includes improved clinical ethics, safety, practicability and enhancement of cell migration in this cell-based therapies [170].

There are currently two clinical MSC-based therapies under development to evaluate their safety and efficiency on severe asthmatic patients [195]. Firstly, a phase 1 clinical trial will be developed at the University of Miami Miller School of Medicine, which will evaluate the effect of allogeneic BM-MSC in patients with moderate asthma. They will administer via *i.v.* 20 or 100 million BM-MSC to three patients per group and they will evaluate lung volume, dyspnea, pulmonary function and side effects every 4 weeks until the end of the study (NCT03137199) [195]. The second study is based on the effect of allogeneic umbilical cord MSC-derived trophic factors in asthma. This clinical trial is being developed by the Punta Pacifica Hospital of Panama City with the aim of studying their safety and efficiency [195]. They administer via *i.n.* MSC trophic factors in a regime of one dose per week for 4 weeks to 20 patients per group and they evaluate side effects and take pulmonary function tests after the one-month surveillance (NCT02192736) [195].

As described above, experimental asthma models have demonstrated the safety and the effects of administered MSC [195]. However, there are several problems to resolve before the use of MSC in a clinical context due to the data obtained from recent clinical trials [195]. Firstly, there is a strong suppression in the immune system which induces the development of infections for a short time period in the airways after MSC-based therapy [197]. Secondly, the regulation of the immune response effect and its migration capacity are reduced with age, which has been studied in BM-MSC-based therapy in idiopathic pulmonary fibrosis (IPF) patients [198]. Thirdly, the local microenvironment could promote MSC' engraft to induce unwanted differentiation from transplanted MSC [199]. Therefore, there is a need to define an optimal number of administered MSC and to identify factors that are implicated in signaling pathways regulations with the aim of getting a satisfactory balance between desirable and undesirable effects, the second of which include a strong suppression of the immune system [199]. Moreover, MSC may promote tumor growth and metastasis through paracrine and endocrine manners, which suppress anti-tumorigenic immunity and induce neovascularization through the secretion of pro-angiogenic factors

(VEGF, HGF, PDGF, angiopoietin-1, and placental growth factor). Consequently, with the aim of defining the possible pro-tumorigenic development induced by MSC administration, studies centralize in the evaluation and monitoring of MSC administered in patients during long durations [199].

HYPOTHESIS AND OBJECTIVES

Hypothesis

Asthma is an immune-mediated disease, pathologically characterized as airway inflammation, airway hyperresponsiveness and subsequent abnormal repair leading to structural changes in the airway wall, known as airway remodeling. Airway smooth muscle cell proliferation is a major feature of airway remodeling where many mediators have been implicated. An infiltration of T cells into the airways is a major feature of asthma, where these cells contribute to the ongoing inflammation through the release of cytokines and chemokines. The increase of ASM mass may be the main contributing factor to airway hyperresponsiveness and asthma severity. Therefore, it is crucial to find an effective treatment to suppress the development of airway remodeling in asthma. Animal models represent a useful system for understanding disease pathobiology and for developing and testing potential drug therapies. Classical experimental asthma models based on intraperitoneally sensitization followed by airway challenge may not fully reflect the immune response involved in actual asthma, where humans are sensitized to airborne allergens through primary exposure in the airways. As research in this area continues to expand, the relative merits and limitations of each model must be defined and understood in order to evaluate the information that is obtained from these models and to extrapolate these findings to humans so that effective drug therapies can be developed. Despite these issues, animal models have been, and will continue to be, vital in understanding the mechanisms that are involved in the development and progression of asthma.

Previous studies in OVA-sensitized rats demonstrated that a direct interaction between ASM cells and $CD4^+$ T cells is involved in the proliferation of ASM cells and the survival of $CD4^+$ T cells. These data support a direct contribution of activated $CD4^+$ T cells to the mechanism of ASM remodeling in asthma. Moreover, other studies demonstrated that MSC may suppress airway inflammation in experimental asthma *in vivo*, but such effects declined under sustained allergen challenge despite a persistent presence of the MSC. These outcomes support furthering research toward a potential use of MSC in asthma, but caution and solid preclinical data building are warranted.

The development of experimental models based on primary airway antigen exposure, and the integrated analysis of the pulmonary airways in such models, may unveil immunological mechanisms relevant to the disease. This research has contributed to the current understanding of how the immune system interacts with the functional respiratory system and pulmonary pathophysiology. Further, animal models remain the easiest way

to help developing new drugs and immunotherapy strategies for the treatment of this complex disease.

Objectives

1. To develop a rat asthma model induced by primary airway antigen exposure through intranasal (*i.n.*) instillation of antigen or control.

    a. To analyze airway hyperresponsiveness as a primary *in vivo* outcome, and profile its development and evolution through a time series of experiments.

    b. To analyze other experimental asthma outcomes including airway inflammation, goblet cell hyperplasia, mucus production, subepithelial fibrosis and airway contractile tissue mass.

    c. To analyze the inflammatory profile recruitment and the quantities of cytokines released.

2. To evaluate suppressive effect of mesenchymal stem cells in airway remodeling by co-culture *in vitro* model.

.

a. To test whether HDM allergen activates effector $CD4^+$ T cells and elicits airway myocyte proliferation upon direct contact.

b. To, investigate whether adipose-derived MSC, added to the $CD4^+$ T cell/ASM co-culture, interfere with ASM proliferation induced by effector $CD4^+$ T cells.

c. To evaluate if the suppressive effect are molecules secreted into the medium or carried by exosomes and interfere with ASM proliferation induced by effector $CD4^+$ T cells.

d. To evaluate the inhibitory capacity of the MSC medium fractionated into molecular weight ranges, added to the $CD4^+$ T cell/ASM co-culture, interfere with ASM proliferation induced by effector $CD4^+$ T cells.

3. To test whether different doses of fractioned MSC medium suppress airway remodeling *in vivo* in rat asthma model.

a. To analyze airway hyperresponsiveness as a primary *in vivo* outcome, and profile its development and evolution through a time series of experiments.

b. To analyze other experimental asthma outcomes including airway inflammation, goblet cell hyperplasia, mucus production, subepithelial fibrosis and airway contractile tissue mass.

c. To analyze the inflammatory profile recruitment and the profile of cytokines released by $CD4^+$ T cells.

METHODS

1. Animals

Female Sprague Dawley (Crl:OFA(SD) rats of 6 weeks of age and 200-250 g body weight were obtained from Charles River Laboratories Inc. (Lyon, France). The rats were maintained at the *Institut de Recerca Hospital de la Santa Creu i Sant Pau* (IIB Sant Pau) animal core facility. They were housed in allergen-free ventilated racks, breathing High-Efficiency Particulate Air (HEPA)-filtered air at room temperature (22-25ºC), under 12:12-hour dark/light cycle, and with *ad libitum* access to standard pellet diet and water. The rats were aged 7 weeks when entered in the experiments.

The Animal Research Ethics Committee of the *Generalitat de Catalunya* approved all procedures, and the animals received care according to European Union Directive 86/609 and the derived Guide for the Care and Use of Laboratory Animals (Royal Decree 1201/2005, Government of Spain). Animal handling, experimental procedures, and data collection and reporting were carried out in compliance with the Animal Research: Reporting In Vivo Experiment (ARRIVE) guidelines [200].

2. Study design

For asthma modeling, the rats were randomly assigned to four groups (n = 10 animals per group for all experiments) according to the agent administered via *i.n.*: control group (receiving saline solution), *Staphylococcal Enterotoxin B* (SEB; Sigma-Aldrich, Jerusalem, Israel) group, standardized House Dust Mite extract group (HDM; Citeq Biologics, Groningen, Netherlands), or a combination of HDM with SEB (HDM+SEB) group. Three experimental designs were carried out: (**A**) low-dose model (10IN) consisting of 2 *i.n.* instillations per week for 5 weeks; (**B**) high-dose model (15IN) consisting of 3 *i.n.* instillations per week during 5 weeks; and (**C**) extended model (30IN), consisting of 3 *i.n.* instillations per week for 10 weeks. For the *i.n.* instillations, HDM was dissolved in sterile 0.9% saline solution to obtain a working concentration of 20 µg/mL, and stored at 4ºC. The doses of HDM used in this work refer to the amount of *Derp 1*. SEB was dissolved in sterile saline for a working concentration of 2 µg/ mL and stored at -20ºC. The animals were *i.n.* instilled with 50 µL per nostril of saline, HDM, SEB or HDM+SEB solution under light anesthesia with inhaled 3% Isoflurane (AbbVie, Madrid, Spain). Forty-eight hours after the last *i.n.* instillation, the rats were subjected to pulmonary function testing under mechanical ventilation.

For *in vitro* experiments, four groups of rats were included (n = 10 each): (**B-type protocol/HDM+SEB**) *i.n.*-instilled with HDM+SEB using the 15IN model; (**D**) receiving intraperitoneal (*i.p.*) injection of HDM extract adsorbed on aluminium hydroxide ($AlOH_3$; InvivoGen-IBIAN Technologies, Zaragoza, Spain) (HDM+$AlOH_3$ group) on days 0 and 14; and (**B-type protocol/saline**) *i.n.*-instilled with saline used the 15IN model (control group). For *i.p.* sensitization to HDM, the animals were lightly anesthetized as for *i.n*. instillations, and 5 µg of HDM adsorbed in 10 mg/mL of $AlOH_3$ was *i.p.* injected in a 0.3-mL PBS volume. Forty-eight hours after the last *i.n*. or *i.p*. dosing, the rats from all groups were euthanized by anaesthesia overdose and tissues for in-vitro investigations were harvested.

For experiments aimed at *in-vivo* testing of the therapeutic effect of MSC-conditioned medium (MSC-CM) we induced experimental asthma by using the 15IN model, and we administered MSC-CM as per the following dose-finding scheme: (**E**) HDM+SEB-sensitized rats received 12.5, 25 or 50 µg of MSC-CM (n = 6 per dose group), delivered through *i.n.* instillation, one dose per week for 2 weeks (1W groups); (**F**) HDM+SEB-sensitized rats received 12.5, 25 or 50 µg MSC-CM, 2 *i.n.*-instilled doses per week for 2 weeks (2W groups). For dose preparation, MSC-CM was dissolved in sterile saline to obtain a working concentration of 12.5, 25 or 50 µg in 0.1 mL, and stored at -80ºC until delivery. The animals received 50 µL of *i.n.* MSC-CM solution into each nostril, under light anaesthesia as described above. For both the 1 and 2-week regimes, the HDM+SEB *i.n.* instillations were continued after the MSC-CM doses to mimic a scenario where human subjects would undergo continuing exposure to an aeroallergen regularly present in their environment. Pulmonary mechanics were performed one week after the last *i.n.*-instilled MSC-CM dose.

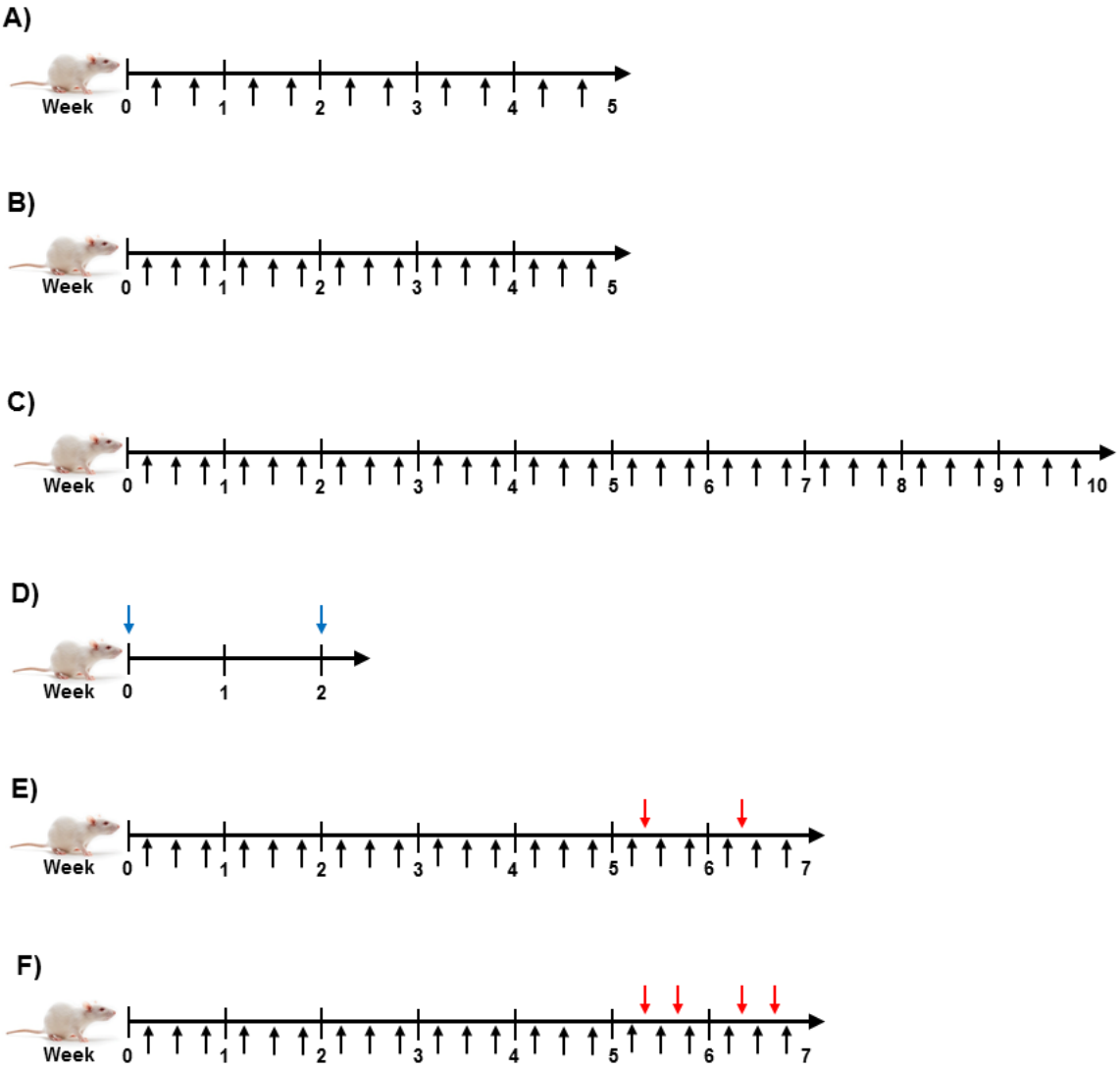

Figure 1| Study design. Sprague Dawley rats were *i.n.*-instilled with saline (CONTROL), SEB (2 µg/mL), HDM (20 µg/ml), or HDM+SEB in same respective concentrations (n = 10 per group of each of the A, B, and C experiments. The rats were assigned to 3 experimental designs: (**A**) low-dose model (10IN), consisting of 2 *i.n.* instillations per week for 5 weeks; (**B**) high-dose model (15IN), consisting of 3 *i.n.* instillations per week for 5 weeks; and (**C**) extended model (30IN), receiving 3 *i.n.* instillations per week for 10 weeks. For in vitro experiments, rats were *i.p.*-sensitized on days 0 and 14 (**D**) with HDM in aluminium hydroxide hydrate ($AlOH_3$) or *i.n.*-instilled with HDM+SEB or saline solution using 15IN model (**B**) (n = 10 per group of each of the B and D experiments). For experiments to test the MSC-CM therapeutic effect (n = 10 per group of each of the E and F experiments), we induced experimental asthma using the 15IN model, and assigned HDM+SEB-sensitized rats to the following dose-finding groups: (**E**) 12.5, 25, or 50 µg/0.1 mL of *i.n.*-instilled MSC-CM, 1 instillation per week for 2 weeks (1W group); and (**F**) 12.5, 25 or 50 µg/0.1 mL of *i.n.*-instilled MSC-CM, 2 *i.n.* instillations per week for 2 weeks (2W group). HDM+SEB *i.n.* instillations were continued after the MSC-CM doses to mimic a scenario where human subjects would undergo continuing exposure to an aeroallergen regularly present in their environment. Small arrows in the time scales indicate *i.n.* instillations (black), *i.p.* sensitization (blue), and MSC-CM doses (red).

3. Experimental procedures *in vivo*

3.1. Lung resistance

Invasive lung function measurements were performed by forced oscillation technique under mechanical ventilation, using eSpira equipment purchased from Electromed Systems (EMMS; London, UK). Forty-eight hours after the last *i.n.* instillation, the rats from the experimental asthma modeling experiments and the MSC-CM therapeutic effect testing were subjected to pulmonary function testing under mechanical ventilation.

For this purpose, the rats were anaesthetized with *i.p.* Ketamine 75 $mg \cdot Kg^{-1}$ (Fatro Ibérica, Barcelona, Spain) and Dexdomitor 0.5 $mg \cdot kg^{-1}$ (Esteve laboratories, Barcelona, Spain). The trachea was cannulated through tracheostomy using a metal endotracheal tube (diameter of 1.07 mm and inner diameter of 0.65 mm; EMMS).

The animals were then connected to a computer-controlled ventilator system (EMMS). Then, neuromuscular blockade was induced with Rocuronium 0.6 $mg \cdot Kg^{-1}$ *i.p.* (Esmeron®-MSD, Madrid, Spain) and lung function measurements were initiated. Ventilator settings used were 90-120 breaths/min respiratory rate, a tidal volume of approximately 10 ml/Kg (body weight-adjusted for each individual animal) and a positive end-expiratory pressure (PEEP) of 2-3 cmH_2O.

Lung resistance (R_L) was assessed upon nebulizing increasing concentrations of methacholine (MCh; Sigma-Aldrich, Madrid, Spain) (20 µl of vehicle, 4, 8, 16, 32, 64, 128, 256 $mg \cdot mL^{-1}$) with an Aeroneb®Lab ultrasonic nebulizer (Aerogen, Galway, Ireland) coupled to the eSpira inspiratory arm. Data collection was performed with EMMS eDaq software (EMMS) using a single-compartment model.

The airway responsiveness profile was presented as the curve generated from the successive peak R_L values obtained after each of the corresponding MCh doses. Airway hyperresponsiveness was considered present when R_L was significantly higher than baseline R_L at 256 mg/mL MCh or earlier, and significantly higher than baseline R_L.

To avoid artifact data due to the formation of atelectases during mechanical ventilation, a total-lung-capacity (TLC) manoeuvre or “sigh” was administered as necessary. During this manoeuvre, the ventilator distends the lungs up to 300 mmH_2O pressure, which usually uncollapses the lung parenchyma and/or plugged airways.

3.2 Blood serum extraction

Following the methacholine challenge test, the rats were euthanized by anesthesia overdose. Blood samples were drawn from the caudal cava vein, centrifuged after clotting (1200·g for 10 min at 22ºC), and the blood serum was harvested and stored at -80ºC.

3.3. Bronchoalveolar lavage (BAL) analysis

BAL was collected for differential leukocyte populations analysis by flow cytometry, and to store samples of its fluid fraction for further analysis.

The endotracheal tube was plugged into a three-way stopcock connected to a syringe, and the lungs were washed with 10 ml of PBS containing 5% Fetal Bovine Serum (FBS; Life Technologies, Madrid, Spain). An initial 2-mL aliquot (S1) and a subsequent 8-mL aliquot (S2) were separately obtained and centrifuged (650·g for 5 min at 22 °C). The supernatant from S1 was recovered as BAL fluid (BALF) and stored at −80°C. The cell pellets obtained from S1 and S2 were merged and resuspended in 1-mL of Red Blood Cell Lysing Buffer (Sigma-Aldrich, Schnelldorf, Germany) for 3 min at RT. The cells were then washed and resuspended in 1-mL of PBS with 5% FBS. Total leukocyte counts were performed in a Neubauer chamber (Zuzi Corp., France), and cell viability was checked by trypan blue dye (Sigma-Aldrich) exclusion. Cell concentration was then adjusted to $1 \cdot 10^6$ cells/mL using PBS with 5% FBS.

For flow cytometry analysis, $1 \cdot 10^5$ cells were immunostained with labeled antibodies as detailed in **Tables 1 and 2**. For this purpose, the cells were washed and blocked with anti-CD32 (BD Biosciences, Madrid, Spain) as per manufacturer's instructions to prevent Fc-mediated, non-specific binding. The cells were then stained with Fixable Viability Dye eFluor®450 (eBioscience-Labclinics S.A., Barcelona, Spain) for 20 min at RT in the dark. Next, the cells were stained with the corresponding labeled antibodies for 20 min at RT in the dark, followed by further washing.

Unless otherwise stated, all flow cytometry procedures in this work were performed with MACSQuant Instrument (Miltenyi Biotec, Cologne, Germany) using MACS Quantify software (Miltenyi Biotec, Cologne, Germany).

Table 1. Monoclonal antibodies for general leukocyte flow cytometry.

Antibody	Fluorochrome	Clone	Supplier
CD32	N/A	D34-485	BD Biosciences
CD3	VioGreen	REA223	Miltenyi Biotec
Granulocyte Marker	FITC	HIS48	eBioscience
CD172	PE	OX-41	Biolegend
CD161	PerCP-eFluor710	10/78	eBioscience
CD45R (B220)	PE-Cy7	HIS24	eBioscience
CD43	Alexa-Fluor™647	W3/I3	Biolegend
CD45	APC-Cy7	OX-1	BD Biosciences

Table 2. Monoclonal antibodies for lymphocyte flow cytometry.

Antibody	Flurochrome	Clone	Supplier
CD32	N/A	D34-485	BD Bioscience
CD3	VioGreen	REA223	Miltenyi Biotec
CD8a	FITC	REA437	Miltenyi Biotec
CD4	APC	REA489	Miltenyi Biotec
CD45	APC-Cy7	OX-1	BD Bioscience

3.4. Lung histopathology

The right ventricle was punctured with a needle and syringe to perfuse the pulmonary vascular circuit with 5000 IU/mL heparin (Sodium heparin l; Hospira Invicta S.A., Madrid, Spain) in PBS before lung extraction. After perfusion, the lungs were excised in bloc from the thoracic cavity, along with the cannulated tracheobronchial tree and heart. The lungs were then inflated at 25 cmH_2O standardized pressure by connecting the tracheal cannula to a recirculation pump with 4% formaldehyde (Sigma-Aldrich) in PBS for 24 hours, for normalized quantitative morphology. After fixation, lung sagittal slices were introduced into histological casettes, immersed in 70% ethanol (Panreac, Barcelona, Spain), and processed for paraffin embedding at the IIB Sant Pau Histopathology core facilities.

For general histopathological assessment, and to identify inflammatory infiltrates in the lungs, haematoxylin-eosin staining (H-E) was employed. To identify mucus-producing cells in the airways, such as goblet cells, periodic acid-Schiff (PAS) stain was used. Masson's trichrome stain was performed for the analysis of extracellular matrix deposition. Contractile airway tissue was detected by immunohistochemistry using an antibody to alpha-smooth muscle actin (α-SMA; Sigma-Aldrich) with methyl green (Sigma-Aldrich) as a counterstain. The slides were examined under a fluorescence microscope (BX50; Olympus, Tokyo, Japan).

3.5. Alpha-smooth muscle actin immunohistochemistry

Alpha-SMA is the predominant actin isoform in the contractile apparatus of smooth muscle cells, and is also present in myofibroblasts.

Five-µm tissue sections, deparaffinized and rehydrated, were subjected to cell membrane permeabilization with 0.2 % Triton X-100 (Sigma-Aldrich) in TBS for 20 minutes at RT and then blocked with 5% normal horse serum (Vector Labs-Palex Medical, Barcelona, Spain) for 30 minutes at RT. A mouse anti-α-SMA IgG2a monoclonal antibody (clone 1A4, Sigma-Aldrich) was used as primary antibody (1:100 dilution, 5 µg/mL) and incubated for 40 min at RT. Following 3 washes with PBS, the tissue sections were then incubated for 30 min at RT with biotinylated anti-mouse IgG (Vector Labs-Palex Medical) (1:1000 dilution, 10 µg/mL) in PBS with 2.5% normal horse serum (Vector Labs-Palex Medical) and 0.1% Tween-20 (Sigma-Aldrich). After 3 PBS washes, an avidin-biotin-alkaline phosphatase complex (Vector Labs-Palex Medical) was added, incubated for 30 minutes, and washed. Vector Red chromogen (Vector Labs-Palex Medical) was then added for signal development under microscope monitoring. Cell nuclei were counterstained with methyl green (Sigma-Aldrich). The stained specimens were mounted with permanent medium (Vector Labs-Palex Medical) optimized for fluorescence microscopy.

3.6. Quantitative morphology

Images from lung sections were acquired with a fluorescence microscope (BX50; Olympus) equipped with a digital camera (DP21; Olympus), and using 10x, 20x, and 40x objectives depending on airway size so as to obtain the largest possible airway image within one field. Cross-sectioned airways (with the largest inner diameter not exceeding 1.5-fold the shortest diameter) were analyzed according to established sampling and standardization criteria [107], [169].

Airway cell counts, and surface area measurements resulting from extracellular matrix and contractile tissue signal extraction, were referenced to the basement membrane perimeter squared (P_{BM}^2), which is considered a constant airway size reference independently from the airway contraction or relaxation status [107]. Quantitative measurements in the upper airway were based on previously reported methods [107]. Stored mucosubstances, extracellular matrix, and α-SMA^+ contractile tissue, expressed as section surface area/P_{BM}^2, are dimensionless.

Image processing for quantitative morphology was performed with ImageJ software (v.1.43m; National Institutes of Health, USA). The digital images acquired from the microscope were calibrated using a standard micrometric ruler slide (Leica Microsystems, Barcelona, Spain).

To measure collagen deposition and epithelial mucosubstances, the Masson's trichrome blue component and PAS staining areas were respectively delimited by a colour extraction algorithm, and measured as particles surface area. For each cross-sectioned intrapulmonary airway, or upper airway section, the particle surface area summation was divided by the P_{BM}^2 or the basement membrane length squared, respectively, and the result was named “extracellular matrix mass” or “mucoid mass”.

For airway contractile tissue quantification, the α-SMA immunofluorescent signal was digitally thresholded, extracted, measured as particle surface area summation/P_{BM}^2, and named "airway contractile tissue mass”.

3.7 Determination of total and specific IgE

Total IgE was measured in BALF and blood serum using a commercial rat IgE quantitative ELISA kit (range of detection (ROD) of 32 to 0.5 ng/mL; Abcam, Cambridge, UK) as per manufacturer's instructions.

HDM-specific IgE concentration was determined by ELISA as previously described [201]. For this purpose, ELISA plates (Sigma-Aldrich) were coated with 50 µL of 5 µg/mL HDM (Citeq Biologics) in PBS and left overnight at room temperature. The plates were washed with PBS 0.05% Tween 20 (PBST) and blocked for 30 min with 4% bovine serum albumin (BSA; Sigma Aldrich) in PBST. Blood serum or BALF samples were added and then incubated overnight at room temperature. After washing, the plates were incubated for 1 hour at room temperature with a biotinylated anti-IgE antibody (clone MARE-1; Abcam) at 0.5 µg/mL. After washing, the plates were then incubated for 40 min at room temperature with horseradish peroxidase-streptavidin (HRP; BD Biosciences). Following a last wash, tetramethylbenzidine substrate (TMB; BD Biosciences) was added to the plates and incubated at room temperature until colour developed. The reaction was stopped with Stop solution (BD Biosciences), and the plates were read at 450 nm (Multiskan Plus Microplate Reader; Labsystems, Lima, Peru). Results are expressed as mean optical density (mOD) over reference rat serum.

The concentration of anti-SEB rat IgE was determined by ELISA as described in previous studies [202]. ELISA plates were coated with SEB (5 µg/mL; Sigma-Aldrich) in 0.05 M bicarbonate buffer (pH 9.6) overnight at RT. After three washes with PBST, the coated plates were blocked with 2% BSA in PBST at 37°C for 1 hour. The plates were washed three times, then blood serum or BALF was added, and incubated at 37°C for 1 hour. As for total IgE detection, biotinylated anti-IgE (clone MARE-1; Abcam) was added at 0.5 $\mu g \cdot mL^{-1}$ after 3 washes, and incubated at 37°C for 1 hour. HRP (BD Biosciences) was then applied after washing, and color developed with TMB (BD Biosciences) and stopped with Stop Solution (BD Biosciences). The signal was measured with the ELISA reader at 450 nm (Multiskan Plus Microplate Reader; Labsystems), and results expressed in mOD as compared to reference rat serum.

3.8. Determination of total IgG

Total IgG was measured in BALF and blood serum using a commercial rat IgG quantitative ELISA kit (ROD of 20 to 0.31 µg/mL; Abcam) as per manufacturer's instructions.

3.9. BAL and blood serum cytokines

The concentration of IFN-y (14.6 to 60.000 pg/mL ROD), TNF-α (2.4 to 10.000 pg/mL ROD), IL-17A (7.3 to 30.000 pg/mL ROD), IL-13 (15.6 to 1000 pg/mL ROD), IL-4, IL-5, and Eotaxin (4.9 to 20.000 pg/mL ROD) was measured in BALF and blood serum. The samples were analyzed by means of a MILLIPLEX MAP Rat Cytokine/Chemokine Magnetic Bad Panel Immunology Multiplex Assay (Merck Millipore, Molsheim, France). IL-13 was analyzed apart by ELISA (Invitrogen, Madrid, Spain) according to the manufacturer's instructions. The total protein was measured by Bradford assay (Bio-rad Laboratories, Madrid, Spain) to obtain the total protein per mg of BAL or serum. The results were expressed as pg/mL cytokine per mg of total protein.

4. Experimental procedures *in vitro*

4.1. Cell isolation

Following the sensitization procedures, the rats were euthanized by anaesthesia overdose and organ tissues were harvested.

4.2. Splenocyte isolation

Spleens from the HDM+$AlOH_3$ and control groups were mechanically disaggregated and washed. The supernatants were discarded, and the pellets resuspended in 1 mL of Red Blood Cell Lysing Buffer (Sigma-Aldrich). After 2 minutes, the cell suspension was washed and filtered through a 50-µm mesh (ImmunoTools, Friesoythe, Germany) and centrifuged at 650·g for 5 min. The supernatants were discarded and the pellets were resuspended in Dulbecco's modified Eagle's medium: Nutrient mixture F-12 (DMEM/F12; Life Technologies) supplemented with 10% FBS (Life Technologies) and 1% penicillin/streptomycin (Life Technologies)(Complete medium). Total cell counts and cell viability were performed in a Neubauer chamber using trypan blue dye exclusion. To evaluate T-cell subpopulations, $1 \cdot 10^6$ splenocytes /mL were stained with the antibodies enumerated in **Table 2**. Briefly, the cells were washed and blocked with anti-CD32 (BD Biosciences) to prevent Fc-mediated, non-specific binding as per manufacturer's instructions. The cells were then stained with Fixable Viability Dye eFluor®450 (BD Biosciences) for 20 min at RT in the dark, and stained with the antibodies for 20 min at RT. After washing, cells were assessed by flow cytometry analysis.

4.3. HDM-specific $CD4^+$ T-cell isolation

Splenocytes were cultured at a $5 \cdot 10^6$ cells/mL concentration in complete DMEM/F12 with 3 µg/ml HDM, 1% nonessential amino acids (Life Technologies), 50-µM 2ß-mercaptoethanol (Life Technologies), and 100 U/mL IL-2 (BD Biosciences) in 20-mm tissue culture dishes (TPP, Trasadingen, Switzerland), and incubated at 37ºC in 5% CO_2 and 95% humidity (Nuaire, Caerphilly, Wales). After 3-day culturing, the medium was replaced with fresh, HDM-free medium, and 3 more days of incubation followed. At this point, T cells were stained with the antibodies listed in **Table 2** through the same

procedure as in Section 4.2. Additionally, HDM-specific $CD4^+$ T-cell proliferation was quantified by flow cytometric detection of 5-ethynyl-2'-deoxyuridine (Edu) incorporation and cell DNA content using a Click Kit™ Plus EdU Alexa Fluor™ 488 Flow Cytometry Assay Kit (Life Technologies) and FxCycle™ Violet Stain (Life Technologies), respectively, according to their manufacturer's instructions. Marker expression was assessed by flow cytometry analysis.

4.4. $CD4^+$ T cell purification

HDM-specific $CD4^+$ T cells, and naive $CD4^+$ T cells, were obtained using a rat $CD4^+$ T Cell Isolation Kit (Stemcell, Grenoble, France) for negative selection, as per manufacturer's instructions. To verify the purity of the isolated cells, the HDM-specific $CD4^+$ T cells were stained with the antibodies detailed in **Table 2** and the same procedure as in previous sections. Marker expression was assessed by flow cytometry analysis.

4.5. Airway smooth muscle (ASM) isolation

Tracheas from the HDM+SEB and control groups were mechanically disaggregated and digested in Hanks' Balanced Salt Solution (HBSS; Life Technologies) with collagenase IV (6 mg per trachea) (Sigma-Aldrich) and elastase IV (0.75 mg per trachea) (Sigma-Aldrich) for 30 min at 37ºC with mild agitation. The supernatant from the digestion was then decanted into a new tube and centrifuged at 600·g for 5 min. The pellets containing ASM cells were resuspended in Smooth Muscle Cell Growth Medium 2 Kit supplemented with 5% FCS, epidermal growth factor (0.5 ng/mL), basic fibroblast growth factor (2 ng/mL), insulin (5 µg/mL), and 1% penicillin/streptomycin (SMC Medium; Promocell-Labclinics S.A., Barcelona, Spain) and then plated into 35-mm cell culture dishes (Sigma-Aldrich). After 24 hours, the cells were washed in PBS, had the medium refreshed, and were incubated at 37ºC in 5% CO_2 and 95% humidity (Nuaire).

After 3 days, the ASM cells were trypsinized (0.25% trypsin; Life Technologies), washed, and $1{\cdot}10^6$ cells/mL cells were blocked with anti-CD32 (BD Biosciences) to prevent Fc-mediated non-specific binding. The cells were then stained with Fixable Viability Dye eFluor®450 (BD Biosciences) for 20 min at RT in the dark, and then with CD45-APC-Cy7 (BD Biosciences) and specific α-SMA-Alexa Fluor™647 (Clone 1A4; Santa Cruz

Biotechnology, Heidelberg, Germany) using Fixation/Permeabilization Kit (BD Biosciences). Cells were assessed by flow cytometry analysis.

At this point, ASM cells were subcultured in 12-well cell culture plates (Sigma-Aldrich) at a seeding density of $2 \cdot 10^4$ cells/well, and incubated at 37ºC in 5% CO_2 and 95% humidity (Nuaire). When the cultures reached approximately 85% confluence, the wells were washed 3 times with PBS and placed in serum-free medium containing 0.2% Bovine Serum Albumin (BSA; Sigma-Aldrich) for 3 days, for cell cycle arrest.

4.6. Mesenchymal stem cell isolation

Abdominal adipose tissue from the control group was mechanically disaggregated and digested in HBSS with 0.05% collagenase IV for 1 hour at 37ºC with mild agitation. The digested tissue was washed in complete medium and centrifuged at 630·g for 10 min. The supernatant was discarded and the cell pellet was filtered through a 50-µm mesh. The cells were washed and then cultured in selective Mesenchymal Stem Cell Basal Medium (MSCBM) supplemented with 10% FBS, 2% L-Glutamine and 0.1% gentamicin sulfate (Lonza-Cultek, Madrid, Spain). Non-adherent cells were discarded through subsequent culture passages. Passage-5 adherent cells were used for the experiments.

To verify the MSC phenotype, the cells were trypsinized and $1 \cdot 10^6$ cells/mL were labeled with the antibodies listed in **Table 3**. As for the general flow cytometry immunostaining procedure described in the previous sections, the cells were washed and blocked with anti-CD32 (BD Biosciences) to prevent Fc-mediated non-specific binding, stained with Fixable Viability Dye eFluor®450 (BD Biosciences) 20 min at RT in the dark, then incubated with the labeled antibodies for 20 min at RT, and washed. Marker expression was assessed by flow cytometry analysis.

Table 3. Monoclonal antibodies for MSC flow cytometry.

Antibody	Fluorochrome	Clone	Supplier
CD32	N/A	D34-485	BD Biosciences
CD90	PE	OX-7	BD Biosciences
CD29	PE-Cy7	HMβ1-1	Biolegend
CD45	APC-Cy7	OX-1	BD Biosciences

4.7. Osteogenic and Adipogenic Differentiation of MSC

Osteogenic differentiation was induced by culturing MSC for up to 4 weeks in Osteogenic Differentiation Medium (Lonza-Cultek). To verify calcium deposition, the cultures were washed once with PBS, fixed with 4% paraformaldehyde (Sigma-Aldrich) in PBS for 15-30 min, and stained for 45 min with Alizarin Red S stain (Sigma-Aldrich) at pH 4.2. Dye excess was removed through several washes with distilled water.

To induce adipogenic differentiation, MSC were cultured for up to 2 weeks in Adipogenic Induction Medium (Lonza-Cultek). Adipocytes were discerned from the undifferentiated cells by phase-contrast microscopy. To further confirm their phenotype, the cells were fixed with 4% paraformaldehyde (Sigma-Aldrich) in PBS for 30 min at RT and stained with Oil Red O solution (Sigma-Aldrich) for 5 min. Dye excess was removed through several washes in distilled water. The cells were additionally stained with Harris haematoxylin (Sigma-Aldrich) for 1 min at RT.

4.8. Co-culture of ASM cells, $CD4^+$ T cells and MSC

Following cell cycle arrest as described in Section 4.5, the ASM cells were either stimulated with 10% FBS or incubated in DMEM/F12 supplemented with 0.5% FBS in the absence or presence of $CD4^+$ T cells. One million HDM-specific $CD4^+$ T cells, or naive $CD4^+$ T cells, were added directly to each well of the serum-deprived ASM cell cultures. MSC at different MSC:$CD4^+$ T-cell ratios, decreasing from 1:5 to 1:1000 for dose-response titration, were added to the ASM/$CD4^+$ T-cell co-cultures, either directly or in the upper chamber of 0.4-µm-pore Transwell Permeable Supports (SARSTEDT, Barcelona, Spain). MSC in Transwell chambers were only added to the co-cultures containing HDM-specific $CD4^+$ T cells. The tri-culture ensembles were incubated for 48 hours. The cell concentrations used were based on previous work [107], [203].

To monitor cell proliferation, 50 µM EdU was added to the culture media after 24 hours of the co-culture period. At the end of the experiment, the cell suspensions were trypsinized, labeled with CD45-APCy-7 (BD Biosciences) and α-SMA-AlexaFluor®647 (Santa Cruz Biotechnologies), and processed for flow cytometric detection of incorporated Edu and cell DNA content using Click Kit™ Plus EdU Alexa®Fluor™ 488 Flow Cytometry Assay Kit (Life Technologies) and FxCycle™ Violet Stain (Life Technologies), respectively. Marker expression was assessed by flow cytometry analysis.

4.9. ASM cells, $CD4^+$ T cells, and MSC co-culture with GW4869 exosome release inhibitor

Subconfluent, cell cycle-arrested ASM cells (see Section 4.5) were either stimulated with 10% FBS or incubated in DMEM/F12 supplemented with 0.5% FBS in the absence or presence of $CD4^+$ T cells. One million HDM-specific $CD4^+$ T cells were added directly to each well. Additionally, MSC were added in the upper chamber of a 0.4-µm-pore Transwell Permeable Support at a 1:5 MSC:$CD4^+$ T cell ratio with GW4869 exosome release inhibitor (Sigma-Aldrich).

To monitor cell proliferation, 50 µM EdU was added to the culture media after 24 hours of a 48-hour co-culture period. The cell suspensions were trypsinized, labeled with CD45-APCy-7 (BD Biosciences), and processed for flow cytometric detection of incorporated Edu and cell DNA content using Click Kit™ Plus EdU Alexa®Fluor™ 488 Flow Cytometry Assay Kit (Life Technologies) and FxCycle™ Violet Stain (Life Technologies) as **in** Section 4.3. The MSC were stained with anti-CD63-APC (Miltenyi Biotec) using a Fixation/Permeabilization Kit (BD Biosciences) as per manufacturer's instructions. Marker expression was assessed by flow cytometry analysis.

4.10. Harvesting of MSC-conditioned media (MSC-CM)

To address a possible immunoregulatory role of MSC on airway inflammation through a paracrine mechanism, MSC-CM was prepared from cultured MSC as previously described [179]. Briefly, cells at 70-80% confluency were washed three times with PBS and incubated with FBS-free DMEM/F12 medium. After 72 hours, the supernatant was gently aspirated and centrifuged at 650·g for 5 min. MSC-CM was concentrated with protein concentrator centrifugal filters (Sigma-Aldrich) with different molecular weight cutoffs to generate MSC-CM at <3 kDa, 3-10 kDa, 10-30 kDa, 30-100 kDa and >100 kDa. For each MSC-CM protein fraction, the total protein concentration was measured by Bradford assay (Bio-rad Laboratories), and lipid concentration was measured with Cobas 6000 analyzer (Roche, Barcelona, Spain).

4.11. Addition of MSC-CM molecular weight fractions to ASM/CD4$^+$ T-cell co-cultures

ASM/HDM-specific CD4$^+$ T-cell co-cultures were set up as in Section 4.8. Different MSC-CM molecular weight fractions, as obtained in Section 4.10, were added to the co-cultures and incubated for 48 hours. ASM cell proliferation and DNA content were determined as detailed in Section 4.8.

4.12. T cell stimulation assay

To analyze T cell cytokine production, blood and lung tissue samples were collected. After the anesthesia overdose, blood from the abdominal cava vein was collected in a tube with 5000 IU/mL heparin (Hospira Invicta S.A.) and centrifuged at 650·g for 5 min. Lung lobes were extracted and chopped with scissors into fragments. The tissue fragments were then suspended in complete DMEM/F12 (Life Technologies) and incubated for 10 min at RT with mild agitation. The suspension was strained using a 50-µm mesh (ImmunoTools) and centrifuged at 650·g for 5 min. The lung and blood cell pellets were lysed using Blood Cell Lysing Buffer as detailed in Section 4.2. After washing, the pellets were resuspended in complete DMEM/F12 and viable cells counted using trypan blue staining solution (Sigma-Aldrich) on Neubauer chamber (ZUZI corp.).

To determine the phenotypes of Th1/Th2/Th17 cells in whole blood and lung tissue, $1{\cdot}10^6$ cells/ml were incubated in a 96-well U bottom plate (Sigma-Aldrich), and 20 ng/mL phorbol 12-myristate 13-acetate (PMA; Sigma-Aldrich) and 500 ng/mL ionomycin (Sigma-Aldrich) were used as cytokine production stimulants, and 2.5 µg/mL brefeldin A (BFA; BD Biosciences) was added as a Golgi apparatus blocker. To identify Treg population, cells were stimulated as described above without BFA. The cells were incubated with this mix for 5 hours.

CD3$^+$ CD8$^-$ T-cell detection was used to help delimitate the CD4$^+$ T-cell subpopulation since CD4$^-$ expression is downregulated when T cells are activated by PMA. The cells were surface-stained with the antibodies listed in **Table 2**, and then fixed and permeabilized using Fixation/Permeabilization Kit (BD Biosciences). Subsequently, anti-IL-17A-PE (clone eBio17B7; eBioscience), anti-IFN-y-PE (clone DB-1; BD Biosciences), anti-IL-4-PE (clone OX-41; BD Biosciences) and anti-Foxp3-PE (clone #376209; R&D Systems, Abington, UK) antibodies were used for intracellular cytokine staining. Isotype

controls (Biolegend-Palex Medical) were used to enable correct flow cytometry compensation and confirm labeling specificity.

After washing, the stained cells were analyzed by flow cytometry. The results were analyzed with MACS Quantify software, and were presented as a percentage of cytokine-producing cells within the $CD4^+$ T-cell subpopulation.

5. Single-dimension SDS gel electrophoresis

Protein concentration was quantified by Bradford assay (Bio-rad Laboratories). Following the determination of MSC-CM protein concentration, the samples were mixed with sample buffer containing 50 mM Tris-HCl (pH 6.8), 10% glycerol, 0.1% bromophenol blue, 2% SDS, and 4% 2ß-mercaptoethanol, heated at 70ºC in a water bath for 10 minutes to denature proteins, and then vortexed before gel loading. Equal amounts (10 µg) of each sample and a SeeBlue Plus2 Pre-stained Standard (Invitrogen) were separated by SDS-polyacrylamide gel electrophoresis on 4-12% Bis/Tris gels (Life Technologies) using 2-(N-morpholino)ethanesulfonic acid (MES) running buffer (diluted 1/20, Life Technologies). The gels were run for 1.5 hours at 35mA and 150V in an XCell Surelock mini gel system (Invitrogen). The membranes were rinsed in distilled water, and Coomassie blue (Invitrogen) was used to stain the gels as per manufacturer's instructions.

6. Proteomics analysis

Each gel lane was cut into 5 bands and stored in distilled water at 4ºC. Mass spectrometry was performed by the Proteomics Platform of the Barcelona Science Park, a member institution of the ProteoRed-ISCIII network.

6.1. Protein digestion

The samples were in-gel digested as follows: The gel bands were washed with ammonium bicarbonate (50 mM NH_4HCO_3) and acetonitrile (ACN). The samples were reduced (DTT 20 mM; 60 min, 60ºC) and alkylated (iodoacetamide 55 mM; 25ºC, 30 min in the dark). Afterwards, the samples were digested overnight at 37ºC with trypsin (sequence grade modified Trypsin, Promega). Finally, the resulting peptide mixtures were

extracted from the gel matrix with 5% formic acid (FA) in 50% ACN, then 100 % ACN, and dried-down in a SpeedVac vacuum system.

6.2. LC-MS/MS analysis

The dried-down peptide mixtures were analyzed in a nanoAcquity liquid chromatographer (Waters) coupled to a LTQ-Orbitrap Velos (Thermo Scientific, USA) mass spectrometer. The tryptic digests were resuspended in 1% FA solution and an aliquot of each sample was injected for chromatographic separation. Peptides were trapped on a Symmetry C18TM trap column (5 µm x 180 µm x 20mm; Waters), and were separated using a C18 reverse-phase capillary column (ACQUITY UPLC BEH column; 130Å, 1.7µm, 75 µm x250 mm, Waters). The gradient used for the elution of the peptides was 1 to 40% B through 30 minutes, followed by 40% to 60% A in 5 min (A: 0.1% FA; B: 100% ACN, 0.1% FA; flow rate : 250 nL/min).

The eluted peptides were subjected to electrospray ionization in an emitter needle (PicoTipTM, New Objective) with an applied voltage of 2000 V. Peptide masses (m/z 300-1700) were analyzed in data dependent mode where a full Scan MS was acquired in the Orbitrap with a resolution of 60,000 FWHM at 400m/z. Up to the 15th most abundant peptides (minimum intensity of 500 counts) were selected from each MS scan, and then fragmented in the linear ion trap using CID (38% normalized collision energy) with helium as the collision gas. The scan time settings were: Full MS: 250 ms (1 microscan) and MSn: 120 ms. Generated .raw data files were collected with Thermo Xcalibur (v.2.2).

6.3. Database search

The .raw data files obtained from the mass spectrometry analyses were used for a search against all *murinae* entries present in the Uniprot public database of 07/06/2019. A small database containing common laboratory contaminants was also entered. The search was performed with SequestHT search engine using Thermo Proteome Discover (v.1.4.1.14).

The following search parameters were applied:

- *Database/Taxonomy:* Uniprot_Murinae_190607_cont.fasta
- *Enzyme:* Trypsin
- *Missed cleavage:* 2
- *Fixed modification:* carbamidomethyl of cysteine
- *Variable modifications:* oxidation of methionine
- *Peptide tolerance:* 10 ppm and 0.6 Da (respectively for MS and MS/MS spectra)
- *Percolator:*
    - Target FDR (Strict): 0.01
    - Target FDR (Relaxed): 0.05
    - Validation based on q-Value

To improve the sensitivity of the database search, Percolator (semi-supervised learning machine) was used in order to discriminate correct from incorrect peptide spectrum matches. Percolator assigns a q-value to each spectrum, which is defined as the minimal FDR at which the identification is deemed correct. These q-values are estimated using the distribution of scores from the decoy database search. The results have been filtered, so only proteins identified with at least 2 medium confidence peptides (FDR≤ 0.05) are included in the list.

7. Data analysis

Statistical analysis was performed using SPSS (version 16.0) software, and graphics were generated using Graphpad Prism 5. Data are presented as mean ± standard error of the mean (SEM) unless otherwise specified. Unpaired t-test was used when comparing two groups, and one-way ANOVA when comparing multiple groups with the appropriate post-ANOVA pairwise comparisons test. When data were found not to be normally distributed, Mann-Whitney's U test was used when comparing two groups, or Kruskal-Wallis test when comparing multiple groups. All treatments were compared to relevant control groups, and the differences were considered significant when $p<0.05$. Bioinformatics analysis and functional classification was performed using PANTHER (http://www.pantherdb.org/) classification system (version 14.1).

RESULTS

1. Development of experimental allergic asthma in a rat model of primary airway allergen exposure.

To mimetize the response to primary allergic sensitization in the airways, the first aim was to investigate whether *i.n.* instillations of standardized *D. pteronyssinus* HDM extract, along with SEB exposure, induce allergic asthma in the Sprague Dawley rat resembling the way sensitization to airborne allergens naturally occurs in humans.

1.1. Primary upper airway exposure to HDM+SEB elicits and modulates airway hyperresponsiveness.

The continued *i.n.* instillation of HDM with SEB induced airway hyperresponsiveness to methacholine in the 15IN model only, as demonstrated by a significant increase in R_L (p<0.001 versus control group) after the 64, 128 and 256 mg/mL MCh doses in comparison with the administration of saline (control group), HDM or SEB alone (**Figure 2B and Table S1 in appendix**). Conversely, co-administration of HDM plus SEB in the 10IN and 30IN models did not induce airway hyperresponsiveness when compared with the respective controls, HDM or SEB groups (**Figure 2A-C and Table S1 in appendix**). These data show that primary allergen exposure of the upper airway induces attenuated airway hyperresponsiveness, which reaches a plateau by week 5 after the first exposure, and fades if *i.n.* antigen exposure continues through 10 weeks.

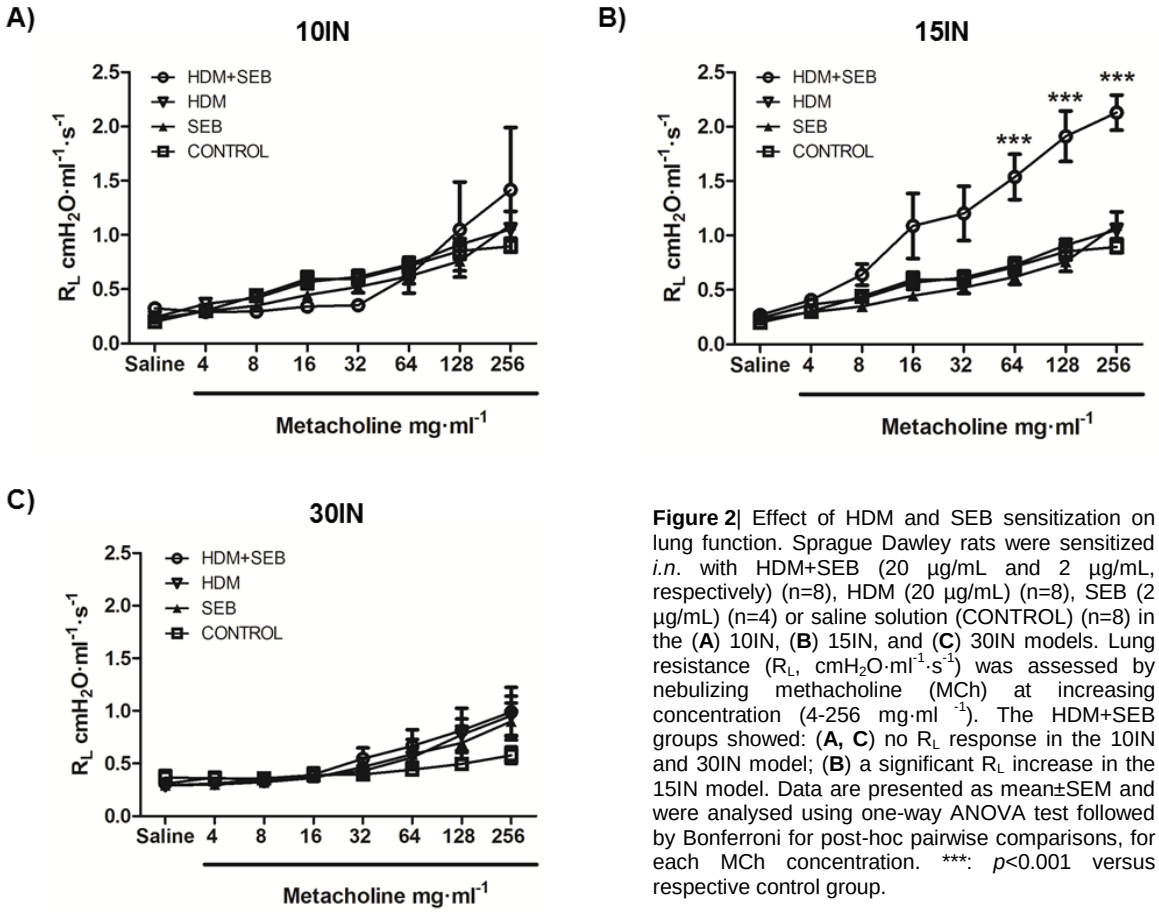

Figure 2| Effect of HDM and SEB sensitization on lung function. Sprague Dawley rats were sensitized *i.n*. with HDM+SEB (20 µg/mL and 2 µg/mL, respectively) (n=8), HDM (20 µg/mL) (n=8), SEB (2 µg/mL) (n=4) or saline solution (CONTROL) (n=8) in the (**A**) 10IN, (**B**) 15IN, and (**C**) 30IN models. Lung resistance (R_L, cmH$_2$O·ml^{-1}·s^{-1}) was assessed by nebulizing methacholine (MCh) at increasing concentration (4-256 mg·ml $^{-1}$). The HDM+SEB groups showed: (**A, C**) no R_L response in the 10IN and 30IN model; (**B**) a significant R_L increase in the 15IN model. Data are presented as mean±SEM and were analysed using one-way ANOVA test followed by Bonferroni for post-hoc pairwise comparisons, for each MCh concentration. ***: p<0.001 versus respective control group.

1.2. Primary exposure with HDM+SEB in the lung increases allergic response.

Total serum IgE was significantly increased (p=0.002 versus control group) in the 15IN model after co-administration of HDM plus SEB, while administration of SEB or HDM alone did not increase total serum IgE, being similar to the control group (**Figure 3B and Table S2 in appendix**). In the 10IN and 30IN models, instillation of HDM+SEB, HDM, or SEB alone did not increase the total IgE response when compared with the respective control animals (**Figure 3A-C and Table S2 in appendix**). Therefore, increased total serum IgE in the HDM+SEB-challenged animals showed a trend consistent with the airway responsiveness data. Total BAL IgE was under the limit of detection (ROD).

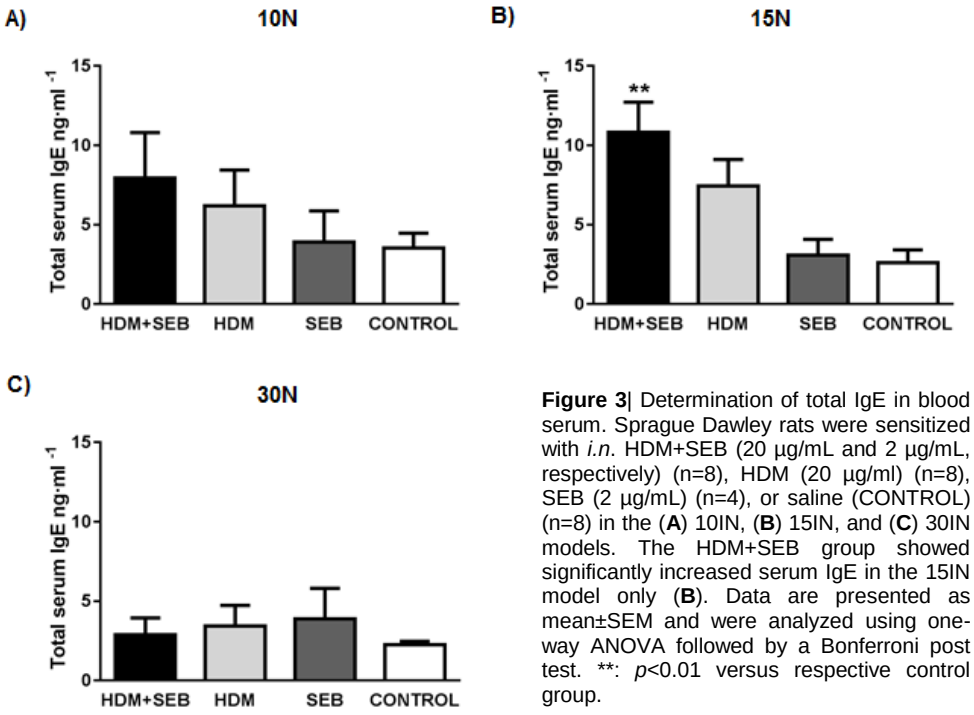

Figure 3| Determination of total IgE in blood serum. Sprague Dawley rats were sensitized with *i.n*. HDM+SEB (20 µg/mL and 2 µg/mL, respectively) (n=8), HDM (20 µg/ml) (n=8), SEB (2 µg/mL) (n=4), or saline (CONTROL) (n=8) in the (**A**) 10IN, (**B**) 15IN, and (**C**) 30IN models. The HDM+SEB group showed significantly increased serum IgE in the 15IN model only (**B**). Data are presented as mean±SEM and were analyzed using one-way ANOVA followed by a Bonferroni post test. **: p<0.01 versus respective control group.

Given that only the 15IN model elicited airway inflammation and hyperresponsiveness associated with an IgE-mediated adaptive immune response, we did not pursue further investigations in the 10IN and 30IN models. We selected the 15IN model for further development.

1.3. Primary airway exposure to HDM+SEB induces a mucoid response, increased subepithelial extracellular matrix deposition, and increased airway contractile mass.

Histological examination of haematoxylin and eosin-stained lung sections from rats of the 15IN-model HDM+SEB group showed strong airway inflammatory infiltrates, narrowing of the airway lumen, and airway wall remodeling. The SEB group showed faint inflammatory infiltrates. The HDM animals were devoid of airway inflammation, as were the control animals (**Figure 4A-D**).

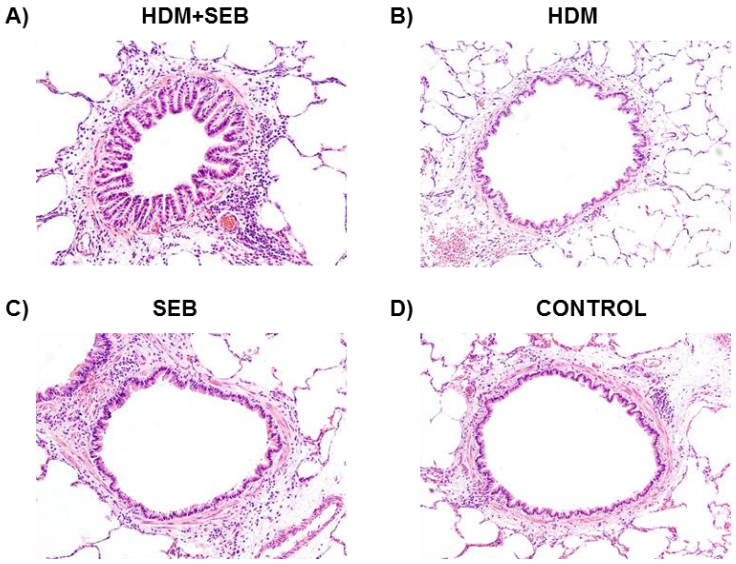

Figure 4| H-E staining of tissue sections. Histological examination of lung tissue sections after sensitization. Sprague Dawley rats were sensitized *i.n.* with HDM+SEB (20 µg/ml and 200 ng/0.1 ml, respectively) (n=8), HDM (20 µg/ml) (n=8), SEB (200 ng/0.1 ml) (n=4) or saline solution (CONTROL) (n=8) in 15IN model. HDM+SEB animals showed strong inflammatory infiltrates (**A**). HDM group (**B**) showed no inflammatory infiltrates in the airways, similarly to the control group (**D**). In the SEB group, the rats showed attenuated infiltrates (**C**).

With the aim of studying the mucous secretory response and goblet cell hyperplasia in the lungs, as features of tissue remodeling in asthma, tissue sections were stained with Periodic acid Schiff (PAS). The load of intraepithelial stored mucus was quantitatively assessed in the upper and lower airways. Co-administration of HDM and SEB, or SEB alone, significantly increased the PAS-positive cells in the airways compared to the control group or HDM individually (**Figure 5A-D**). Therefore, the mucus load in the airway epithelium was more patent in HDM plus SEB (p<0.001 versus control group) or SEB alone (p=0.006 versus control group), while HDM alone did not increase the mucus load, being in this case similar to the control animals (**Figure 5E and Table S3 in appendix**).

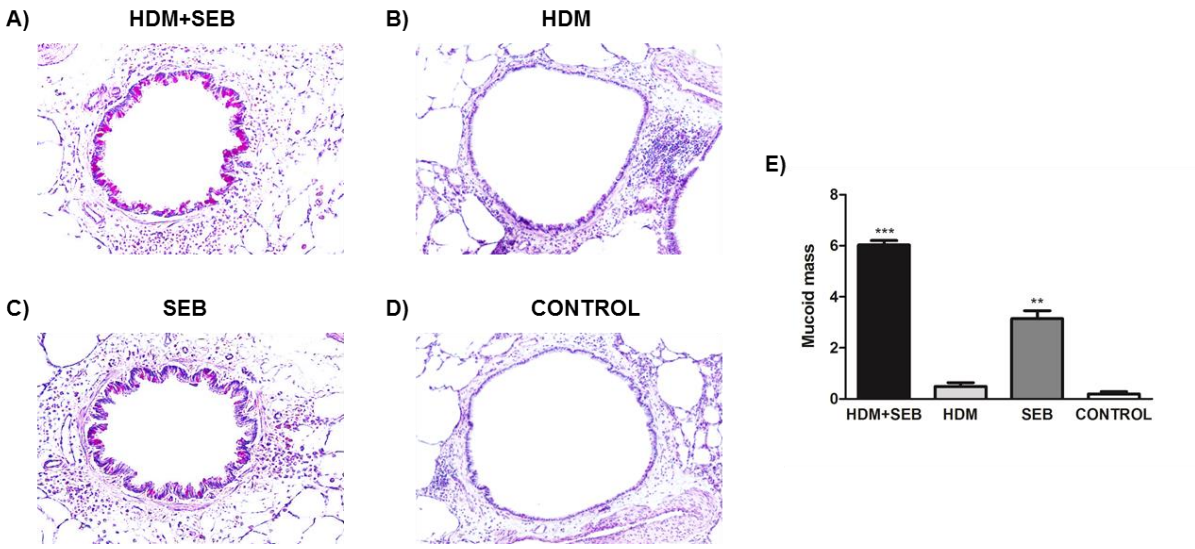

Figure 5| PAS staining of tissue sections. Histological examination of lung tissue sections after sensitization. Lung tissue sections were stained with PAS to quantify goblet cell number and mucus load. Sprague Dawley rats were sensitized *i.n.* with HDM+SEB (20 µg/ml and 2 µg/mL, respectively) (n=8), HDM (20 µg/ml) (n=8), SEB (2 µg/mL) (n=4) or saline solution (CONTROL) (n=8) in 15IN model. The micrographs show representative airways from the (**A**) HDM+SEB, (**B**) HDM, (**C**) SEB, and (**D**) control groups. (**E**) Mucus load quantification. The HDM+SEB group showed a strong mucus response, while the SEB group showed a significant but attenuated response. The control and HDM groups showed no mucous response in the lungs. Data are presented as mean±SEM and were analyzed using one-way ANOVA. ***: $p<0.001$; **: $p<0.01$ versus control group.

To evaluate subepithelial fibrosis as an asthma airway remodeling feature, Masson's trichrome stained lung sections were processed to extract and measure the trichrome blue dye component, which overall reflects extracellular matrix deposition. The dimensionless index resulting from normalization by airway size was termed “extracellular matrix mass”. The extracellular matrix mass was significantly increased in the HDM plus SEB group ($p=0.007$ versus control group) or SEB alone ($p=0.030$ versus control group), while HDM alone did not increase the extracellular matrix deposition (**Figure 6 and Table S4 in appendix**).

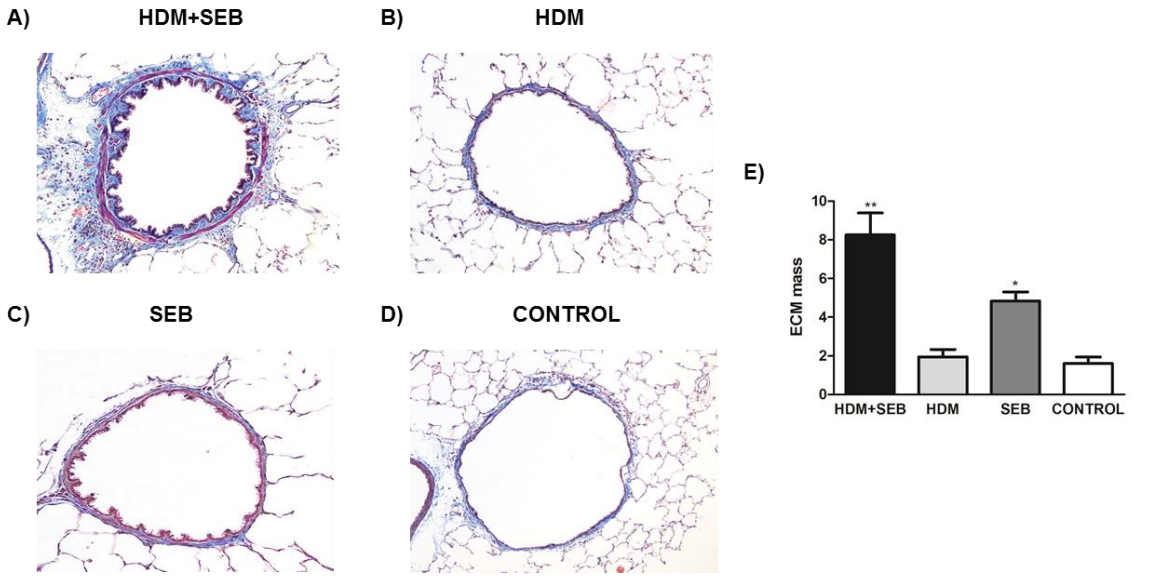

Figure 6| Trichrome staining of tissue sections. Sprague Dawley rats were sensitized *i.n.* with HDM+SEB (20 µg/ml and 2 µg/mL, respectively) (n=8), HDM (20 µg/ml) (n=8), SEB (2 µg/mL) (n=4) or saline solution (CONTROL) (n=8) in the 15IN model. Masson's trichrome was employed to evaluate subepithelial fibrosis, quantitatively evaluated as extracellular matrix mass (ECM). The extracellular matrix stained blue, and the ECM mass was calculated by digital color extraction. Representative airways of challenged animals in the (**A**) HDM+SEB, (**B**) HDM, (**C**) SEB, and (**D**) control groups are shown. (**E**) ECM was significantly increased in the HDM+SEB and SEB groups. Conversely, the HDM group showed light subepithelial collagen deposition similar to the control animals. Data are presented as mean±SEM and were analyzed using one-way ANOVA. *: $p<0.05$; **: $p<0.01$ versus control group.

Airway contractile tissue mass was quantified based on α-SMA immunofluorescence and digital signal extraction and processing. The dimensionless index resulting from normalization by airway size was termed “airway contractile mass”. In the HDM+SEB and SEB groups, the ASM mass was significantly increased in comparison with the control group or HDM alone (**Figure 7A-C**). Co-administration of HDM and SEB increased the airway contractile mass ($p=0.001$ versus control group). In the SEB group, it was weakly but significantly increased ($p=0.023$ versus control group). The HDM group did not show any increment in the ASM mass (**Figure 7E and Table S5 in appendix**).

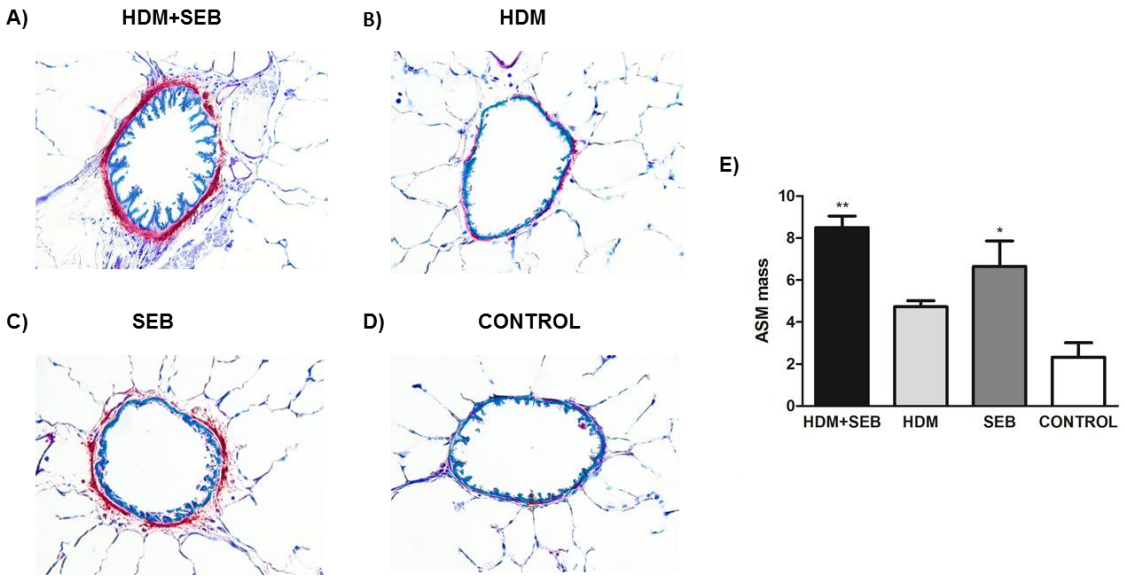

Figure 7| Immunohistochemical detection of alpha-SMA and airway contractile tissue mass (ASM mass) quantification in airway sections. Sprague Dawley rats were sensitized *i.n.* with HDM+SEB (20 µg/ml and 2 µg/mL, respectively) (n=8), HDM (20 µg/ml) (n=8), SEB (2 µg/mL) (n=4) or saline solution (CONTROL) (n=8), 3 times per week, for 5 weeks. The (**A**) HDM+SEB and (**C**) SEB groups showed significantly increased ASM mass versus (**D**) control, while increased ASM mass was absent in (**B**) the HDM group. Data are presented as mean±SEM and were analyzed using one-way ANOVA. *: $p<0.05$; **: $p<0.01$ versus control group.

1.4. Primary airway exposure to HDM+SEB generates eosinophilic recruitment in the lung.

To further confirm that sensitization to HDM and SEB leads to an increased number of leukocytes in the lungs, we performed flow cytometry analysis of BAL from all groups using specific leucocyte biomarkers.

We used antibodies targeted against a range of cell surface antigens (**Table 1**) and a gating strategy accordingly (**Figure 8**). To select singlets, we used the FSC-H and FSC-W parameters to identify and exclude cells stuck together (doublets) and larger clumps. This gating resulted in a population of single live leukocytes, which were then sequentially separated, first for the $CD172^+$ and $CD172^-$ populations. Next, the $CD172^-$ population was separated to identify T lymphocytes by CD3 expression. NK cells were identified by CD161, and B Cells by CD45R, within the $CD3^-$ population. We gated on negative CD172 expression and high granularity marker HIS48 to identify eosinophils. $CD172^+$ cells were gated to identify neutrophils and macrophages. Neutrophils were identified by high HIS48 and CD43 expression, while macrophages were negative for these markers (**Figure 8**).

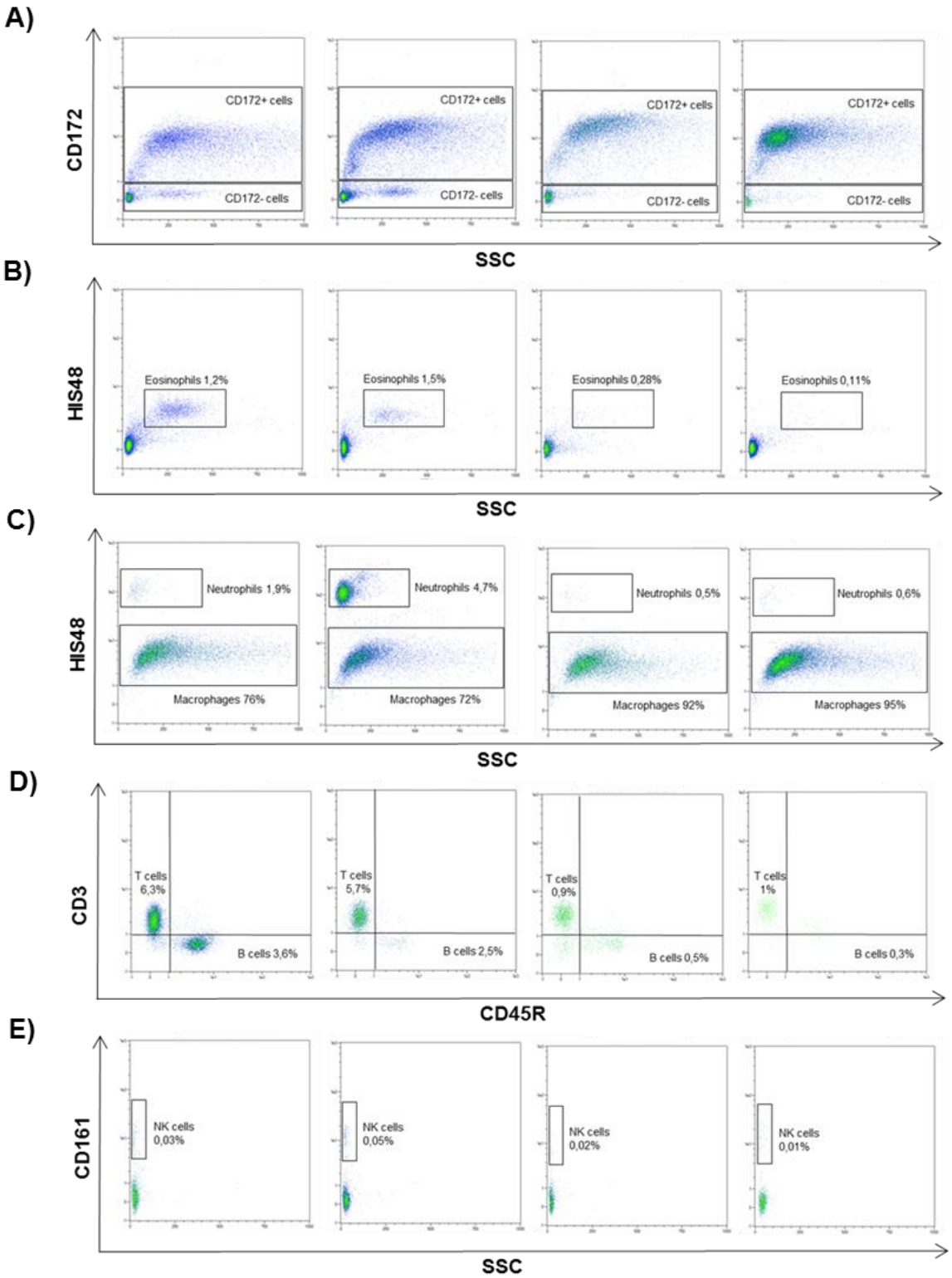

Figure 8| Flow cytometry analysis of bronchoalveolar lavage (BAL). Sprague Dawley rats were sensitized *i.n.* with saline HDM+SEB (20 µg/ml and 2 µg/mL, respectively) (n=8), HDM (20 µg/ml) (n=8), SEB (2 µg/mL) (n=4) or saline solution (CONTROL) (n=8), 3 times per week, for 5 weeks. Representative dot plots show the gating strategy. Cells were first gated by Fixable Viability dye cell marker. The negative (viable) cell population was gated by CD45 labeling, and the $CD45^+$ population was selected to identify leukocytes. Then, the $CD172^+$ population (**A**) was selected and gated by HIS48 versus SSC to identify neutrophils and macrophages (**C**). The $CD172^-$ cells were gated to identify eosinophils by HIS48 versus SSC (**B**). Lymphocytes were selected and gated by CD3 and CD45R to identify T and B cells (**D**), while double negative CD3 and CD45R population was used to select NK cells by CD161 expression (**E**).

Macrophages were decreased in the HDM+SEB (p=0.034 versus control) and HDM groups (p=0.013 versus control group), but not in the SEB group (**Figure 9A and Table S6 in appendix**). Neutrophils were only increased when the rats were treated with HDM alone (p=0.006 versus control group), while SEB alone or HDM+SEB did not significantly increase this cell subset (**Figure 9B and Table S6 in appendix**). Eosinophil recruitment to BAL was increased after co-administration of HDM with SEB (p=0.024 versus control group) or HDM alone (p=0.026 versus control). However, SEB alone did not increase the eosinophil numbers compared to the control group (**Figure 9C and Table S6 in appendix**). NK cells increased in the HDM rats only (p=0.010 versus control group), while SEB alone or HDM+SEB did not significantly modify these cells when compared to the control animals (**Figure 9D and Table S6 in appendix**). We observed that the adaptive T cell response was increased by co-administration of HDM with SEB (p=0.008 versus control group) or HDM alone (p=0.032 versus control group). SEB alone did not increase T-cell recruitment, being similar to the control group (**Figure 9E and Table S6 in appendix**). B cells numbers were increased when the rats were co-administered HDM plus SEB (p=0.005 versus control group) but not SEB or HDM alone (**Figure 9F and Table S6 in appendix**).

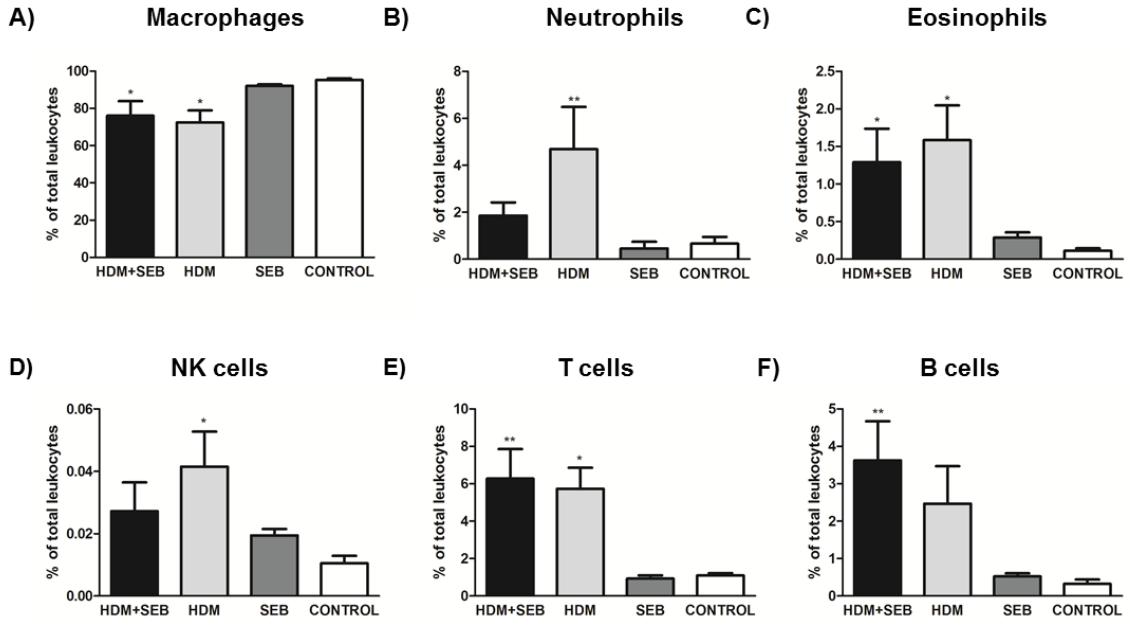

Figure 9| Effect of HDM in combination with SEB on cell recruitment in bronchoalveolar lavage (BAL). Sprague Dawley rats were sensitized *i.n.* with saline solution, HDM+SEB (20 µg/ml and 2 µg/mL, respectively) (n=8), HDM (20 µg/ml) (n=8), SEB (2 µg/mL) (n=4), or saline solution (CONTROL) (n=8), 3 times per week, for 5 weeks. The HDM+SEB animals showed strong recruitment of eosinophils (**C**) and B cells (**F**) in comparison with the control group. The HDM or SEB alone groups showed no recruitment of these cells compared with the control group. The HDM+SEB and HDM groups showed recruitment of T cells (**E**) with the macrophages (**A**) decreased in comparison with the control group. Only the HDM group generated neutrophil (**B**) an NK-cell (**D**) recruitment. Data are presented as mean±SEM and analyzed with one-way ANOVA. *: p<0.05; **: p<0.01 versus control group.

We observed down-regulation of CD161 expression by B cells after co-administration of HDM plus SEB (p=0.003 versus control), while SEB or HDM alone did not significantly decrease this marker (**Figure 10A, B and Table S6 in appendix**).

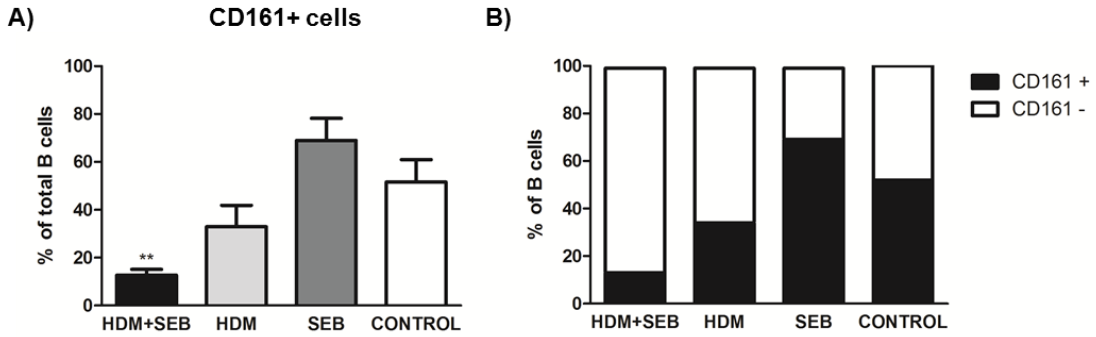

Figure 10| Effect of HDM in combination with SEB on CD161 expression by B cells in bronchoalveolar lavage (BAL). Sprague Dawley rats were sensitized *i.n.* with HDM+SEB (20 µg/ml and 2 µg/mL, respectively) (n=8), HDM (20 µg/ml) (n=8), SEB (2 µg/mL) (n=4) or saline (CONTROL) (n=8), 3 times per week, for 5 weeks. The HDM+SEB group showed decreased CD161 expression by B cells in comparison with the control group. The HDM and SEB groups were similar to the control group. Data are presented as mean±SEM and analyzed with one-way ANOVA. **: p<0.01 versus control group.

1.5. Airway allergic inflammation is HDM-specific, not SEB-specific.

Sensitization with HDM+SEB led to significantly increased (p<0.001 versus control) levels of HDM-specific IgE in BAL, while SEB or HDM alone had no effect over control (**Figure 11A and Table S7 in appendix**). HDM+SEB, but not HDM alone, also led to significantly increased serum HDM-specific IgE (p<0.002 versus control group). (**Figure 11C and Table S7 in appendix**). The increased HDM-specific IgE in the HDM+SEB-challenged animals showed a trend consistent with the total IgE data. We did not observe any significant difference in the concentration of BAL or serum SEB-specific IgE upon sensitization with HDM+SEB, HDM, or SEB individually, in comparison with the control group (**Figure 11B, D; Table S8 in appendix**).

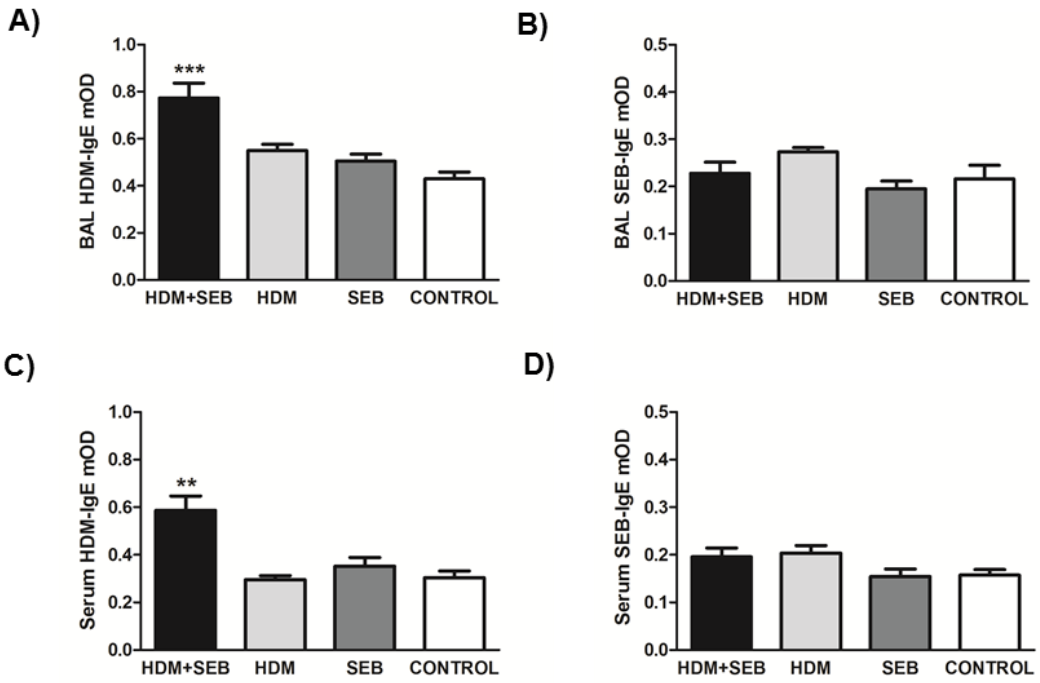

Figure 11| Determination of HDM- and SEB-specific IgE in bronchoalveolar lavage (BAL) and blood serum. Data are protein concentration as measured by ELISA. Sprague Dawley rats were sensitized *i.n.* with HDM+SEB (20 µg/mL and 2 µg/ mL, respectively) (n=8), HDM (20 µg/ml) (n=8), SEB (2 µg/mL) (n=4) or saline solution (CONTROL) (n=8), 3 times per week, for 5 weeks. BAL (**A**) and serum (**C**) HDM-specific IgE was significantly increased in the HDM+SEB group, while the HDM and SEB groups showed no HDM-specific response compared to the control group. All groups showed no BAL (**B**) or serum (**D**) SEB-specific IgE response. Data are presented as mean±SEM optical density (mOD) and analyzed with one-way ANOVA. **: $p<0.01$; ***: $p<0.001$ versus control group.

1.6. Primary airway exposure to HDM+SEB decreases the IgG response.

BAL levels of total IgG were significantly decreased after HDM+SEB instillations ($p<0.034$ versus control group), while administration of SEB or HDM alone did not increase total IgG (**Figure 12 and Table S9 in appendix**). Serum IgG was under the limit of detection (ROD).

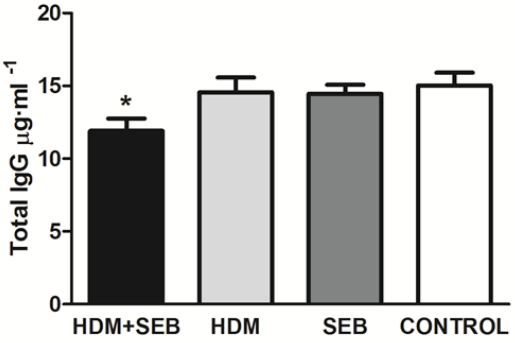

Figure 12| Determination of total IgG in bronchoalveolar lavage (BAL). Data are protein expression as measured by ELISA. Sprague Dawley rats were sensitized *i.n.* with HDM+SEB (20 µg/mL and 2 µg/mL, respectively) (n=8), HDM (20 µg/ml) (n=8), SEB (2 µg/mL) (n=4) or saline solution (CONTROL) (n=8), 3 times per week, for 5 weeks. The HDM+SEB group showed significant total IgG decrease, while the HDM and SEB groups were similar to the control group. Data are presented as mean±SEM and analyzed with one-way ANOVA. *: $p<0.05$ versus control group.

1.7. The allergic response to HDM+SEB induces the release of Th2 cytokines.

To investigate the mechanism underlying the observed allergic inflammation, we measured a range of asthma-related cytokines in BAL and serum. IL-4 was increased in BAL of the HDM+SEB (p=0.005 versus control group) and SEB rats (p=0.022 versus control group). HDM alone did not increase IL-4 (**Figure 13A and Table S10 in appendix**). IL-13 was increased in the HDM+SEB (p=0.009 versus control) and SEB (p=0.007 versus control group) groups, while HDM alone did not significantly modify IL-13 production (**Figure 13B and Table S10 in appendix**). IL-17A was increased in the HDM+SEB group (p=0.043 versus control) and HDM (p=0.035 versus control), but not the SEB group (**Figure 13C and Table S10 in appendix**). IFN-γ was increased in the HDM+SEB group only (p=0.012 versus control) and HDM (p=0.035) (**Figure 13D and Table S10 in appendix**). IL-5 was increased in the HDM+SEB (p=0.006 versus control), SEB (p=0.046 versus control), and HDM (p=0.005 versus control) groups (**Figure 13E and Table S10 in appendix**). Eotaxin was increased in the HDM+SEB (p=0.002 versus control) and HDM (p=0.003 versus control), while SEB alone did not modify eotaxin production (**Figure 13F and Table S10 in appendix**). TNF-α was under the ROD.

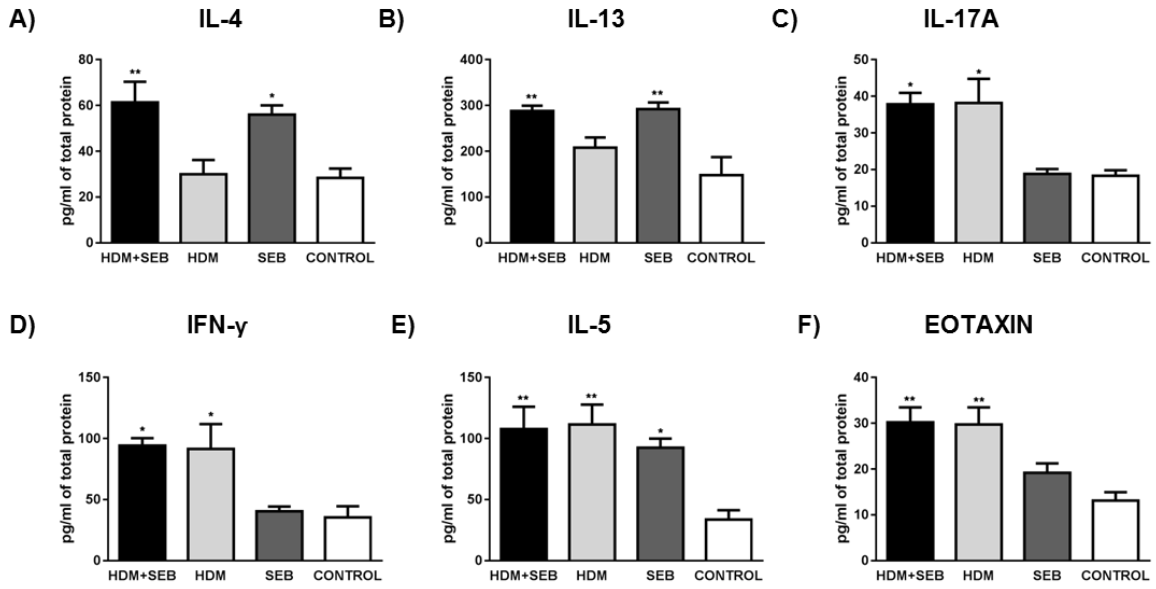

Figure 13| Determination of cytokine concentrations in bronchoalveolar lavage (BAL). Sprague Dawley rats were sensitized *i.n.* with HDM+SEB (20 µg/mL and 2 µg/mL, respectively) (n=6), HDM (20 µg/ml) (n=6), SEB (2 µg/mL) (n=4) or saline (CONTROL) (n=6), 3 times per week, for 5 weeks. The HDM+SEB and SEB groups showed significantly increased IL-4 (**A**) and IL-13 (**B**), but not the HDM group. IL-17 (**C**), IFN-γ (**D**) and Eotaxin (**F**) were significantly increased in the HDM+SEB and HDM groups, and not in the SEB group. All groups showed increased IL-5 (**E**). Data are presented as mean±SEM and analyzed using one-way ANOVA. *: p<0.05; **: p<0.01, versus control group.

In blood serum, IL-5 was increased in the HDM+SEB (p<0.001 versus control) and SEB (p<0.001 versus control) groups. HDM alone did not lead to increased IL-5 (**Figure 14A and Table S11 in appendix**). None of the groups had increased IL17-A, IL-13, eotaxin, or TNF-α when compared with the control animals (**Figure 14C-E and Table S11 in appendix**). The serum concentration of IFN-y and IL-4 was under the ROD.

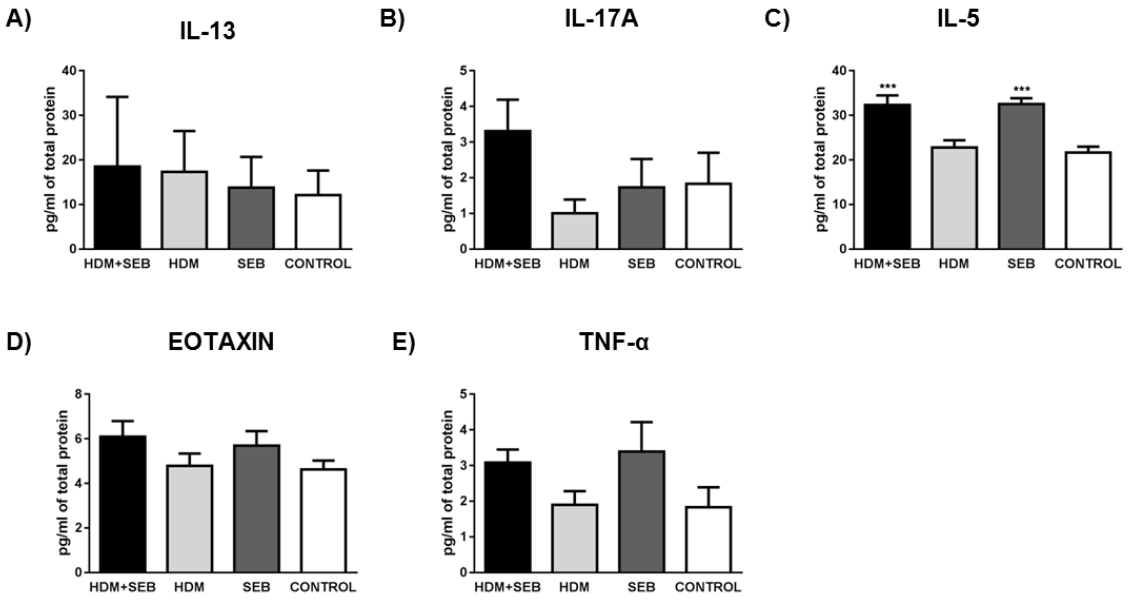

Figure 14| Determination of cytokine concentrations in blood serum. Sprague Dawley rats were sensitized *i.n.* with HDM+SEB (20 µg/mL and 2 ng/mL, respectively) (n=6), HDM (20 µg/ml) (n=6), SEB (2 µg/mL) (n=5), or saline (CONTROL) (n=6), 3 times per week, for 5 weeks. IL-13 (**A**), IL-17 (**B**), Eotaxin (**D**), and TNF-α (**E**) were similar to the control group. The HDM+SEB and SEB groups showed increased IL-5, while the HDM group was similar to the control group (**C**). Data are presented as mean±SEM and were analyzed using one-way ANOVA. *: p<0.05; ***: p<0.001 versus the control group.

2. Role of MSC in airway remodeling *in vitro*: pathogenic versus suppressive arms.

As a second objective of the present work, we tested whether HDM allergen activates effector $CD4^+$ T cells and elicits airway myocyte proliferation upon direct contact *in vitro*, as previously shown for OVA [107]. We reproduced consistent results showing that direct contact between HDM-specific $CD4^+$ T cells and ASM induces ASM cell proliferation and $CD4^+$ T cell survival *in vitro*. We then employed this model to investigate whether adipose-derived MSC, added to the $CD4^+$ T cell/ASM co-culture, interfere with ASM proliferation induced by effector $CD4^+$ T cells.

2.1. ASM cell and MSC isolation and culture

To verify the proper phenotype and purity of the ASM cell and MSC cultures, we performed flow cytometry analysis as previously reported [169]. MSC cultured in selective differentiation medium produced calcified extracellular matrix upon culture in osteogenic differentiation medium as demonstrated by alizarin-red staining (**Figure 15A**), or fat deposits upon culture in adipogenic differentiation medium as shown by oil-red O staining (**Figure 15B**). Using antibodies against a range of cell surface antigens (**Table 3**), the adherent cell population cultured in MSC selective medium was SSC^{high} and $CD45^-$ $CD29^+$ $CD90^+$ (**Figure 15C**). As for the ASM cells cultured in SMC selective medium, multiparameter flow cytometry analysis showed a SSC^{high}, $CD45^-$ and $\alpha\text{-SMA}^+$ phenotype (**Figure 15D**).

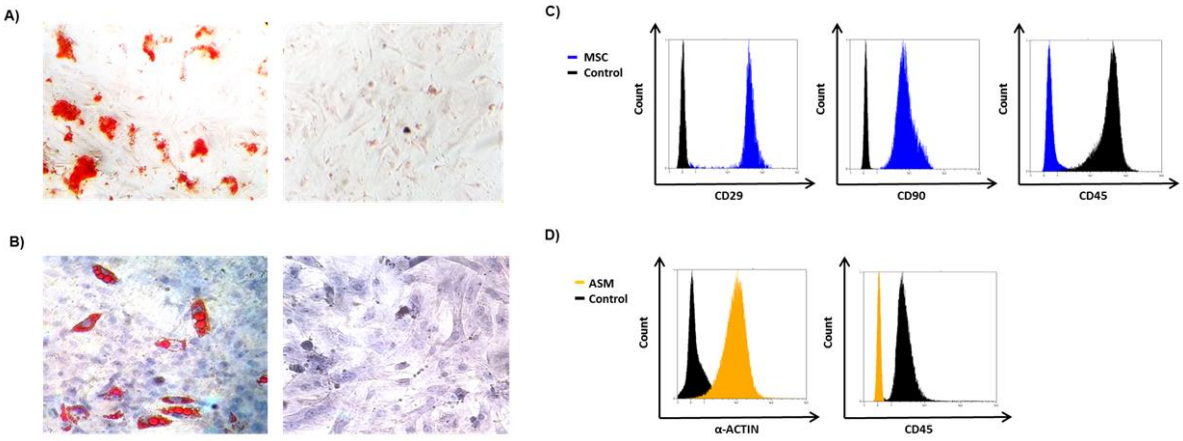

Figure 15| Phenotyping of ASM cells and MSC. (**A**) MSC produced calcified extracellular matrix upon culture in osteogenic differentiation medium as demonstrated by alizarin-red staining, and (**B**) fat deposits upon culture in adipogenic differentiation medium as shown by oil-red O staining. Cells cultured in non-MSC-selective medium were used as a negative control. (**C**) Cell phenotyping by flow cytometry. Black histograms are from control cultures. MSC are $CD29^+$ $CD90^+$ $CD45^-$. (**D**) ASM cell populations are $CD45^-$ and alpha-smooth muscle $actin^+$. Data are representative from n= 6 independent experiments.

2.2. Generation of HDM-specific CD4+ T cells by *in vitro* antigen stimulation

We performed *in vitro* antigen stimulation to generate HDM-specific $CD4^+$ T cells from rats i.p.-sensitized to HDM adsorbed on $AlOH_3$ suspension. These cells can then be identified by flow cytometry as $CD45^+$, $CD3^+$, and $CD4^+$. Following culture of total splenocytes, the percentage of live $CD4^+$ T cells was enriched through the stimulation time in culture, increasing from 35.65% to 52.87% by day 6 (p=0.014 versus day 0) (**Figure 16A and Table S12 in appendix**). This enrichment is attributable to combined clonal expansion of activated, antigen-specific $CD4^+$ T cells and extensive apoptosis of other cell subsets. Proliferating $CD4^+$ T cell, identified as per EdU incorporation, were increased in the HDM-activated cultures on day 6, compared with naive $CD4^+$ T cells (cultured from unsensitized animals and with no *in vitro* stimulation) (p<0.001 versus CD4ns) or CD4s cells prior to stimulation (p=0.004 versus CD4s day 0) (**Figure 16B, C and Table S12 in appendix**). We found no differences in proliferative activity (EdU incorporation) between activated and naive $CD4^+$ T cells on day 0 (**Figure 16B and Table S12 in appendix**).

The antigen-stimulated cells upregulated CD4 expression from day 0 to 6 (p=0.024, day 6 versus day 0) as an effect of activation. Such CD4 upregulation was also significant in comparison with the naive $CD4^+$ T cells (p=0.034, CD4s on day 6 versus CD4ns). No difference in CD4 mean fluorescence intensity (MFI) was found between the antigen-stimulated $CD4^+$ T cells on day 0 and their naive counterpart (**Figure 16D and Table S12 in appendix**). We obtained efficient purification of CD4s and CD4n T cells (>95%) for co-culture experiments (**Figure 16A**).

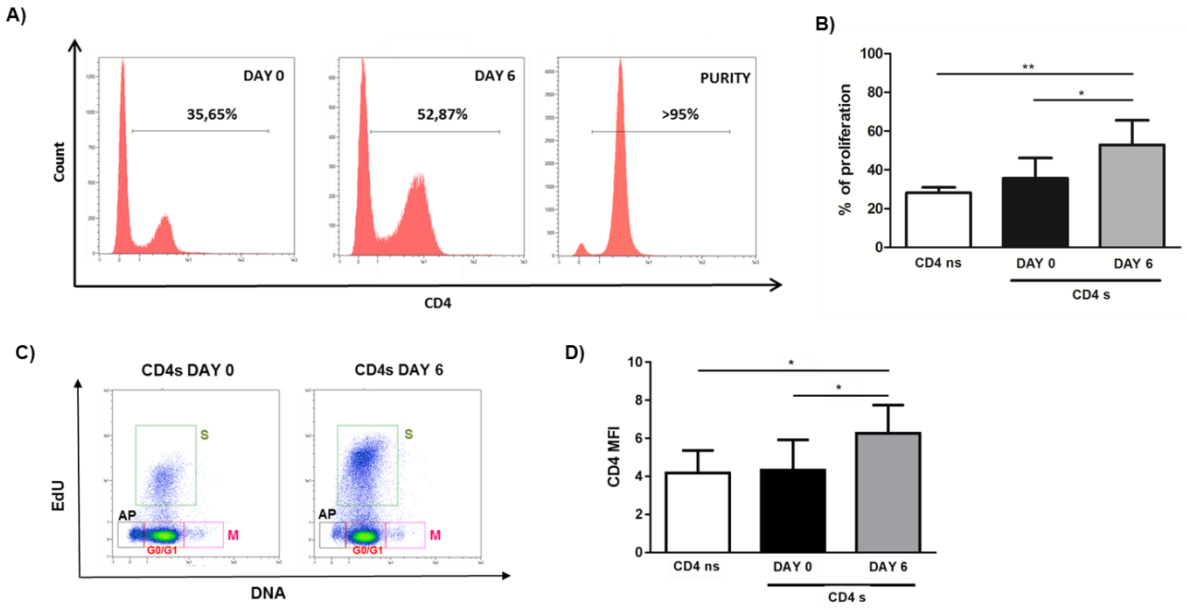

Figure 16| $CD4^+$ T cell isolation and HDM-specific $CD4^+$ T cell activation. (**A**) HDM stimulation of whole splenocyte cultures from rats *i.p.*-sensitized with HDM+$AlOH_3$ led to progressive enrichment of $CD4^+$ T cells, which yielded high $CD4^+$ T-cell purity after immunomagnetic separation. (**B**) Percentage of $CD4^+$ T cells with EdU incorporation in splenocyte cultures from naive and HDM+$AlOH_3$-sensitized rats on day 0 and upon 6-day stimulation. (**C**) Analysis of $CD4^+$ T-cell proliferation and cell cycle by EdU incorporation and cell DNA content. Cell cycle phases G0/G1, S, and M are shown. Apoptotic (AP) cells are identified as subdiploid as per DNA content. (**D**) CD4 mean expression of $CD4^+$ T cells from spleen of naive and HDM+$AlOH_3$-sensitized rats on day 0 and at 6 days of stimulation. Data (n= 6) independent experiments per group. *: p<0.05; **: p<0.01; ***: p<0.001.

2.3. Cell contact between cultured ASM cells and activated $CD4^+$ T cells induces ASM cell proliferation.

We tested whether, in line with an OVA-based previous study employing Brown Norway rats [108], direct T-cell/ASM-cell contact induces myocyte proliferation by using Sprague Dawley rat splenocytes and stimulation with HDM. We co-cultured cell cycle-arrested ASMs or ASMns cells with $CD4^+$ T cells isolated from HDM-sensitized donors. The $CD4^+$ T cells had been either activated with HDM *in vitro* or let stay with no antigen stimulation. The ASM cells were cell cycle-arrested and, after 48 hours of co-culture, ASM cell proliferation was analysed by flow cytometry on the basis of EdU incorporation during the last 24 hours and cell cycle profiling by DNA content. Following trypsin treatment of the co-cultures, using antibodies targeted against a range of surface antigens our gating strategy in co-culture (**Figure 17**). Following activation by HDM *in vitro* and 48 hours of subsequent co-culture with the ASM cells, a fraction of the $CD4^+$ T cells progressed through the cell cycle and synthesized DNA. Both the ASM and T cells comprised EdU^+ cells that were in S phase of the cell cycle. Another fraction of the $CD4^+$ T cells, likely comprising non-HDM-specific T cells, did not incorporate EdU and stayed as quiescent

(EdU$^-$ cells in G0/G1 phase), live post-mitotic (EdU$^-$ cells in G2/M phase), or apoptotic cells (EdU$^-$ cells with sub-diploid DNA content) (**Figure 17**).

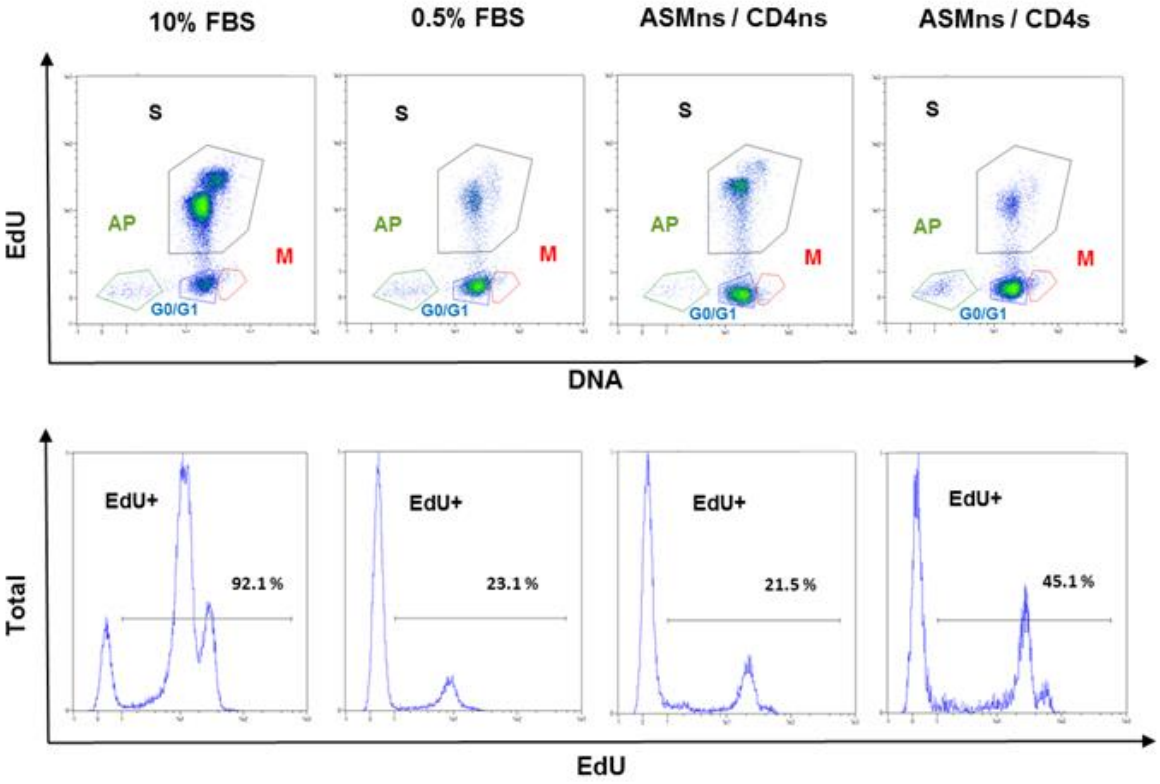

Figure 17| Activated, HDM-specific CD4$^+$ T cells induce airway myocyte proliferation, dependent on direct ASM-cell/CD4$^+$ T cell contact. Top: ASM-cell EdU incorporation. Bottom: ASM cell cycle. The plots show representative examples of proliferation positive control (10% fetal bovine serum, FBS), negative control (0.5% FBS), and co-culture with naive or activated HDM-specific CD4$^+$ T cells, respectively. Data (n = 6) independent experiments per group.

Mean baseline EdU incorporation by ASM cells cultured with 0.5% FBS after cell cycle arrest was 23.13%. Direct contact between CD4s T cells and either ASMs or ASMns cells induced DNA synthesis by the myocytes (p<0.001 versus 0.5% FBS group) (**Figure 18A and Table S13 in appendix**). Whether the ASM cells were ASMs or ASMns, it did not influence the EdU incorporation response induced by direct contact with CD4s cells (p=0.389). There was also no difference in EdU incorporation by the ASM cells, whether ASMs or ASMns, upon co-culture with CD4n T cells in contact or through Transwell (**Figure 18A and Table S13 in appendix**). Direct contact between ASMs or ASMns cells with CD4s cells increased the number of CD4s cells in S phase (p=0.005 versus ASMns+CD4ns and p=0.003 versus ASMs+CD4ns), and decreased the ASM cells in G0/G1 phase (p=0.002 versus ASMns + CD4ns group and p=0.023 versus ASMs + CD4ns group) (**Figure 18C and Table S13 in appendix**). For the CD4$^+$ T cells in direct contact with ASM cells, no differences were observed in the apoptotic or G2/M states (**Figure 18C and Table S13 in appendix**). We did not observe any differences in EdU

incorporation by ASMs or ASMns cells, or S-phase differences, when co-cultured with CD4ns or CD4s T cells separated by a Transwell chamber (**Figure 18B and Table S14 in appendix**). We did observe that co-culture of ASMs or ASMns cells with CD4s T cells separated by a Transwell chamber increased the frequency of CD4s and CD4ns apoptotic cells (p=0.009 versus ASMns + CD4ns group and p=0.008 versus ASMs + CD4ns group), and decreased the numbers of cells in G0/G1 phase (p=0.003 versus ASMns + CD4ns group and p=0.003 versus ASMs + CD4ns group) (**Figure 18D and Table S14 in appendix**). No differences were observed in the G2/M state under any of the experimental conditions.

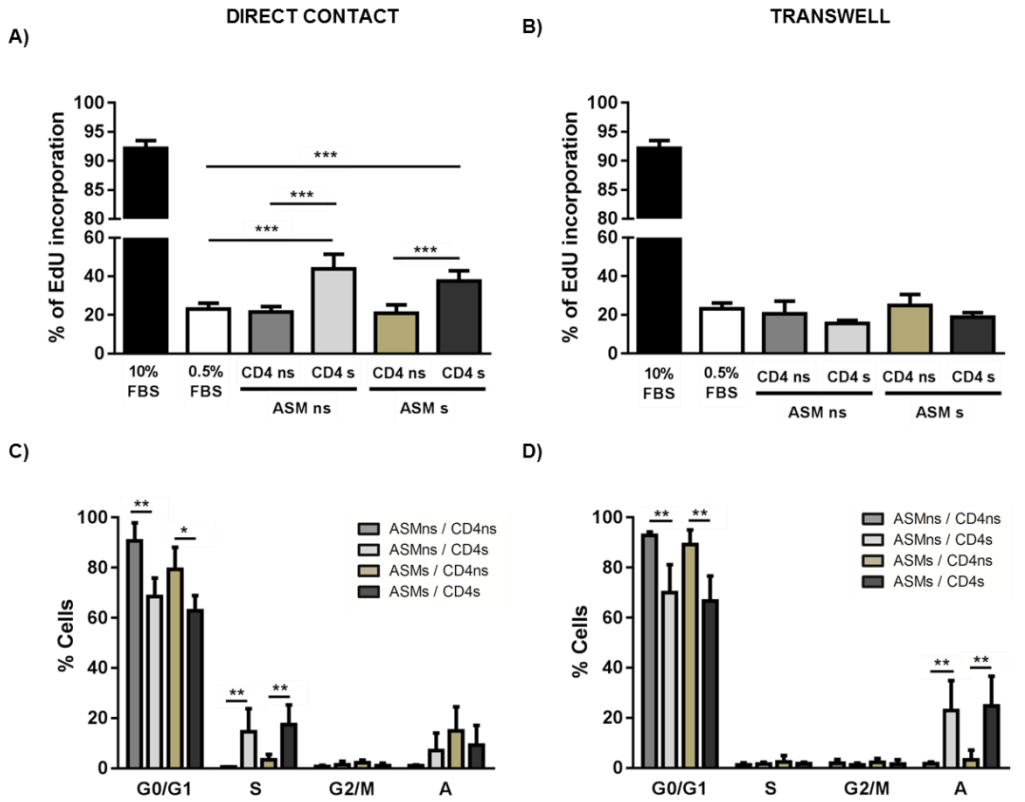

Figure 18| Activated, HDM-specific $CD4^+$ T cells induce airway myocyte proliferation, dependent on direct ASM-cell/T-cell contact. (**A** and **B**) EdU incorporation by ASM cells. ASM cells incubated with 0.5% FBS was the negative control for cell proliferation. Addition of 10% FBS served as positive control for proliferation. The ASMs and ASMns were co-cultured in direct contact o separated by Transwell membrane with CD4n or CD4s T cells. Co-culture of ASMs or ASMns cells in direct contact with CD4s T cells elicited a significant increase in EdU incorporation. (**C** and **D**) Cell cycle analysis by EdU incorporation and total cell DNA content of $CD4^+$ T cells defines different regions: G_0/G_1 phase; S phase; M phase; Apoptotic. The positive control show more cells in S phase than the negative control. The $CD4^+$ T cells analysis of the co-cultured trigger an increase S phase of $CD4_s$ in contact with ASM_s or ASM_{ns}. Data (n= 6) independent experiments per group. **: p<0.01; ***: p<0.001.

2.4. The addition of MSC in the upper chamber of a Transwell, but not in direct ASM-cell contact, had a suppressive effect on the proliferation of ASMns cells co-cultured with activated $CD4^+$ T cells.

We analysed the effect of MSC addition to ASMs/CD4s co-cultures on ASM cell proliferation. ASMns and CD4s cells were co-cultured in direct contact for induction of ASM cell cycle, and the MSC were either added, in varying MSC:CD4s ratios, in free contact with the ASMns/CD4s co-cultures or in upper Transwell chambers. EdU incorporation during the last 24 hours of triple co-culture, and cell DNA content, were analyzed by flow cytometry and gated to the ASM cells. The presence of MSC in upper Transwell chambers significantly inhibited myocyte DNA synthesis and EdU incorporation (S phase) when added in 1:5 and 1:10 ratios ($p<0.001$ and $p=0.008$ versus ASMns+CD4s, respectively) (**Figure 19B and Table S15 in appendix**). Lower MSC/CD4s (1:100 and 1:1000) ratios in upper Transwell chambers, or MSC in free co-culture contact at any ratio, did not result in any effect on ASM cell proliferation (**Figure 19A-B and Table S15 and S16**).

The effect of MSC on $CD4^+$ T cell proliferation was also analyzed. Only MSC in upper Transwell chambers had a suppressive effect on CD4s T cell proliferation, seen at 1:5, 1:10, 1:100, and 1:1000 ratios ($p<0.001$, $p<0.001$, $p=0.011$ and $p=0.023$, respectively, versus ASMns+CD4s) (**Figure 19D and Table S15 in appendix**). We did not observe such effect when the MSC were added in direct contact with the ASMs/CD4s co-culture (**Figure 19C and Table S16 in appendix**). We did not observe any differences in $CD4^+$ T cell apoptosis or G2/M phase (**Figure 19C-D and Table S15 and S16 in appendix**).

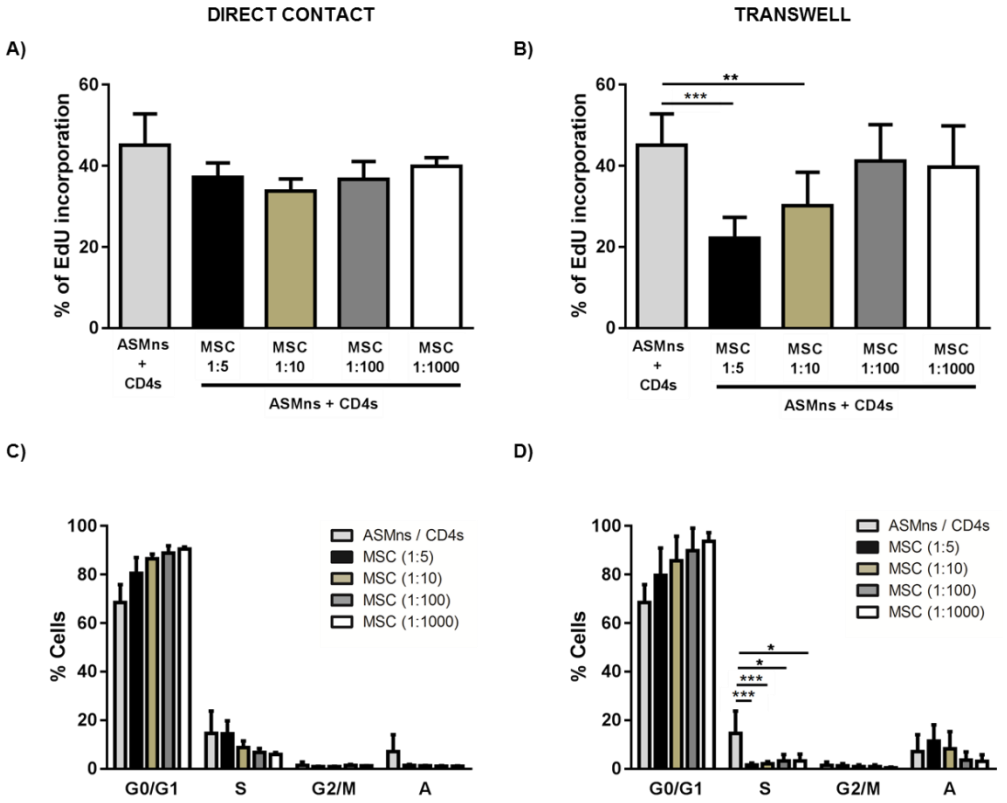

Figure 19| MSC, added in upper Transwell chambers at high MSC:CD4s ratios, inhibit ASM and CDs T-cell proliferation. (**A**-**B**) EdU incorporation by ASM cells. (**A**) MSC added in direct contact with co-cultured ASMs and CD4s do not have any effect on myocyte proliferation. (**B**) MSC added on upper Transwell chambers at 1:5 and 1:10 ratios inhibited myocyte proliferation. (**C-D**) Analysis of EdU incorporation and total cell DNA content of $CD4^+$ T cells. The G_0/G_1, S, and M cell cycle phases, and sub-diploid apoptotic cells, are indicated. (**C**) MSC in direct contact with the ASMns/CD4s co-cultures did not have any effect on $CD4_s$ proliferation at any ratio. (**D**) MSC in upper Transwell chambers inhibited $CD4_s$ proliferation at all ratios tested, with a greater inhibitory effect at high ratios (1:5 and 1:10). Data (n= 6) independent experiments per group. *: p<0.05; **: p<0.01; ***: p<0.001

2.5. The suppressive effect of MSC on ASM cell proliferation is not mediated by exosomes.

We explored the role of exosomes in the suppressive effect of MSC on $CD4^+$ T cell-induced ASM cell proliferation. MSC were cultured with GW4869, a neutral sphingomyelinase inhibitor, which is the most widely used pharmacological agent for blocking exosome generation [204]. We analysed the effects of MSC, in high MSC:CD4s ratio (1:5), on EdU incorporation by the ASM cells. First, we verified that the release of exosomes from MSC was effectively blocked by GW4869, as indicated by a significant upregulation of CD63 MFI expression when compared with MSC without GW4869 (p<0.005 versus control group) (**Figure 20A and Table S17 in appendix**). Consistently with previous studies demonstrating GW4869-specific fluorescence using 405-nm excitation and 450/50-nm emission filters [204], we also observed increased MFI in MSC cultured with GW4869 (p<0.003 versus no-GW4869 control) (**Figure 20B and Table S17**

in appendix). Next, we tested the effect of exosome release blockade on the inhibition of CD4s-induced ASM cell proliferation by MSC. MSC cultured in upper Transwell chambers, in 1:5 MSC:CD4s ratio, inhibited myocyte DNA synthesis and proliferation in the presence of GW4869 (p<0.001 versus ASMs+CD4s), to a similar extent as MSC without GW4869 (**Figure 20C and Table S18 in appendix**). The data showed, therefore, that the inhibitory effect of MSC on $CD4^+$ T cell-induced ASM cell proliferation was not altered by the blockade of exosome release with GW4869 (**Figure 20C and Table S18 in appendix**).

Exosome blockade also abrogated the effect of MSC on CD4s T cell proliferation. MSC with GW4869 consistently decreased CD4s T-cell proliferation (p<0.001 versus ASMs+CD4s), as reported above on the effect of Transwell-contained MSC on ASMns/CD4s co-cultures. In the presence of GW4869, the CD4s T cells showed boosted proliferation (p<0.001 versus ASMs+CD4s) (**Figure 20D and Table S18 in appendix**). No differences were observed in CD4s T-cell apoptosis, or G0/G1 or G2/M cell cycle phases (**Figure 20D and Table S18 in appendix**).

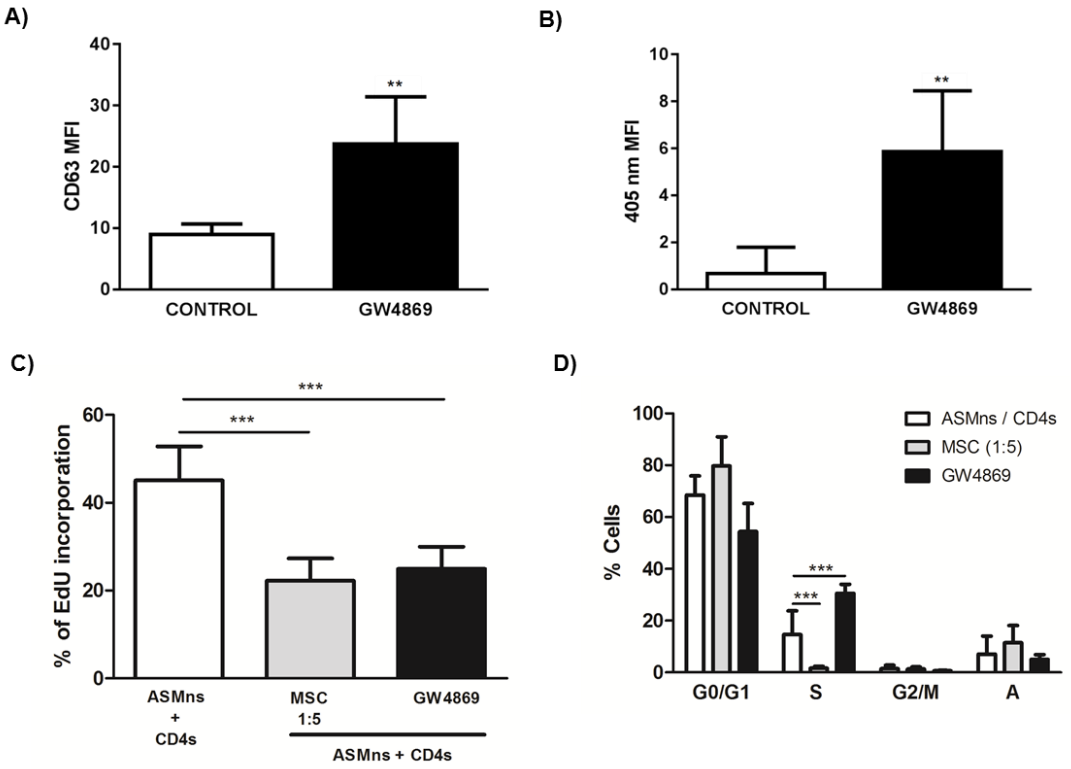

Figure 20| Blocking exosome release with GW4869 in MSC induces airway myocyte arrested-proliferation and enhances CD4s proliferation. (**A**) The amount of unreleased $CD63^+$ exosomes was significantly increased in MSC cultivated with the exosome release inhibitor GW4869. (**B**) GW4869-specific fluorescence was detected at 405 nm by flow cytometry in MSC cultivated with GW4869. (**C**) EdU incorporation by ASM. Co-cultured ASMns and CD4s preserved the myocyte proliferation activity when the MSC were added in upper Transwell chambers, at 1:5 MSC:CD4s ratio, with GW4869. (**D**) Analysis of EdU incorporation and total cell DNA content of $CD4^+$ T cells defines the G_0/G_1, S, and M cell cycle phases, and sub-diploid apoptotic cells. MSC added with GW4869 enhanced $CD4_s$ proliferation. Data (n= 6) independent experiments per group. **: p<0.01; ***: p<0.001.

2.6. MSC-conditioned medium inhibits ASM cell proliferation induced by ASM/CD4$^+$ T-cell contact.

We analyzed the effect of MSC-conditioned medium on CD4$^+$ T cell-induced ASM cell proliferation. MSC were cultured in serum-free media for 72 hours, and the conditioned medium collected. The addition of MSC-conditioned medium to ASMns/CD4s co-cultures inhibited myocyte DNA synthesis and proliferation (p<0.001 versus ASMns+CD4s group), to a similar degree as the MSC added in 1:5 MSC/CD4s ratio in upper Transwell chambers (**Figure 21A and Table S19 in appendix**).

The MSC-conditioned medium also had a suppressive effect on CD4s T cell proliferation (p<0.001 versus ASMns+CD4s), similarly to the suppressive effect of MSC co-cultured in 1:5 ratio and separated by Transwell membrane (p<0.001 versus ASMns+CD4s group) (**Figure 21B and Table S19 in appendix**). We did not observe any difference in the suppression of CD4$^+$ T cell-induced ASM cell proliferation between adding MSC-conditioned medium or MSC in high ratio (1:5) separated by a Transwell membrane (p>0.999) (**Figure 21B and Table S19 in appendix**). No significant differences were observed in the apoptotic, G0/G1, or G2/M states (**Figure 21B and Table S19 in appendix**).

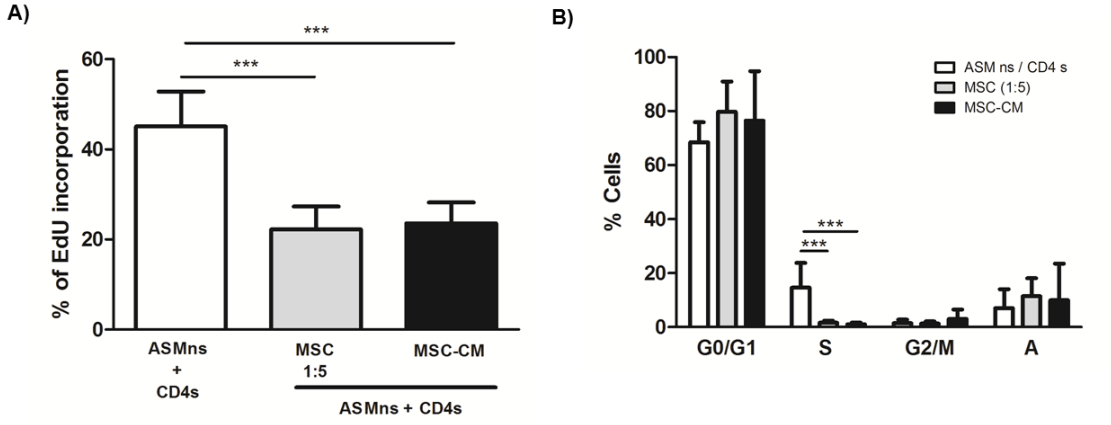

Figure 21| Conditioned MSC medium inhibits ASMns and $CD4_s$ proliferation in ASMns/CD4s co-cultures. (**A**) EdU incorporation by ASM. The addition of conditioned MSC medium to co-cultured ASMns and CD4s inhibits myocyte proliferation. (**B**) Analysis of EdU incorporation and total cell DNA content of CD4$^+$ T cells defines the G_0/G_1, S, and M phases of the cell cycle, and the sub-diploid apoptotic cells. MSC-conditioned medium inhibits $CD4_s$ cell proliferation. Data (n= 6) independent experiments per group. ***: p<0.001.

2.7. The MSC-conditioned medium agent(s) that carry the suppressive effect on $CD4^+$ T-cell-induced ASM cell proliferation fall within a limited range of protein molecular weight

To encircle a limited set of molecules carrying the inhibitory effect of MSC-conditioned medium on $CD4^+$ T cell-induced ASM cell proliferation, we generated and tested serial molecular-weight range cut-offs. MSC were cultured in serum-free media for 72 hours, and different cut-off ranges of protein molecular weight (<3 kDa, 3-10 kDa, 10-30 kDa, 30-100 kDa and >100 kDa) were separated through centrifugal filtration steps. We analyzed the effect of each fraction on ASM cell proliferation in ASMns/CD4s cells co-cultures. Only the 30-100-kDa cut-off range inhibited myocyte DNA synthesis and proliferation when compared with the suppressive effect of whole MSC-conditioned medium (p>0.999 versus CM) (all p<0.001 versus ASMns+CD4s) (**Figure 22A and Table S20 in appendix**). The <3 kDa, 3-10 kDa, 10-30 kDa and >100 kDa cut-off ranges did not have a suppressive effect on $CD4^+$ T-cell-induced ASM proliferation (all p<0.001 versus CM) (**Figure 22A and Table S20 in appendix**).

We did not observe a significant suppressive effect on CD4s T-cell proliferation when 3-10 kDa (p=0.004 versus MSC-CM), 10-30 kDa (p<0.016 versus MSC-CM) or >100 kDa (p<0.020 versus MSC-CM) fractions were added to the co-culture (**Figure 22B and Table S20 in appendix**). We did observe a significant suppressive effect on CD4s T-cell proliferation with the <3 kDa and 30-100 kDa fractions, which resulted similar to the whole CM (both p<0.001 versus ASMns+CD4s) (**Figure 22B and Table S20 in appendix**).

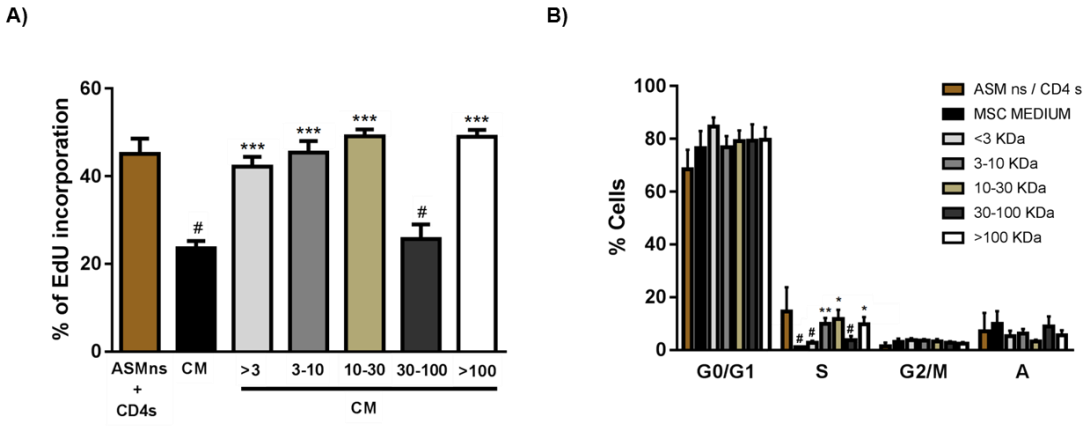

Figure 22| The MSC-conditioned medium, 30-100 kDa protein molecular weight range inhibits airway myocyte and CD4s cell proliferation. (**A**) EdU incorporation by ASM cells. Addition of the 30-100 kDa CM fraction to ASMns/CD4s co-culture inhibited myocyte proliferation. (**B**) Analysis of EdU incorporation and total cell DNA content of $CD4^+$ T cells showing the G_0/G_1, S, and M cell cycle phases, and sub-diploid apoptotic cells. The <3 kDa and 30-100 kDa CM fractions inhibited CD4s T-cell proliferation. Data (n= 6) independent experiments per group. *: p<0.05 versus CM; **: p<0.01 versus CM; ***: p<0.001 versus CM; $^{\#}p$<0.001 versus ASMns+CD4s.

To further characterize the MSC-conditioned medium, we measured the protein content of the CM fractions. We observed significantly increased protein content in the 10-30 kDa and 30-100 kDa fractions (p<0.032 and p<0.040, respectively, versus control DMEM culture). No differences were observed for the rest of the fractions (**Figure 23A and Table S21 in appendix**). We also analyzed the 30-100 kDa fraction for lipid content (cholesterol, triglycerides, and phospholipids) with a negative result for both the MSC-conditioned medium and DMEM control culture medium (**Figure 23B**).

A)

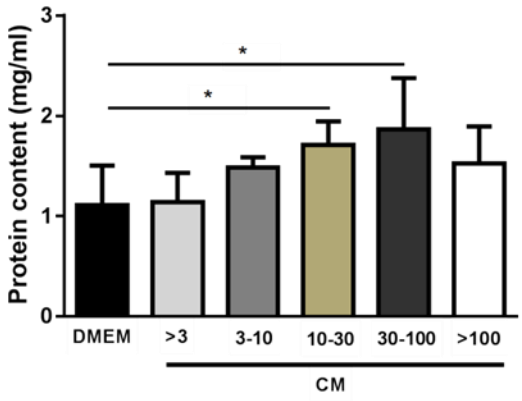

B)

	DMEM 30-100 KDa	MSC MEDIUM 30-100 KDa
CHO2I	Negative	Negative
TRIGL	Negative	Negative
PL-T	Negative	Negative

Figure 23| Protein and lipid content in serial MSC-conditioned medium fractions by protein molecular-weight ranges. (**A**) Protein concentration in mg/mL. The 3-10 kDa and 30-100 kDa MSC-conditioned medium (CM) fractions had increased protein content in comparison with control DMEM cultures. (**B**) Lipid content in the 30-100 kDa fraction of MSC-conditioned medium and control DMEM culture shown as concentration in mMol/L. Lipid detection resulted negative in all cases. CHO2I: Cholesterol TRIGL: Triglycerides PL-T: Phospholipids. Data (n= 6) in (**A**) are presented as mean±SEM. *: p<0.05. Data (n= 4) in (**B**) are presented as negative or positive detection.

3. Effect of the 30-100 kDa MSC-conditioned medium (MSC-CM) fraction on experimental asthma outcomes *in vivo*.

Next, we aimed at demonstrating the role of MSC-CM in experimental asthma. To test the effect of MSC-CM on ongoing disease, we conducted experiments on a rat model of experimental asthma induced by primary HDM+SEB exposure in the airways. For this purpose, the animals received *i.n.* HDM+SEB instillations under the same regime and protocol duration as the 15IN model described in Section 1. Upon reaching 15 HDM+SEB instillations, the rats showed airway hyperresponsiveness and a significant increase in lung airway contractile tissue mass and total BAL cells, consistent with the model description. On histopathological examination, they showed inflammatory lung infiltrates comprising mononuclear cells and eosinophils, and mucus overproduction in the airway epithelium.

To explore the MSC-CM suppressive effect on airway smooth muscle remodeling, we instilled serial *i.n.* doses of the 30-100 kDa MSC-CM fraction, in a dose-finding fashion, on day 35 of the *i.n.* instillation protocol. The model was then continued up to completing one dose per week during two weeks (termed hereinafter 1-week [1W] model, 23 total instillations) or two doses per week during two weeks (2W model, 25 total instillations) of further *i.n.* HDM+SEB and MSC-CM fraction.

3.1. MSC-CM attenuates airway inflammation and hyperresponsiveness.

The repeated *i.n.* HDM+SEB instillations induced airway hyperresponsiveness to methacholine, as demonstrated by a significant increase in R_L (p<0.001 versus saline control group) at 64, 128, and 256 mg/mL MCh doses. All MSC-CM-treated groups in the 1W and 2W models showed significantly decreased R_L (p<0.001 versus HDM+SEB group), whose curve was flattened in closeness to the control animals (**Figure 24A-B and Table S22 in appendix**).

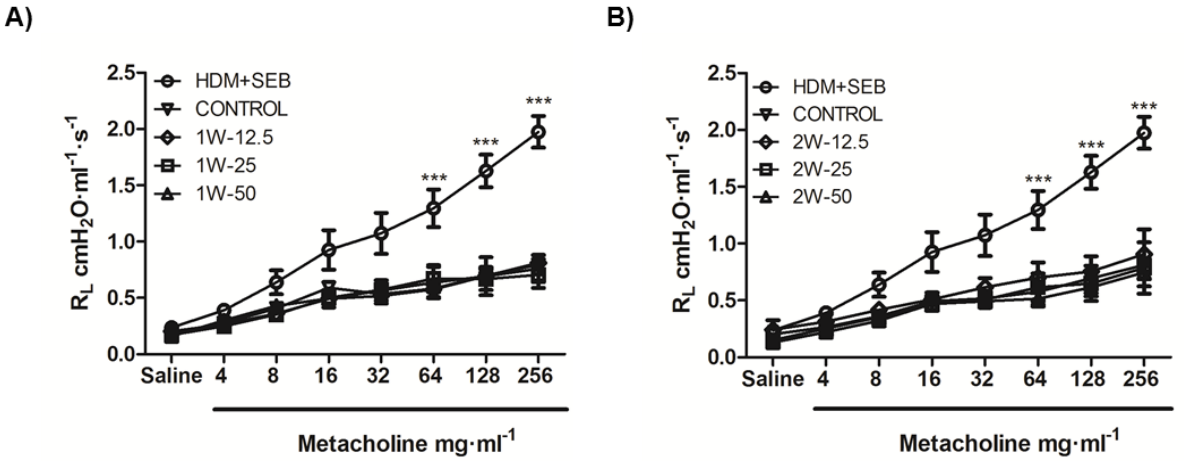

Figure 24| Effect of MSC-CM on lung function in rats with experimental asthma. Sprague Dawley rats were *i.n.*-instilled with saline (CONTROL) or HDM+SEB (20 µg/mL and 2 µg/mL, respectively), 3 times weekly. Upon completion of 5 weeks on instillations, the HDM+SEB rats received additional HDM+SEB or saline instillations and different doses (12.5, 25 or 50 µg) of MSC-CM, *i.n.*-instilled. (**A**) One dose per week (1W) model. (**B**) Two doses per week (2W) model. Following *i.n.* Instillation of the MSC-CM doses, pulmonary mechanics and specimen harvesting were performed upon completion two weeks. Mean lung resistance (R_L, $cmH2O \cdot ml^{-1} \cdot s^{-1}$) was measured through 4-256 $mg \cdot ml^{-1}$ methacholine (MCh) nebulizations. All MSC-CM-treated groups, in both the 1W and 2W models, showed no R_L response in comparison with the respective HDM+SEB groups, and were similar to the control, saline-instilled animals. Data (n= 6 per group) are presented as mean±SEM and were analysed using one-way ANOVA test, followed by Bonferroni for post-hoc pairwise comparisons, for each MCh concentration. ***: $p<0.001$ versus HDM+SEB group.

3.2. MSC-CM decreases total serum IgE.

Total serum IgE was significantly increased (p=0.006 versus control group) after the co-administration of HDM plus SEB. We found a significant decrease of total serum IgE in the 1W model at 12.5, 25, and 50-µg MSC-CM doses (p=0.005, p=0.032, and p=0.003 versus HDM+SEB group, respectively) (**Figure 25A and Table S23 in appendix**). Such reduction in total serum IgE persisted in the 2W model at the three MSC-CM doses tested (p=0.018, p=0.044, and p=0.044 versus HDM+SEB group, respectively) (**Figure 25B and Table S23 in appendix**). Total BAL IgE was under the ROD limit.

Total BAL IgG was significantly decreased by the co-administration of HDM plus SEB (p=0.040 versus control group). Total BAL IgG was similar to the saline control animals in the MSC-CM-treated animals for the 12.5, 25, and 50-µg MCS-CM doses (p=0.039, p=0.020, and p=0.013 for the 1W model; and p=0.025, p=0.027, p=0.020 for the 2W model, versus HDM+SEB group, respectively) (**Figure 25C-D and Table S24 in appendix**). Total serum IgG was under to the ROD limit.

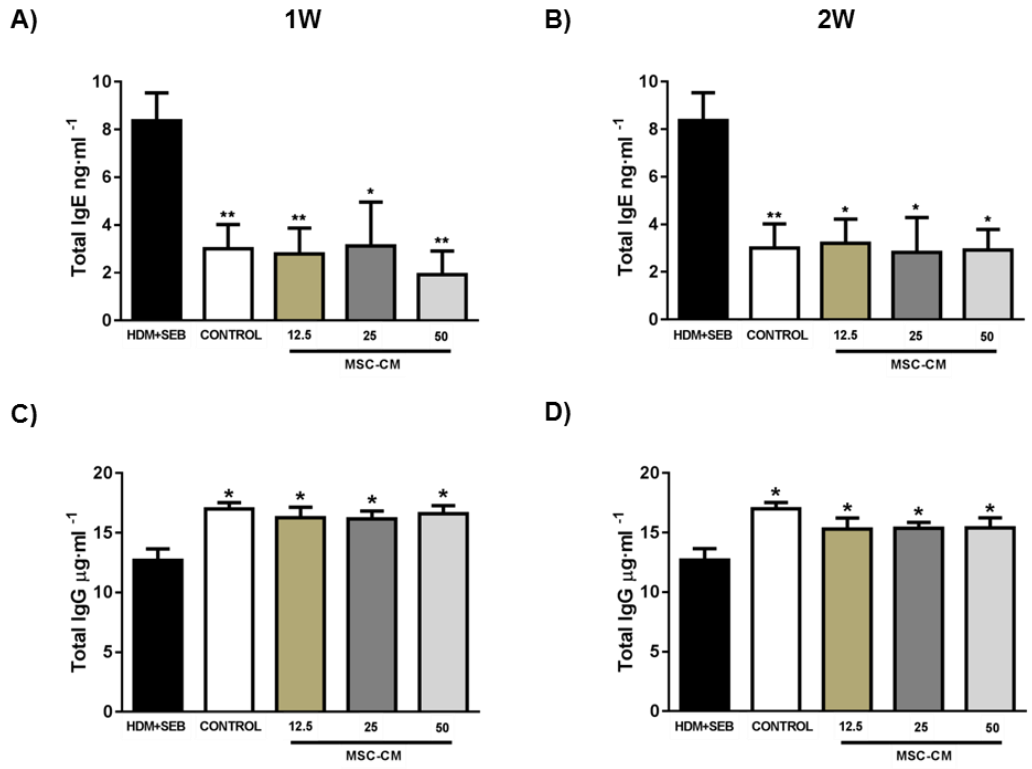

Figure 25| Determination of total IgE and IgG in BAL and blood serum. Sprague Dawley rats were *i.n.*-instilled with saline (CONTROL) or HDM+SEB (20 µg/mL and 2 µg/mL, respectively), 3 times weekly. Upon completion of 5 weeks on instillations, the HDM+SEB rats received additional HDM+SEB or saline instillations and different doses (12.5, 25 or 50 µg) of MSC-CM, *i.n.*-instilled: One dose per week (1W, **A** and **C**) model or two doses per week (2W, **B** and **D**) model. During the MSC-CM dosing, the animals continued under HDM+SEB *i.n.* instillations for 2 weeks. (**A-B**) All MSC-CM-treated groups, in both the 1W and 2W models, had decreased total IgE in serum, which reached a concentration similar to the saline control animals. (**C-D**) All MSC-CM-treated groups, in both the 1W and 2W models, had total BAL IgG concentration comparable to the saline control animals. Data (n= 6) are presented as mean±SEM, and were analyzed using one-way ANOVA. *: $p<0.05$; **: $p<0.01$ versus HDM+SEB group.

3.3. MSC-CM attenuates the HDM-specific IgE response.

HDM+SEB led to significantly increased BAL HDM-specific IgE (p=0.002 versus saline control group). There was a significant decrease of BAL HDM-specific IgE in the MSC-CM-treated animals, in both the 1W and 2W models at the 12.5, 25, and 50-µg MSC-CM doses (p=0.001, p=0.002, and p=0.002; p=0.003, p=0.001, and p=0.003, versus HDM+SEB group, respectively). (**Figure 26A-B and Table S25 in appendix**). Serum HDM-specific IgE behaved similarly, with a significant increase in the HDM+SEB-instilled animals (p=0.006 versus saline control), and its concentrations decreased to saline-control level in the MSC-CM-treated animals at the three MCS-CM-tested doses (p=0.002, p=0.002, p=0.004; and p=0.002, p=0.002, p=0.004 versus the HDM+SEB groups, 1W and 2W models, respectively) (**Figure 26C-D and Table S25 in appendix**).

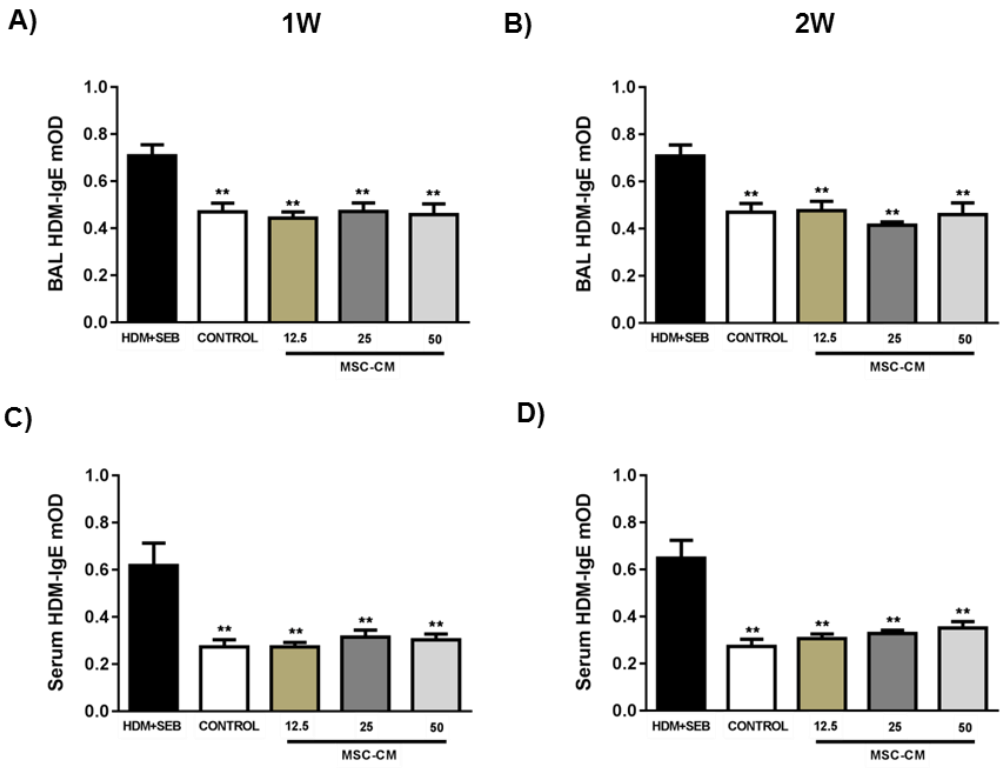

Figure 26| Determination of HDM-specific IgE in bronchoalveolar lavage (BAL) and blood serum. Sprague Dawley rats were *i.n.*-instilled with saline (CONTROL) or HDM+SEB (20 µg/mL and 2 µg/mL, respectively), 3 times weekly. Upon completion of 5 weeks on instillations, the HDM+SEB rats received additional HDM+SEB or saline instillations and different doses (12.5, 25 or 50 µg) of MSC-CM, *i.n.*-instilled: One dose per week (1W, **A** and **C**) model or two doses per week (2W, **B** and **D**) model. During the MSC-CM dosing, the animals continued under HDM+SEB *i.n.* instillations for 2 weeks. In both the 1W and 2W models, BAL (**A** and **B**) and serum (**C** and **D**) HDM-specific IgE was significantly decreased in comparison with the HDM+SEB groups. Data (n= 6) are presented as mean±SEM optical density (mOD) and were analyzed using one-way ANOVA. **: $p<0.01$.

We did not observe any significant differences in BAL or serum SEB-specific IgE across any of the experimental groups (**Figure 27A-D and Table S26 in appendix**).

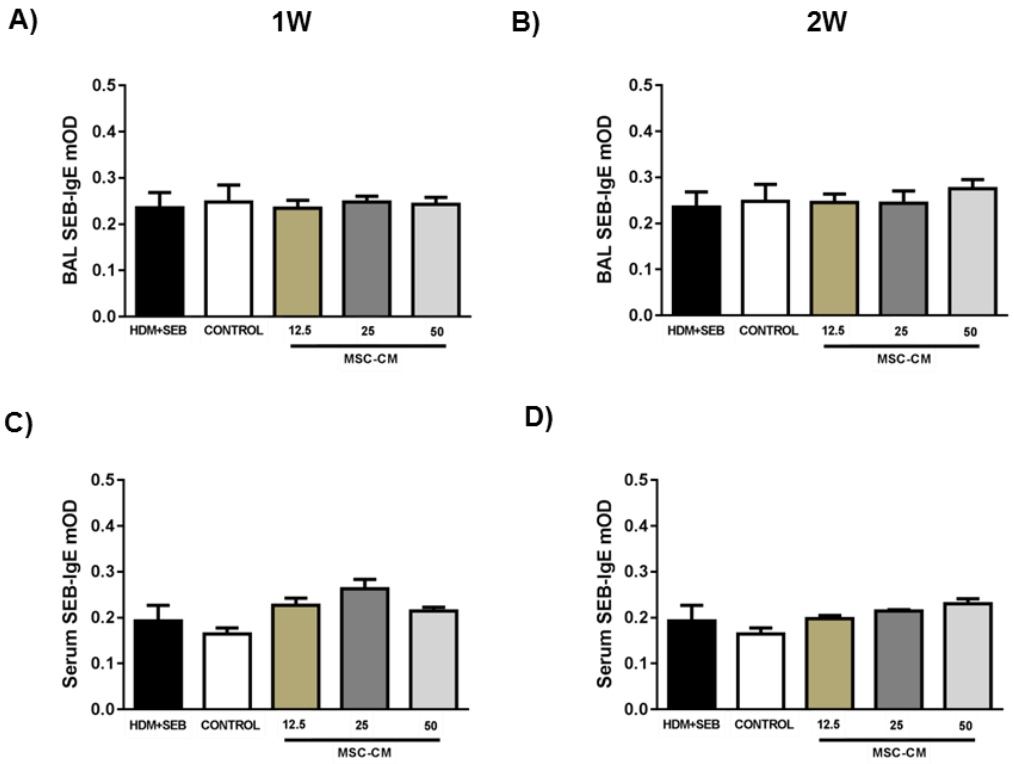

Figure 27| Determination of SEB-specific IgE in bronchoalveolar lavage (BAL) and blood serum. Sprague Dawley rats were *i.n.*-instilled with saline (CONTROL) or HDM+SEB (20 µg/mL and 2 µg/mL, respectively), 3 times weekly. Upon completion of 5 weeks on instillations, the HDM+SEB rats received additional HDM+SEB or saline instillations and different doses (12.5, 25 or 50 µg) of MSC-CM, *i.n.*-instilled: One dose per week (1W, **A** and **C**) model or two doses per week (2W, **B** and **D**) model. During the MSC-CM dosing, the animals continued under HDM+SEB *i.n.* instillations for 2 weeks. SEB-specific IgE, in BAL (**A** and **B**) and serum (**C** and **D**), was approximate across all experimental groups in both the 1W and 2W models. Data (n= 6) are presented as mean±SEM optical density (mOD) and were analyzed using one-way ANOVA.

3.4. MSC-CM decreases airway mucus production, subepithelial collagen deposition, and contractile tissue mass.

Examination of H-E-stained lung tissue sections from rats instilled with *i.n.* HDM+SEB showed a marked increase in airway inflammatory infiltrates, narrowing of the airway lumen, and airway wall remodeling, in comparison with the saline control group. The airway inflammatory infiltrates were attenuated or abrogated in the MSC-CM-treated groups in both the 1W (**Figure 28C-E**) and 2W (**Figure 28F-H**) models.

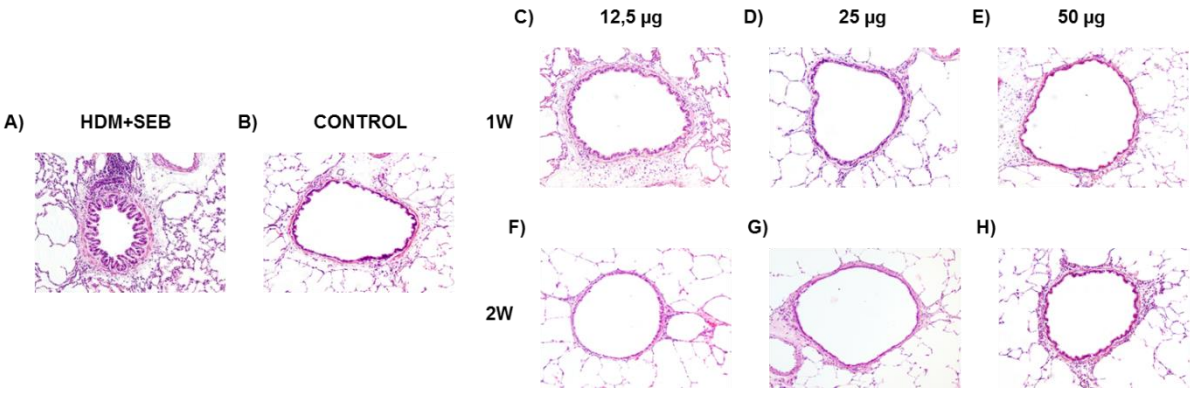

Figure 28| H-E staining of tissue sections. Sprague Dawley rats were *i.n.*-instilled with saline (CONTROL) or HDM+SEB (20 µg/mL and 2 µg/mL, respectively), 3 times weekly. Upon completion of 5 weeks on instillations, the HDM+SEB rats received additional HDM+SEB or saline instillations and different doses (12.5, 25 or 50 µg) of MSC-CM, *i.n.*-instilled: One dose per week (1W, **C-E**) model or two doses per week (2W, **F-H**) model. During the MSC-CM dosing, the animals continued under HDM+SEB *i.n.* instillations for 2 weeks. The micrographs show representative airways of HDM+SEB animals (**A**), the respective saline control (**B**), and the MSC-CM dosing groups in the 1W model (12.5 (**C**), 25 (**D**), and 50 (**E**) µg), and 2W model (12.5 (**F**), 25 (**G**), and 50 (**H**) µg). The HDM+SEB animals showed strong airway inflammatory infiltrates, which were attenuated or abrogated in the MSC-CM-dosed groups.

To assess the degree of goblet cell hyperplasia and mucin overproduction, lung sections were stained with PAS and the airway intraepithelial mucus load was quantitatively assessed. Co-administration of HDM+SEB increased the PAS-positive cells in the airways compared to the saline control group (p<0.001 versus control group). The administration of MSC-CM induced an overall trend towards decreased airway mucous load over time, through the 1W and 2W models, yet this tendency only reached statistical significance for the 12.5-µg dose in the 2W model (**Figure 29I-J and Table S27 in appendix**).

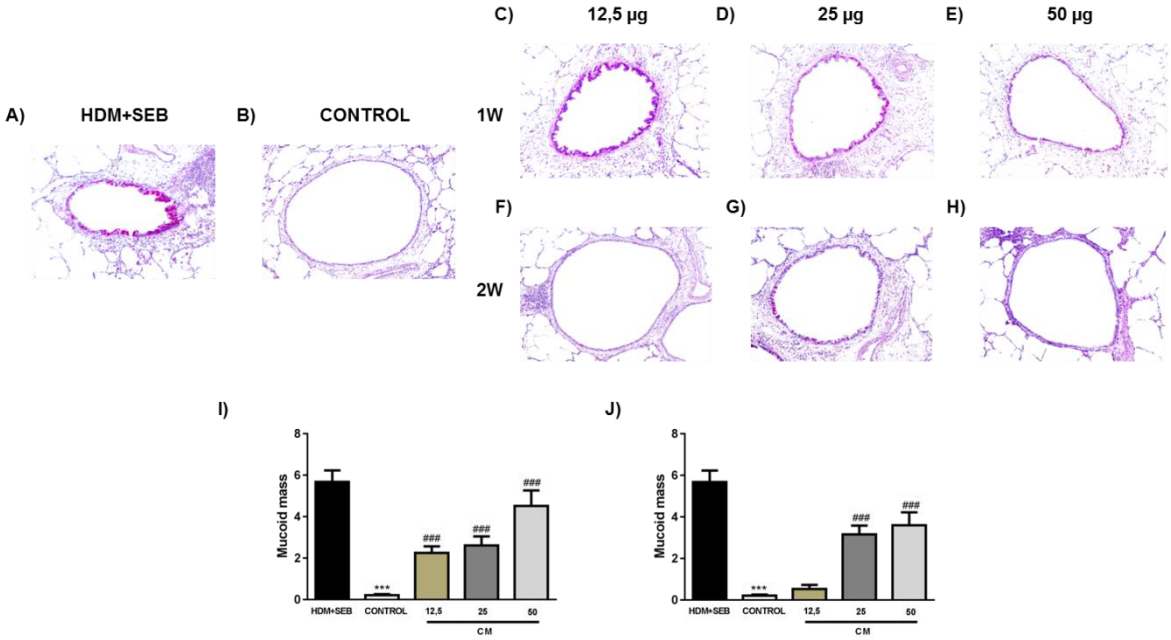

Figure 29| PAS staining of tissue sections. Histological examination of lung tissue sections after sensitization. Sprague Dawley rats were *i.n.*-instilled with saline (CONTROL) or HDM+SEB (20 µg/mL and 2 µg/mL, respectively), 3 times weekly. Upon completion of 5 weeks on instillations, the HDM+SEB rats received additional HDM+SEB or saline instillations and different doses (12.5, 25 or 50 µg) of MSC-CM, *i.n.*-instilled: One dose per week (1W, **C-E**) model or two doses per week (2W, **F-H**) model. During the MSC-CM dosing, the animals continued under HDM+SEB *i.n.* instillations for 2 weeks. The micrographs show representative airways of HDM+SEB animals (**A**), the respective saline control (**B**), and the MSC-CM dosing groups in the 1W model (12.5 (**C**), 25 (**D**), and 50 (**E**) µg), and 2W model (12.5 (**F**), 25 (**G**), and 50 (**H**) µg). The HDM+SEB animals showed a strong mucous response. The 12.5-µg MSC-CM group in the 2W model showed attenuated mucus production, similar to the control group. Data (n= 6) are presented as mean±SEM and were analyzed using one-way ANOVA. ***: $p<0.001$ versus HDM+SEB group; $^{###}$: $p<0.001$ versus control group.

To evaluate subepithelial fibrosis as an asthma airway remodeling feature, Masson's trichrome-stained lung sections were processed to extract and measure the trichrome blue dye component, which reflects collagen deposition. The dimensionless index resulting from normalization by airway size was termed “extracellular matrix mass”. In the HDM+SEB group, the extracellular matrix mass was significantly increased ($p<0.001$ versus saline control group). Administration of MSC-CM at the 12.5, 25, and 50-µg doses did not significantly decrease subepithelial fibrosis in the 1W model (**Figure 30C-E, I; and Table S28 in appendix**). In the 2W model, the animals treated with 12.5-µg MSC-CM showed decreased collagen deposition ($p<0.001$ versus HDM+SEB group), while 25 or 50 µg did not decrease subepithelial fibrosis, being similar to asthmatic group (**Figure 30F-H, J; and Table S28 in appendix**).

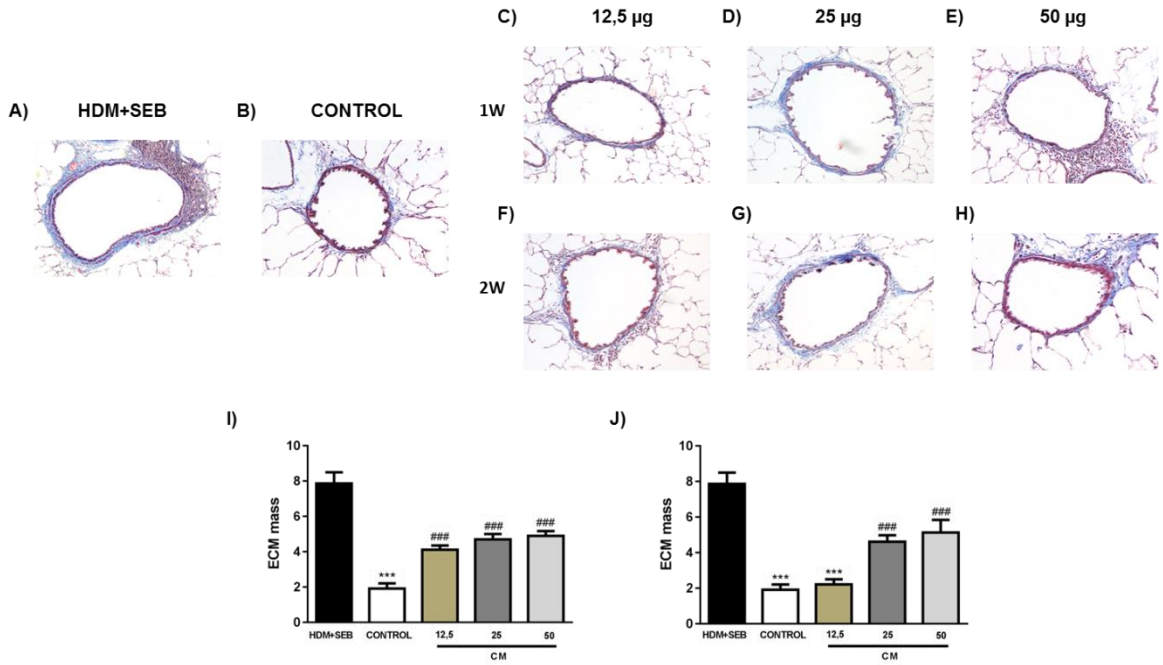

Figure 30| Subepithelial extracellular matrix mass (ECM mass) quantification. Sprague Dawley rats were *i.n.*-instilled with saline (CONTROL) or HDM+SEB (20 µg/mL and 2 µg/mL, respectively), 3 times weekly. Upon completion of 5 weeks on instillations, the HDM+SEB rats received additional HDM+SEB or saline instillations and different doses (12.5, 25 or 50 µg) of MSC-CM, *i.n.*-instilled: One dose per week (1W, **C-E**) model or two doses per week (2W, **F-H**) model. During the MSC-CM dosing, the animals continued under HDM+SEB *i.n.* instillations for 2 weeks. The micrographs show representative airways of HDM+SEB animals (**A**), the respective saline control (**B**), and the MSC-CM dosing groups in the 1W model (12.5 (**C**), 25 (**D**), and 50 (**E**) µg), and 2W model (12.5 (**F**), 25 (**G**), and 50 (**H**) µg). ECM mass was significantly increased in the HDM+SEB group. The 12.5-µg MSC-CM-treated group in the 2W model showed significantly decreased ECM mass, similar to the control animals. Data (n= 6) are presented as mean±SEM and were analyzed using one-way ANOVA. ***: $p<0.001$ versus HDM+SEB group; $^{###}$: $p<0.001$ versus control group.

Airway contractile tissue mass was quantified on the basis of α-SMA immunofluorescence and digital signal extraction and processing. The dimensionless index resulting from normalization by airway size was termed “airway contractile mass”. We showed that HDM+SEB animals showed an increase of airway contractile tissue mass when compared to control group as described above ($p<0.001$ versus control group). We observed that administration of MSC-CM (12.5, 25 and 50 µg) in 1W model not decreased α-actin positive cells, being similarly to asthmatic group (**Figure 31C-E**). Conversely, treated animals with MSC-CM at 12.5 µg doses decreased airway contractile mass, while 25 or 50 µg doses being more similarly to HDM+SEB group (**Figure 31F-H**).

Therefore, ASM mass was maintained when rats treated with MSC-CM (12.5, 25 and 50 µg) in 1W model (**Figure 31I and Table S29 in appendix**). However, airway contractile mass was decreased in 2W model at 12.5 µg ($p<0.001$ versus HDM+SEB group), while 25 or 50 µg not decreased ASM mass, being more similarly to asthmatic group (**Figure 31J and Table S29 in appendix**).

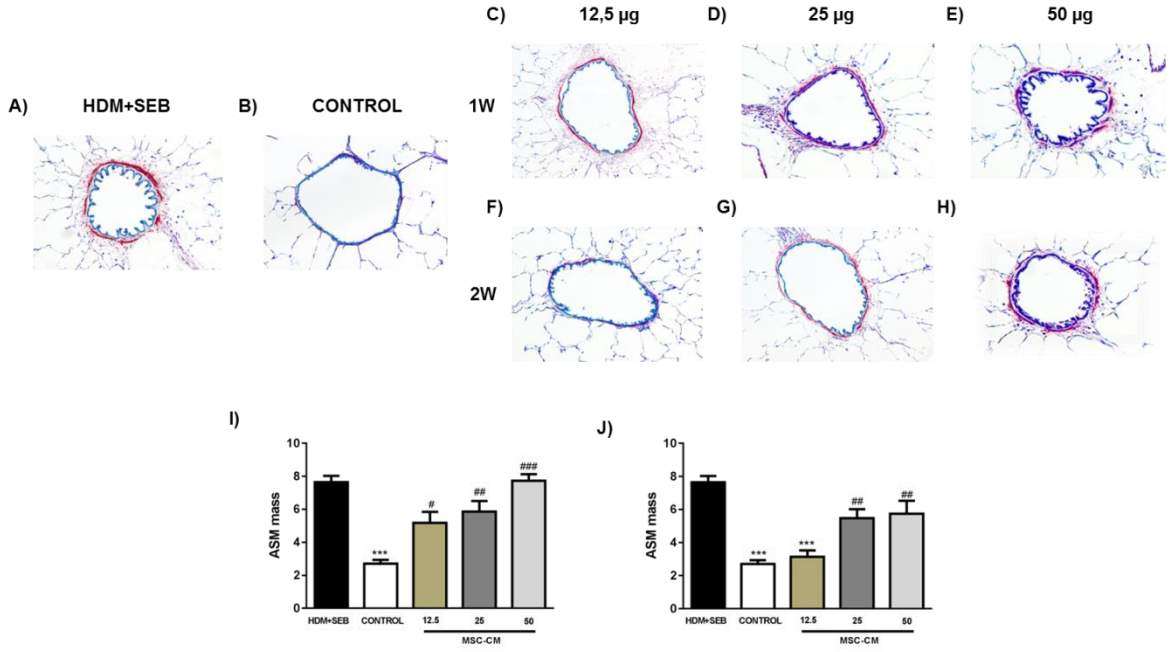

Figure 31| Immunohistochemical detection of alpha-SMA and airway contractile tissue mass (ASM mass) quantification in lungs after sensitization. Histological examination of lung tissue sections after sensitization. Sprague Dawley rats were *i.n.*-instilled with saline (CONTROL) or HDM+SEB (20 µg/mL and 2 µg/mL, respectively), 3 times weekly. Upon completion of 5 weeks on instillations, the HDM+SEB rats received additional HDM+SEB or saline instillations and different doses (12.5, 25 or 50 µg) of MSC-CM, *i.n.*-instilled: One dose per week (1W, **C-E**) model or two doses per week (2W, **F-H**) model. During the MSC-CM dosing, the animals continued under HDM+SEB *i.n.* instillations for 2 weeks. Representative airways of HDM+SEB (**A**) animals at different doses of MSC-CM in the 1W model (12.5 (**C**), 25 (**D**) or 50 (**E**) µg) and 2W model (12.5 (**F**), 25 (**G**) or 50 (**H**) µg) with respective control (**B**) group. The HDM+SEB animals showed increased airway contractile tissue mass. The increased ASM mass was absent in the 12.5-µg MSC-CM group in the 2W model, where it was similar to the control group. Data (n= 6) are presented as mean±SEM and were analyzed using one-way ANOVA. ***: p<0.001 versus HDM+SEB group; $^{\#}$: p<0.05 versus control group; $^{\#\#}$: p<0.01 versus control group; $^{\#\#\#}$: p<0.001 versus control group.

3.5. Primary airway exposure to HDM+SEB elicits eosinophil recruitment but decreases B-cell infiltration.

To further support that sensitization to HDM+SEB leads to increased airway leukocytes, we performed BAL flow cytometry analysis from all groups. In the 1W model, macrophages were decreased in the HDM+SEB-instilled animals (p<0.045 versus control group), as well as in all groups treated with MSC-CM (12.5, 25, and 50-µg doses) (**Figure 32A and Table S30 in appendix**). Neutrophils were increased in the rats treated with all MSC-CM doses (12.5, 25 and 50 µg; p=0.030, p=0.039, and p=0.040, respectively, versus HDM+SEB group) (**Figure 32B and Table S30 in appendix**). Eosinophil recruitment in BAL was increased in the HDM+SEB group (p<0.010 versus saline control). MSC-CM treatment, at the three doses tested (12.5, 25 and 50 µg), did not have any significant effect in terms of eosinophil reduction (**Figure 32C and Table S30 in appendix**). There were no significant differences in NK cell recruitment across the experimental groups (**Figure 32D and Table S30 in appendix**). T cells were increased in the HDM+SEB group

(*p*<0.001 versus saline control), and all MSC-CM groups (12.5, 25 and 50 µg) (**Figure 32E and Table S30 in appendix**). B cells were increased in the HDM+SEB group (*p*<0.001 versus saline control), while all MSC-CM doses (12.5, 25, and 50 µg) decreased B cells (*p*=0.002, *p*=0.004, and *p*=0.002, respectively, versus HDM+SEB group) (**Figure 32F and Table S30 in appendix**).

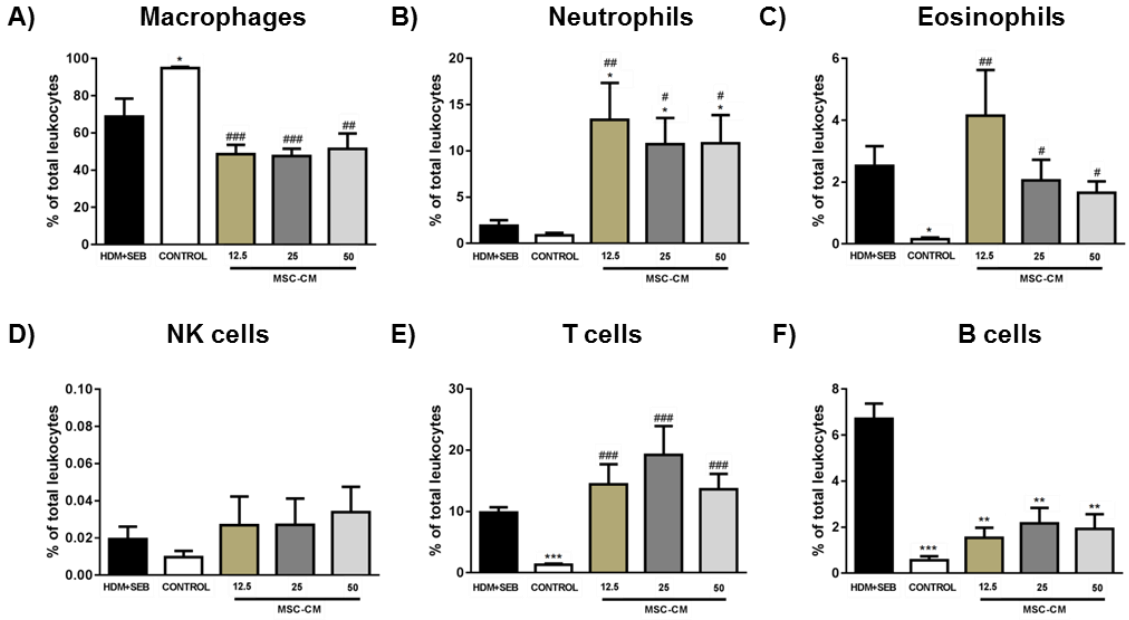

Figure 32| Effect of MSC-CM on leukocyte recruitment in bronchoalveolar lavage (BAL), in the 1W model. Sprague Dawley rats were *i.n.*-instilled with saline (CONTROL) or HDM+SEB (20 µg/mL and 2 µg/mL, respectively), 3 times weekly. Upon 5 weeks on instillations, respective HDM+SEB groups received one dose per week (1W) of different *i.n.* doses (12.5, 25, or 50 µg) of MSC-CM. During the MSC-CM dosing, the animals continued under HDM+SEB *i.n.* instillations for 2 weeks. The MSC-CM treatment did not lead to differences in BAL eosinophils (**C**), NK (**D**), or T cells (**E**). All MSC-CM doses induced neutrophil recruitment (**B**) and B-cell reduction (**F**) compared with the HDM+SEB group. Data (n= 6) are presented as mean±SEM and were analyzed with one-way ANOVA. *: *p*<0.05 versus HDM+SEB group; **: *p*<0.01 versus HDM+SEB group; ***: *p*<0.001 versus HDM+SEB group; $^{\#}$: *p*<0.05 versus control group; $^{\#\#}$: *p*<0.01 versus control group; $^{\#\#\#}$: *p*<0.001 versus control group.

In the 2W model, BAL macrophages were decreased in the HDM+SEB-instilled animals (*p*=0.045 versus saline control), and all MSC-CM doses (12.5, 25, and 50 µg) (**Figure 33A and Table S30 in appendix**). Neutrophils were increased in the rats treated with 25 and 50-µg MSC-CM (*p*=0.047 and *p*=0.028, respectively, versus HDM+SEB group) (**Figure 33B and Table S30 in appendix**). Eosinophils were increased in the HDM+SEB group (*p*<0.010 versus saline control), and in all MSC-CM doses (12.5, 25 and 50 µg) similarly (**Figure 33C and Table S30 in appendix**). The 12.5-µg MSC-CM dose increased NK cells significantly (*p*<0.033 versus HDM+SEB group), while the 25 and 50 µg doses showed a similar trend not reaching significance (**Figure 33D and Table S30 in**

appendix). T cells were similarly increased in the HDM-SEB group and all MSC-CM-dosed groups (**Figure 33E and Table S30 in appendix**). B cells were decreased with all MSC-CM doses (p<0.001 versus HDM+SEB) (**Figure 33F and Table S30 in appendix**).

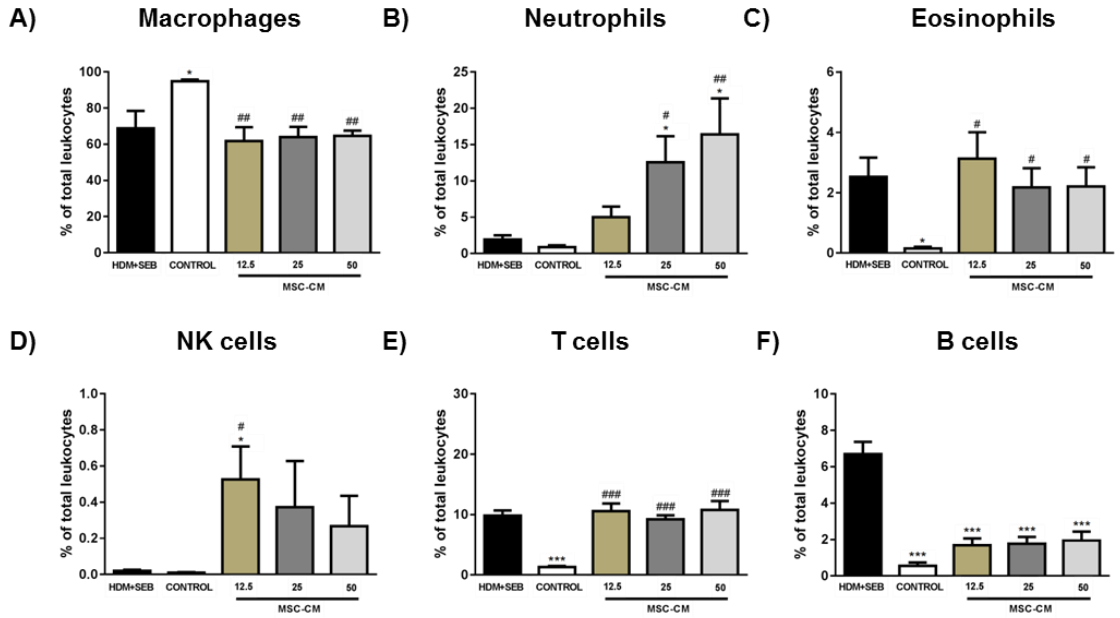

Figure 33| Effect of MSC-CM on BAL leukocyte cell recruitment in the 2W model. Sprague Dawley rats were *i.n.*-instilled with saline (CONTROL) or HDM+SEB (20 µg/mL and 2 µg/mL, respectively), 3 times weekly. Upon 5 weeks on instillations, respective HDM+SEB groups received two doses per week (2W) different *i.n.* doses (12.5, 25, or 50 µg) of MSC-CM. During the MSC-CM dosing, the animals continued under HDM+SEB *i.n.* instillations for 2 weeks. All groups showed decreased macrophage numbers (**A**) compared with the HDM+SEB group. The 25 and 50-µg doses induced neutrophils recruitment (**B**), and the 12.5-µg dose increased NK cells (**D**). MSC-CM had no significant effect on eosinophils (**C**) and T cells (**E**) compared with the HDM+SEB group. All groups showed decreased B cells (**F**) compared with the HDM+SEB group. Data (n= 6) are presented as mean±SEM and were analysed using one-way ANOVA. *: p<0.05 versus HDM+SEB group; ***: p<0.001 versus HDM+SEB group; $^{\#}$: p<0.05 versus control group; $^{\#\#}$: p<0.01 versus control group; $^{\#\#\#}$: p<0.001 versus control group.

We analyzed the effect MSC-CM on the frequency of BAL T-lymphocyte subpopulations. None of the experimental conditions in either model, including MSC-CM treatment, modified the $CD4^+$ or $CD8^+$ T-cell subpopulations (**Figure 34 and Table S30 in appendix**).

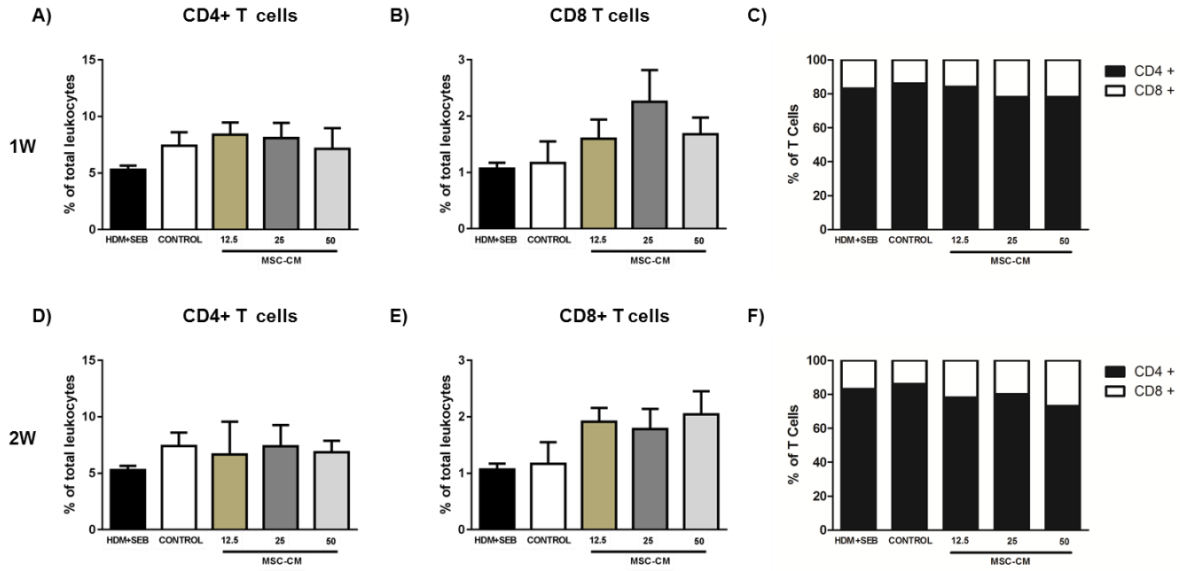

Figure 34| Effect of MSC-CM on CD4 and CD8 T cell recruitment in bronchoalveolar lavage (BAL). Sprague Dawley rats were *i.n.*-instilled with saline (CONTROL) or HDM+SEB (20 µg/mL and 2 µg/mL, respectively), 3 times weekly. Upon completion of 5 weeks on instillations, the HDM+SEB rats received additional HDM+SEB or saline instillations and different doses (12.5, 25 or 50 µg) of MSC-CM, *i.n.*-instilled: One dose per week (1W, **A-C**) model or two doses per week (2W, **D-F**) model. During the MSC-CM dosing, the animals continued under HDM+SEB *i.n.* instillations for 2 weeks. None of the MSC-CM doses altered the BAL $CD4^+$ or $CD8^+$ T-cell subpopulations. Data (n= 6) are presented as mean±SEM and were analyzed using one-way ANOVA.

Curiously, we observed down-regulation in the expression of CD161 on B cells after co-administration of HDM plus SEB treatment (p<0.001 versus control group) as described above. Moreover, we showed that all doses of MSC-CM in 1W model not significantly increase this marker expression when compared to asthmatic animals (**Figure 35A-C and Table S30 in appendix**). However, only 12.5 µg doses in 2W model generated an up-regulation of CD161 on B cells (p<0.041 versus HDM+SEB group), while the 25 and 50 µg doses not significantly increase this marker expression, being similarly to HDM+SEB group (**Figure 35D-F and Table S30 in appendix**).

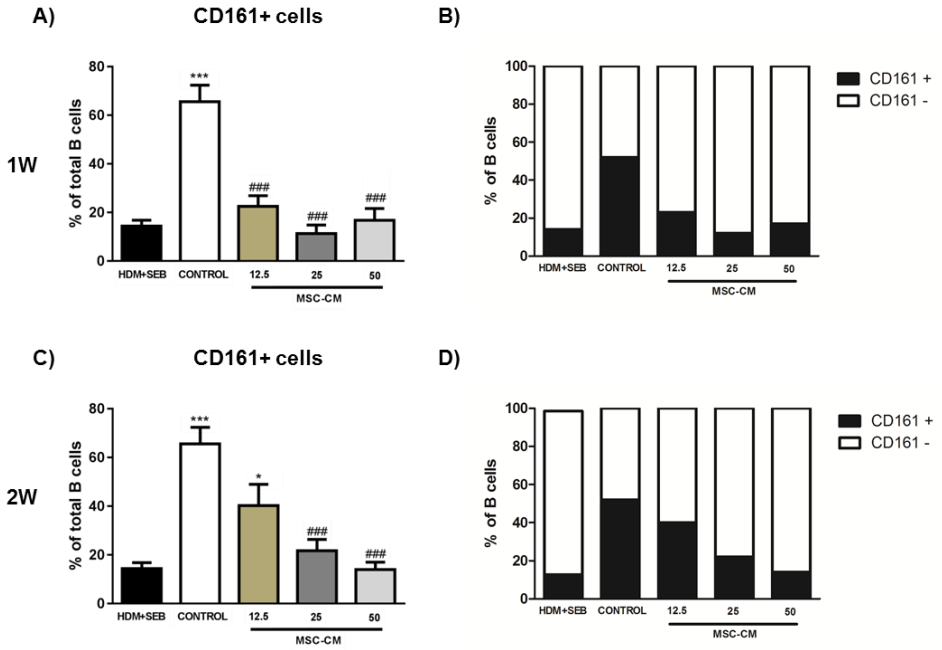

Figure 35| The effect of CM in 1W model on CD161$^+$ B cell expression in bronchoalveolar lavage (BAL). Sprague Dawley rats were *i.n.*-instilled with saline (CONTROL) or HDM+SEB (20 µg/mL and 2 µg/mL, respectively), 3 times weekly. Upon completion of 5 weeks on instillations, the HDM+SEB rats received additional HDM+SEB or saline instillations and different doses (12.5, 25 or 50 µg) of MSC-CM, *i.n.*-instilled: One dose per week (1W, **A-B**) model or two doses per week (2W, **C-D**) model. During the MSC-CM dosing, the animals continued under HDM+SEB *i.n.* instillations for 2 weeks. All doses of MSC-CM showed a decrease of CD161$^+$ B cell expression, similarly to HDM+SEB group (**A**, **B** and **C**). Data (n= 6) are presented as mean±SEM and were

3.6. Conditioned media decreased Th2 deviation in lung and blood.

To further determine if conditioned media generate changes in cytokine production by CD4$^+$ T cells, we performed a flow cytometry analysis of lung and blood from all groups. Using antibodies targeted against a range of surface antigens (**Table 2**) our gating strategy in lung and blood (**Figure 36**). To remove singlets, we utilized the FSC-H and FSC-W parameters to identify and exclude cells stuck together (doublets) and larger clumps. This resulted in a population of live single leukocytes which were separated to obtain T lymphocytes by CD3 expression. Further, T lymphocytes were further delineated by CD4 and CD8. Moreover, CD4$^+$ T cells were gated and delineated by IFN-y, IL-4 or IL-17 with FSC to identify cytokine production. Control isotype was used as negative control.

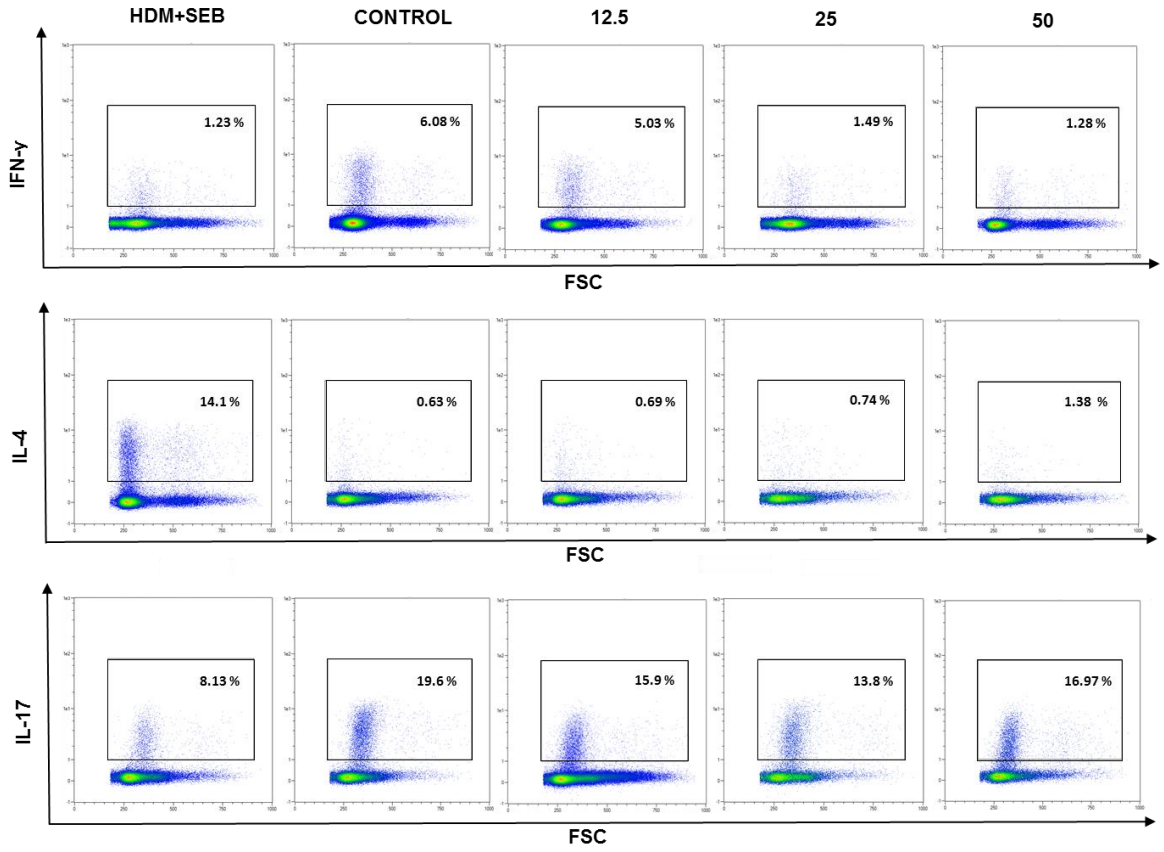

Figure 36| The effect of MSC-CM in 2W model on $CD4^+$ T cell cytokine production in lung. Sprague Dawley rats were *i.n.*-instilled with saline (CONTROL) or HDM+SEB (20 µg/mL and 2 µg/mL, respectively), 3 times weekly. Upon completion of 5 weeks on instillations, the HDM+SEB rats received additional HDM+SEB or saline instillations and different doses (12.5, 25 or 50 µg) of MSC-CM, *i.n.*-instilled: One dose per week (1W) model or two doses per week (2W,) model. During the MSC-CM dosing, the animals continued under HDM+SEB *i.n.* instillations for 2 weeks. Data (n= 4) are presented as mean±SEM.

We observed that frequencies of IFN-y secreted by $CD4^+$ T cells in lung decreased in HDM+SEB-challenged animals (p=0.021 versus HDM+SEB group). We showed that all doses of MSC-CM in 1W model not increased IFN-y production when compared to asthmatic group. However, only 12.5 µg doses of MSC-CM in 2W model increased frequencies of IFN-y secreted by $CD4^+$ T cells (p=0.026 versus HDM+SEB group), while no differences observed when rats were treated with 25 and 50 µg of MSC-CM (**Figure 37A and D and Table S31 in appendix**).

Further, HDM+SEB-challenged animals showed an increased production of IL-4 in lung (p<0.001 versus control group).Curiously, all doses of MSC-CM (12.5, 25 and 50 µg) in 1W and 2W model decreased the IL-4 production by $CD4^+$ T cells, being similarly to control animals MSC-CM (**Figure 37B and E and Table S31 in appendix**).

We showed that frequencies of IL-17 production by $CD4^+$ T cells in lung decreased in HDM+SEB-challenged animals (p=0.018 versus HDM+SEB group). Moreover, we showed that all doses of MSC-CM (12.5, 25 or 50 µg) in 1W model significantly increase in IL-17

production (p=0.013, p=0.015 and p=0.026 respectively, versus HDM+SEB group) (**Figure 37C and F Table S31 in appendix**). Further, when rats were treated with 12.5, 25 or 50 µg doses of MSC-CM in 2W model increased frequencies of IL-17 secretion by $CD4^+$ T cells (p=0.020, p=0.040 and p=0.040 respectively, versus HDM+SEB group) (**Figure 37C and F Table S31 in appendix**).

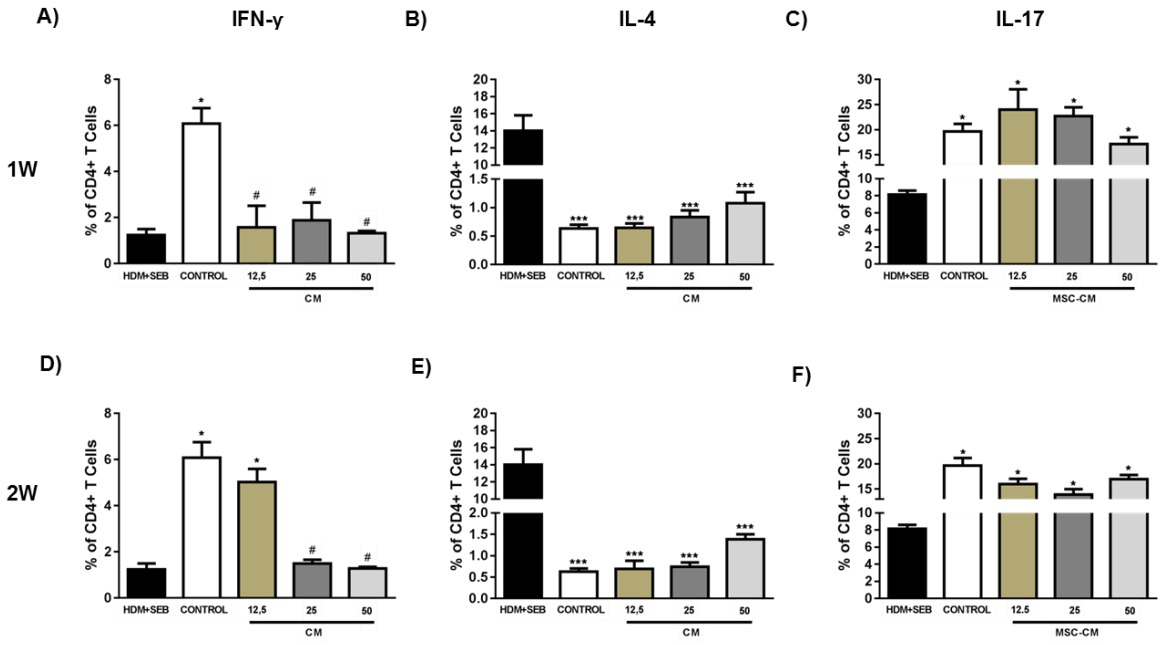

Figure 37| The effect of CM in 1W and 2W models on $CD4^+$ T cell cytokine production in lung. Sprague Dawley rats were *i.n.*-instilled with saline (CONTROL) or HDM+SEB (20 µg/mL and 2 µg/mL, respectively), 3 times weekly. Upon completion of 5 weeks on instillations, the HDM+SEB rats received additional HDM+SEB or saline instillations and different doses (12.5, 25 or 50 µg) of MSC-CM, *i.n.*-instilled: One dose per week (1W, **A-C**) model or two doses per week (2W, **D-F**) model. During the MSC-CM dosing, the animals continued under HDM+SEB *i.n.* instillations for 2 weeks. All groups showed IL-4 decrease in lung when compared with asthmatic group (**B** and **E**). All doses in 1W and 2W model showed an increase of IL-17 (**C** and **F**), similarly to the control animals. Only 12.5 µg doses in 2W model generated IFN-y production in lung versus HDM+SEB group (**D**), while no differences observed in 1W model doses (**A**). Data (n= 4) are presented as mean±SEM and were analyzed using the one-way ANOVA test. *: p<0.05 versus HDM+SEB group; ***: p<0.001 versus HDM+SEB group; $^{\#}$: p<0.05 versus control group.

We observed that frequencies of IFN-y secreted by $CD4^+$ T cells in blood decreased in HDM+SEB-challenged animals (p=0.011 versus HDM+SEB group). We showed that all doses of MSC-CM in 1W model not increased IFN-y production when compared to asthmatic group (**Figure 38A and Table S31 in appendix**). However, when rats were treated with 12.5 doses of MSC-CM in 2W model increased frequencies of IFN-y secreted by $CD4^+$ T cells (p=0.035 versus HDM+SEB group), while no differences observed when rats were treated with 25 or 50 µg of MSC-CM (**Figure 38D and Table S31 in appendix**).

Further, HDM+SEB-challenged animals showed an increased production of IL-4 in blood (p<0.001 versus control group). Curiously, all doses of MSC-CM (12.5, 25 and 50 µg) in

1W and 2W model decreased the IL-4 production by $CD4^+$ T cells, being similarly to control animals MSC-CM (**Figure 38B and E and Table S31 in appendix**).

We showed that frequencies of IL-17 production by $CD4^+$ T cells in blood were similarly in HDM+SEB-challenged animals when compared to control group. Curiously, no differences observed when rats were treated with all different doses of MSC-CM (12.5, 25 and 50 µg) in 1W and 2W model (**Figure 38C and F and Table S31 in appendix**).

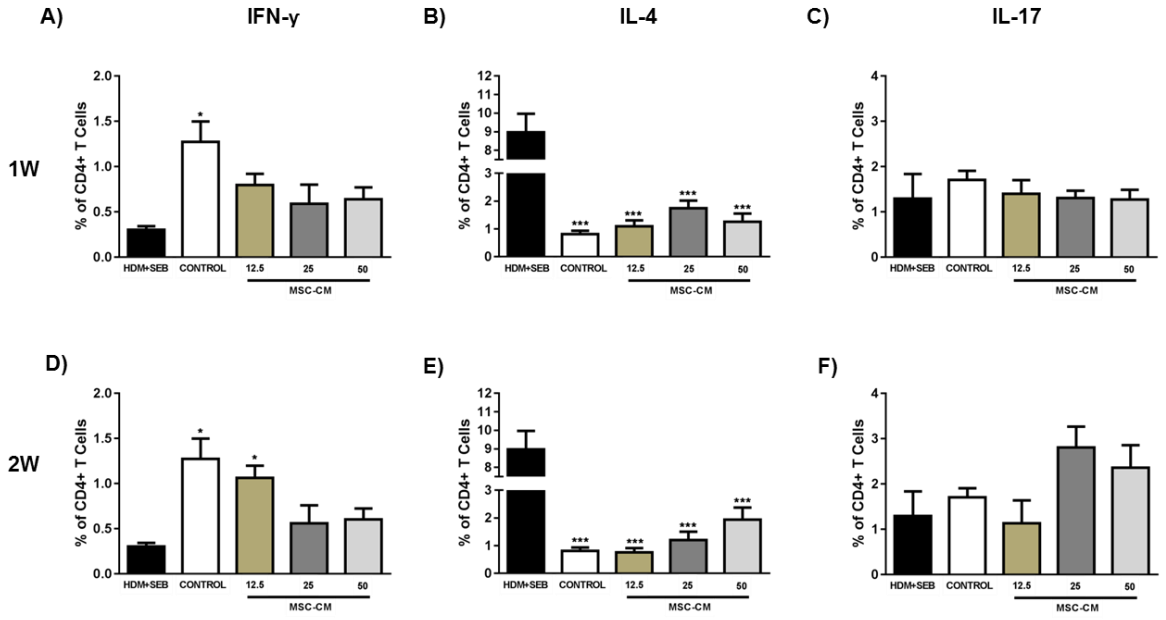

Figure 38| The effect of CM in 1W and 2W models on CD4 T cell cytokine production in blood. Sprague Dawley rats were *i.n.*-instilled with saline (CONTROL) or HDM+SEB (20 µg/mL and 2 µg/mL, respectively), 3 times weekly. Upon completion of 5 weeks on instillations, the HDM+SEB rats received additional HDM+SEB or saline instillations and different doses (12.5, 25 or 50 µg) of MSC-CM, *i.n.*-instilled: One dose per week (1W, **A-C**) model or two doses per week (2W, **D-F**) model. During the MSC-CM dosing, the animals continued under HDM+SEB *i.n.* instillations for 2 weeks. All groups showed IL-4 decrease in lung when compared with asthmatic group (**B** and **E**). Only 12.5 µg doses in 2W model generated IFN-γ production in lung versus HDM+SEB group (**D**), while no differences observed in 1W model doses (**A**). No differences showed in 1W (**C**) and 2W (**F**) IL-17 production when compared with HDM+SEB group. Data (n= 4) are presented as mean±SEM and were analyzed using the one-way ANOVA test. *: $p<0.05$; ***: $p<0.001$ versus HDM+SEB group.

3.7. Proteomic analysis of fractioned MSC-CM

One-dimensional SDS-PAGE of the soluble protein extracts demonstrated differences in the intensity of the staining and the number of bands between medium alone and the 30-100 kDa molecular weight range of MSC-CM, where the MSC-CM electrophoresis showed limited complexity in its composition as demonstrated by few stained bands (**Figure 39A**). A total of 37 proteins were identified by mass spectrometry. **Table 4** presents detailed information on the identification of proteins in each band. Each data set

was subjected to gene ontology using PANTHER, which facilitated the characterization of identified proteins.

When the identified proteins were classified by biological process, it resulted in 40.5 % of the proteins allocated to cellular process functions, 9.5% to response to stimulus, 9.5% to developmental processes, and 7.1% to multicellular organismal processes (**Figure 39B**).

As for classification by molecular function, 29.4% of the proteins were attributed to binding processes, 14.7% to structural molecule activity, 5.9% to regulation functions, and 2.9% to transcription regulator activity (**Figure 39C**).

Classification by protein class with PANTHER identified 25% of the proteins as hydrolases, 8.3% as enzyme modulators, 8.3% as transferases, 4.2% as oxidoreductases, 4.2% as lyases, and 4.2% as transcription factors (**Figure 39D**).

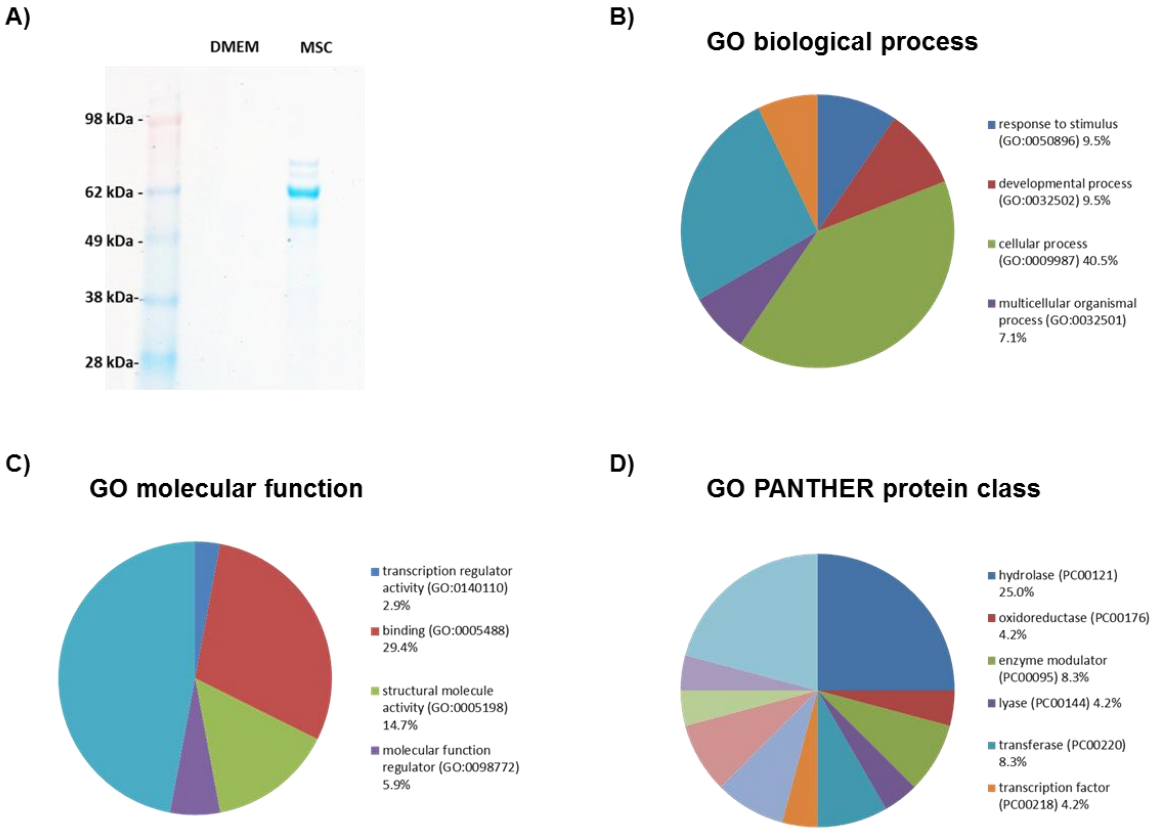

Figure 39| Protein identification in the 30-100-kDa MSC-CM fraction. The 30-100-kDa molecular weight fraction of MSC-CM or DMEM medium was subjected to SDS-PAGE. Ten µg of protein from MSC-CM or DMEM was loaded and run on a gel, and stained with Coomassie blue (**A**). The proteins identified through proteomics were classified by molecular biological processes (**B**), molecular function (**C**), and protein class (**D**), via PANTHER (Protein Analysis through Evolutionary Relationships) Classification System (www.pantherdb.org/).

Table 4| Identification of proteins contained in MSC-CM.

Accesion number	Name
P11598	Protein disulfide-isomeraseA3
G3V9E3	Caldesmon 1
P50398	Rab GDP dissociation inhibitor alpha
D3ZVR9	Phosphoglucomutase 5
PO4785	Protein disulfide•isomerase
Q6IRK9	CarboxypeptidaseQ
P40124	Adenylyl cyclase-associated protein
A0A097PUG1	Anti-lox-1 15C4 heavy chain
008553	Dihydropyrimidinase-related protein 2
Q3TJXO	Lcp1 protein
AOA1C7CYVO	Plastin-3 (Fragment)
P30349	LeukotrieneA-4 hydrolase
P26043	Radixin
AOAOG2K890	Ezrin
F7FLB2	Pgm2 protein
A0A1W2Q6E9	Moesin
Q9ROHS	Keratin, type II cytoskeletal 71
A0A09713W25	Periostin
Q3UD81	Actgl protein
P18418	Calreticulin
A0A0G2JUN7	Thioredoxin reductase 1
P32261	Antithrombin-III
P04785	Protein disulfide-isomerase
Q9EPB1	Dipeptidyl peptidase 2
Q4QQV4	Dead end homolog 1
Q5I0D7	Xaa-pro dipeptidase
Q3TJ52	Rad23b protein
P49088	Asparagine synthetase
A0A0G2K509	Keratin, type II cytoskeletal 5
P40142	Transketolase
P33434	72 kDa type IV collagenase
P06761	Endoplasmatic reticulum chaperone BIP
Q504P4	Heat shock cognate 71 kDa protein
P02454	Collagen-alpha (I) chain
G3V6T7	Protein disulfide-isomerase A4
E9Q1S3	Protein transport protein SEC23
Q3TGJ9	Gsn protein

DISCUSSION

The uses of experimental asthma animal models enhance the study of biological and immunological mechanisms with a depth that is not possible on humans. Many questions originated from clinical observation in patients could be understood using experimental models, and these can be translated to the human context. The molecular and cellular basis of allergic asthma is becoming better understood through animal studies, which show how genotypic variations result in specific phenotypic outcomes [123], [137]. Therefore, animal models have an important role in the preclinical development of new therapies by the pharmaceutical research.

There is a variety of studies that use different animal species to develop an efficient model of asthma [121], [124], [128], [138]. The animal most used by researchers is the mouse, due to its low price and the similarities observed between murine and human asthma [18]. However, because of important anatomical and physiological differences between mice and humans, the translation of results to humans needs to be evaluated with care [18].These discrepancies between species explain many problems to translate findings from mouse to human clinical practice [18]. Recently, the rat has been used by numerous investigators over other animals [121]. The rat, compared to other laboratory animal species, exhibit many features of allergic asthma that are comparable to those observed by humans, and its respiratory system anatomy and bronchial circulation are closer to those of humans [121].

It is well accepted in experimental rat studies that their susceptibility to develop allergic and physiological responsiveness to allergen challenge are strain dependent [123], [137]. The Brown Norway (BN) rat is genetically Th2-predisposed and has been the most widely used strain for studying allergic inflammation [137]. Conversely, the BN demonstrates high baseline response when are untreated. These problems combined with heterogeneous response in the strength of allergic response between interindividual animals generate confusion of the allergic pathophysiology [123].

Previous studies demonstrated that Lewis (LW) and Sprague Dawley (SD) rats had lower baseline responses than BN rats when are untreated. Further, there are differences to histopathology lesions, Th2 cytokine levels, and eosinophil levels in the BAL, which suggested that BN strain could have inappropriate for develop an animal model for asthma research [123]

Further, previous studies showed that local allergen sensitization generated an increase of AHR in SD rats after five challenges, which was similar as the BN allergic response. Conversely, LW rats did not develop AHR under any circumstances [123]. It is now well studied that allergic asthma is a chronic disease resulting from continued or recurrent interaction to an allergen. Moreover, the airway is exposed to a prolonged chronic inflammatory state that leads to different structural changes collectively attributed to as airway remodeling [205]. In fact, it is possible to emulate human asthma features in the rat, such as abnormalities in the structural airway system reflecting airway remodeling and airway hyperresponsiveness resulting to airflow obstruction with nonspecific challenge. Airway hyperresponsiveness is an important asthma feature due to correlation role between airway remodeling and inflammation [120], [206]. Moreover, this animal can reproduce airway eosinophil infiltration in the lung with the development of adaptive immune response to an allergen, mediated by activated $CD4^+$ T cells with a Th2 biased phenotype [121].

However, there are limitations when interpreting the animal models data in the human translation context. In most studies observed on animal asthma models, the disease was developed by OVA sensitization and challenge that reproduce the inflammatory and immunological process in the lung [121]. However, it has been postulated that the need of OVA with an artificial adjuvant does not correctly mimic how asthmatic patients become sensitized to aeroallergens [139]. These limitations should prompt investigators to find more appropriate methods that allow closer comparison with humans [121]. Therefore, questions about the relevance of OVA have promoted the use of alternative allergens considered more appropriate to represent the human condition, including HDM [18]. However, antigenic sensitization occurs depending on immunological factors, such as pathogenic and non-pathogenic microorganisms that affect innate and adaptive immune responses. We showed that bacterial factors such as SEB could break a state of tolerance and lead to the development of an allergic immune response in the airways when inhaled together with an allergen [144], [145]**.** It has been reported that SEB induces the production of other cytokines such as IL-2, IL-4, IL-5 and IL-13 in the human allergic mucosa [207].

In the work presented in this thesis, we aimed at studying the effect of mesenchymal stem cells on airway remodeling in a new experimental asthma model based on local exposure, to better reproduce the natural immunological response and development of asthma

features to airborne allergen. For the animal asthma model development, the animals were exposed to an allergen or control through different continued protocol.

We chose *i.n.* instillation as the procedure for airway allergen exposure based on previous studies in our laboratory by us [208], and others who reported that antigens administered by *i.n.* instillation reaches the intrathoracic airways and is deposited into the lungs [209]. Other approaches for airway allergen exposure have been less used and present practical inconveniences or limited lung deposition. Antigen delivery through orotracheal intubation or tracheotomy requires general anesthesia and surgery in the latter case. Such methods are controversial as a repeated procedure on the same animal due to the invasive intervention required. Another approach is the exposure of awake animals to allergen nebulized into a chamber, which results in a reduced deposition in the airways and facilitates bowel allergen exposure, partly indirectly through skin deposition and licking, which may induce immune tolerance [210].

In order to profile the timeline of the immune response and associated experimental disease driven by *i.n.* instillation, we developed the 10IN, 15IN and 30IN models. The 10IN and 15IN model cut-off were chosen as the time point where the time elapsed from the first contact with the antigen generated asthma disease. It has been reported that 5-week exposed mice treated with HDM demonstrated a significant and severe increase in airway reactivity, as evidenced by the slope of the dose response curve to MCh [211]. Finally, the results obtained in the in 15IN model led us to develop the 30IN model, to represent extended chronicity and analyze whether the experimental asthma features elicited in the 15IN model would worsen, plateau or decline.

We chose R_L responsiveness to MCh, an *in vivo* lung function output sensitive to airway hyperresponsiveness, as the primary outcome to evaluate the development of experimental disease through the 10IN, 15IN and 30IN models. The inhalation of nebulized MCh, an acetylcholine analog cholinergic agent [136], stimulates muscarinic receptors in the airway smooth muscle and induces smooth muscle contraction, which in turn increases R_L. In animals with experimental asthma, R_L increases significantly through progressive MCh doses in comparison with control animals. Testing R_L responsiveness to MCh under mechanical ventilation in experimental animals serves indeed as a close analog to spirometric testing of airway hyperresponsiveness in humans.

In the experiments presented in this thesis, we observed that only HDM+SEB-challenged animals in 15IN showed a significant R_L increase at the highest MCh doses (64, 128, 256 $mg \cdot ml^{-1}$) versus the control group, which reflects airway hyperresponsiveness to an

inhaled cholinergic agonist as also seen in clinical MCh testing on asthmatic subjects. In the 10IN model, the R_L response profile of the HDM+SEB animals closely followed that control group, an expected outcome in the absence of an adaptive immune response and dependent IgE and effector T cell-driven inflammatory mechanisms. Given the 15IN model data, we enquired whether the attenuated airway response would fully develop into consolidated airway hyperresponsiveness should airway antigen challenge continue for a prolonged period. This was tested in the 30IN model where, conversely, the R_L response in the HDM+SEB-challenged animals declined and closely approached the control group, such as in the 10IN model. Moreover, in the animals that received SEB or HDM alone in the different models, the R_L response profile did not show a significant increase versus the control group and no airway hyperresponsiveness to inhaled MCh occurred.

In summary, thus our interpretation of this result was that the inhalational exposure to a combination of HDM with SEB for a prolonged period induces airway hyperresponsiveness, declined upon sustained airway antigen challenge. These results were concordance with previous studies, showed that after systemic immunization and challenge with HDM alone, only the Brown Norway rats developed a strong AHR compared with challenged controls [123]. Conversely, Sprague Dawley and Lewis rats did not develop AHR under the same conditions [123]. Therefore, this AHR was attributable to the mechanisms elicited by primary antigen exposure in the airways, and the resulting adaptive immune response, along with potentiating pathways contributed by the presence of SEB.

Due to immunoglobulins play important roles in mediating inflammatory reactions and hypersensitivity, we investigated the concentration of several IgE levels in serum that have been implicated in B-cell immune responses. Serum IgE was also increased only in HDM+SEB-challenged animals on 15IN model when compared to their respective control group, and was correlated with the airway responsiveness data. In the 10IN model, the IgE levels of the HDM+SEB animals not increase and was similar to the control group due to the absence of an adaptive immune response and dependent IgE mechanisms. Moreover, in the 30IN model, the IgE levels declined and and was similar to the control group, such as in the 10IN model. Moreover, in the animals that received SEB or HDM alone in the different models, the IgE profile did not show a significant increase versus their respective control groups. Previous studies demonstrated that SEB is capable of polyclonal T-cell stimulation and induces the production of pro-inflammatory and Th2-polarizing cytokines such as IL-4, IL-5, IL-13 and other cytokines [212]. These data

suggest that repeated exposure to HDM in combination with SEB increases serum IgE in association with an inflammatory response in the airways.

Airway inflammation was evaluated by histopathological examination of lung tissue sections with H-E staining. We show that rats receiving repeated *i.n.* exposure to HDM with SEB induced increased peribronchial inflammatory cells and a marked narrowing of the airway lumen versus the respective control group. Moreover, we observed attenuated cell infiltration in the SEB-challenged animals, while animals treated with HDM alone being similarly to control animals.

Mucus overproduction in the airways was evaluated by PAS color extraction and quantification (mucoid mass).The HDM+SEB treated group showed significantly increased mucus production when compared with the control group. In the SEB group, animals showed an important increment of mucoid mass in the airways, while animals treated with HDM alone not increased mucus production and being similar to healthy rats.

Subepithelial fibrosis was measured by the presence of collagen deposits in the airways. This feature was evaluated by Masson's trichrome color extraction and digital analysis. The SEB and HDM+SEB-challenged rats showed significantly increased collagen deposition in the lamina propria in the bronchus. Conversely, there were no differences when rats were treated with HDM alone.

Airway smooth muscle alterations, which include hyperplasia and hypertrophy, is the most important feature of airway remodeling and was correlated with AHR [33]. We used α-SMA detection, the most detectable biomarker molecule to airway smooth muscle quantification. The analysis of airway contractile tissue mass in the HDM+SEB group and SEB-challenged animals demonstrated large increments of airway contractile tissue, whereas the rats treated with HDM alone not showed significant differences when compared to control animals.

Previous studies demonstrated that HDM in combination with SEB induced allergic chronic rhinosinusitis nasal polyps (CRSwNP) in mice. This model showed eosinophil infiltration, mucus overproduction and subepithelial fibrosis similar to human CRSwNP [213]. Moreover, in the airways, the location of the inflammatory cells also differs [214]. In the mouse, leukocyte accumulation is largely perivascular with edema around blood vessels, while the peribronchial component is diffuse and variable. In humans, immune cell accumulation is in the bronchial wall [215]. In our study, we observed peribronchial distribution of immune cells in rats treated with concomitant application of HDM with SEB,

which reflects an optimized approach to the pathophysiology of human asthma. Therefore, the combination of HDM with SEB for a prolonged period induces a peribronchial influx of inflammatory cells, a marked narrowing of the airway lumen and histopathological signs of airway wall remodeling, a capacity that exposure to SEB or HDM alone does not have.

Airway inflammation was evaluated identifying by different leukocyte subpopulations in BAL by flow cytometry analysis. It has been reported that asthma induced in mice by treatment with OVA and SEB is characterized by T-cell migration and pulmonary allergic Th2 response with eosinophilic recruitment in BAL. We demonstrated that concomitant exposure to HDM with SEB generated inflammatory cell infiltration into the rat airway. We could detect an increase in eosinophils, T and B lymphocytes as compared with the control group. This can be observed in the rat [201] and the immunological mechanisms responsible remain understood. HDM extracts have been composed by some other contaminants generate inflammatory pathway stimulation [44], [216]. Previous studies described that Brown Norway rats have eosinophils in BAL under basal conditions (30-40%) [123], while in human asthma is 1-5% [18]. In this work, we obtained similar levels of eosinophils in BAL fluid as compared to human asthma, which reflects an optimized approach to the pathophysiology of this disease.

However, studies in OVA-allergic asthma model on SD rats demonstrated that not develop eosinophil infiltration and airway hyperresponsiveness following OVA challenge [217]. We suggest that further research to understand this mechanisms in important to reveal immunological pathways and could potentially discover new relevant mechanisms involved in pathogenesis of this disease. CD161 has been shown a regulatory role of lymphocyte tissue recruitment [218], and $CD161^+$ T cells are mainly memory cells [219]. Therefore, they might have a potential commitment in the regulation of asthma condition, and especially in asthma exacerbations, through their migration to the airways and the local production of IFN-y [220]. Increased activation of $CD161^+$ cells with a Th1 cytokine-profile polarization in asthma attack patients may suggest that these cells are part of the mechanisms to compensate the Th2-biased response associated with asthma during the attack [220]. Curiously, we observed decreased expression of CD161 on B lymphocytes after HDM+SEB treatment, which suggests a homeostatic role of this marker in the airways. In addition, this is the first study that demonstrated the differential expression of CD161 on this cell type. This information supports a possible immunoregulatory role of $CD161^+$ B cells in the reestablishment of the altered homeostasis in asthma disease. The mechanisms that induce these alterations in asthma are poorly understood. Whether CD161 expression on B cells may lead to sustained control of asthma condition is an

outstanding question of particular relevance in Th1-cytokine profile polarization in asthma attacks, which requires further studies.

The data obtained by ELISA showed that HDM+SEB induced significantly increased levels of total serum IgE as described above. Further, we determinate the antigen-specific immune response evaluating the BAL and serum levels of specific HDM- and SEB-IgE by ELISA as previously described [201], [202]. We showed that HDM+SEB led to significantly increased levels of specific HDM-IgE in both BAL and serum as compared with controls. It has been reported that rats also received HDM with an adjuvant during sensitization showed significant levels of serum HDM-specific IgE. Conversely, Sprague Dawley rats that did not receive the adjuvant failed to observe the direct inflammatory response to inhaled HDM [201]. Moreover, a combination of OVA+SEB resulted in increased serum levels of OVA-specific IgE as compared to OVA and SEB alone groups [145]**.** Additionally, HDM in combination with SEB allergic induced airway inflammation and increases the total serum IgE in mice [213]. These data suggest that HDM induced the production of allergen-specific IgE in combination with SEB and that observed airway inflammation is part of an allergic phenotype.

In order to determine whether SEB was on its own capable of eliciting the production of specific anti-SEB IgE antibodies, serum and BAL were also tested for the presence of anti-SEB IgE. The data obtained showed no significant differences in anti-SEB IgE titers in BAL or serum among the study groups. These results prove that exposure to SEB via repeated *i.n.* instillation does not generate specific anti-SEB IgE. These results do not exclude the hypothesis that SEB exposure might have led to the production of other anti-SEB antibody isotypes (IgA, IgG or IgM) as was previously described [202]. However, such anti-SEB antibody levels were shown to significantly decline within several hours after SEB exposure [202].

In addition, we evaluate the adaptive immune response deviation measuring BAL and serum levels of total IgG by ELISA. Conversely to IgE results, BAL levels of total IgG were significantly decreased after the concomitant application of HDM with SEB in comparison with the control group. Previously studies showed that the high IgG1 shows a Th1 component of allergen sensitization, as also indicated by the Th1 cytokine responses to HDM allergens in T-cell studies [221], [222]. Moreover, the less important allergens did not induce IgG4, so for HDM allergy, allergenicity correlates with immunogenicity rather than a response deviated away from IgG [223]. These data demonstrated that concomitant application of HDM and SEB induced a Th2 sensitization with increased

levels of IgE as well as decreased the levels of IgG, which is known to block mast cell degranulation and IgE-mediated allergen presentation [223].

Treatment of rats with the combination of HDM and SEB showed a marked elevation of IL-4, IL-5, IL-13, IL-17A, IFN-y and eotaxin levels in BAL fluid of the rats exposed as compared with the control group as we as increased levels of serum IL-5. Moreover, we not observed any differences in all other cytokines between all groups in serum. Th17 immunological response has an important role during allergic inflammation and asthma features were significantly reduced in mice knock-out for IL-17 cytokine. It has been reported that allergic asthma features was attenuated in the absence of IL-17A or IL-17F, and was observed due to a reduction of AHR, eosinophilic infiltration and mucus overproduction [224]. Previous studies showed that SEB treatment increased production of the IFN-y. At this time, the secretion of TNF-α was inhibited [225]. In addition, it has been reported that intranasal SEB increased the levels of IL-4, IL-5 and IFN-y in serum, while local administration in the lungs increase the OVA-specific IgE in serum [212]. Further, it has been reported that HDM treatment increased eotaxin levels in SD rats [201]. These results show that airway contact with SEB is capable of aggravating several features of bronchial allergic inflammation. Therefore, airway contact with HDM plus SEB may be crucial to favor a Th2 response with increased IL-4, IL-5 and IL-13 production that results in an enhanced response to antigen challenge.

However, studies in mice that were chronically exposed to low doses of SEB demonstrated increased levels of TGF-β1 and Th2-cytokines [226]. These observations prompted us to suggest that continued *i.n.* sensitization to HDM and SEB might induce increased levels of TFG-β1 and Th2 cytokines in comparison to the administration of SEB alone, which could increase levels of IL-10. Furthermore, the presence of SEB during allergen exposure could potentiate the Th2 driven immune response to the allergen. To measure IL-10 and TGF-β1 levels in bronchoalveolar lavage, to explore mechanisms on how a hypothetical SEB synergism with allergic sensitization may contribute to airway remodeling.

In conclusion, our observation in the first part of this work demonstrated that the repeated primary airway exposure to *D. pteronyssinus* in combination with SEB in a Th1/Th2 neutral immunocompetent rat strain provides a novel and robust model of atopic experimental asthma with an optimized approach to the pathophysiology of human atopic asthma.

Asthma is an immune-mediated disease, pathologically characterized as airway inflammation, airway hyperresponsiveness and subsequent abnormal repair leading to structural changes in the airways, known as airway remodeling. Infiltration of T lymphocytes into the lungs is a major hallmark of asthma. The close proximity of T lymphocytes with structural cells has been reported in many studies [107], [108]. Several studies have examined the effects of T lymphocytes on biological processes in airway structural cells, which included airway smooth muscle cells and epithelial cells [106], [107], [205]. Airway smooth muscle cell proliferation is the most important feature of airway remodeling and many mediators have been implicated [120]. The increase of ASM mass may be a critical factor that is implicated in AHR and the asthma clinical significance [120]. ASM cells play a pivotal role in asthma as a structural cell which contracts in response to a bronchoconstrictor [120]. Direct contact of this structural cell with other cells has been documented in the context of asthma in recent years [106], [107].

Although reported by Brightling *et al.* that T cells did not infiltrate the ASM layer in asthmatic subjects [227], subsequent studies have clearly demonstrated the presence of T lymphocytes within the muscle bundles and in close proximity to the ASM cells. However, the interaction of T lymphocytes and structural cells also leads to a response in T cells, such as an increase in survival [107]. Further, little is known on the effect of structural cells on inflammatory cells. It has been reported a direct interaction between T cells and ASM, where via ICAM-1, VCAM-1 and CD44 are implicated and induced ASM proliferation [106]. However, the T cell-derived mediators responsible for mediating the increase of ASM cell hyperplasia had not been addressed to our knowledge. Therefore, it is crucial to find an effective treatment to suppress the development of airway remodeling in asthma. MSC are a promising candidate for the treatment of asthma due to their immunomodulatory features. These cells have the ability to repair deteriorated lungs and enhance the resistance to infections due to their suppressive effect [168]. In addition, previous studies in our laboratory demonstrated that MSC may suppress airway inflammation in experimental asthma *in vivo* [169].

In the second aim of the present work, we tested whether HDM allergen activates effector $CD4^+$ T cells and elicits airway myocyte proliferation upon direct contact *in vitro*, as previously shown for OVA. We demonstrated whether direct contact between HDM-specific $CD4^+$ T cells and ASM induces ASM proliferation and $CD4^+$ T cell survival *in vitro*. Moreover, we investigate whether adipose-derived MSC, added to the $CD4^+$ T cell/ASM co-culture, interfere with ASM proliferation induced by effector $CD4^+$ T cells *in vitro*.

We based on studies and methodology of Ramos-Barbon *et al*., who showed that OVA-specific $CD4^+$ T cells airway smooth muscle cell proliferation in direct contact and the reciprocal effect, the myocytes prevented post-activation antigen-specific $CD4^+$ T cell apoptosis [107]. We demonstrate here that $CD4^+$ T cells activated by HDM, but not naïve T cells, induced sensitized ASM cell proliferation in direct T cell-myocyte contact with prevented $CD4^+$ T cell apoptosis. These data suggest that in allergen-sensitized rats, repeated airway sensitization induced ASM proliferation mediated for the antigen-specific $CD4^+$ T cell contact. Several studies have shown that monoclonal antibody depletion of $CD4^+$ T cells in a mouse model inhibits AHR and eosinophilic infiltration [111]. Depletion of $CD4^+$ T cells by repeated ovalbumin challenges in BALB/c mice resulted in a marked decrease of AHR and specific features of airway remodeling, including subepithelial fibrosis, epithelial thickening and mucous cell hyperplasia and metaplasia [112]. However, the immunological and molecular pathways that have been implicated in airway remodeling and ASM proliferation remain understood. The most documented mechanism of molecular exchange between cells is the secretion of mediators, which bind to receptors on target cells. However, the direct contact of $CD4^+$ T cells and ASM cells is essential for the ASM proliferation. Studies in humans and OVA-sensitized rats demonstrated that $CD4^+$ T cells adhered to ASM cells via adhesion molecules and CD44 to generate ASM proliferation [228], [229]. Recent studies demonstrated that inhibition of CD44 or MMP-9 is sufficient in preventing ASM cell proliferation [228]. Such adhesion molecules as immune receptors lead to stimulation of molecular pathways that may be implicated in proliferation, which include MAPK and PI3K activation [228]. Our data demonstrate that HDM-activated $CD4^+$ T cells induced proliferation of cell cycle-arrested ASM cells, which could regulate AHR by the secretion of soluble factors and adhesion molecules [228]. These effects might induce the contact of $CD4^+$ T cells and progress the tissue repair induced the remodeling of ASM. Recent studies demonstrate that activated T cells communicate with ASM cells and are involved in T cell survival [229]. Furthermore, *in vitro* ASM cells largely inhibit apoptosis of the OVA-activated $CD4^+$ T cells [107]. ASM cells may have a proinflammatory effect in asthma through the secretion of soluble factors [228]. In contrast, other studies suggest that $CD4^+$ T cells are not required for airway remodeling during allergen challenges after the development of acute eosinophilic lung inflammation in a murine model [114]. Further studies are needed to determine the molecular pathways that may be implicated in the regulation of AHR by $CD4^+$ T cell interaction. In summary, $CD4^+$ T cells activated by antigen in direct contact with ASM cells induce the myocyte DNA synthesis and proliferation, and the reciprocal effect, the myocytes prevented post-activation antigen-specific $CD4^+$ T cell apoptosis.

In order to determinate the therapeutic effect of MSC in airway remodeling, we used different ratios of these cells in the ASM/ $CD4^+$ T cell co-culture model performed above. We observed that only high doses of MSC (1:5/1:10) separated by a membrane could inhibit ASM proliferation. After verifying that the direct contact between ASM and $CD4^+$ T cells is necessary to induce the ASM proliferation we aimed at probing whether MSC might promote an anti-inflammatory therapy. The optimal asthma treatment should relieve symptoms, attenuate inflammation and prevent remodeling. There are reported that administered MSC have the ability to migrate to injured tissues and contribute to their regenerative effect [51]. Moreover, an important point of this effect is modulated by the microenvironment. Depending on inflammatory stimuli, MSC have the ability to regulate immunological pathways, but stimulate effect was observed in other context [51]. Previously studies demonstrate that MSC have a suppressive effect on naïve and memory T cells [203]. There are reported a significant suppressive effect when high number of MSC were added (MSC:lymphocyte ratio >1:10) [203]. Human MSC have the ability to inhibit T and B cells when were separated by Transwell, whereas mouse MSC require cell interaction to do this effect [203]. By in contrast, MSC at a low ratio (MSC:lymphocyte 1:100 – 1:1000) often enhances T cell proliferation [203]. In our data, we cultivated 1:5, 1:10, 1:100 and 1:1000 (MSC:lymphocytes) of MSC in direct contact with T cell-myocyte or in the upper of a Transwell. Our data demonstrate that the MSC in contact with T cell-myocyte allows the $CD4^+$ T cells to proliferate. Further, we demonstrate that rat MSC seems at human MSC because only T cells were suppressive when MSC were separated by a Transwell, being suppressive in high ratios (1:15/1:10). The data suggest that some MSC suppressive factors might rapidly downregulate airway remodeling in association with inhibit the $CD4^+$ T cell proliferation and the subsequent T cell-myocyte interaction. On the contrary, co-culture experiments using Transwells to separate MSC and lymphocytes result in marked suppressive effect on lymphocyte proliferation and were blocked when MSC were added in direct contact [230]. However, when specific CD95L and TGF-β antibodies were added, they inhibit MSC suppressive effect on activated T cells, but anti-IL10 had no effect [231]. Pro-inflammatory cytokines such as INF-γ and TNF-α trigger that MSC produce large amounts of nitrogen oxide (NO) (in mice) or indoleamine 2,3-dioxygenase (IDO), which are involved in the MSC suppressive effect [51]. MSC might inhibit T-cell proliferation through the production of IDO [203]. IDO is induced by IFN-γ, inhibit T cell responses by tryptophan depletion [232]. IDO is a critical molecule that regulated the immunomodulation of MSC, and is an important target to maintain their suppressive effect [51].

Furthermore, these data suggest that the T cells proliferation maybe change the Th2 subpopulation. Other studies demonstrate that MSC increase the portions of $CD4^+$ $CD25^{high}$ population, the called regulatory T cells which have potent suppressor activity [203]. On the other hand, PGE2, which is synthesized by cyclooxygenase enzymes, have the ability to stimulate regulatory T cells [203]. On the other hand, MSC express COX-1 and COX-2, and in culture with T cells COX-2 and PGE2 production increase [203]. However, previously studies *in vivo* in asthma mouse model suggest that MSC administered rapidly downregulate airway inflammation and mucus production in association with a rise of Th1 cytokines in the lung, but such effects declined under sustained allergen challenge despite a persistent presence of the MSC [169]. However, whether repeated MSC doses may lead to sustained anti-inflammatory activity is a standing question of particular relevance for clinical translation that requires more studies [169]. In summary MSC have the ability to ASM arrested-proliferation. Furthermore, the degree of activated $CD4^+$ T cell suppression is dose dependent, only when larger numbers of MSC are present in a Transwell we observe a marked immunosuppression. Nevertheless, MSC trigger anti-inflammatory feature inducing inhibition of T cell and ASM proliferation.

MSC release exosomes with the capacity to enhance lung tissue regeneration and this may be of use in alleviating airway remodeling in asthma [192]. In asthma, exosomes can regulate immune and inflammatory responses in a beneficial and detrimental manner [192]. The severity of asthma has been linked with distinct exosomal pools and/or content which have important roles in disease at least in primary cells and in in vivo models of disease [192]. Previous studies suggested that the fraction contain extracellular vesicles are composed by exosomes and microvesicles are released by MSC, which contribute in the suppressive effects of conditioned media [192].

To confirm if exosomes act as a vehicle for suppressive ASM proliferation factor and $CD4^+$ T cell inhibitor, we first used GW4869 to inhibit the exosomes secretion in cultivated MSC. GW4869 controls ceramide synthesis and regulates the secretion of exosomes [233]. Previous studies demonstrated a GW4869-specific fluorescence that was detected using a 405 nm excitation filter and 450/50 nm emission filter [204]. First, we demonstrated the blocking exosome release in MSC cultivated with GW4869. The data demonstrated an increase of CD63, an exosomal marker, in MSC cultivated with GW4869 when compared with MSC without inhibitor. In addition, we observed GW4869-specific fluorescence using a 405 nm excitation in MSC carrying the inhibitor as described above. In proteomic analysis of the MSC secretome, many factors involved in immune system regulation and

matrix components were reported, which include with extracellular vesicles such as CD63 or CD81 and are enriched on exosomes, small microvesicles, 30-100 nm in diameter, which are stored within multivesicular bodies and released into the environment by fusion with the cell membrane [234]. Our data showed that high doses of MSC (1:5) cultivated with GW4869 and separated by a membrane can inhibit ASM proliferation. It has been reported that exosomes derived from adipose derived MSC regulate cell apoptosis and induce cell proliferation in a cisplatin-induced acute kidney injury model [234], [235]; and an acute kidney injury model where MSC activate a proliferative program in tubular cells [236]. Further, we demonstrate that rat MSC cultivated with GW4869 enhance $CD4^+$ T cell proliferation.

Conditioned MSC medium from high doses (1:5) of cultivated MSC can inhibit ASM proliferation and was T cell immunosuppressive. In the lung, using an *in vitro* system, Liang *et al.* showed that bone marrow MSC-CM can inhibit the proliferation of pulmonary artery smooth muscle cells, an effect not observed with fibroblast-CM [237]. This observation demonstrated that, in addition to the immunomodulatory effect of MSC on lung inflammation, these cells release factors with an anti-proliferative activity on smooth muscle cells, directly inhibiting vascular remodeling. Previous studies demonstrated that MSC-CM was can alter the proliferative response of pulmonary artery smooth muscle cells *in vitro*, and this treatment ameliorated pH and early pulmonary inflammation in a hypoxic mouse model [238]. Further, other data showed that stem cell-secreted growth factors are responsible for some of the therapeutic effects of stem cells inside the body, it seems logical that the paracrine functions of MSC driven by secretome could be monitored in the supernatant MSC-CM [239]. Moreover, other studies revealed that systemic injection of MSC-CM in repeated doses could be effective in the alleviation of chronic asthmatic changes in lung tissues [185]. On the contrary, MSC-CM in a single dosage did not yield any beneficial effects in lung tissues of sensitized rats, which was reinforced by our recently findings [185]. Significantly, MSC had shown to release growth factors when stressed by hypoxia *in vitro* [240], [241], and as discussed by Foronjy and Majka, understanding the lung microenvironment is important because the endogenous MSC niche interact with differents pathways and are dependent by the microenvironment [242]. Finally, the administration of MSC-CM shortly after hyperoxic exposure abrogated the inflammatory lung infiltration, pointing to the existence of anti-inflammatory mediators in the medium [243]. In addition, we demonstrate that MSC conditioned media had suppressive $CD4^+$ T cells. The data suggest that some MSC suppressive factors might rapidly inhibit the $CD4^+$ T cell proliferation and the subsequent T cell-myocyte interaction,

and MSC not require the previous signaling to secrete this factor. Previous studies revealed that systemic administration of MSC-CM in repeated doses could significantly reduce pathological injuries in OVA-sensitized rats by the regulation of expression of T-bet and GATA-3 in the airways [179], [182], [189]. In a bleomycin-induced pulmonary fibrosis model, Jun et al. reported a loss of resident MSC with an associated impaired T-cell response, while administration of exogenous lung MSC, isolated as the side population, or their MSC-CM, conferred a protective effect [244]. Finally, in this study we have shown that MSC have the ability to release inhibitory factors when cultured without stimulants and demonstrate that their effect is an intrinsic mechanism. In this study we have demonstrated that soluble factors released in MSC-CM from the cultures possess the ability to inhibit T lymphocyte proliferation without previous stimulation. Moreover, previous studies showed that human amniotic MSC were not stimulated prior to MSC-CM collection and suppress T lymphocyte proliferation [245]. On the contrary, MSC from BM [246], [247] not possess this intrinsic effect and have suppressive when were cultured with activating stimulus, such as proinflammatory cytokines which include TNF-α, IFN-y or IL-1β [248]. In addition, other studies showed that Th1 cells have a crucial role to stimulate the suppressive effect by MSC in mice and is mediated by the secretion of IDO [249].

To establish the molecular weight which contains the inhibitory factor(s) in MSC-CM, we fractionate the conditioned medium. All fractions were then tested for their effects on activated ASM/$CD4^+$ T cell co-culture. The fraction containing molecules with a molecular weight of 30-100 kDa was the only fraction maintaining an inhibitory effect on activated ASM/$CD4^+$ T cell co-culture. However, the other fractions obtained by the conditioned medium did not show any inhibitory effect. Further, the level of $CD4^+$ T cell suppression achieved with the fraction containing molecules <3 kDa and 30-100 kDa was maintained when compared with the other fractions. Further, previous studies demonstrated that the inhibitory factor(s) main a non-proteinaceous nature and possess <3 kDa of molecular weight [149]. The lists of candidate mediators released by MSC include TNF-α, IL-10, IDO, PGE2 among others [264]. It has been reported that IDO and NO have an important candidates in the inhibitory effect on T-cell proliferation [250], [251].

In summary, the results in this second part point to the direction that only antigen-specific $CD4^+$ T cells induce ASM remodeling through a mechanism involving direct interaction with T cells. On the other hand, the addition of MSC in the T cell-myocyte co-culture suggests that it would be an asthma therapy. MSC may ameliorate ASM remodeling and airway hyperresponsiveness by anti-inflammatory and immunosuppressive features and ASM arrested-proliferation only when these cells were separated by Transwell membrane.

Thus, MSC have a variable modulation of the immune system than their inhibitory effect. In this part of the work, we observed that the therapeutic effect of MSC *in vitro* is characterized by a suppressive action and has induced in a paracrine mechanism. These observations reveal a suppressive effect of MSC and their conditioned media and have a good point to be more efficacious than cell transplantation.

Given the lack of definite therapeutic advantages and the progressive nature of the disease, new strategic approaches seem to be essential for facilitating the regeneration rate of asthmatic changes [182]. It has been demonstrated that systemic transplantation of MSC or MSC-CM could significantly shift $CD4^+$ T lymphocyte population from Th2 cells toward a Th1 phenotype, alleviating airway inflammation during lung injury [185], [252]. However, underlying mechanisms governed by MSC during asthma have still not been fully addressed. Rat models of asthma not completely, but considerably, mimic many of the features of human allergic asthma [121]. Indeed, understand the mechanisms directed by MSC in a rat model of asthma will promote clinical application of stem cells for asthmatic subjects as one of the most promising candidates for regenerative medicine field and cellular therapy [182].

The most beneficial effects of MSC administration seen in previous studies in our laboratory were demonstrated that MSC migrate and recruited in the airways when inflammatory factors were secreted in injured lungs [169]. MSC immunoregulatory effects and allogeneic tolerance led to investigations into the treatment of severe immune-mediated diseases, which in turn attracted interest in anti-inflammatory MSC as a potential asthma treatment [253]. However, the use of MSC for asthma may face significant limitations. There is evidence that airway remodeling, a relevant feature of asthma pathophysiology, may originated by circulating progenitor cells that migrated and differentiated in myofibroblasts and airways smooth muscle cells into the lungs [254]. Therefore, MSC administered for therapeutic treatment in asthma occur due to their anti-inflammatory effect, but in contrary their potential to differentiate in airway structural cells improve airway remodeling.

Due to the existence of immune regulatory features of MSC, mainly orchestrated by paracrine mechanisms, this makes them an important candidate for a range of inflammatory disorders such as asthma [255]. However, the administration of MSC-CM could alone attenuate some of the disadvantages associated with direct transplantation of MSC such as immune responses, tumorigenic risk, infectious agents, total costs, and long-term for stem cell expansion [256]. Increasing evidence in animal studies

demonstrated that systemic direction of MSC or MSC-CM could alleviate airway inflammation by modulating Th1/Th2 cytokines and suppressing airway recruitment of inflammatory cells [169], [185]. Although the immunomodulatory properties of MSC have attracted significant interest, nevertheless, the precise mechanisms of immune regulation by MSC are still unknown.

In the last chapter of this work, we evaluated the possible role of MSC-CM in the regulation on airway responsiveness and the inflammatory context. To test the effect of MSC-CM on the asthma disease, we established these experiments on a rat model of experimental asthma induced by local HDM+SEB exposure as described in the first chapter. For this purpose, the animals were *i.n.* instilled with HDM+SEB under the same regime as the 15IN model. When the protocol ends, rats showed airway hyperresponsiveness, reflected as a significant R_L increase on the 64, 128 and 256 mg/mL MCh doses compared with the saline solution instilled animals, which acted as a control group. The HDM+SEB-challenged animals also showed a significant increase in airway tissue mass and total BAL cells, as described above. On histopathological examination, they showed inflammatory lung infiltrates composed by lymphocytes and eosinophils with mucus overproduction in the airways.To explore the MSC-CM suppressive effect, we instilled different doses of MSC-CM with different timelines on day 35 of the *i.n.* instillation protocol and continued the protocol up to finished on day 49 (21 HDM+SEB instillations).

We chose R_L responsiveness to MCh, an in vivo lung function to measure AHR, as the primary outcome to evaluate the therapeutic effect in the experimental asthma disease through the 1W and 2W models. It has been described that systemic administration of MSC-CM in repeated doses, but not in single dose, could ameliorate asthmatic changes, by the modulation of Th1/Th2 effector cells via regulation of T-bet and GATA-3 expression in OVA-sensitized male rats [185]. To our knowledge, there is little data related to the administration of the repeated doses of MSC-CM in OVA-induced asthmatic rats. In line with this issue, more investigations are needed to unveil the therapeutic effect of MSC-CM administered in repeated doses in comparison with a single dose in asthmatic rats [185].

In the experiments presented, we observed that all MSC-CM treated groups in 1W and 2W model demonstrated a significant decrease in R_L curve that was flattened in closeness to the control animals and significant differences observed when compared with asthmatic animals. Previous studies revealed that systemic presentation of MSC-CM in repeated doses could significantly reduce pathological injuries in OVA-sensitized rats, while a single

dosage did not yield any beneficial effects in lung tissues of sensitized rats which were reinforced by recent findings [185]. Unlike our results, some experiments showed that systemic transplantation of MSC-CM in a single dose in animal models of lung injury could protect the lung architecture against inflammation [257]. Conversely, previous studies in our laboratory revealed that MSC administered on established experimental asthma rapidly downregulated airway inflammation and mucus production in association with a rise of Th1 cytokines in the lung, but such effects declined under sustained allergen challenge despite a persistent presence of the MSC [169]. The logic explanation for these controversial results could be presumably related to the volume and content of MSC-CM injection. Although the therapeutic benefits of MSC-CM are clear, some issues must be considered before clinical application. MSC-CM contains only a limited amount of growth factor which could easily be distributed in the peripheral tissues and not reach efficiently into the target tissues [258]. In addition, the fact that the therapeutic effects of MSC-CM are associated to dose, content and repeated administration without the risk of rejection by the recipient needs to be ascertained by several studies [259].

We investigated the concentration of several IgE levels in serum that have been implicated in B-cell immune responses. In addition, we showed a significant decrease in total IgE serum when rats were treated with MSC-CM in 1W and 2W model, being similar to the control group. Conversely, all MSC-CM treated groups in 1W and 2W model showed increased BAL total IgG. Furthermore, the increased IgG levels in the HDM+SEB-challenged group showed a trend consistent with decreased total IgE data.

We determinate the antigen-specific immune response evaluating the BAL and serum levels of specific HDM- and SEB-IgE by ELISA. Furthermore, all BAL and serum HDM-specific IgE levels in 1W and 2W models were significantly decreased in comparison with the asthmatic group. However, all BAL and serum SEB-specific IgE levels in 1W and 2W models were similar to the HDM+SEB group. Previous studies showed that MSC significantly reduced inflammatory infiltrate and serum specific IgE in mice challenged with OVA [174]. Conversely, previous studies in our laboratory showed that MSC rapidly attenuated, but did not abrogate airway inflammation without modifying its eosinophilic profile and concomitantly decreased serum IgE [169].

Airway inflammation was evaluated by histopathological examination of lung tissue sections. We observed attenuated infiltrates in all MSC-CM treated groups in the 1W model. However, we observed that 12.5 µg in the 2W model were devoid of airway inflammation, being similar to control animals. Conversely, 25 or 50 µg doses in the 2W

model showed attenuated infiltrates as evidenced by H-E stain. Moreover, mucus overproduction in the airways was evaluated by PAS color extraction and quantification (mucoid mass), with both approaches yielding equivalent results. We showed that the administration of MSC-CM in the 1W model not decreased goblet cell hyperplasia and mucus overproduction, being similar to the asthmatic group. Conversely, treated animals with MSC-CM at 12.5 µg doses decreased intraepithelial PAS-positive cells and mucous load, while 25 or 50 µg doses being more similar to HDM+SEB group. In addition, subepithelial fibrosis was measured by the presence of collagen deposits in the airways. This feature was evaluated by Masson's trichrome color extraction and digital analysis. We demonstrated that the administration of MSC-CM in the 1W model not decreased subepithelial fibrosis, being similar to the asthmatic group. Conversely, treated animals with MSC-CM at 12.5 µg doses decreased collagen deposition, while 25 or 50 µg doses being more similar to the HDM+SEB group. Airway smooth muscle alterations, which include hyperplasia and hypertrophy, is the most important feature of airway remodeling. We use the most detectable α-SMA biomarker to airway smooth muscle quantification and color extraction analysis. We observed that the administration of MSC-CM in the 1W model not decreased α-actin positive cells, being similar to the asthmatic group. Conversely, treated animals with MSC-CM at 12.5 µg doses decreased airway contractile mass, while 25 or 50 µg doses being more similar to the HDM+SEB group. The reduction of airway remodeling is consistent with previous data [169], [179], [185]. Studies showed that local and systemic injection of MSC and MSC-CM palliated the lung injury, airway inflammation rate and histopathological changes during respiratory disorders [169], [185]. Moreover, other data demonstrated that systemic presentation of MSC-CM in repeated doses could significantly reduce pathological injuries in OVA-sensitized rats. On the contrary, MSC-CM in a single dosage did not yield any beneficial effects in lung tissues of sensitized rats, which were reinforced by recent findings [185]. Conversely, previous studies in our laboratory showed that MSC anti-inflammatory effect rebounded and airway inflammation was appeared after 2 weeks of continued allergen challenge, with a rebound effect on infiltrates, goblet cell hyperplasia, serum IgE, and BAL cells [169]. Furthermore, the research on asthma MSC therapy has overlooked the evidence on a role for recruited precursors in airway smooth muscle remodeling.

The logic explanation for these controversial results could be presumably related to the volume and content of MSC-CM injection. Although the therapeutic benefits of MSC-CM are clear, some issues must be considered before application. MSC-CM contains only a limited amount of growth factor which could easily be distributed in the peripheral tissues

and not reach efficiently into the target tissues. In addition, the fact that the therapeutic effects of MSC-CM are related to dose and content of MSC-CM and repeated administration of MSC-CM is without the risk of rejection by the recipient needs to be ascertained by several studies [259].

Airway inflammation was evaluated by identifying different leukocyte subpopulations in BAL by flow cytometry analysis. We could detect that rats treated with MSC-CM in the 1W model increased neutrophil recruitment when compared with asthmatic rats. Curiously, rats treated with 25 µg and 50 µg MSC-CM increased neutrophil infiltration when compared with HDM+SEB-challenged animals, while 12.5 µg doses had similar levels that control and asthmatic rats. MSC secrete high levels of IL-6 and IL-8, which promote the recruitment and activation of PBMC [260], [261]. In addition, other studies reported that previous stimulation of MSC with LPS induced the recruitment of neutrophils due to the secretion of IL-8 and the regulation of apoptosis [261]. Conversely with our data, studies reported that the administration of MSC in OVA-sensitized rats reduced neutrophil counts in BAL [262]. However, all doses of MSC-CM in the 1W and 2W model maintained eosinophil levels in BAL. Previous studies showed that eosinophil and neutrophil levels were reduced after sensitization with MSC in OVA asthmatic rats. However, rats receiving MSC-CM not decrease eosinophil and neutrophil recruitment. In addition, previous studies in our laboratory demonstrated that MSC not modifying eosinophilic profile and airway inflammation. Conversely, previous data revealed that MSC reduced eosinophil counts in BAL [262]. Further, all doses of MSC-CM in the 1W and 2W model maintained T cell recruitment and not altering the proportion of CD4/CD8 T cells in BAL. Other studies showed that T cell levels return to baseline conditions when OVA asthmatic rats were treated with MSC. However, in this study, rats receiving MSC-CM not decrease T cell recruitment, being similarly to asthmatic animals [262]. Curiously, only 12.5 µg doses of MSC-CM in 2W model increased NK cell recruitment, while decreased B cell infiltration. Previous reports have studied the anti-inflammatory effects of MSC and showed that reduced NK cell functions [263].

Conversely, previous studies reported that exist an interaction between MSC and NK cells when were cultured with poly(I:C), a model stimulus for viral infection. They reported that short-term stimulation of MSC resulted in NK cell activation, while more prolonged stimulation of MSC and prolonged exposure of NK cells to factors secreted by these MSC result in NK regulation. Previous studies showed that a reduction of B cell levels might have associated with the resolution of lung inflammation after administration of serum-stimulated MSC, as B cells promote the secretion of allergen-specific IgE and are also

involved in antigen presentation and T-cell proliferation, which intensify immune responses against the allergen [262]. In addition, we evaluated CD161 expression on B cells, given that they might have a potential participation in the control of asthma condition, and especially in asthma attacks, through their migration to the airways and the local production of IFN-y [220]. Moreover, we showed that all doses of MSC-CM in the 1W model did not significantly increase CD161 expression on B cells when compared to asthmatic animals. However, only 12.5 µg doses in the 2W model generated an up-regulation of CD161 on B cells, while the 25 and 50 µg doses not significantly increase this marker expression, being similarly to HDM+SEB group.

Chronic pathologic changes in allergic asthma, including reversible airway obstruction, airways hyperresponsiveness, mucus hypersecretion and airway remodeling are associated initially with an imbalance of Th1/Th2 cells. To investigate the therapeutic effects of MSC-CM in asthmatic rats, evaluated the cytokine production of $CD4^+$ T cells in lung and blood by flow cytometry analysis. Considering the therapeutic impact of MSC-CM and peculiarly MSC, we did emphasize that an efficient suppression of asthma by an increase of INF-y and reduction of IL-4 levels.

In the lung, we observed that frequencies of IL-17 and IFN-y secreted by $CD4^+$ T cells were decreased in HDM+SEB-challenged animals, while showed an increased production of IL-4 when compared to control animals. Consistent with previous experiments, we confirmed the potential dynamic of proinflammatory cytokine IL-4 in advancing the status of asthma [111]. The irregularity between $CD4^+$ Th1 and Th2 immune responses has been recognized as the major contributing factor to the pathogenesis of asthma [264]. IL-4 plays a crucial role in the differentiation of Th2 cells of naive $CD4^+$ T cells and also promotes IgG to IgE isotype switching on B cells required for an initial sensitization to allergens [111]. IFN-y, a predominant cytokine produced by Th1, is involved in diminishing Th2-cell responses and IgE synthesis by B cells to confine the progress of disease [264]. In our experiments, we observed that levels of IFN-y producing by $CD4^+$ T cells in lung and blood were similar between the asthmatic group and rats treated with different doses of MSC-CM in the 1W model. However, only 12.5 µg doses of MSC-CM in the 2W model increased frequencies of IFN-y secreted by $CD4^+$ T cells in lung and blood, while no differences observed when rats were treated with 25 and 50 µg of MSC-CM. Further, all doses of MSC-CM in the 1W and 2W model decreased the IL-4 production by $CD4^+$ T cells in lung and blood, being similar to control animals. Curiously, we showed that all doses of MSC-CM in the 1W and 2W model significantly increase in IL-17 production in the lung, while no differences were observed in the blood. Previous studies showed that

the anti-inflammatory effects of MSC-CM governed likely by restoring the Th1/Th2 balance via modulation of T-bet and GATA-3 expression in OVA-sensitized male rats [185]. Notably, the upregulation of Th2 cytokines in allergic airways potentiates VCAM-1 and ICAM-1 expression on lung microvascular endothelial cells, leading to continuous eosinophil entrance to inflammatory niche, and finally exacerbates the asthmatic condition. Thus, the control of Th2 cytokines could result in a decreased VCAM-1 and ICAM-1 endothelial distribution [265]. Other studies showed that pre- and post-MSC-CM transplantation could show that the anti-inflammatory effects of MSC occurred likely by restoring the Th1/Th2 balance via downregulating of ICAM-1 and VCAM-1 expression [189].

Conversely with our data, previous reports revealed that human MSC mediates a phenotypic deviation from Th17 cells through a direct cell contact interaction. Moreover, when MSC were used, only regulate the phenotypic switch when cells are in contact, while cells separated by Transwell blocked this effect [266]. It has been reported that MSC-T cell interaction induced the production of IL-17 and deviation toward Th17 phenotype and its regulated by caspase 1 activation [266].

However, other studies showed that pre-exposure to IL-1β (an example of a proinflammatory cytokine that might be encountered by MSC when introduced into multiple sclerosis patients) augmented the reciprocal effects of human MSC on Th1 and Th17 responses [266]. A similar effect on human Th17 responses was recently reported with human fetal MSC, suggesting that the potential to induce Th17 responses may be an intrinsic property of human MSC under certain conditions [267]. For example, IFN-y and TNF-α have also been implicated in the immunosuppressive activity of MSC, which may explain our IL-17–producing cells results. Other factors that alter MSC behavior may be encountered *in vivo*. Thus, the outcome of MSC-T-cell interactions in patients may be shaped by the state of the T cells (i.e. recent *in vivo* activation) and by MSC-independent factors in the microenvironment (i.e. inflammatory cytokines, toll-like receptor ligands) [267].

Therefore, our results show that although MSC may have an immunomodulatory activity by deviation Th2 to Th1 profile, they may, in parallel, propagate inflammation by the Th17 response and amplifying proinflammatory IL-17 cytokine secretion as described previously [252]. However, it has been demonstrated a synergistic effect on *IL6*, *IL1B*, and *IL8* mRNA expression when TNF-α and IFN-y were combined with IL-17A, suggesting that the environment may play a role in the secretion of proinflammatory cytokines by MSC. The

positive role of IFN-y in IL-17A mediated cytokine production was described previously. On the contrary, it has been reported that IFN-y negatively regulates the development of Th17 cells [266]. However, IL-17A and IFN-y have also been shown to potentiate neutrophil attraction in hapten-challenged skin, supporting the idea that under certain conditions, IL-17A and IFN-y can act in simultaneously [268].

Mass spectrometry analysis provides an efficient method to show the complete profile of cellular and ECM molecules from MSC. The characterization of MSC-CM by proteome analysis can originated good possible candidates to obtain a precise clinical research. The proteomic profiles using 30-100 kDa cut-off molecular weight range of MSC-CM demonstrated using 1D gels showed that there were differences in the band profiles when compared with medium alone. When the number of identified proteins were compared, there were a higher number of protein identifications (37 proteins), indicating a more complex proteome in these MS-CM. Moreover, previous studies revealed the identified proteins in MSC-CM obtained in our experiments [269]–[271]. Our data have provided proteins for our better understanding of the underlying mechanisms that are responsible for the therapeutic effect of MSC-CM, thus assisting in the application of MSC in cell-based therapy for asthma. We obtained identified proteins, i.e. calreticulin or periostin, which it has been demonstrated beneficial effects on bronchial smooth muscle proliferation in asthma [272], [273]. Conversely, other proteins revealed in MSC-CM (i.e. MMP-2) demonstrated a positive role in airway remodeling and asthma severity [274]. These result have significant implications for the therapeutic effect, revealing the necessity of approaches to improve the functionality of MSC-CM. It is necessary to identify proteins involved in decreased cell proliferation to validate and improve our *in vitro* ASM/$CD4^+$ T cell co-culture model with the objective to develop new strategic therapies.

In summary, repeated low doses of MSC-CM administered on established experimental asthma decrease airway inflammation and mucus production in association with an increase of Th1 and Th17 cytokines in the lung, but Th1 effects declined if single or high repeated doses were added. These data suggest that an immune deviation mechanism may be responsible for the loss of anti-inflammatory effect. Whether repeated MSC-CM doses may lead to sustained anti-inflammatory activity is a standing question of particular relevance for clinical translation that requires pharmacodynamics-like studies. Conversely, AwCT mass showed a strong reduction, associated with a tendency to attenuate airway hyperresponsiveness, regardless of the continued pathogenic stimuli and T cell inflammatory recruitment. Our data suggest that adipose-derived MSC-CM infused as an asthma therapy may be free of unwanted pro-remodeling effects and may ameliorate

AwCT remodeling and airway hyperresponsiveness. These results support the research toward a potential use of MSC-CM in asthma, but caution and robust preclinical data are needed.

CONCLUSIONS

I. Primary airway exposure to HDM with SEB, and repeated challenge, induces experimental asthma in the Sprague Dawley rat with a HDM-specific, Th2 adaptive immune response, airway hyperresponsiveness, eosinophilic airway inflammation, and airway remodeling encompassing mucous metaplasia, subepithelial fibrosis, and increased airway contractile tissue mass. Prolonged continuation of airway challenges leads to downregulation of airway hyperresponsiveness and the HDM-specific IgE response.

II. Direct cell contact between co-cultured, HDM-activated $CD4^+$ T cells and ASM cells induces ASM cell proliferation and inhibits $CD4^+$ T-cell apoptosis.

III. MSC inhibit $CD4^+$ T cell-induced ASM cell proliferation through soluble mediators in a dose-response fashion. High MSC ratios in Transwell are T-cell immunosuppressive, while low MSC ratios or MSC in direct co-culture contact enhance T cell proliferation.

IV. MSC-CM has a suppressive effect on $CD4^+$ T-cell-induced ASM cell proliferation that does not require previous signaling to secrete soluble mediators. This suppressive effect is not carried by MSC-secreted exosomes.

V. MSC-CM fractionation by protein molecular weight leads to a 30-100 kDa fraction that carries the suppressive effect on $CD4^+$ T-cell-induced ASM cell proliferation *in vitro*.

VI. Low repeated doses of the 30-100 kDa MSC-CM fraction, administered by intranasal instillation on established experimental asthma, downregulate airway hyperresponsiveness, inflammation, and mucus production, and reduce subepithelial fibrosis and airway contractile mass, in association with a rise of Th1 and Th17 cytokines *in vivo*.

VII. Proteomics analysis of the 30-100 kDa MSC-CM fraction reveals an encircled set of identified proteins of varied biochemical class and function.

REFERENCES

[1] M. Masoli, D. Fabia, S. Holt, and R. Beasley, “Global Initiative for Asthma (GINA) Program: the global burdan of asthma: executive summary of the GINA Dissemination Committee report.,” *Allergy*, vol. 59, pp. 469–478, 2004.

[2] V. Plaza Moral, “[GEMA(4.0). Guidelines for Asthma Management].,” *Arch. Bronconeumol.*, vol. 51 Suppl 1, pp. 2–54, Jan. 2015, doi: 10.1016/S0300-2896(15)32812-X.

[3] S. G. Marketos and C. N. Ballas, “Bronchial asthma in the medical literature of greek antiquity,” *J. Asthma*, vol. 19, no. 4, pp. 263–269, 1982, doi: 10.3109/02770908209104771.

[4] E. K. Chu and J. M. Drazen, “Asthma one hundred years of treatment and onward,” *Am. J. Respir. Crit. Care Med.*, vol. 171, no. 11, pp. 1202–1208, 2005, doi: 10.1164/rccm.200502-257OE.

[5] L. Pembrey *et al.*, “Understanding asthma phenotypes: the World Asthma Phenotypes (WASP) international collaboration,” *ERJ Open Res.*, vol. 4, no. 3, pp. 00013–02018, 2018, doi: 10.1183/23120541.00013-2018.

[6] B. N. Lambrecht and H. Hammad, “The immunology of asthma,” *Nat. Immunol.*, vol. 16, no. 1, pp. 45–56, 2015, doi: 10.1038/ni.3049.

[7] J. Bousquet, P. K. Jeffery, W. W. Busse, M. Johnson, and A. M. Vignola, “Asthma. From bronchoconstriction to airways inflammation and remodeling.,” *Am. J. Respir. Crit. Care Med.*, vol. 161, no. 5, pp. 1720–1745, May 2000, doi: 10.1164/ajrccm.161.5.9903102.

[8] W. Busse *et al.*, “Omalizumab, anti-IgE recombinant humanized monoclonal antibody, for the treatment of severe allergic asthma,” *J. Allergy Clin. Immunol.*, vol. 108, no. 2, pp. 184–190, 2001, doi: 10.1067/mai.2001.117880.

[9] J. V Fahy, “Nihms677010.Pdf,” vol. 15, no. 1, pp. 57–65, 2015, doi: 10.1038/nri3786.Type.

[10] S. S. Braman, “The Global Burden of Asthma,” *Chest*, vol. 130, no. 1, Supplement, pp. 4S-12S, 2006, doi: https://doi.org/10.1378/chest.130.1_suppl.4S.

[11] M. Asher *et al.*, “Worldwide time trends in the prevalence of symptoms of asthma, allergic rhinoconjunctivitis, and eczema in childhood,” *Lancet*, vol. 368, no. 9537, pp. 733–743, 2006, doi: 10.1016/S0140-6736(06)69283-0.

[12] L. García-Marcos *et al.*, “Stabilization of asthma prevalence among adolescents and increase among schoolchildren (ISAAC phases I and III) in Spain,” *Allergy Eur. J. Allergy Clin. Immunol.*, vol. 59, no. 12, pp. 1301–1307, 2004, doi: 10.1111/j.1398-9995.2004.00562.x.

[13] R. Loddenkemper, *European Lung White Book. The first comprehensive survey on respiratory health in Europe.* Sheffield, UK: European Respiratory Society, 2003.

[14] S. Gilles *et al.*, “The role of environmental factors in allergy: A critical reappraisal,” *Exp. Dermatol.*, vol. 27, no. 11, pp. 1193–1200, 2018, doi: 10.1111/exd.13769.

[15] A. A. Litonjua, V. J. Carey, H. A. Burge, S. T. Weiss, and D. R. Gold, “Parental history and the risk for childhood asthma: Does mother confer more risk than father?,” *Am. J. Respir. Crit. Care Med.*, vol. 158, no. 1, pp. 176–181, 1998, doi: 10.1164/ajrccm.158.1.9710014.

[16] A. B. Mukherjee and Z. Zhang, “Allergic asthma: Influence of genetic and environmental factors,” *J. Biol. Chem.*, vol. 286, no. 38, pp. 32883–32889, 2011, doi: 10.1074/jbc.R110.197046.

[17] P. Cullinan and A. N. Taylor, “Asthma: Environmental and occupational factors,” *Br. Med. Bull.*, vol. 68, pp. 227–242, 2003, doi: 10.1093/bmb/ldg021.

[18] K. Mullane and M. Williams, “Animal models of asthma: Reprise or reboot?,” *Biochem. Pharmacol.*, vol. 87, no. 1, pp. 131–139, 2014, doi: 10.1016/j.bcp.2013.06.026.

[19] S. E. Wenzel, “Asthma phenotypes: The evolution from clinical to molecular approaches,” *Nat. Med.*, vol. 18, no. 5, pp. 716–725, 2012, doi: 10.1038/nm.2678.

[20] D. G. Chapman, J. E. Tully, J. D. Nolin, Y. M. Janssen-Heininger, and C. G. Irvin, “Animal models of allergic airways disease: Where are we and where to next?,” *J. Cell. Biochem.*, vol. 115, no. 12, pp. 2055–2064, 2014, doi: 10.1002/jcb.24881.

[21] J. Pekkanen, J. Lampi, J. Genuneit, A. L. Hartikainen, and M. R. Järvelin, “Analyzing atopic and non-atopic asthma,” *Eur. J. Epidemiol.*, vol. 27, no. 4, pp. 281–286, 2012, doi: 10.1007/s10654-012-9649-y.

[22] N. Pearce, J. Pekkanen, and R. Beasley, “How much asthma is really attributable to atopy?,” *Thorax*, vol. 54, no. 3, pp. 268–272, 1999, doi: 10.1136/thx.54.3.268.

[23] I. Pavord, “Asthma phenotypes,” *Semin. Respir. Crit. Care Med.*, vol. 33, no. 6, pp. 645–652, 2012, doi: 10.1055/s-0032-1326962.

[24] J. L. Simpson, R. Scott, M. J. Boyle, and P. G. Gibson, “SIMPSON ET AL_2006_Inflammatory subtypes in asthma Assessment and identification using induced sputum.pdf,” pp. 54–61, 2006.

[25] P. Haldar and I. D. Pavord, “Noneosinophilic asthma: A distinct clinical and pathologic phenotype,” *J. Allergy Clin. Immunol.*, vol. 119, no. 5, pp. 1043–1052, 2007, doi: 10.1016/j.jaci.2007.02.042.

[26] D. Charpin, A. Magnan, A. Lanteaume, and D. Vervloet, “Original article Allergic vs nonallergic asthma : what makes the difference ?,” *Allergy*, vol. 57, no. 10, pp. 607–613, 2002.

[27] J. J. CURRY, “Clinical appraisal of demerol, benadryl and pyribenzamine,” *Med. Clin. North Am.*, vol. 30, no. 5, pp. 1138–1148, 1946, doi: 10.1016/S0025-7125(16)35911-9.

[28] D. W. COCKCROFT, R. E. RUFFIN, J. DOLOVICH, and F. E. HARGREAVE, “Allergen-induced increase in non-allergic bronchial reactivity,” *Clin. Exp. Allergy*, vol. 7, no. 6, pp. 503–513, 1977, doi: 10.1111/j.1365-2222.1977.tb01481.x.

[29] M. Tomaki and M. Ichinose, “Measurement of airway hyperresponsiveness,” *Nippon rinsho. Japanese J. Clin. Med.*, vol. 59, no. 10, pp. 1945–1949, 2001.

[30] N. Carroll, J. Elliot, A. Morton, and A. James, “The structure of large and small airways in nonfatal and fatal asthma,” *Am. Rev. Respir. Dis.*, vol. 147, no. 2, pp. 405–410, 1993, doi: 10.1164/ajrccm/147.2.405.

[31] N. A. Flavahan, L. L. Aarhus, T. J. Rimele, and P. M. Vanhoutte, “Respiratory epithelium inhibits bronchial smooth muscle tone,” *J. Appl. Physiol.*, vol. 58, no. 3, pp. 834–838, 1985.

[32] R. Lundgren, M. Soderberg, P. Horstedt, and R. Stenling, “Morphological studies of bronchial mucosal biopsies from asthmatics before and after ten years of treatment with inhaled steroids,” *Eur. Respir. J.*, vol. 1, no. 10, pp. 883–889, 1988.

[33] Y. Sumi and Q. Hamid, “Airway Remodeling in Asthma,” *Allergol. Int.*, vol. 56, no. 4, pp. 341–348, 2007, doi: 10.2332/allergolint.R-07-153.

[34] J. V. Fahy, “Remodeling of the airway epithelium in asthma.,” *Am. J. Respir. Crit. Care Med.*, vol. 164, no. 10 Pt 2, 2001, doi: 10.1164/rccm2106066.

[35] B. NAYLOR, “The shedding of the mucosa of the bronchial tree in asthma.,” *Thorax*, vol. 17, pp. 69–72, 1962, doi: 10.1136/thx.17.1.69.

[36] S. T. Holgate, “Epithelium dysfunction in asthma,” *J. Allergy Clin. Immunol.*, vol. 120, no. 6, pp. 1233–1244, 2007, doi: 10.1016/j.jaci.2007.10.025.

[37] A. M. Vignola *et al.*, “Airway inflammation in mild intermittent and in persistent asthma,” *Am. J. Respir. Crit. Care Med.*, vol. 157, no. 2, pp. 403–409, 1998, doi: 10.1164/ajrccm.157.2.96-08040.

[38] M. J. Evans, L. S. Van Winkle, M. V. Fanucchi, and C. G. Plopper, “The attenuated fibroblast sheath of the respiratory tract epithelial-mesenchymal trophic unit,” *Am. J. Respir. Cell Mol. Biol.*, vol. 21, no. 6, pp. 655–657, 1999, doi: 10.1165/ajrcmb.21.6.3807.

[39] Y. Nakamura *et al.*, “Bronchial epithelial cells regulate fibroblast proliferation,” *Am. J. Physiol. - Lung Cell. Mol. Physiol.*, vol. 269, no. 3 13-3, 1995.

[40] L. M. Reid, “The presence or absence of bronchial mucus in fatal asthma,” *J. Allergy Clin. Immunol.*, vol. 80, no. 3, Part 2, pp. 415–416, 1987, doi: https://doi.org/10.1016/0091-6749(87)90064-9.

[41] D. Pavia, J. R. M. Bateman, N. F. Sheahan, J. E. Agnew, and S. W. Clarke, “Tracheobronchial mucociliary clearance in asthma: Impairment during remission,” *Thorax*, vol. 40, no. 3, pp. 171–175, 1985, doi: 10.1136/thx.40.3.171.

[42] M. Saetta, A. Di Stefano, C. Rosina, G. Thiene, and L. M. Fabbri, “Quantitative structural analysis of peripheral airways and arteries in sudden fatal asthma,” *Am. Rev. Respir. Dis.*, vol. 143, no. 1, pp. 138–143, 1991, doi: 10.1164/ajrccm/143.1.138.

[43] H. C. Atherton, G. Jones, and H. Danahay, “IL-13-induced changes in the goblet cell density of human bronchial epithelial cell cultures: MAP kinase and phosphatidylinositol 3-kinase regulation,” *Am. J. Physiol. - Lung Cell. Mol. Physiol.*, vol. 285, no. 3 29-3, pp. 730–739, 2003.

[44] T. Gray *et al.*, “Interleukin-1β-induced mucin production in human airway epithelium is mediated by cyclooxygenase-2, prostaglandin E2 receptors, and cyclic AMP-protein kinase A signaling,” *Mol. Pharmacol.*, vol. 66, no. 2, pp. 337–346, 2004, doi: 10.1124/mol.66.2.337.

[45] P. D. Vermeer, R. Harson, L. A. Einwalter, T. Moninger, and J. Zabner, “Interleukin-9 induces goblet cell hyperplasia during repair of human airway

epithelia," *Am. J. Respir. Cell Mol. Biol.*, vol. 28, no. 3, pp. 286–295, 2003, doi: 10.1165/rcmb.4887.

[46] W. R. Roche, J. H. Williams, R. Beasley, and S. T. Holgate, "SUBEPITHELIAL FIBROSIS IN THE BRONCHI OF ASTHMATICS Bronchoscopy , Lavage , and Biopsy," pp. 520–524, 1986.

[47] A. Chetta, A. Foresi, M. Del Donno, G. Bertorelli, A. Pesci, and D. Olivieri, "Airways remodeling is a distinctive feature of asthma and is related to severity of disease," *Chest*, vol. 111, no. 4, pp. 852–857, 1997, doi: 10.1378/chest.111.4.852.

[48] K. Prikk *et al.*, "Airway obstruction correlates with collagenase-2 (MMP-8) expression and activation in bronchial asthma," *Lab. Investig.*, vol. 82, no. 11, pp. 1535–1545, 2002, doi: 10.1097/01.LAB.0000035023.53893.B6.

[49] S. E. Wenzel, S. Balzar, M. Cundall, and H. W. Chu, "Subepithelial basement membrane immunoreactivity for matrix metalloproteinase 9: Association with asthma severity, neutrophilic inflammation, and wound repair," *J. Allergy Clin. Immunol.*, vol. 111, no. 6, pp. 1345–1352, 2003, doi: 10.1067/mai.2003.1464.

[50] J. M. and V. A. Bousquet J, Jeffery PK, Buse WW, S. Of, and T. H. E. Art, "State of the Art State of the Art :," *8th Nord. Grouting Conf.*, vol. 36, pp. 20–23, 2017, doi: 10.1007/978-3-642-40308-8_2.

[51] P. G. Woodruff *et al.*, "Hyperplasia of smooth muscle in mild to moderate asthma without changes in cell size or gene expression," *Am. J. Respir. Crit. Care Med.*, vol. 169, no. 9, pp. 1001–1006, 2004, doi: 10.1164/rccm.200311-1529OC.

[52] P. Joubert and Q. Hamid, "Role of airway smooth muscle in airway remodeling," *J. Allergy Clin. Immunol.*, vol. 116, no. 3, pp. 713–716, 2005, doi: 10.1016/j.jaci.2005.05.042.

[53] A. L. James *et al.*, "Airway smooth muscle hypertrophy and hyperplasia in asthma," *Am. J. Respir. Crit. Care Med.*, vol. 185, no. 10, pp. 1058–1064, 2012, doi: 10.1164/rccm.201110-1849OC.

[54] W. T. Gerthoffer, "Migration of airway smooth muscle cells," *Proc. Am. Thorac. Soc.*, vol. 5, no. 1, pp. 97–105, 2008, doi: 10.1513/pats.200704-051VS.

[55] D. W. Cockcroft, "Direct challenge tests: Airway hyperresponsiveness in asthma: Its measurement and clinical significance," *Chest*, vol. 138, no. 2 SUPPL., pp. 18S-24S, 2010, doi: 10.1378/chest.10-0088.

[56] N. Regamey *et al.*, "Increased airway smooth muscle mass in children with asthma, cystic fibrosis, and non-cystic fibrosis bronchiectasis," *Am. J. Respir. Crit. Care Med.*, vol. 177, no. 8, pp. 837–843, 2008, doi: 10.1164/rccm.200707-977OC.

[57] N. K. Malavia, C. B. Raub, S. B. Mahon, M. Brenner, R. A. Panettieri, and S. C. George, "Airway epithelium stimulates smooth muscle proliferation," *Am. J. Respir. Cell Mol. Biol.*, vol. 41, no. 3, pp. 297–304, 2009, doi: 10.1165/rcmb.2008-0358OC.

[58] P. R. A. Johnson, C. L. Armour, D. Carey, and J. L. Black, "Heparin and PGE2 inhibit DNA synthesis in human airway smooth muscle cells in culture," *Am. J. Physiol. - Lung Cell. Mol. Physiol.*, vol. 269, no. 4 13-4, 1995.

[59] M. Ebina, T. Takahashi, T. Chiba, and M. Motomiya, "Cellular hypertrophy and hyperplasia of airway smooth muscles underlying bronchial asthma: A 3-D

morphometric study," *Am. Rev. Respir. Dis.*, vol. 148, no. 3, pp. 720–726, 1993, doi: 10.1164/ajrccm/148.3.720.

[60] L. Benayoun, A. Druilhe, M. C. Dombret, M. Aubier, and M. Pretolani, "Airway structural alterations selectively associated with severe asthma," *Am. J. Respir. Crit. Care Med.*, vol. 167, no. 10, pp. 1360–1368, 2003, doi: 10.1164/rccm.200209-1030OC.

[61] J. K. Bentley *et al.*, "Airway smooth muscle hyperplasia and hypertrophy correlate with glycogen synthase kinase-33 phosphorylation in a mouse model of asthma," *Am. J. Physiol. - Lung Cell. Mol. Physiol.*, vol. 296, no. 2, pp. 176–185, 2009, doi: 10.1152/ajplung.90376.2008.

[62] J. S. Mohamed, M. A. Lopez, and A. M. Boriek, "Mechanical stretch up-regulates microRNA-26a and induces human airway smooth muscle hypertrophy by suppressing glycogen synthase kinase-3β," *J. Biol. Chem.*, vol. 285, no. 38, pp. 29336–29347, 2010, doi: 10.1074/jbc.M110.101147.

[63] H. Hammad and B. N. Lambrecht, "Dendritic cells and epithelial cells: Linking innate and adaptive immunity in asthma," *Nat. Rev. Immunol.*, vol. 8, no. 3, pp. 193–204, 2008, doi: 10.1038/nri2275.

[64] B. N. Lambrecht and H. Hammad, "The airway epithelium in asthma," *Nat. Med.*, vol. 18, p. 684, May 2012.

[65] P. J. Barnes, "Immunology of asthma and chronic obstructive pulmonary disease," *Nat. Rev. Immunol.*, vol. 8, no. 3, pp. 183–192, 2008, doi: 10.1038/nri2254.

[66] L. Borish, "The immunology of asthma: Asthma phenotypes and their implications for personalized treatment," *Ann. Allergy, Asthma Immunol.*, vol. 117, no. 2, pp. 108–114, 2016, doi: 10.1016/j.anai.2016.04.022.

[67] A. G. Besnard, D. Togbe, N. Guillou, F. Erard, V. Quesniaux, and B. Ryffel, "IL-33-activated dendritic cells are critical for allergic airway inflammation," *Eur. J. Immunol.*, vol. 41, no. 6, pp. 1675–1686, 2011, doi: 10.1002/eji.201041033.

[68] B. D. Bell *et al.*, "STAT5 is critical in dendritic cells for development of Th2- but not Th1- dependent immunity," *Nat. Immunol.*, vol. 14, no. 4, pp. 364–371, 2013, doi: 10.1038/ni.2541.STAT5.

[69] D. K. Chu *et al.*, "IL-33, but not thymic stromal lymphopoietin or IL-25, is central to mite and peanut allergic sensitization," *J. Allergy Clin. Immunol.*, vol. 131, no. 1, pp. 187-200.e8, 2013, doi: 10.1016/j.jaci.2012.08.002.

[70] C. Viret and C. A. Janeway, "MHC and T cell development," *Rev. Immunogenet.*, vol. 1, no. 1, p. 91—104, 1999.

[71] C. C. Tydell, E.-S. David-Fung, J. E. Moore, L. Rowen, T. Taghon, and E. V. Rothenberg, "Molecular Dissection of Prethymic Progenitor Entry into the T Lymphocyte Developmental Pathway," *J. Immunol.*, vol. 179, no. 1, pp. 421–438, 2007, doi: 10.4049/jimmunol.179.1.421.

[72] K. Shortman and L. Wu, "Early T Lymphocyte Progenitors," *Annu. Rev. Immunol.*, vol. 14, no. 1, pp. 29–47, 1996, doi: 10.1146/annurev.immunol.14.1.29.

[73] Q. Yu, J. H. Park, L. L. Doan, B. Erman, L. Feigenbaum, and A. Singer, "Cytokine signal transduction is suppressed in preselection double-positive thymocytes and

restored by positive selection," *J. Exp. Med.*, vol. 203, no. 1, pp. 165–175, 2006, doi: 10.1084/jem.20051836.

[74] A. Singer, S. Adoro, and J. H. Park, "Lineage fate and intense debate: Myths, models and mechanisms of CD4- versus CD8-lineage choice," *Nat. Rev. Immunol.*, vol. 8, no. 10, pp. 788–801, 2008, doi: 10.1038/nri2416.

[75] A. Singer and R. Bosselut, "CD4/CD8 coreceptors in thymocyte development, selection, and lineage commitment: Analysis of the CD4/CD8 lineage decision," *Adv. Immunol.*, vol. 83, pp. 91–131, 2004, doi: 10.1016/S0065-2776(04)83003-7.

[76] H. Kishimoto and J. Sprent, "Negative selection in the thymus includes semimature T cells," *J. Exp. Med.*, vol. 185, no. 2, pp. 263–271, 1997, doi: 10.1084/jem.185.2.263.

[77] A. D. Griesemer, E. C. Sorenson, and M. A. Hardy, "The role of the thymus in tolerance," *Transplantation*, vol. 90, no. 5, pp. 465–474, 2010, doi: 10.1097/TP.0b013e3181e7e54f.

[78] U. H. Von Andrian and T. R. Mempel, "Homing and cellular traffic in lymph nodes," *Nat. Rev. Immunol.*, vol. 3, no. 11, pp. 867–878, 2003, doi: 10.1038/nri1222.

[79] L. J. Picker and E. C. Butcher, "Physiological and Molecular Mechanisms of Lymphocyte Homing," *Annu. Rev. Immunol.*, vol. 10, no. 1, pp. 561–591, 1992, doi: 10.1146/annurev.iy.10.040192.003021.

[80] E. C. Butcher, M. Williams, K. Youngman, L. Rott, and M. Briskin, "Lymphocyte trafficking and regional immunity," *Adv. Immunol.*, vol. 72, no. 72, pp. 209–253, 1999.

[81] C. Théry and S. Amigorena, "The cell biology of antigen presentation in dendritic cells," *Curr. Opin. Immunol.*, vol. 13, no. 1, pp. 45–51, 2001, doi: 10.1016/S0952-7915(00)00180-1.

[82] M. A. M. Willart and H. Hammad, "Alarming dendritic cells for allergic sensitization," *Allergol. Int.*, vol. 59, no. 2, pp. 95–103, 2010, doi: 10.2332/allergolint.09-RAI-0162.

[83] L. S. Van Rijt and B. N. Lambrecht, "Dendritic cells in asthma: A function beyond sensitization," *Clin. Exp. Allergy*, vol. 35, no. 9, pp. 1125–1134, 2005, doi: 10.1111/j.1365-2222.2005.02321.x.

[84] J. M. Brewer, M. Conacher, C. A. Hunter, M. Mohrs, F. Brombacher, and J. Alexander, "Aluminium hydroxide adjuvant initiates strong antigen-specific Th2 responses in the absence of IL-4- or IL-13-mediated signaling.," *J. Immunol.*, vol. 163, no. 12, pp. 6448–54, 1999.

[85] S. K. Jeong *et al.*, "Mite and cockroach allergens activate protease-activated receptor 2 and delay epidermal permeability barrier recovery," *J. Invest. Dermatol.*, vol. 128, no. 8, pp. 1930–1939, 2008, doi: 10.1038/jid.2008.13.

[86] R. M. Steinman, "Dendritic cells and the control of immunity," *Exp. Hematol.*, vol. 26, no. 8, p. 681, 1998.

[87] H. Bour-Jordan and J. A. Bluestone, "CD28 function: A balance of costimulatory and regulatory signals," *J. Clin. Immunol.*, vol. 22, no. 1, pp. 1–7, 2002, doi: 10.1023/A:1014256417651.

[88] H. Gudmundsdottir, A. D. Wells, and L. A. Turka, “Dynamics and requirements of T cell clonal expansion in vivo at the single-cell level: effector function is linked to proliferative capacity.,” *J. Immunol.*, vol. 162, no. 9, pp. 5212–23, 1999.

[89] M. M. Curtis *et al.*, “Pathogen Lifestyle,” vol. 8, no. 2, pp. 612–626, 2011, doi: 10.1016/j.chom.2010.07.006.Fidelity.

[90] T. R. Mosmann and R. L. Coffman, “TH1 and TH2 cells: Different patterns of lymphokine secretion lead to different functional properties,” *Annu. Rev. Immunol.*, vol. 7, pp. 145–173, 1989.

[91] G. Hansen, G. Berry, R. H. DeKruyff, and D. T. Umetsu, “Allergen-specific Th1 cells fail to counterbalance Th2 cell-induced airway hyperreactivity but cause severe airway inflammation,” *J. Clin. Invest.*, vol. 103, no. 2, pp. 175–183, 1999, doi: 10.1172/JCI5155.

[92] B. T. Defrance, P. Carayon, G. Billian, J. Guillemot, S. A. Minty, and S. D. Caput, “Interleukin 13 Is a B Cell Stimulating Factor By Thierry Defrance, ~ Pierre Carayon,~ Gis~le Billian,* Jean-Claude Guillemot,S Adrian Minty, S Daniel Caput,$ and Pascual Ferrara~,” vol. 179, no. January, 1994.

[93] T. Kouro and K. Takatsu, “IL-5- and eosinophil-mediated inflammation: From discovery to therapy,” *Int. Immunol.*, vol. 21, no. 12, pp. 1303–1309, 2009, doi: 10.1093/intimm/dxp102.

[94] D. Amsen, A. Antov, and R. A. Flavell, “The different faces of Notch in T-helper-cell differentiation,” *Nat. Rev. Immunol.*, vol. 9, no. 2, pp. 116–124, 2009, doi: 10.1038/nri2488.

[95] N. Hosken, K. Shibuya, A. Heath, and KM, “The effect of antigen dose on CD4+ T helper cell phenotype development in a T cell receptor-alpha beta-transgenic model.,” *J.*, vol. 182, no. November, pp. 20–22, 1995.

[96] C. Leonard, V. Tormey, C. Burke, and L. W. Poulter, “Allergen-induced Cytokine Production in Atopic Disease and Its Relationship to Disease Severity,” *Am. J. Respir. Cell Mol. Biol.*, vol. 17, no. 3, pp. 368–375, 1997, doi: 10.1165/ajrcmb.17.3.2797.

[97] F. Annunziato *et al.*, “Phenotypic and functional features of human Th17 cells,” *J. Exp. Med.*, vol. 204, no. 8, pp. 1849–1861, 2007, doi: 10.1084/jem.20070663.

[98] E. Bettelli *et al.*, “Reciprocal developmental pathways for the generation of pathogenic effector TH17 and regulatory T cells,” *Nature*, vol. 441, no. 7090, pp. 235–238, 2006, doi: 10.1038/nature04753.

[99] Z. Yao *et al.*, “Human IL-17: a novel cytokine derived from T cells.,” *J. Immunol.*, vol. 155, no. 12, pp. 5483–5486, 1995.

[100] P. Ye *et al.*, “Requirement of interleukin 17 receptor signaling for lung CXC chemokine and granulocyte colony-stimulating factor expression, neutrophil recruitment, and host defense,” *J. Exp. Med.*, vol. 194, no. 4, pp. 519–527, 2001, doi: 10.1084/jem.194.4.519.

[101] F. Fossiez *et al.*, “at the third Annual Conference of The International Cytokine Society on 12-15,” vol. 183, no. June, 1995.

[102] R. H. Wilson, G. S. Whitehead, H. Nakano, M. E. Free, J. K. Kolls, and D. N. Cook, “Allergic sensitization through the airway primes Th17-dependent neutrophilia and airway hyperresponsiveness,” *Am. J. Respir. Crit. Care Med.*, vol. 180, no. 8, pp. 720–730, 2009, doi: 10.1164/rccm.200904-0573OC.

[103] M. Akdis, K. Blaser, and C. A. Akdis, “T regulatory cells in allergy: Novel concepts in the pathogenesis, prevention, and treatment of allergic diseases,” *J. Allergy Clin. Immunol.*, vol. 116, no. 5, pp. 961–968, 2005, doi: 10.1016/j.jaci.2005.09.004.

[104] F. Cottrez, S. D. Hurst, R. L. Coffman, and H. Groux, “T Regulatory Cells 1 Inhibit a Th2-Specific Response In Vivo,” *J. Immunol.*, vol. 165, no. 9, pp. 4848–4853, 2000, doi: 10.4049/jimmunol.165.9.4848.

[105] C. J. Corrigan and A. B. Kay, “CD4 T-lymphocyte activation in acute severe asthma. Relationship to disease severity and atopic status,” *Am. Rev. Respir. Dis.*, vol. 141, no. 4 I, pp. 970–977, 1990.

[106] A. L. Lazaar, S. M. Albelda, J. M. Pilewski, B. Brennan, E. Puré, and R. A. Panettieri, “T Lymphocytes adhere to airway smooth muscle cells via integrins and CD44 and induce smooth muscle cell DNA synthesis,” *J. Exp. Med.*, vol. 180, no. 3, pp. 807–816, 1994, doi: 10.1084/jem.180.3.807.

[107] D. Ramos-Barbón, J. F. Presley, Q. A. Hamid, E. D. Fixman, and J. G. Martin, “Antigen-specific CD4 + T cells drive airway smooth muscle remodeling in experimental asthma,” *J. Clin. Invest.*, vol. 115, no. 6, pp. 1580–1589, 2005, doi: 10.1172/JCI19711.

[108] D. Ramos-Barbón *et al.*, “T cells localize with proliferating smooth muscle α-actin + cell compartments in asthma,” *Am. J. Respir. Crit. Care Med.*, vol. 182, no. 3, pp. 317–324, 2010, doi: 10.1164/rccm.200905-0745OC.

[109] K. M. Hawker, P. R. A. Johnson, J. M. Hughes, and J. L. Black, “Interleukin-4 inhibits mitogen-induced proliferation of human airway smooth muscle cells in culture,” *Am. J. Physiol. - Lung Cell. Mol. Physiol.*, vol. 275, no. 3 19-3, pp. 469–477, 1998.

[110] P. A. Risse *et al.*, “Interleukin-13 inhibits proliferation and enhances contractility of human airway smooth muscle cells without change in contractile phenotype,” *Am. J. Physiol. - Lung Cell. Mol. Physiol.*, vol. 300, no. 6, pp. 958–967, 2011, doi: 10.1152/ajplung.00247.2010.

[111] G. G. Brusselle *et al.*, “Attenuation of allergic airway inflammation in IL-4 deficient mice,” *Clin. Exp. Allergy*, vol. 24, no. 1, pp. 73–80, 1994, doi: 10.1111/j.1365-2222.1994.tb00920.x.

[112] P. S. Foster, M. Yang, C. Herbert, and R. K. Kumar, “CD4+ T-lymphocytes regulate airway remodeling and hyper-reactivity in a mouse model of chronic asthma,” *Lab. Investig.*, vol. 82, no. 4, pp. 455–462, 2002, doi: 10.1038/labinvest.3780438.

[113] Q. Wang, H. Li, Y. Yao, D. Xia, and J. Zhou, “The Overexpression of Heparin-Binding Epidermal Growth Factor Is Responsible for Th17-Induced Airway Remodeling in an Experimental Asthma Model,” *J. Immunol.*, vol. 185, no. 2, pp. 834–841, 2010, doi: 10.4049/jimmunol.0901490.

[114] T. A. Doherty, P. Soroosh, D. H. Broide, and M. Croft, “CD4+ cells are required for chronic eosinophilic lung inflammation but not airway remodeling,” *Am. J. Physiol. - Lung Cell. Mol. Physiol.*, vol. 296, no. 2, 2009, doi: 10.1152/ajplung.90543.2008.

[115] K. Tsuchiya *et al.*, “Depletion of CD8 + T cells enhances airway remodelling in a rodent model of asthma,” *Immunology*, vol. 126, no. 1, pp. 45–54, 2009, doi: 10.1111/j.1365-2567.2008.02876.x.

[116] T. L. Bonfield, M. Koloze, D. P. Lennon, B. Zuchowski, S. E. Yang, and A. I. Caplan, “Human mesenchymal stem cells suppress chronic airway inflammation in the murine ovalbumin asthma model,” *Am. J. Physiol. - Lung Cell. Mol. Physiol.*, vol. 299, no. 6, pp. 760–771, 2010, doi: 10.1152/ajplung.00182.2009.

[117] L. P. Boulet, “Airway remodeling in asthma: Update on mechanisms and therapeutic approaches,” *Curr. Opin. Pulm. Med.*, vol. 24, no. 1, pp. 56–62, 2018, doi: 10.1097/MCP.0000000000000441.

[118] R. Berair and C. E. Brightling, “Asthma therapy and its effect on airway remodelling,” *Drugs*, vol. 74, no. 12, pp. 1345–1369, 2014, doi: 10.1007/s40265-014-0250-4.

[119] M. L. Fajt and S. E. Wenzel, “Aair-9-3,” vol. 9, no. 1, pp. 3–14, 2017.

[120] A. Shifren, C. Witt, C. Christie, and M. Castro, “Mechanisms of Remodeling in Asthmatic Airways,” *J. Allergy*, vol. 2012, pp. 1–12, 2012, doi: 10.1155/2012/316049.

[121] I. Kucharewicz, A. Bodzenta-łukaszyk, and W. Bucko, “Experimental asthma in rats,” *Pharmacol. Reports*, vol. 60, no. 6, pp. 783–788, 2008.

[122] J. Auer and P. A. Lewis, “The physiology of the immediate reaction of anaphylaxis in the guinea-pig,” *J. Exp. Med.*, vol. 12, no. 2, pp. 151–175, 1910, doi: 10.1084/jem.12.2.151.

[123] P. Singh *et al.*, “Phenotypic comparison of allergic airway responses to house dust mite in three rat strains,” *Am. J. Physiol. - Lung Cell. Mol. Physiol.*, vol. 284, no. 4 28-4, pp. 588–598, 2003.

[124] A. L. de Weck, P. Mayer, B. Stumper, B. Schiessl, and L. Pickart, “Dog Allergy, a Model for Allergy Genetics,” *Int. Arch. Allergy Immunol.*, vol. 113, no. 1–3, pp. 55–57, 1997, doi: 10.1159/000237507.

[125] J. C. Delehunt, A. P. Perruchoud, L. Yerger, B. Marchette, J. S. Stevenson, and W. M. Abraham, “The Role of Slow-Reacting Substance of Anaphylaxis in the Late Bronchial Response after Antigen Challenge in Allergic Sheep,” *Am. Rev. Respir. Dis.*, vol. 130, no. 5, pp. 748–754, 1984, doi: 10.1164/arrd.1984.130.5.748.

[126] J. A. Phills, A. J. Harrold, G. V Whiteman, and L. Perelmutter, “Pulmonary Infiltrates, Asthma and Eosinophilia Due to Ascaris suum Infestation in Man,” *N. Engl. J. Med.*, vol. 286, no. 18, pp. 965–970, 1972, doi: 10.1056/NEJM197205042861802.

[127] P. Padrid, “Chronic lower airway disease in the dog and cat,” *Probl. Vet. Med.*, vol. 4, no. 2, p. 320—344, 1992.

[128] P. Padrid, “Feline asthma: Diagnosis and treatment,” *Vet. Clin. North Am. - Small Anim. Pract.*, vol. 30, no. 6, pp. 1279–1293, 2000, doi: 10.1016/S0195-5616(00)06007-1.

[129] B. Herszberg, D. Ramos-Barbón, M. Tamaoka, J. G. Martin, and J. P. Lavoie, “Heaves, an asthma-like equine disease, involves airway smooth muscle remodeling,” *J. Allergy Clin. Immunol.*, vol. 118, no. 2, pp. 382–388, 2006, doi: 10.1016/j.jaci.2006.03.044.

[130] Y. S. Shin, K. Takeda, and E. W. Gelfand, “Understanding asthma using animal models,” *Allergy, Asthma Immunol. Res.*, vol. 1, no. 1, pp. 10–18, 2009, doi: 10.4168/aair.2009.1.1.10.

[131] J. A. Elias, C. G. Lee, T. Zheng, B. Ma, R. J. Homer, and Z. Zhu, “New insights into the pathogenesis of asthma,” *J. Clin. Invest.*, vol. 111, no. 3, pp. 291–297, 2003, doi: 10.1172/JCI17748.

[132] C. G. Irvin and J. H. T. Bates, “Measuring the lung function in the mouse: The challenge of size,” *Respir. Res.*, vol. 4, pp. 1–9, 2003, doi: 10.1186/rr199.

[133] J. J. Lee *et al.*, “Defining a link with asthma in mice congenitally deficient in eosinophils,” *Science (80-.).*, vol. 305, no. 5691, pp. 1773–1776, 2004, doi: 10.1126/science.1099472.

[134] A. Datta *et al.*, “Specific allergen immunotherapy attenuates allergic airway inflammation in a rat model of Alstonia scholaris pollen induced airway allergy,” *Int. Immunopharmacol.*, vol. 30, pp. 111–120, 2016, doi: 10.1016/j.intimp.2015.12.004.

[135] M. Kianmehr, V. Ghorani, and M. H. Boskabady, “Animal model of asthma, various methods and measured parameters, a methodological review,” *Iran. J. Allergy, Asthma Immunol.*, vol. 15, no. 6, pp. 445–465, 2016.

[136] S. Sapienza, T. Du, D. H. Eidelman, N. S. Wang, and J. G. Martin, “Structural changes in the airways of sensitized Brown Norway rats after antigen challenge,” *Am. Rev. Respir. Dis.*, vol. 144, no. 2, pp. 423–427, 1991, doi: 10.1164/ajrccm/144.2.423.

[137] M. N. Hylkema, M. O. Hoekstra, M. Luinge, and W. Timens, “The strength of the OVA-induced airway inflammation in rats is strain dependent,” *Clin. Exp. Immunol.*, vol. 129, no. 3, pp. 390–396, 2002, doi: 10.1046/j.1365-2249.2002.01938.x.

[138] T. Akkoç, “Animal models of asthma,” *Turkish J. Immunol.*, vol. 18, no. 2, p. 2, 2012, doi: 10.1111/j.1365-2222.2007.02740.x.

[139] M. A. Birrell, A. J. M. Van Oosterhout, and M. G. Belvisi, “Do the current house dust mite-driven models really mimic allergic asthma?,” *Eur. Respir. J.*, vol. 36, no. 5, pp. 1220–1221, 2010, doi: 10.1183/09031936.00069110.

[140] E. R. Tovey and B. A. Baldo, “Standardization of allergens. Qualitative definition of house dust mite extracts following electroblotting and detection of components with antibody and lectin probes.,” *Int. Arch. Allergy Appl. Immunol.*, vol. 75, no. 4, pp. 322–329, 1984.

[141] S. J. Thompson, H. J. Whitley, J. D. Naysmith, and F. Carswell, “IgE antibodies to D. pteronyssinus in atopic patients,” *Immunology*, vol. 64, no. 2, pp. 311–314, 1988.

[142] U. Herz *et al.*, “The relevance of murine animal models to study the development of allergic bronchial asthma,” *Immunol. Cell Biol.*, vol. 74, no. 2, pp. 209–217, 1996, doi: 10.1038/icb.1996.30.

[143] J. N. Liu *et al.*, “The prevalence of serum specific IgE to superantigens in asthma and allergic rhinitis patients,” *Allergy, Asthma Immunol. Res.*, vol. 6, no. 3, pp. 263–266, 2014, doi: 10.4168/aair.2014.6.3.263.

[144] O. Krysko *et al.*, “The adjuvant-like activity of staphylococcal enterotoxin B in a murine asthma model is independent of IL-1R signaling,” *Allergy Eur. J. Allergy Clin. Immunol.*, vol. 68, no. 4, pp. 446–453, 2013, doi: 10.1111/all.12102.

[145] W. Huvenne *et al.*, “Staphylococcus aureus enterotoxin B facilitates allergic sensitization in experimental asthma,” *Clin. Exp. Allergy*, vol. 40, no. 7, pp. 1079–1090, 2010, doi: 10.1111/j.1365-2222.2010.03464.x.

[146] T. Squillaro, G. Peluso, and U. Galderisi, “Clinical trials with mesenchymal stem cells: An update,” *Cell Transplant.*, vol. 25, no. 5, pp. 829–848, 2016, doi: 10.3727/096368915X689622.

[147] N. Kim and S. G. Cho, “Clinical applications of mesenchymal stem cells,” *Korean J. Intern. Med.*, vol. 28, no. 4, pp. 387–402, 2013, doi: 10.3904/kjim.2013.28.4.387.

[148] J. L. Dragoo *et al.*, “Tissue-engineered cartilage and bone using stem cells from human infrapatellar fat pads,” *J. Bone Jt. Surg. - Ser. B*, vol. 85, no. 5, pp. 740–747, 2003, doi: 10.1302/0301-620X.85B5.13587.

[149] R. H. Lee *et al.*, “Intravenous hMSCs improve myocardial infarction in mice because cells embolized in lung are activated to secrete the anti-inflammatory protein TSG-6.,” *Cell Stem Cell*, vol. 5, no. 1, pp. 54–63, Jul. 2009, doi: 10.1016/j.stem.2009.05.003.

[150] B. T. Estes, B. O. Diekman, J. M. Gimble, and F. Guilak, “Isolation of adipose-derived stem cells and their induction to a chondrogenic phenotype.,” *Nat. Protoc.*, vol. 5, no. 7, pp. 1294–1311, Jul. 2010, doi: 10.1038/nprot.2010.81.

[151] G. Pelled, O. Mizrahi, N. Kimelman-Bleich, and D. Gazit, “Mesenchymal stem cells for bone gene therapy,” *Princ. Bone Regen.*, pp. 81–96, 2012, doi: 10.1007/978-1-4614-2059-0_7.

[152] I. Ullah, R. B. Subbarao, and G. J. Rho, “Human mesenchymal stem cells - Current trends and future prospective,” *Biosci. Rep.*, vol. 35, 2015, doi: 10.1042/BSR20150025.

[153] F. Gao *et al.*, “Mesenchymal stem cells and immunomodulation: current status and future prospects,” *Cell Death Dis.*, vol. 7, p. e2062, 2016, doi: 10.1038/cddis.2015.327.

[154] J. M. Ryan, F. Barry, J. M. Murphy, and B. P. Mahon, “Interferon-γ does not break, but promotes the immunosuppressive capacity of adult human mesenchymal stem cells,” *Clin. Exp. Immunol.*, vol. 149, no. 2, pp. 353–363, 2007, doi: 10.1111/j.1365-2249.2007.03422.x.

[155] G. Ren *et al.*, “Mesenchymal Stem Cell-Mediated Immunosuppression Occurs via Concerted Action of Chemokines and Nitric Oxide,” *Cell Stem Cell*, vol. 2, no. 2, pp. 141–150, 2008, doi: 10.1016/j.stem.2007.11.014.

[156] O. DelaRosa *et al.*, “Requirement of IFN-gamma-mediated indoleamine 2,3-dioxygenase expression in the modulation of lymphocyte proliferation by human adipose-derived stem cells.,” *Tissue Eng. Part A*, vol. 15, no. 10, pp. 2795–2806, Oct. 2009, doi: 10.1089/ten.TEA.2008.0630.

[157] L. Jarvinem *et al.*, “Jornal of Immunology,” vol. 181, no. 6, pp. 4389–4396, 2013.

[158] W. Ge, J. Jiang, J. Arp, W. Liu, B. Garcia, and H. Wang, “Regulatory T-cell generation and kidney allograft tolerance induced by mesenchymal stem cells associated with indoleamine 2,3-dioxygenase expression,” *Transplantation*, vol. 90, no. 12, pp. 1312–1320, 2010, doi: 10.1097/TP.0b013e3181fed001.

[159] P. Terness *et al.*, “Inhibition of allogeneic T cell proliferation by indoleamine 2,3-dioxygenase-expressing dendritic cells: Mediation of suppression by tryptophan metabolites,” *J. Exp. Med.*, vol. 196, no. 4, pp. 447–457, 2002, doi: 10.1084/jem.20020052.

[160] M. Sioud, A. Mobergslien, A. Boudabous, and Y. Fløisand, “Mesenchymal stem cell-mediated T cell suppression occurs through secreted galectins,” *Int. J. Oncol.*, vol. 38, no. 2, pp. 385–390, 2011, doi: 10.3892/ijo.2010.869.

[161] M. Sioud, A. Mobergslien, A. Boudabous, and Y. Fløisand, “Evidence for the involvement of galectin-3 in mesenchymal stem cell suppression of allogeneic T-cell proliferation,” *Scand. J. Immunol.*, vol. 71, no. 4, pp. 267–274, 2010, doi: 10.1111/j.1365-3083.2010.02378.x.

[162] M. Najar *et al.*, “Adipose-Tissue-Derived and Wharton’s jelly-derived mesenchymal stromal cells suppress lymphocyte responses by secreting leukemia inhibitory factor,” *Tissue Eng. - Part A*, vol. 16, no. 11, pp. 3537–3546, 2010, doi: 10.1089/ten.tea.2010.0159.

[163] K. H. Han *et al.*, “Immunosuppressive mechanisms of embryonic stem cells and mesenchymal stem cells in alloimmune response,” *Transpl. Immunol.*, vol. 25, no. 1, pp. 7–15, 2011, doi: 10.1016/j.trim.2011.05.004.

[164] M. Krampera *et al.*, “Krampera et al,” vol. 101, no. 9, pp. 3722–3729, 2003, doi: 10.1182/blood-2002-07-2104.Supported.

[165] A. Augello *et al.*, “Bone marrow mesenchymal progenitor cells inhibit lymphocyte proliferation by activation of the programmed death 1 pathway,” *Eur. J. Immunol.*, vol. 35, no. 5, pp. 1482–1490, 2005, doi: 10.1002/eji.200425405.

[166] A. L. Guangwen Ren, Xin Zhao, Liying Zhang, Jimin Zhang and W. Ling, “Inflammatory Cytokine-Induced Intercellular Adhesion,” *J. Immunol.*, vol. 184, no. 5, pp. 2321–2328, 2010, doi: 10.4049/jimmunol.0902023.Inflammatory.

[167] X. L. Fan, Z. Zhang, C. Y. Ma, and Q. L. Fu, “Mesenchymal stem cells for inflammatory airway disorders: Promises and challenges,” *Biosci. Rep.*, vol. 39, no. 1, pp. 1–13, 2019, doi: 10.1042/BSR20182160.

[168] S. G. Royce, S. Rele, B. R. S. Broughton, K. Kelly, and C. S. Samuel, “Intranasal administration of mesenchymoangioblast-derived mesenchymal stem cells abrogates airway fibrosis and airway hyperresponsiveness associated with chronic allergic airways disease,” *FASEB J.*, vol. 31, no. 9, pp. 4168–4178, 2017, doi: 10.1096/fj.201700178R.

[169] L. Mariñas-Pardo *et al.*, “Mesenchymal stem cells regulate airway contractile tissue remodeling in murine experimental asthma,” *Allergy Eur. J. Allergy Clin. Immunol.*, vol. 69, no. 6, pp. 730–740, 2014, doi: 10.1111/all.12392.

[170] Y. Q. Sun *et al.*, “Human pluripotent stem cell-derived mesenchymal stem cells prevent allergic airway inflammation in mice,” *Stem Cells*, vol. 30, no. 12, pp. 2692–2699, 2012, doi: 10.1002/stem.1241.

[171] T. Bonfield, M. Sutton, D. Lennon, and A. Caplan, “Mesenchymal stem cells: new directions in treating asthma (THER2P.955),” *J. Immunol.*, vol. 194, no. 1 Supplement, pp. 67.6--67.6, 2015.

[172] B. D. Goldstein, M. E. Lauer, A. I. Caplan, and T. L. Bonfield, “Chronic asthma and Mesenchymal stem cells: Hyaluronan and airway remodeling,” *J. Inflamm. (United Kingdom)*, vol. 14, no. 1, pp. 1–9, 2017, doi: 10.1186/s12950-017-0165-4.

[173] Y. Li, T. Qu, L. Tian, T. Han, Y. Jin, and Y. Wang, “Human placenta mesenchymal stem cells suppress airway inflammation in asthmatic rats by modulating Notch signaling,” *Mol. Med. Rep.*, vol. 17, no. 4, pp. 5336–5343, 2018, doi: 10.3892/mmr.2018.8462.

[174] R. Habibian, N. Delirezh, and A. A. Farshid, “The effects of bone marrow-derived mesenchymal stem cells on ovalbumin-induced allergic asthma and cytokine responses in mice,” *Iran. J. Basic Med. Sci.*, vol. 21, no. 5, pp. 483–488, 2018, doi: 10.22038/IJBMS.2018.26898.6575.

[175] K. Takeda *et al.*, “Mesenchymal Stem Cells Recruit CCR2(+) Monocytes To Suppress Allergic Airway Inflammation.,” *J. Immunol.*, vol. 200, no. 4, pp. 1261–1269, Feb. 2018, doi: 10.4049/jimmunol.1700562.

[176] S. Bin Fang *et al.*, “Human iPSC-MSCs prevent steroid-resistant neutrophilic airway inflammation via modulating Th17 phenotypes,” *Stem Cell Res. Ther.*, vol. 9, no. 1, pp. 1–12, 2018, doi: 10.1186/s13287-018-0897-y.

[177] H. Kavanagh and B. P. Mahon, “Allogeneic mesenchymal stem cells prevent allergic airway inflammation by inducing murine regulatory T cells,” *Allergy Eur. J. Allergy Clin. Immunol.*, vol. 66, no. 4, pp. 523–531, 2011, doi: 10.1111/j.1398-9995.2010.02509.x.

[178] A. P. Wong *et al.*, “Targeted cell replacement with bone marrow cells for airway epithelial regeneration,” *Am. J. Physiol. - Lung Cell. Mol. Physiol.*, vol. 293, no. 3, pp. 740–753, 2007, doi: 10.1152/ajplung.00050.2007.

[179] M. Ahmadi, R. Rahbarghazi, M. R. Aslani, A. A. Shahbazfar, M. Kazemi, and R. Keyhanmanesh, “Bone marrow mesenchymal stem cells and their conditioned media could potentially ameliorate ovalbumin-induced asthmatic changes,” *Biomed. Pharmacother.*, vol. 85, pp. 28–40, 2017, doi: 10.1016/j.biopha.2016.11.127.

[180] S. C. Abreu *et al.*, “Bone marrow mononuclear cell therapy in experimental allergic asthma: Intratracheal versus intravenous administration,” *Respir. Physiol. Neurobiol.*, vol. 185, no. 3, pp. 615–624, 2013, doi: 10.1016/j.resp.2012.11.005.

[181] J. E. Trzil *et al.*, “Long-term evaluation of mesenchymal stem cell therapy in a feline model of chronic allergic asthma.,” *Clin. Exp. Allergy*, vol. 44, no. 12, pp. 1546–1557, Dec. 2014, doi: 10.1111/cea.12411.

[182] M. Ahmadi, R. Rahbarghazi, S. Soltani, M. R. Aslani, and R. Keyhanmanesh, “Contributory Anti-Inflammatory Effects of Mesenchymal Stem Cells, Not Conditioned Media, On Ovalbumin-Induced Asthmatic Changes in Male Rats,” *Inflammation*, vol. 39, no. 6, pp. 1960–1971, 2016, doi: 10.1007/s10753-016-0431-2.

[183] M. Gnecchi, Z. Zhang, A. Ni, and V. J. Dzau, “Paracrine mechanisms in adult stem cell signaling and therapy,” *Circ. Res.*, vol. 103, no. 11, pp. 1204–1219, 2008, doi: 10.1161/CIRCRESAHA.108.176826.

[184] D. Kyurkchiev, “Secretion of immunoregulatory cytokines by mesenchymal stem cells,” *World J. Stem Cells*, vol. 6, no. 5, p. 552, 2014, doi: 10.4252/wjsc.v6.i5.552.

[185] R. Keyhanmanesh, R. Rahbarghazi, M. R. Aslani, M. Hassanpour, and M. Ahmadi, “Systemic delivery of mesenchymal stem cells condition media in repeated doses acts as magic bullets in restoring IFN-γ/IL-4 balance in asthmatic rats,” *Life Sci.*, vol. 212, no. July, pp. 30–36, 2018, doi: 10.1016/j.lfs.2018.09.049.

[186] N. Taechangam, S. S. Iyer, N. J. Walker, B. Arzi, and D. L. Borjesson, “Mechanisms utilized by feline adipose-derived mesenchymal stem cells to inhibit T lymphocyte proliferation,” *Stem Cell Res. Ther.*, vol. 10, no. 1, pp. 1–12, 2019, doi: 10.1186/s13287-019-1300-3.

[187] K. C. Clark *et al.*, “Human and feline adipose-derived mesenchymal stem cells have comparable phenotype, immunomodulatory functions, and transcriptome,” *Stem Cell Res. Ther.*, vol. 8, no. 1, pp. 1–16, 2017, doi: 10.1186/s13287-017-0528-z.

[188] M. Krampera *et al.*, “Role for Interferon-γ in the Immunomodulatory Activity of Human Bone Marrow Mesenchymal Stem Cells,” *Stem Cells*, vol. 24, no. 2, pp. 386–398, 2006, doi: 10.1634/stemcells.2005-0008.

[189] R. Keyhanmanesh, R. Rahbarghazi, and M. Ahmadi, “Systemic Transplantation of Mesenchymal Stem Cells Modulates Endothelial Cell Adhesion Molecules Induced by Ovalbumin in Rat Model of Asthma,” *Inflammation*, vol. 41, no. 6, pp. 2236–2245, 2018, doi: 10.1007/s10753-018-0866-8.

[190] A. G. Kay *et al.*, “Mesenchymal Stem Cell-Conditioned Medium Reduces Disease Severity and Immune Responses in Inflammatory Arthritis,” *Sci. Rep.*, vol. 7, no. 1, pp. 1–11, 2017, doi: 10.1038/s41598-017-18144-w.

[191] B. Johnstone and K. March, “A Stem-Cell-Derived Cell-Free Therapy for Stroke: Moving Conditioned Medium into Clinical Trial,” *Cell Ther. Brain Inj.*, pp. 247–265, 2015, doi: 10.1007/978-3-319-15063-5_14.

[192] F. F. Cruz *et al.*, “ Systemic Administration of Human Bone Marrow-Derived Mesenchymal Stromal Cell Extracellular Vesicles Ameliorates Aspergillus Hyphal Extract-Induced Allergic Airway Inflammation in Immunocompetent Mice ,” *Stem Cells Transl. Med.*, vol. 4, no. 11, pp. 1302–1316, 2015, doi: 10.5966/sctm.2014-0280.

[193] J. H. Lee, J. Park, and J.-W. Lee, “Therapeutic use of mesenchymal stem cell-derived extracellular vesicles in acute lung injury.,” *Transfusion*, vol. 59, no. S1, pp. 876–883, Feb. 2019, doi: 10.1111/trf.14838.

[194] L. L. De Castro *et al.*, “Human adipose tissue mesenchymal stromal cells and their extracellular vesicles act differentially on lung mechanics and inflammation in experimental allergic asthma,” *Stem Cell Res. Ther.*, vol. 8, no. 1, pp. 1–12, 2017, doi: 10.1186/s13287-017-0600-8.

[195] C. R. Harrell, C. Fellabaum, N. Jovicic, V. Djonov, N. Arsenijevic, and V. Volarevic, “Molecular Mechanisms Responsible for Therapeutic Potential of Mesenchymal Stem Cell-Derived Secretome,” *Cells*, vol. 8, no. 5, p. 467, 2019, doi: 10.3390/cells8050467.

[196] F. F. Cruz and P. R. M. Rocco, “Stem-cell extracellular vesicles and lung repair,” *Stem Cell Investig.*, vol. 4, no. 9, pp. 1–11, 2017, doi: 10.21037/sci.2017.09.02.

[197] M. K. Glassberg *et al.*, “Allogeneic Human Mesenchymal Stem Cells in Patients With Idiopathic Pulmonary Fibrosis via Intravenous Delivery (AETHER): A Phase I Safety Clinical Trial,” *Chest*, vol. 151, no. 5, pp. 971–981, 2017, doi: 10.1016/j.chest.2016.10.061.

[198] N. Cárdenes *et al.*, “Senescence of bone marrow-derived mesenchymal stem cells from patients with idiopathic pulmonary fibrosis,” *Stem Cell Res. Ther.*, vol. 9, no. 1, pp. 1–10, 2018, doi: 10.1186/s13287-018-0970-6.

[199] V. Volarevic *et al.*, “Ethical and safety issues of stem cell-based therapy,” *Int. J. Med. Sci.*, vol. 15, no. 1, pp. 36–45, 2018, doi: 10.7150/ijms.21666.

[200] C. Kilkenny, W. Browne, I. C. Cuthill, M. Emerson, and D. G. Altman, “Animal research: reporting in vivo experiments: the ARRIVE guidelines.,” *Br. J. Pharmacol.*, vol. 160, no. 7, pp. 1577–1579, Aug. 2010, doi: 10.1111/j.1476-5381.2010.00872.x.

[201] J. De Alba *et al.*, “House dust mite induces direct airway inflammation in vivo: Implications for future disease therapy?,” *Eur. Respir. J.*, vol. 35, no. 6, pp. 1377–1387, 2010, doi: 10.1183/09031936.00022908.

[202] Ching-Feng Weng, “Interactions of immune and neuroendocrine systems in response to the superantigens Staphylococcal enterotoxin B,” 1994.

[203] K. Le Blanc and O. Ringdén, “Immunomodulation by mesenchymal stem cells and clinical experience,” *J. Intern. Med.*, vol. 262, no. 5, pp. 509–525, 2007, doi: 10.1111/j.1365-2796.2007.01844.x.

[204] S. Vuckovic *et al.*, “The cationic small molecule GW4869 is cytotoxic to high phosphatidylserine-expressing myeloma cells,” *Br. J. Haematol.*, vol. 177, no. 3, pp. 423–440, 2017, doi: 10.1111/bjh.14561.

[205] K. Raemdonck *et al.*, “CD4+ and CD8+ T cells play a central role in a HDM driven model of allergic asthma,” *Respir. Res.*, vol. 17, no. 1, pp. 1–17, 2016, doi: 10.1186/S12931-016-0359-Y.

[206] S. T. Holgate, “Airway inflammation and remodeling in asthma: Current concepts,” *Appl. Biochem. Biotechnol. - Part B Mol. Biotechnol.*, vol. 22, no. 2, pp. 179–189, 2002, doi: 10.1385/MB:22:2:179.

[207] W. Huvenne *et al.*, “Staphylococcus aureus enterotoxin B augments granulocyte migration and survival via airway epithelial cell activation.,” *Allergy*, vol. 65, no. 8, pp. 1013–1020, Aug. 2010, doi: 10.1111/j.1398-9995.2009.02313.x.

[208] R. Fraga-Iriso *et al.*, “Development of a Murine Model of Airway Inflammation and Remodeling in Experimental Asthma,” *Arch. Bronconeumol.*, vol. 45, no. 9, pp. 422–428, 2009, doi: 10.1016/S1579-2129(09)73484-6.

[209] C. McCusker, M. Chicoine, Q. Hamid, and B. Mazer, “Site-specific sensitization in a murine model of allergic rhinitis: Role of the upper airway in lower airways disease,” *J. Allergy Clin. Immunol.*, vol. 110, no. 6, pp. 891–898, 2002, doi: 10.1067/mai.2002.130048.

[210] P. Burney, “Variations in the prevalence of respiratory symptoms, self-reported asthma attacks, and use of asthma medication in the European Community Respiratory Health Survey (ECRHS),” *Eur. Respir. J.*, vol. 9, no. 4, pp. 687–695, 1996, doi: 10.1183/09031936.96.09040687.

[211] J. R. Johnson *et al.*, “Continuous Exposure to House Dust Mite Elicits Chronic Airway Inflammation and Structural Remodeling,” *Am. J. Respir. Crit. Care Med.*, vol. 169, no. 3, pp. 378–385, 2004, doi: 10.1164/rccm.200308-1094OC.

[212] P. W. Hellings *et al.*, “Aggravation of bronchial eosinophilia in mice by nasal and bronchial exposure to Staphylococcus aureus enterotoxin B,” *Clin. Exp. Allergy*, vol. 36, no. 8, pp. 1063–1071, 2006, doi: 10.1111/j.1365-2222.2006.02527.x.

[213] R. Khalmuratova, M. Lee, D. W. Kim, J. W. Park, and H. W. Shin, “Induction of nasal polyps using house dust mite and Staphylococcal enterotoxin B in C57BL/6 mice,” *Allergol. Immunopathol. (Madr).*, vol. 44, no. 1, pp. 66–75, 2016, doi: 10.1016/j.aller.2015.04.004.

[214] A. R. Abbas *et al.*, “Lung gene expression in a rhesus allergic asthma model correlates with physiologic parameters of disease and exhibits common and distinct pathways with human asthma and a mouse asthma model.,” *Am. J. Pathol.*, vol. 179, no. 4, pp. 1667–1680, Oct. 2011, doi: 10.1016/j.ajpath.2011.06.009.

[215] J. A. Boyce and K. F. Austen, “No audible wheezing: Nuggets and conundrums from mouse asthma models,” *J. Exp. Med.*, vol. 201, no. 12, pp. 1869–1873, 2005, doi: 10.1084/jem.20050584.

[216] S. Post *et al.*, “The composition of house dust mite is critical for mucosal barrier dysfunction and allergic sensitisation,” *Thorax*, vol. 67, no. 6, pp. 488–495, 2012, doi: 10.1136/thoraxjnl-2011-200606.

[217] T. Schneider, D. van Velzen, R. Moqbel, and A. C. Issekutz, “Kinetics and quantitation of eosinophil and neutrophil recruitment to allergic lung inflammation in a brown Norway rat model.,” *Am. J. Respir. Cell Mol. Biol.*, vol. 17, no. 6, pp. 702–712, Dec. 1997, doi: 10.1165/ajrcmb.17.6.2849.

[218] A. Poggi, P. Costa, M. R. Zocchi, and L. Moretta, “Phenotypic and functional analysis of CD4+ NKRP1A+ human T lymphocytes. Direct evidence that the NKRP1A molecule is involved in transendothelial migration,” *Eur. J. Immunol.*, vol. 27, no. 9, pp. 2345–2350, 1997, doi: 10.1002/eji.1830270932.

[219] T. Takahashi, S. Dejbakhsh-Jones, and S. Strober, “Expression of CD161 (NKR-P1A) Defines Subsets of Human CD4 and CD8 T Cells with Different Functional Activities,” *J. Immunol.*, vol. 176, no. 1, pp. 211–216, 2006, doi: 10.4049/jimmunol.176.1.211.

[220] Y. González-Hernández *et al.*, “Peripheral blood CD161+ T cells from asthmatic patients are activated during asthma attack and predominantly produce IFN-γ,” *Scand. J. Immunol.*, vol. 65, no. 4, pp. 368–375, 2007, doi: 10.1111/j.1365-3083.2006.01885.x.

[221] R. M. O’Brien, H. Xu, J. M. Rolland, K. A. Byron, and W. R. Thomas, “Allergen-specific production of interferon-γ by peripheral blood mononuclear cells and CD8 T cells in allergic disease and following immunotherapy,” *Clin. Exp. Allergy*, vol. 30, no. 3, pp. 333–340, 2000, doi: 10.1046/j.1365-2222.2000.00700.x.

[222] T. Heaton *et al.*, “An immunoepidemiological approach to asthma: identification of in-vitro T-cell response patterns associated with different wheezing phenotypes in children.,” *Lancet*, vol. 365, no. 9454, pp. 142–149, 2005.

[223] B. J. Hales *et al.*, “IgE and IgG anti-house dust mite specificities in allergic disease,” *J. Allergy Clin. Immunol.*, vol. 118, no. 2, pp. 361–367, 2006, doi: 10.1016/j.jaci.2006.04.001.

[224] P. Chenuet *et al.*, “Neutralization of either IL-17A or IL-17F is sufficient to inhibit house dust mite induced allergic asthma in mice,” *Clin. Sci.*, vol. 131, no. 20, pp. 2533–2548, 2017, doi: 10.1042/CS20171034.

[225] R. Plaza, J. L. Rodriguez-Sanchez, and C. Juarez, “Staphylococcal enterotoxin B in vivo modulates both gamma interferon receptor expression and ligand-induced activation of signal transducer and activator of transcription 1 in T cells,” *Infect. Immun.*, vol. 75, no. 1, pp. 306–313, 2007, doi: 10.1128/IAI.01220-06.

[226] G. Rajagopalan, A. Y. Tilahun, Y. W. Asmann, and C. S. David, “Early gene expression changes induced by the bacterial superantigen staphylococcal enterotoxin B and its modulation by a proteasome inhibitor,” *Physiol. Genomics*, vol. 37, no. 3, pp. 279–293, 2009, doi: 10.1152/physiolgenomics.90385.2008.

[227] C. E. Brightling, P. Bradding, F. A. Symon, S. T. Holgate, A. J. Wardlaw, and I. D. Pavord, “Mast-cell infiltration of airway smooth muscle in asthma,” *N. Engl. J. Med.*, vol. 346, no. 22, pp. 1699–1705, 2002, doi: 10.1056/NEJMoa012705.

[228] A. L. Lazaar and R. A. Panettieri, “Airway smooth muscle: A modulator of airway remodeling in asthma,” *J. Allergy Clin. Immunol.*, vol. 116, no. 3, pp. 488–495, 2005, doi: 10.1016/j.jaci.2005.06.030.

[229] S. Al Heialy *et al.*, “ Nanotubes Connect CD4 + T Cells to Airway Smooth Muscle Cells: Novel Mechanism of T Cell Survival ,” *J. Immunol.*, vol. 194, no. 12, pp. 5626–5634, 2015, doi: 10.4049/jimmunol.1401718.

[230] H. Sheng *et al.*, “A critical role of IFNγ in priming MSC-mediated suppression of T cell proliferation through up-regulation of B7-H1,” *Cell Res.*, vol. 18, no. 8, pp. 846–857, 2008, doi: 10.1038/cr.2008.80.

[231] J. Liu *et al.*, “Suppression of human peripheral blood lymphocyte proliferation by immortalized mesenchymal stem cells derived from bone marrow of Banna Minipig Inbred-line,” *Transplant. Proc.*, vol. 36, no. 10, pp. 3272–3275, 2004, doi: 10.1016/j.transproceed.2004.11.090.

[232] D. H. Munn *et al.*, “Prevention of allogeneic fetal rejection by tryptophan catabolism,” *Science (80-.).*, vol. 281, no. 5380, pp. 1191–1193, 1998, doi: 10.1126/science.281.5380.1191.

[233] N. Kosaka, H. Iguchi, Y. Yoshioka, F. Takeshita, Y. Matsuki, and T. Ochiya, “Secretory mechanisms and intercellular transfer of microRNAs in living cells,” *J. Biol. Chem.*, vol. 285, no. 23, pp. 17442–17452, 2010, doi: 10.1074/jbc.M110.107821.

[234] A. Dorronsoro and P. D. Robbins, “Regenerating the injured kidney with human umbilical cord mesenchymal stem cell-derived exosomes,” *Stem Cell Res. Ther.*, vol. 4, no. 2, pp. 8–10, 2013, doi: 10.1186/scrt187.

[235] Y. Zhou *et al.*, “exosomes UCB.pdf,” 2013.

[236] S. Bruno *et al.*, “Mesenchymal stem cell-derived microvesicles protect against acute tubular injury,” *J. Am. Soc. Nephrol.*, vol. 20, no. 5, pp. 1053–1067, 2009, doi: 10.1681/ASN.2008070798.

[237] O. D. Liang *et al.*, “Mesenchymal stromal cells expressing heme oxygenase-1 reverse pulmonary hypertension.,” *Stem Cells*, vol. 29, no. 1, pp. 99–107, Jan. 2011, doi: 10.1002/stem.548.

[238] C. Lee *et al.*, “Exosomes mediate the cytoprotective action of mesenchymal stromal cells on hypoxia-induced pulmonary hypertension,” *Circulation*, vol. 126, no. 22, pp. 2601–2611, 2012, doi: 10.1161/CIRCULATIONAHA.112.114173.Exosomes.

[239] D. Drago, C. Cossetti, N. Iraci, E. Gaude, and G. Musco, “Europe PMC Funders Group The stem cell secretome and its role in brain repair,” *Biochimie*, vol. 95, no. 12, pp. 2271–2285, 2014, doi: 10.1016/j.biochi.2013.06.020.The.

[240] Y. Luan, X. Zhang, F. Kong, G. H. Cheng, T. G. Qi, and Z. H. Zhang, “Mesenchymal stem cell prevention of vascular remodeling in high flow-induced pulmonary hypertension through a paracrine mechanism,” *Int. Immunopharmacol.*, vol. 14, no. 4, pp. 432–437, 2012, doi: 10.1016/j.intimp.2012.08.001.

[241] K. M. Patel *et al.*, “Mesenchymal Stem Cells Attenuate Hypoxic Pulmonary Vasoconstriction by a Paracrine Mechanism,” *J. Surg. Res.*, vol. 143, no. 2, pp. 281–285, 2007, doi: 10.1016/j.jss.2006.11.006.

[242] R. F. Foronjy and S. M. Majka, “The Potential for Resident Lung Mesenchymal Stem Cells to Promote Functional Tissue Regeneration: Understanding Microenvironmental Cues,” *Cells*, vol. 1, no. 4, pp. 874–885, 2012, doi: 10.3390/cells1040874.

[243] M. Aslam *et al.*, “Bone marrow stromal cells attenuate lung injury in a murine model of neonatal chronic lung disease,” *Am. J. Respir. Crit. Care Med.*, vol. 180, no. 11, pp. 1122–1130, 2009, doi: 10.1164/rccm.200902-0242OC.

[244] D. Jun *et al.*, “The pathology of bleomycin-induced fibrosis is associated with loss of resident lung mesenchymal stem cells that regulate effector T-cell proliferation.,” *Stem Cells*, vol. 29, no. 4, pp. 725–735, Apr. 2011, doi: 10.1002/stem.604.

[245] D. Rossi, S. Pianta, M. Magatti, P. Sedlmayr, and O. Parolini, “Characterization of the Conditioned Medium from Amniotic Membrane Cells: Prostaglandins as Key Effectors of Its Immunomodulatory Activity,” *PLoS One*, vol. 7, no. 10, 2012, doi: 10.1371/journal.pone.0046956.

[246] M. E. Groh, B. Maitra, E. Szekely, and O. N. Koç, “Human mesenchymal stem cells require monocyte-mediated activation to suppress alloreactive T cells,” *Exp. Hematol.*, vol. 33, no. 8, pp. 928–934, 2005, doi: 10.1016/j.exphem.2005.05.002.

[247] G. Li Pira, F. Ivaldi, L. Bottone, R. Quarto, and F. Manca, “Human Bone Marrow Stromal Cells Hamper Specific Interactions of CD4 and CD8 T Lymphocytes with Antigen-Presenting Cells,” *Hum. Immunol.*, vol. 67, no. 12, pp. 976–985, 2006, doi: 10.1016/j.humimm.2006.08.298.

[248] N. G. Singer and A. I. Caplan, “Mesenchymal Stem Cells: Mechanisms of Inflammation,” *Annu. Rev. Pathol. Mech. Dis.*, vol. 6, no. 1, pp. 457–478, 2011, doi: 10.1146/annurev-pathol-011110-130230.

[249] K. English, F. P. Barry, C. P. Field-Corbett, and B. P. Mahon, “IFN-γ and TNF-α differentially regulate immunomodulation by murine mesenchymal stem cells,” *Immunol. Lett.*, vol. 110, no. 2, pp. 91–100, 2007, doi: 10.1016/j.imlet.2007.04.001.

[250] K. Sato *et al.*, “Nitric oxide plays a critical role in suppression of T-cell proliferation by mesenchymal stem cells,” *Blood*, vol. 109, no. 1, pp. 228–234, 2007, doi: 10.1182/blood-2006-02-002246.

[251] R. Meisel, A. Zibert, M. Laryea, U. Göbel, W. Däubener, and D. Dilloo, “Human bone marrow stromal cells inhibit allogeneic T-cell responses by indoleamine 2,3-dioxygenase-mediated tryptophan degradation,” *Blood*, vol. 103, no. 12, pp. 4619–4621, 2004, doi: 10.1182/blood-2003-11-3909.

[252] M. Goodwin *et al.*, “Bone marrow-derived mesenchymal stromal cells inhibit Th2-mediated allergic airways inflammation in mice.,” *Stem Cells*, vol. 29, no. 7, pp. 1137–1148, Jul. 2011, doi: 10.1002/stem.656.

[253] J. García-Castro, C. Trigueros, J. Madrenas, J. A. Pérez-Simón, R. Rodriguez, and P. Menendez, “Mesenchymal stem cells and their use as cell replacement therapy and disease modelling tool,” *J. Cell. Mol. Med.*, vol. 12, no. 6B, pp. 2552–2565, 2008, doi: 10.1111/j.1582-4934.2008.00516.x.

[254] V. A. Dolgachev, M. R. Ullenbruch, N. W. Lukacs, and S. H. Phan, “Role of stem cell factor and bone marrow-derived fibroblasts in airway remodeling,” *Am. J. Pathol.*, vol. 174, no. 2, pp. 390–400, 2009, doi: 10.2353/ajpath.2009.080513.

[255] P. K. L., S. Kandoi, R. Misra, V. S., R. K., and R. S. Verma, “The mesenchymal stem cell secretome: A new paradigm towards cell-free therapeutic mode in regenerative medicine,” *Cytokine Growth Factor Rev.*, vol. 46, no. February, pp. 1–9, 2019, doi: 10.1016/j.cytogfr.2019.04.002.

[256] L. Timmers *et al.*, “Human mesenchymal stem cell-conditioned medium improves cardiac function following myocardial infarction,” *Stem Cell Res.*, vol. 6, no. 3, pp. 206–214, 2011, doi: 10.1016/j.scr.2011.01.001.

[257] L. Ionescu *et al.*, “Stem cell conditioned medium improves acute lung injury in mice: In vivo evidence for stem cell paracrine action,” *Am. J. Physiol. - Lung Cell. Mol. Physiol.*, vol. 303, no. 11, 2012, doi: 10.1152/ajplung.00144.2011.

[258] S. H. Bhang, S. Lee, J. Y. Shin, T. J. Lee, H. K. Jang, and B. S. Kim, “Efficacious and clinically relevant conditioned medium of human adipose-derived stem cells for therapeutic angiogenesis,” *Mol. Ther.*, vol. 22, no. 4, pp. 862–872, 2014, doi: 10.1038/mt.2013.301.

[259] J. A. Pawitan, “Prospect of stem cell conditioned medium in regenerative medicine,” *Biomed Res. Int.*, vol. 2014, pp. 7–9, 2014, doi: 10.1155/2014/965849.

[260] S. Brandau *et al.*, “Mesenchymal stem cells augment the anti-bacterial activity of neutrophil granulocytes,” *PLoS One*, vol. 9, no. 9, 2014, doi: 10.1371/journal.pone.0106903.

[261] S. Brandau *et al.*, “Tissue-resident mesenchymal stem cells attract peripheral blood neutrophils and enhance their inflammatory activity in response to microbial challenge,” *J. Leukoc. Biol.*, vol. 88, no. 5, pp. 1005–1015, 2010, doi: 10.1189/jlb.0410207.

[262] S. C. Abreu *et al.*, “Serum from Asthmatic Mice Potentiates the Therapeutic Effects of Mesenchymal Stromal Cells in Experimental Allergic Asthma,” *Stem Cells Transl. Med.*, vol. 8, no. 3, pp. 301–312, 2019, doi: 10.1002/sctm.18-0056.

[263] D. Chatterjee *et al.*, “Human umbilical cord-derived mesenchymal stem cells utilise activin-A to suppress interferon-gamma production by natural killer cells,” *Front. Immunol.*, vol. 5, no. DEC, pp. 1–8, 2014, doi: 10.3389/fimmu.2014.00662.

[264] H. W. Guo *et al.*, “Mangiferin attenuates Th1/Th2 cytokine imbalance in an ovalbumin-induced asthmatic mouse model,” *PLoS One*, vol. 9, no. 6, pp. 1–12, 2014, doi: 10.1371/journal.pone.0100394.

[265] J. H. Lee, J. H. Sohn, S. Y. Ryu, C. S. Hong, K. D. Moon, and J. W. Park, “A novel human anti-VCAM-1 monoclonal antibody ameliorates airway inflammation and remodelling,” *J. Cell. Mol. Med.*, vol. 17, no. 10, pp. 1271–1281, 2013, doi: 10.1111/jcmm.12102.

[266] A. Eljaafari *et al.*, “Bone marrow-derived and synovium-derived mesenchymal cells promote Th17 cell expansion and activation through caspase 1 activation: Contribution to the chronicity of rheumatoid arthritis,” *Arthritis Rheum.*, vol. 64, no. 7, pp. 2147–2157, 2012, doi: 10.1002/art.34391.

[267] P. J. Darlington *et al.*, “Reciprocal Th1 and Th17 regulation by mesenchymal stem cells: Implication for multiple sclerosis,” *Ann. Neurol.*, vol. 68, no. 4, pp. 540–545, 2010, doi: 10.1002/ana.22065.

[268] D. D. Kish, X. Li, and R. L. Fairchild, “CD8 T cells producing IL-17 and IFN-gamma initiate the innate immune response required for responses to antigen skin challenge.,” *J. Immunol.*, vol. 182, no. 10, pp. 5949–5959, May 2009, doi: 10.4049/jimmunol.0802830.

[269] Y. Tachida, H. Sakurai, and J. Okutsu, “Proteomic Comparison of the Secreted Factors of Mesenchymal Stem Cells from Bone Marrow, Adipose Tissue and Dental Pulp,” *J. Proteomics Bioinform.*, vol. 8, no. 12, pp. 266–273, 2015, doi: 10.4172/jpb.1000379.

[270] Y. Nakashima *et al.*, “A liquid chromatography with tandem mass spectrometry-based proteomic analysis of primary cultured cells and subcultured cells using mouse adipose-derived mesenchymal stem cells,” *Stem Cells Int.*, vol. 2019, 2019, doi: 10.1155/2019/7274057.

[271] S. Rolandsson Enes *et al.*, “Quantitative proteomic characterization of lung-MSC and bone marrow-MSC using DIA-mass spectrometry,” *Sci. Rep.*, vol. 7, no. 1, p. 9316, 2017, doi: 10.1038/s41598-017-09127-y.

[272] N. Miglino, M. Roth, D. Lardinois, M. Tamm, and P. Borger, “Calreticulin Is a Negative Regulator of Bronchial Smooth Muscle Cell Proliferation,” *J. Allergy*, vol. 2012, pp. 1–7, 2012, doi: 10.1155/2012/783290.

[273] W. Li *et al.*, “Periostin: Its role in asthma and its potential as a diagnostic or therapeutic target,” *Respir. Res.*, vol. 16, no. 1, pp. 1–10, 2015, doi: 10.1186/s12931-015-0218-2.

[274] K. Grzela, A. Strzelak, W. Zagórska, and T. Grzela, “Matrix Metalloproteinases in Asthma-Associated Airway Remodeling – Dr. Jekyll or Mr. Hyde ?,” 2016.

APPENDIX

I. Data tables

Table S1. R_L responsiveness to MCh. IN models.

Model	Group	D0	D4	D8	D16	D32	D64	D128	D256
10 IN	CONTROL	0.20±0.021	0.32±0.076	0.49±0.117	0.57±0.078	0.57±0.072	0.64±0.077 ---	0.73±0.073 ---	0.81±0.089 ---
	HDM	0.25±0.037	0.35±0.023	0.40±0.043	0.51±0.065	0.53±0.039	0.68±0.035 ---	0.94±0.046 ---	1.07±0.074 ---
	SEB	0.24±0.033	0.26±0.037	0.29±0.039	0.40±0.093	0.52±0.118	0.63±0.147 ---	0.78±0.178 ---	1.13±0.215 ---
	HDM+SEB	0.32±0.039	0.29±0.018	0.29±0.009	0.34±0.027	0.35±0.029	0.62±0.159 ---	1.05±0.439 ---	1.41±0.574 ---
15 IN	CONTROL	0.20±0.013	0.30±0.032	0.44±0.050	0.59±0.068	0.59±0.041	0.71±0.075 ---	0.85±0.078 ---	0.89±0.052 ---
	HDM	0.24±0.027	0.36±0.021	0.41±0.025	0.56±0.066	0.61±0.060	0.72±0.067 ---	0.91±0.055 ---	1.05±0.039 ---
	SEB	0.22±0.017	0.29±0.017	0.34±0.023	0.44±0.045	0.52±0.053	0.62±0.070 ---	0.76±0.090 ---	1.09±0.124 ---
	HDM+SEB	0.26±0.032	0.40±0.041	0.64±0.097	1.08±0.298	1.20±0.249	1.53±0.208 *p<0.001	1.91±0.232 *p<0.001	2.12±0.161 *p<0.001
30 IN	CONTROL	0.36±0.068	0.35±0.059	0.36±0.051	0.39±0.045	0.39±0.041	0.44±0.033 ---	0.49±0.046 ---	0.57±0.078 ---
	HDM	0.29±0.020	0.31±0.018	0.34±0.018	0.38±0.019	0.43±0.043	0.55±0.088 ---	0.77±0.149 ---	0.95±0.187 ---
	SEB	0.29±0.014	0.30±0.014	0.32±0.009	0.36±0.021	0.46±0.082	0.58±0.142 ---	0.69±0.158 ---	0.90±0.176 ---
	HDM+SEB	0.30±0.034	0.36±0.051	0.33±0.022	0.39±0.061	0.54±0.101	0.66±0.154 ---	0.81±0.210 ---	0.99±0.233 ---

Data are mean ± standard error of the mean. 10IN, 15IN and 30IN models: primary airway exposure models with 10, 15 and 30 *i.n.* instillations, respectively. CONTROL: respective control groups, *i.n.*-instilled with saline solution. HDM: respective HDM challenged groups. SEB: respective SEB challenged groups. HDM+SEB: respective HDM plus SEB challenged groups. D0 to D256: MCh doses (0, 4, 8, 16, 32, 64, 128 and 256 mg/mL, respectively). ---: P>0.05 intragroup. *: versus intragroup CONTROL.

Table S2. Total IgE serum. 10IN, 15IN and 30IN models.

Model	Group	IgE ng/ml
10 IN	**CONTROL**	3.52±1.061
	HDM	6.18±2.312
	SEB	3.89±1.893
	HDM+SEB	7.95±2.862
15 IN	**CONTROL**	2.61±0.814
	HDM	7.43±1.667
	SEB	3.08±0.992
	HDM+SEB	10.8±1.907 *p=0.002
30 IN	**CONTROL**	2.24±0.225
	HDM	3.44±1.281
	SEB	3.89±1.920
	HDM+SEB	2.88±1.062

Data are mean ± standard error of the mean. CONTROL, HDM, SEB and HDM+SEB as described. *: versus intragroup CONTROL.

Table S3. Quantitative morphology for mucoid mass in intrapulmonary airways.

Model	Group	Mucoid mass (dimensionless)	
15 IN	**CONTROL**	0.19±0.087	
	HDM	0.49±0.146	
	SEB	3.14±0.314	*p=0.006
	HDM+SEB	6.03±0.170	*p<0.001

Data are mean ± standard error of the mean. CONTROL, HDM, SEB and HDM+SEB as described. *: versus CONTROL.

Table S4. Quantitative morphology for subepithelial collagen deposition in intrapulmonary airways.

Model	Group	ECM mass (dimensionless)
15 IN	**CONTROL**	1.60±0.335
	HDM	1.94±0.383
	SEB	4.84±0.466 *p=0.030
	HDM+SEB	8.25±1.128 *p=0.007

Data are mean ± standard error of the mean. CONTROL, HDM, SEB and HDM+SEB as described. *: versus CONTROL.

Table S5. Quantitative morphology of airway contractile tissue mass (ASM mass).

Model	Group	ASM mass (dimensionless)	
15 IN	**CONTROL**	2.32±0.684	
	HDM	4.72±0.286	
	SEB	6.64±1.213	*p=0.030
	HDM+SEB	8.49±0.552	*p=0.007

Data are mean ± standard error of the mean. CONTROL, HDM, SEB and HDM+SEB as described. *: versus CONTROL.

Table S6. Flow cytometry analysis of BAL leucocytes subpopulations.

	15IN				
Groups	**CONTROL**	**HDM**		**SEB**	**HDM+SEB**
Macrophagues	95.2±0.775	72.4±6.427	*p=0.013	92.1±0.805	76.1±7.797 *p=0.034
Neutrophils	0.66±0.287	4.68±1.800	*p=0.006	0.45±0.281	1.85±0.562
Eosinophils	0.11±0.034	1.58±0.461	*p=0.026	0.28±0.067	1.29±0.444 *p=0.024
NK cells	0.01±0.002	0.04±0.011	*p=0.010	0.02±0.002	0.03±0.009
T cells	1.09±0.122	5.73±1.124	*p=0.032	0.93±0.171	6.27±1.583 *p=0.008
B cells	0.32±0.115	2.47±0.998		0.52±0.082	3.62±1.046 *p=0.005
CD161+ B cells	51.6±9.324	32.9±8.917		68.9±9.251	12.7±2.373 *p=0.002

Data are mean percentage ± standard error. CONTROL, HDM, SEB and HDM+SEB as described. *: versus CONTROL.

Table S7. HDM-specific IgE in BAL and serum.

		HDM-IgE mOD	
Model	**Group**	**BAL**	**SERUM**
15 IN	**CONTROL**	0.4296±0.02944	0.3041±0.02783
	HDM	0.5492±0.02684	0.2956±0.01650
	SEB	0.5046±0.03023	0.3518±0.03671
	HDM+SEB	0.7726±0.06358 *p<0.001	0.5868±0.06010 *p=0.002

Data are mean ± standard error of the mean. CONTROL, HDM, SEB and HDM+SEB as indicated. mOD: mean optical density. *: versus CONTROL.

Table S8. SEB-specific IgE in BAL and serum.

		SEB-IgE mOD	
Model	**Group**	**BAL**	**SERUM**
15 IN	**CONTROL**	0.21±0.028	0.15±0.011
	HDM	0.27±0.009	0.20±0.016
	SEB	0.19±0.016	0.15±0.015
	HDM+SEB	0.22±0.023	0.19±0.018

Data are mean ± standard error of the mean. CONTROL, HDM, SEB and HDM+SEB as indicated. mOD: mean optical density. *: versus CONTROL.

Table S9. Total BAL IgG.

Model	Group	IgG µg/ml
15 IN	**CONTROL**	15.03±0.878
	HDM	14.57±1.001
	SEB	14.46±0.611
	HDM+SEB	11.91±0.854 *p=0.034

Data are mean ± standard error of the mean. CONTROL, HDM, SEB and HDM+SEB as described. *: versus CONTROL.

Table S10. BAL cytokines.

Model	Group	IL-4	IL-13	IL-17A	IFN-γ	IL-5	EOTAXIN
15 IN	CONTROL	28.3±0.408	147±3.959	20.9±0.293	35.43±9.191	33.5±0.775	13.1±0.182
	HDM	30.6±0.518	208±2.219	37.8±0.572 *p=0.035	91.41±20.39 *p=0.035	111±1.618 *p=0.005	29.7±0.376 *p=0.003
	SEB	55.9±0.411 *p=0.022	292±1.435 *p=0.007	18.7±0.135	40.26±4.109	92.5±0.742 *p=0.046	19.1±0.210
	HDM+SEB	61.3±0.903 *p=0.005	288±1.146 *p=0.009	37.8±0.306 *p=0.043	94.31±5.983 *p=0.012	107±1.843 *p=0.006	30.1±0.330 *p=0.002

Data are mean ± standard error of the mean. CONTROL, HDM, SEB and HDM+SEB as described. *: versus CONTROL.

Table S11. Serum cytokines.

Model	Group	IL-13	IL-17A	IL-5	EOTAXIN	TNF-α
15 IN	CONTROL	12.0±0.319	1.82±0.087	21.6±0.135	4.62±0.039	1.83±0.056
	HDM	17.2±0.459	1.07±0.038	22.8±0.159	4.75±0.054	1.86±0.038
	SEB	13.8±0.397	1.74±0.080	32.5±0.132 *$p<0.001$	5.67±0.065	3.38±0.082
	HDM+SEB	18.4±0.783	3.33±0.087	32.3±0.214 *$p<0.001$	6.09±0.071	3.02±0.036

Data are mean ± standard error of the mean. CONTROL, HDM, SEB and HDM+SEB as described. *: versus CONTROL.

Table S12. $CD4^+$ T cell stimulation.

Groups	% Proliferation	% EdU incorporation	CD4 MFI
CD4n	28.16±1.399	2.26±1.111	4.17±0.591
CD4s DAY 0	35.66±3.692	2.34±0.957	4.33±0.561
CD4s DAY 6	52.87±4.515 *p=0.003 **p=0.014	19.8±2.280 *p=0.004 **p<0.001	6.27±0.520 *p=0.034 **p=0.024

Data are mean ± standard error of the mean. CD4n and CD4s as described. *: versus CD4s DAY 0; **: versus CD4n.

Table S13. Direct contact ASM/CD4+ T cell co-culture.

Groups		%EdU ASM	CD4 G0/G1 phase	CD4 S phase	CD4 G2/M phase	CD4 Apoptotic
ASM 10% FBS		92.17±0.469				
ASM 0.5% FBS		23.13±1.112				
ASM ns	**CD4 ns**	21.58±1.274	93.85±0.368	0.54±0.047	0.82±0.178	1.04±0.172
	CD4 s	45.10±3.455 *p<0.001 **p<0.001	73.67±5.921 **p=0.002	14.6±4.581 **p=0.005	1.48±0.584	7.06±3.115
ASM s	**CD4 ns**	20.78±1.818	79.41±4.361	3.49±0.841	2.23±0.437	14.9±3.900
	CD4 s	37.03±1.697 *p<0.001 ***p<0.001	62.86±2.268 ***p=0.023	17.4±2.981 ***p=0.003	1.08±0.359	9.17±2.990

Data are mean ± standard error of the mean. ASMs, ASM ns, CD4n and CD4s as described. *: versus ASM 0.5%; FBS **: versus ASM ns+CD4ns; ***: versus ASM s+CD4 ns.

Table S14. Transwell ASM/CD4^{+} T cell co-culture.

Groups		%EdU ASM	CD4 G0/G1 phase	CD4 S phase	CD4 G2/M phase	CD4 Apoptotic
ASM 10% FBS		92.17±0.469				
ASM 0.5% FBS		23.13±1.112				
ASM ns	**CD4 ns**	20.59±2.886	92.78±0.6344	1.23±0.364	1.97±0.627	1.76±0.285
	CD4 s	15.55±0.8069	69.98±5.588 ***p*=0.003	1.58±0.355	1.28±0.345	22.9±5.985 ***p*=0.009
ASM s	**CD4 ns**	24.89±2.535	89.24±2.610	1.75±0.261	1.63±0.836	3.22±1.731
	CD4 s	18.75±1.213	66.67±4.975 ****p*=0.003	2.40±1.152	2.31±0.676	24.77±5.928 ****p*=0.008

Data are mean ± standard error of the mean. ASMs, ASM ns, CD4n and CD4s as described. **: versus ASM ns+CD4 ns; ***: versus ASM s+CD4 ns.

Table S15. MSC/ASM/CD4^{+} T cell co-culture, direct cell contact.

Groups		%EdU ASM	CD4 G0/G1 phase	CD4 S phase	CD4 G2/M phase	CD4 Apoptotic
ASM ns + CD4 s		45.10±3.455	73.67±5.921	14.6±4.581	1.48±0.584	7.06±3.115
ASM ns + CD4 s	MSC (1:5)	37.23±1.754	80.53±3.259	14.4±2.649	0.90±0.074	1.33±0.223
ASM ns + CD4 s	MSC (1:10)	33.77±1.505	86.53±0.947	8.71±1.356	0.99±0.037	1.24±0.085
ASM ns + CD4 s	MSC (1:100)	36.71±2.195	88.87±1.524	6.79±0.792	1.43±0.164	1.08±0.097
ASM ns + CD4 s	MSC (1:1000)	39.92±1.066	90.50±0.455	5.84±0.430	1.17±0.0491	1.02±0.104

Data are mean ± standard error of the mean. ASM ns, CD4s and MSC (1:5, 1:10, 1:100 and 1:1000) as described. *: versus ASM ns+CD4s

Table S16. ASM/CD4^{+} T cell co-culture with MSC in upper Transwell chamber

Groups		%EdU ASM	CD4 G0/G1 phase	CD4 S phase	CD4 G2/M phase	CD4 Apoptotic
ASM ns + CD4 s		45.10±3.455	73.67±5.921	14.6±4.581	1.48±0.584	7.06±3.115
ASM ns + CD4 s	MSC (1:5)	22.25±1.538 *p<0.001	79.73±3.543	1.59±0.282 **p<0.001	1.26±0.268	11.5±2.105
ASM ns + CD4 s	MSC (1:10)	30.21±2.598 *p=0.008	85.74±3.169	2.00±0.296 **p<0.001	0.85±0.244	8.29±2.221
ASM ns + CD4 s	MSC (1:100)	41.20±3.170	89.88±3.494	4.22±1.288 **p=0.011	0.87±0.256	3.56±1.281
ASM ns + CD4 s	MSC (1:1000)	39.67±3.852	90.99±2.951	3.19±1.084 **p=0.023	0.49±0.073	3.05±1.044

Data are mean ± standard error of the mean. ASM ns, CD4s and MSC (1:5, 1:10, 1:100 and 1:1000) as described. *: versus ASM ns+CD4s

Table S17.Blocking exosome production by MSC.

Groups		405 nm MFI		CD63 MFI	
MSC(1:5)	**CONTROL**	0.67±0.457		8.99±0.693	
	GW4869	4.88±1.029	*p=0.003	20.4±3.202	*p=0.005

Data are mean ± standard error of the mean. MSC (1:5), CONTROL and GW4869 as described. *: versus CONTROL.

Table S18. Blocked exosome MSC in ASM/CD4^{+} T cell co-culture.

Groups	%EdU ASM	CD4 G0/G1 phase	CD4 S phase	CD4 G2/M phase	CD4 Apoptotic
ASM ns + CD4 s	45.10±3.455	73.67±5.921	14.6±4.581	1.48±0.584	7.06±3.115
MSC (1:5)	22.25±1.538 *p<0.001	79.73±3.543	1.59±0.282	1.26±0.268	11.5±2.105
MSC (1:5) + GW4869	24.95±2.057 *p<0.001	54.35±4.424	30.5±1.774 *p<0.001 **p<0.001	0.61±0.087	5.03±0.822

Data are mean ± standard error of the mean. ASM ns, CD4s, MSC (1:5) and MSC (1:5)+GW4869 as described. *: versus ASM ns+CD4s; **: versus MSC (1:5).

Table S19. MSC-CM effect in ASM/CD4^{+} T cell co-culture.

Groups	%EdU ASM	CD4 G0/G1 phase	CD4 S phase	CD4 G2/M phase	CD4 Apoptotic
ASM ns + CD4 s	45.1±3.455	73.6±5.921	14.6±4.581	1.48±0.584	7.06±3.115
MSC (1:5)	22.2±1.538 *p<0.001	79.7±3.543	1.59±0.282 *p<0.001	1.26±0.268	11.5±2.105
CM	23.5±1.634 *p<0.001	76.4±6.484	1.07±0.250 *p<0.001	3.07±1.231	9.92±4.822

Data are mean ± standard error of the mean. ASM ns, CD4s, MSC (1:5) and CM as described. *: versus ASM ns+CD4s.

Table S20. Cut-off MSC-CM effect in ASM/CD4^{+} T cell co-culture.

Groups	%EdU ASM	CD4 G0/G1 phase	CD4 S phase	CD4 G2/M phase	CD4 Apoptotic
ASM ns + CD4 s	45.1±3.455	73.6±5.921	14.6±4.581	1.48±0.584	7.06±3.115
CM	23.5±1.634 $^{**}p<0.001$	76.4±6.484	1.07±0.250 $^{\#}p<0.001$	3.07±1.231	9.92±4.822
<3 kDa	42.2±2.183 $^{*}p<0.001$	84.7±3.419	2.70±0.773 $^{**}p<0.001$	3.77±0.647	5.24±2.022
3-10 kDa	45.4±2.574 $^{*}p<0.001$	76.89±4.134	9.94 ± 2.200 $^{*}p=0.004$	3.52±0.565	6.20±1.727
10-30 kDa	49.1±1.575 $^{*}p<0.001$	79.2±3.977	11.7±3.436 $^{*}p=0.016$	3.21±0.897	3.25±0.617
30-100 kDa	25.6±3.348 $^{**}p<0.001$	79.3±6.163	3.78±1.501 $^{**}p<0.001$	2.78±0.475	8.85±3.818
>100 kDa	48.9±1.586 $^{*}p<0.001$	79.6±4.801	9.73±2.749 $^{*}p=0.020$	2.46±0.469	5.56±1.919

Data are mean ± standard error of the mean. CM and different cut-offs (<3 kDa, 3-10 kDa, 10-30 kDa, 30-100 kDa and >100 kDa) as described.
*: versus CM; **: versus ASM+CD4s.

Table S21. Protein content in different cut-offs of MSC-CM

Groups	Protein content (mg/ml)	
DMEM	1.10±0,162	
<3 kDa	1.13±0,103	
3-10 kDa	1.48±0,041	
10-30 kDa	1.71±0,094	*p=0.032
30-100 kDa	1.86±0,180	*p=0.040
>100 kDa	1.52±0,139	

Data are mean ± standard error of the mean. DMEM and different cut-offs of MSC-CM (<3 kDa, 3-10 kDa, 10-30 kDa, 30-100 kDa and >100 kDa) as described. *: versus DMEM.

Table S22. R_L responsiveness to MCh. IN models.

Model	Group	Subgroup	D0	D4	D8	D16	D32	D64	D128	D256
HDM+SEB			0.23±0.026	0.39±0.045	0.63±0.107	0.92±0.175	1.07±0.182	1.29±0.167 **p<0.001	1.62±0.145 **p<0.001	1.97±0.141 **p<0.001
CONTROL			0.20±0.018	0.26±0.018	0.36±0.040	0.49±0.077	0.51±0.066	0.57±0.068 *p<0.001	0.69±0.060 *p<0.001	0.81±0.041 *p<0.001
HDM+SEB	1W	12,5	0.17±0.028	0.24±0.014	0.35±0.026	0.50±0.054	0.57±0.054	0.67±0.119 **p<0.001	0.66±0.097 **p<0.001	0.70±0.115 **p<0.001
		25	0.16±0.011	0.30±0.029	0.42±0.046	0.49±0.050	0.56±0.091	0.63±0.139 **p<0.001	0.69±0.169 **p<0.001	0.76±0.120 **p<0.001
		50	0.18±0.030	0.27±0.019	0.40±0.017	0.59±0.049	0.53±0.030	0.58±0.039 **p<0.001	0.70±0.071 **p<0.001	0.79±0.087 **p<0.001
	2W	12,5	0.24±0.083	0.31±0.060	0.41±0.031	0.50±0.036	0.61±0.080	0.70±0.132 **p<0.001	0.75±0.132 **p<0.001	0.90±0.219 **p<0.001
		25	0.15±0.008	0.25±0.024	0.35±0.029	0.47±0.051	0.50±0.071	0.61±0.123 **p<0.001	0.64±0.155 **p<0.001	0.78±0.226 **p<0.001
		50	0.13±0.006	0.22±0.017	0.32±0.033	0.47±0.060	0.49±0.055	0.51±0.069 **p<0.001	0.61±0.078 **p<0.001	0.74±0.121 *p<0.001

Data are mean ± standard error of the mean. HDM+SEB model: primary airway exposure models with 15 i.n. instillations, respectively. CONTROL: respective control groups, HDM+SEB: respective HDM plus SEB challenged groups. HDM+SEB groups were challenged with different doses of CM (12.5, 25 and 50) one (1W) or two (2W) times per week during two weeks.D0 to D256: MCh doses (0, 4, 8, 16, 32, 64, 128 and 256 mg/mL, respectively). *: versus HDM+SEB. **: versus CONTROL.

Table S23. Total IgE serum. 1W or 2W model with different doses of MSC-CM.

Model	Group	Subgroup	IgE ng/ml	
HDM+SEB			8.36±1.181	
CONTROL			3.01±1.010	*p=0.006
HDM+SEB	**1W**	**12,5**	2.79±1.077	*p=0.005
		25	3.12±1.845	*p=0.032
		50	1.92±0.994	*p=0.003
	2W	**12,5**	3.20±1.015	*p=0.018
		25	2.83±1.460	*p=0.044
		50	2.93±0.860	*p=0.044

Data are mean ± standard error of the mean. HDM+SEB and 1W or 2W at different doses of MSC-CM (12.5, 25 and 50) as described. *: versus HDM+SEB.

Table S24. Total BAL IgG, 1W and 2W models, with serial MSC-CM doses.

Model	Group	Subgroup	IgG µg/ml	
HDM+SEB			12.67±0.990	
CONTROL			17.01±0.510	*p=0.040
HDM+SEB	**1W**	**12,5**	16.28±0.867	*p=0.039
		25	16.15±0.664	*p=0.020
		50	16.59±0.682	*p=0.013
	2W	**12,5**	15.31±0.916	*p=0.025
		25	16.51±0.613	*p=0.027
		50	15.83±0.823	*p=0.020

Table S25. Total BAL and serum HDM-IgE, 1W and 2W models, with serial MSC-CM doses.

			HDM-IgE mOD			
Model	**Group**	**Subgroup**	**BAL**		**SERUM**	
HDM+SEB			0.70±0.046		0.61±0.095	
CONTROL			0.47±0.036	*p=0.002	0.27±0.030	*p=0.006
HDM+SEB	**1W**	**12,5**	0.41±0.033	*p=0.002	0.27±0.018	*p=0.002
		25	0.47±0.036	*p=0.002	0.38±0.070	*p=0.002
		50	0.45±0.045	*p=0.002	0.30±0.024	*p=0.004
	2W	**12,5**	0.47±0.040	*p=0.003	0.30±0.019	*p=0.002
		25	0.39±0.018	*p=0.002	0.32±0.013	*p=0.002
		50	0.46±0.049	*p=0.003	0.35±0.027	*p=0.004

Data are mean ± standard error of the mean. HDM+SEB and 1W or 2W at different doses of MSC-CM (12.5, 25 and 50) as described. *: versus HDM+SEB.

Table S26. Total BAL and serum SEB-IgE, 1W and 2W models, with serial MSC-CM doses.

			SEB-IgE mOD	
Model	**Group**	**Subgroup**	**BAL**	**SERUM**
HDM+SEB			0.23±0.032	0.19±0,033
CONTROL			0.24±0.036	0.16±0.012
HDM+SEB	**1W**	**12,5**	0.23±0.017	0.22±0.015
		25	0.24±0.012	0.26±0.020
		50	0.24±0.014	0.21±0.008
	2W	**12,5**	0.24±0.018	0.19±0.006
		25	0.24±0.026	0.21±0.003
		50	0.27±0.019	0.23±0.011

Data are mean ± standard error of the mean. HDM+SEB and 1W or 2W at different doses of MSC-CM (12.5, 25 and 50) as described. *: versus HDM+SEB.

Table S27. Quantitative morphology of mucous load in intrapulmonary airways, 1W and 2W models, with serial MSC-CM doses.

Model	Group	Subgroup	Mucoid mass (dimensioneless)	
HDM+SEB			5.68±0.553	
CONTROL			0.21±0.041	*p<0.001
HDM+SEB	**1W**	**12,5**	2.24±0.321	**p<0.001
		25	2.61±0.432	**p<0.001
		50	4.52±0.744	**p<0.001
	2W	**12,5**	0.52±0.202	*p<0.001
		25	3.16±0.415	**p<0.001
		50	3.60±0.621	**p<0.001

Data are mean ± standard error of the mean. HDM+SEB and 1W or 2W at different doses of MSC-CM (12.5, 25 and 50) as described. *: versus HDM+SEB; **: versus CONTROL.

Table S28. Quantitative morphology of subepithelial collagen deposition in intrapulmonary airways, 1W and 2W models, with serial MSC-CM doses.

Model	Group	Subgroup	ECM (dimensioneless)	
HDM+SEB			7.86±0.633	
CONTROL			1.92±0.292	*p<0.001
HDM+SEB	**1W**	**12,5**	4.11±0.242	**p<0.001
		25	4.69±0.351	**p<0.001
		50	4.89±0.278	**p<0.001
	2W	**12,5**	2.21±0.287	*p<0.001
		25	4.61±0.370	**p<0.001
		50	5.12±0.718	**p<0.001

Data are mean ± standard error of the mean. HDM+SEB and 1W or 2W at different doses of MSC-CM (12.5, 25 and 50) as described. *: versus HDM+SEB; **: versus CONTROL.

Table S29. Quantitative morphology for airway contractile tissue mass (ASM mass). 1W or 2W model with different doses of CM.

Model	Group	Subgroup	ASM mass (dimensioneless)	
HDM+SEB			7.65±0.381	
CONTROL			2.70±0.231	*p<0.001
HDM+SEB	**1W**	**12,5**	5.17±0.676	**p=0.029
		25	5.86±0641	**p=0.003
		50	7.73±0.398	**p<0.001
	2W	**12,5**	3.14±0.383	*p<0.001
		25	5.48±0.543	**p<0.003
		50	5.73±0.797	**p<0.005

Data are mean ± standard error of the mean. HDM+SEB and 1W or 2W at different doses of MSC-CM (12.5, 25 and 50) as described. *: versus HDM+SEB; **: versus CONTROL.

Table S30. Flow cytometry analysis of BAL leucocyte subpopulations, 1W and 2W models, with serial MSC-CM doses.

	HDM+SEB							
		1W			2W			
Groups	HDM+SEB	CONTROL	12.5	25	50	12.5	25	50
Macrophagues	69.1±10.11	94.5±0.992 *p=0.045	48.5±5.075 **p<0.001	47.5±4.005 **p<0.001	51.4±8.189 **p=0.003	61.7±7.785 **p=0.007	63.9±5.642 **p=0.002	64.5±2.978 **p=0.002
Neutrophils	1.92±0.720	0.72±0.348	11.1±3.878 *p=0.030 **p=0.008	10.7±2.835 *p=0.039 **p=0.011	10.8±3.069 *p=0.040 **p=0.011	5.01±1.458 **p=0.021	12.5±3.606 *p=0.047 **p=0.016	12.1±4.177 *p=0.028 **p=0.009
Eosinophils	2.28±0.550	0.13±0.049 *p=0.010	4.15±1.477 **p=0.009	2.05±0.672 **p=0.040	1.65±0.369 **p=0.011	3.12±0.877 **p=0.019	2.17±0.632 **p=0.032	2.20±0.634 **p=0.031
NK cells	0.02±0.007	0.01±0.003	0.02±0.015	0.02±0.014	0.03±0.013	0.52±0,183 *p=0.033 **p=0.031	0.37±0.255	0.26±0.167
T cells	8.87±0.890	1.22±0.129 *p<0.001	14.4±3.256 **p<0.001	19.2±4.713 **p<0.001	13.6±2.528 **p<0.001	10.5±1.284 **p<0.001	9.22±0.654 **p<0.001	10.7±1.464 **p<0.001
B cells	6.37±1.174	0.54±0.176 *p<0.001	1.53±0.446 *p=0.002	2.16±0.667 *p=0.004	3.93±1.551 *p=0.002	1.69±0.368 *p<0.001	1.76±0.379 *p<0.001	1.94±0.489 *p<0.001
CD161+ B cells	14.8±2.693	64.4±7.322 *p<0.001	22.5±4.312 **p<0.001	11.3±3.455 **p<0.001	16.8±4.835 **p<0.001	40,2±8,742 *p=0.041	21.7±4.640 **p<0.001	13.9±3.111 **p<0.001
CD4 T cells	5.29±0.359	7.40±1.205	8.38±1.086	8.08±1.347	7.13±1.833	6.65±2.915	7.39±1.879	6.86±1.020
CD8 T cells	1.06±0.103	1.16±0.381	1.60±0.338	2.25±0.562	1.67±0.295	1.91±0.246	1.78±0.359	2.04±0.410

Data are mean ± standard error of the mean. HDM+SEB and 1W or 2W at different doses of CM (12.5, 25 and 50) as described. *: versus HDM+SEB; **: versus CONTROL.

Table S31. Flow cytometry analysis of cytokine production by CD4^{+} T cells in lung and blood, 1W and 2W models, with serial MSC-CM doses.

Model	Group	Subgroup	IFN-Y		IL-4		IL-17		FOXP3		CI	
			LUNG	BLOOD	LUNG	BLOOD	LUNG	BLOOD	LUNG	BLOOD	LUNG	BLOOD
HDM+SEB			1.23±0.265	0.29±0.065	14.1±1.790	8.97±1.000	8.13±0.465	1.29±0.545	0	0	0.12±0.080	0.29±0.030
CONTROL			6.08±0.680 *p=0.021	1.27±0.225 *p=0.011	0.63±0.070 *p<0.001	1.93±0.435 *p<0.001	19.6±1.525 *p=0.018	1.70±0.205	0	0	0.19±0.010	0.13±0.020
HDM+SEB	1W	12,5	1.58±0.930 **p=0.043	0.79±0.125	0.64±0.075 *p<0.001	0.89±0.095 *p<0.001	24.1±4.020 *p=0.013	1.10±0.025	0	0	0.51±0.055	0.26±0.105
		25	2.38±1.270 **p=0.041	0.59±0.210	0.83±0.120 *p<0.001	2.01±0.090 *p<0.001	22.7±1.760 *p=0.015	1.30±0.165	0	0	0.32±0.180	0.30±0.115
		50	1.31±0.105 **p=0.020	0.64±0.130	1.07±0.195 *p<0.001	0.98±0.175 *p<0.001	17.1±1.405 *p=0.026	1.27±0.220	0	0	0.09±0.050	0.14±0.085
	2W	12,5	5.03±0.570 *p=0.026	1.06±0.135 *p=0.035	0.69±0.190 *p<0.001	0.75±0.155 *p<0.001	15.9±1.030 *p=0.020	1.13±0.505	0	0	0.19±0.115	0.15±0.050
		25	1.49±0.165 **p=0.022	0.56±0.198	0.74±0.095 *p<0.001	1.20±0.295 *p<0.001	13.8±1.105 *p=0.040	2.80±0.465	0	0	0.06±0.040	0.08±0.020
		50	1.28±0.070 **p=0.019	0.79±0.075	1.38±0.115 *p<0.001	0.81±0.120 *p<0.001	16.9±0.828 *p=0.040	2.36±0.500	0	0	0.13±0.020	0.02±0.010

Data are mean ± standard error of the mean. HDM+SEB and 1W or 2W at different doses of CM (12.5, 25 and 50) as described. *: versus HDM+SEB; **: versus CONTROL.

II. Summary

Castellano

El asma es una enfermedad inflamatoria crónica que afecta aproximadamente a unos 300 millones de personas en todo el mundo. Durante las últimas décadas, especialmente en los países industrializados, su prevalencia y morbimortalidad se han incrementado. Esta enfermedad se caracteriza principalmente por un conjunto de alteraciones estructurales en las vías respiratorias, conocidos mediante el término de “remodelación”, el cual se ha asociado con la severidad de la enfermedad. De entre estas alteraciones, el aumento de la masa de músculo liso inducido por una hiperplasia e hipertrofia de células musculares lisas, es el factor considerado de mayor importancia debido a su influencia sobre la obstrucción irreversible del flujo aéreo y a la hiperreactividad de las vías respiratorias. Actualmente, el tratamiento del asma se basa en el control de la inflamación, sin efecto demostrado sobre el mecanismo de remodelación irreversible. El único tratamiento capaz de actuar sobre esta alteración es la termoplastia invasiva, con coste-efectividad discutido y varios fracasos terapéuticos. En este contexto, las células madre mesenquimales (MSC) ejercen efectos inmunoreguladores de potencial interés terapéutico en la remodelación bronquial. Sin embargo, su infusión como terapia crónica se enfrenta a la posibilidad de que a través de su reclutamiento y diferenciación puedan participar en la remodelación de las vías respiratorias, particularmente en el crecimiento del músculo liso. Por otra parte, datos adicionales obtenidos en asma experimental sugieren que el efecto terapéutico anti-remodelador de las MSC está vehiculados por mediadores. Por tanto, existe por una parte la necesidad de comprender los mecanismos inmunológicos que contribuyen en el proceso de remodelación y por otra parte el desarrollo de modelos animales de enfermedad experimental capaces de reproducir los mecanismos biológicos con un detalle y profundidad los más similar posible en sujetos humanos y permitir una mejor comprensión y tratamiento del asma. Por todo ello, en el presente trabajo de tesis doctoral se propuso desarrollar un modelo de asma alérgica basado en la exposición local de un alérgeno, y estudiar en este modelo la posible implicación de las células T CD4 sobre la remodelación del músculo bronquial *in vitro*. Adicionalmente, se estudió los mecanismos inmunomoduladores de las MSC como terapia supresora sobre esta alteración estructural mediante sistemas de co-cultivo *in vitro* y en el modelo desarrollado *in vivo*. Los resultados obtenidos demostraron un papel inductor de las células T $CD4^+$

alérgeno-específicas en la remodelación del músculo liso mediante un mecanismo de contacto directo, la cual se midió mediante análisis de ciclo celular por citometría de flujo. Adicionalmente, las MSC son capaces de inhibir la proliferación de células musculares lisas inducidas por células T $CD4^+$ solamente cuando están separados mediante una membrana permeable "Transwell" y se encuentran en ratios elevados (MSC:linfocito). Además, se observó que este efecto supresor no estaba vehiculado por exosomas y era secretado espontáneamente sin previa señalización requerida. Asimismo, solamente los factores solubles comprendidos en un rango de 30 a 100 kDa de peso molecular que conforman este medio condicionado (CM) son capaces de inducir este efecto supresor sobre las células musculares lisas. Este CM (30-100 kDa) obtenido, fue testado a diferentes dosis *in vivo* en el modelo desarrollado con anterioridad, observándose un efecto supresor en los mecanismos inmunológicos y el proceso de remodelación solamente cuando se trataban a los animales con dosis bajas repetidas de CM. Este efecto es generado por una posible desviación de la respuesta inmunitaria de un fenotipo característico Th2 en asma alérgico, hacia un fenotipo Th1/Th17 en las vías respiratorias. En este contexto, el CM de las MSC se postula como una estrategia terapéutica prometedora sobre la reversión de la remodelación bronquial debido a una desviación de la respuesta inmunitaria.

Català

L'asma es una malaltia inflamatòria crònica que afecta aproximadament a 300 milions de persones en tot el mon. Durant les últimes dècades, especialment en els països industrialitzats, la prevalença i la morbimortalitat s'han incrementat. Aquesta malaltia es caracteritza principalment per un conjunt d'alteracions estructurals en les vies respiratòries, conegudes amb el terme de "remodelació", el qual s'ha associat amb la severitat de la malaltia. De totes aquestes alteracions, l'augment de la massa de musculatura llisa induït per una hiperplàsia e hipertrofia de cèl·lules musculars llises, es el factor de major importància degut a la seva influencia sobre la obstrucció irreversible del flux i la hiperreactivitat de les vies respiratòries. Actualment, el tractament de l'asma es basa en el control de la inflamació, sense efecte demostrat sobre aquesta remodelació irreversible. L'únic tractament capaç d'actuar sobre aquesta l'alteració es la termoplàstia invasiva, amb un cost-efectivitat discutit i diversos fracassos terapèutics. En aquest context, les cèl·lules mare mesenquimals (MSC) exerceixen efectes inmunoreguladors de potencial interès terapèutic en la remodelació bronquial. No obstant, la seva infusió com a teràpia crònica s'enfronta a la possibilitat de que a traves del seu reclutament i diferenciació puguin participar en la remodelació bronquial, particularment en l'augment

de la musculatura llisa. D'altra banda, dades addicionals obtingudes en asma experimental suggereixen que l'efecte terapèutic anti-remodelador de les MSC estan vehiculats per mediadors. Per tant, existeix d'una banda la necessitat d'entendre els mecanismes immunològics involucrats en el procés de remodelació i d'altra banda el desenvolupament de models animals de malaltia experimental amb capacitat de reproduir els mecanismes biològics amb un detall i profunditat lo mes similar possible als humans i permetre una millora en la comprensió i tractament de l'asma. Per tot això, en el present treball de tesis doctoral es va proposar desenvolupar un model d'asma al·lèrgica basat en l'exposició local d'un al·lergen, i estudiar en aquest model la possible implicació de les cèl·lules T $CD4^+$ sobre la remodelació de la musculatura bronquial *in vitro*. Addicionalment, es van estudiar els mecanismes immunològics de les MSC com a teràpia supressora sobre l'alteració estructural mitjançant sistemes de co-cultiu *in vitro* i en models desenvolupats *in vivo*. Els resultats obtinguts van demostrar un paper inductor de les cèl·lules T $CD4^+$ al·lergen-especifiques en la remodelació de la musculatura llisa mitjançant mecanismes de contacte directe, la qual es va mesurar amb un anàlisis del cicle cel·lular per citometria de flux. Addicionalment, les MSC tenen la capacitat d'inhibir la proliferació de cèl·lules musculars llises induïdes per cèl·lules T $CD4^+$ nomes quan estan separades mitjançant una membrana permeable "Transwell" i es troben en ratios elevats (MSC:limfòcit). Es va observar que l'efecte supressor no estava vehiculat per exosomes i era secretat espontàniament sense prèvia senyalització. Així mateix, únicament els factors solubles compresos en un rang 30 a 100 kDa de pes molecular en aquest medi condicionat (CM) tenen la capacitat de induir aquest efecte supressor sobre les cèl·lules musculars llises. Aquest CM (30-100 kDa) generat, va ser testat a diferents dosis *in vivo* en el model desenvolupat amb anterioritat, i es va observar un efecte supressor en els mecanismes immunològics i el procés de remodelació únicament quan es tractaven als animals amb dosis baixes repetides de CM. Aquest efecte es generat per una possible desviació de la resposta immunitària d'un fenotip característic Th2 en asma al·lèrgic, cap a un fenotip Th1/Th17 en les vies respiratòries. En aquest context, el CM de les MSC es postula com una estratègia terapèutica propicia sobre la reversió de la remodelació bronquial degut a una desviació en la resposta immunitària.